STAPLING AND UNSTAPLING PEPTIDES AND PROTEINS WITH *s*-TETRAZINE

Stephen P. Brown

A DISSERTATION

in

Chemistry

Presented to the Faculties of the University of Pennsylvania

In Partial Fulfillment of the Requirements for the

Degree of Doctor of Philosophy

2015

Supervisor of Dissertation

_____

Amos B. Smith, III
Rhodes-Thompson Professor of Chemistry

Graduate Group Chairperson

_____

Gary A. Molander
Hirschmann-Makineni Professor of Chemistry

Dissertation Committee:

David M. Chenoweth, Assistant Professor of Chemistry
E. James Petersson, Associate Professor of Chemistry
Virgil Percec, P. Roy Vagelos Professor of Chemistry

To My Family

ACKNOWLEDGMENTS

First of all, I would like to thank my advisor, Professor Amos B. Smith, III. I am grateful for being given the chance to work in his group on such an interesting and challenging project. I really admire Professor Smith's work ethic, which I have tried to emulate in pushing myself forward. Many thanks for the guidance, encouragement and support that has been given to me during all of those challenging times.

Special thanks to my dissertation committee: Professor David Chenoweth, Professor E. James Petersson and Professor Virgil Percec for helpful and insightful discussions during our meetings.

Our collaborator, Professor Robin M. Hochstrasser, whom sadly passed away in February of 2013, provided invaluable advice as well as 2D IR experiments to evaluate the ultrafast refolding process of the kinked helix. Additionally, Drs. Matthew Tucker and Jianxin Chen for acquiring the photophysical and 2D IR data. Also, thanks to Professor Feng Gai for continuing our collaboration in the phototriggering area.

Dr. George Furst for assisting in the collection of high resolution NMR spectra for most of the peptides in this thesis with only 1-2 milligram samples.

Dr. Joel Courter conducted the synthesis of a model *S,S*-tetrazine for photophysical studies and Dr. Mohannad Abdo for the development of the fragment coupling procedure and synthesis of the helices kinked with the s-tetrazine. Also, Matthew Bunner for continuing the work with *Cl,S*- and *S,N*-tetrazine peptides

All of the Smith group members deserve great credit for providing such a supportive environment, in particular Bruno Melillo, Mark Farrell, Joel Courter, Mohannad Abdo, Dave Jones and Jason Melvin.

I would like to express my deepest gratitude to my Mom, Dad, sister Laurie and especially my wife Choja for their patience and support along the way. Anything that I could write here would simply not do justice to the support that you have given me along the way. –Thank you

ABSTRACT

STAPLING AND UNSTAPLING PEPTIDES AND PROTEINS WITH *s*-TETRAZINE

Stephen P. Brown

Professor Amos B. Smith, III

This thesis will focus on the design, synthesis, and validation of synthetic techniques to introduce *s*-tetrazine into peptides and proteins. The *s*-tetrazine molecule is effective for restricting peptides/proteins to macrocyclic conformations (i.e. stapling). Importantly, the incorporated *s*-tetrazine chromophore will undergo photodisassociation upon absorption of a photon permitting the release of the restricted conformations (i.e. unstapling).

In chapter one, we aimed to study a fundamental folding process known as the helix-coil transition by phototriggering coupled with transient two-dimensional infrared spectroscopy (2D IR). The *s*-tetrazine molecule possesses the photochemical properties of an ideal phototrigger, as such, *s*-tetrazine was employed towards the development of techniques capable of capturing the fastest structural transitions of biomolecules with both high spatial and high temporal resolution. Tripeptide linchpins, containing the *s*-tetrazine phototrigger, were prepared by solid-phase peptide synthesis. The latter were then employed toward the construction kinked helices near equilibrium via a fragment coupling procedure. The relaxation of the kinked helical structures were observed by pump/probe transient 2D IR spectroscopy.

In chapter two, new synthetic protocols have been developed and validated for the introduction of *s*-tetrazine into peptides and proteins to staple and unstaple the conformations. Conditions for the introduction of *s*-tetrazine into cysteine sulfhydryl groups of unprotected peptides conducted with aqueous biphasic conditions, permitting the construction of macrocyclic peptides with a wide range of functionally and ring topology, bridging from one to 27 amino acid residues adjoining the cysteines. Importantly, the stapled conformations were released photochemically to their thiocyanate counterparts, and in turn the resulting thiocyanates removed to regenerate the native peptide. To the best of our knowledge *s*-tetrazine comprises the first example of a readily removable peptide staple. Finally, the stapling and unstapling protocol has been extended to include thioredoxin as an example of a protein with an incorporated *s*-tetrazine construct that can also serve a useful role in conjugation strategies.

TABLE OF CONTENTS

Table of Figures

Table of Schemes

CHAPTER 1. Development of a Phototriggering Strategy to Measure the Ultrafast Non-Equilibrium Dynamics of Peptides

Introduction

Proteins and peptides, dynamic entities comprised of amino acids linked together into a linear chain, are responsible for a wide array of functions in biochemistry.[1-4] These chains of amino acids ultimately fold into three-dimensional structures, exploiting conformational changes and transient molecular interactions, which in turn, determines the underlying mechanism of a protein's biological function. The early kinetic events that govern conformational dynamics in peptides and proteins are critical for the development and refinement of model systems that relate dynamic structure to the observed biological function.[5-7] X-ray crystallography[8-9] and nuclear magnetic resonance measurements[10] can achieve atomic resolution static structures, however these techniques do not provide information of the transient, non-equilibrium structures. Techniques such as infrared (IR) spectroscopy, Raman spectroscopy and fluorescence resonance energy transfer (FRET) have also been developed to capture the structural transitions of biomolecules. However, none of the existing methods are capable of following the ultrafast folding dynamics with both high spatial and temporal resolution.[11] The development of methods to achieve atomic resolution transient structures within the ultrafast time regime holds the promise towards understanding the process that peptides and proteins undergo to self-assemble into well-ordered three-dimensional structures and in turn reveal significant insight into protein folding diseases.

Exploration of the Helix-Coil Transition

With the goal of developing a technique capable of capturing the fastest structural transitions of biomolecules with both high spatial and high temporal resolution, we began with a basic folding process. The helix-coil transition is a fundamental folding transition commonly used by peptides and proteins. The rates for the helix-coil folding processes had not previously been measured, but had been estimated to be on the order of pico- to nanoseconds with computer simulated values conflicting by more than two-orders of magnitude.[12-14] To achieve our goals, a successful method would require both structurally defined starting and end points in the folding process for spatial control, coupled with a technique capable of observing the backbone folding process on an ultrafast timescale.

Two-Dimensional Infrared Spectroscopy

Two-dimensional infrared spectroscopy (2D IR) has been developed and refined by Hochstrasser to monitor the ultrafast conformational changes in peptides.[15] In the broadest sense 2D IR permits a fourier transform infrared (FTIR) spectrum to be transposed onto two axes (Figure 1.1).[16] This technique uses a series of pulses which are separated by

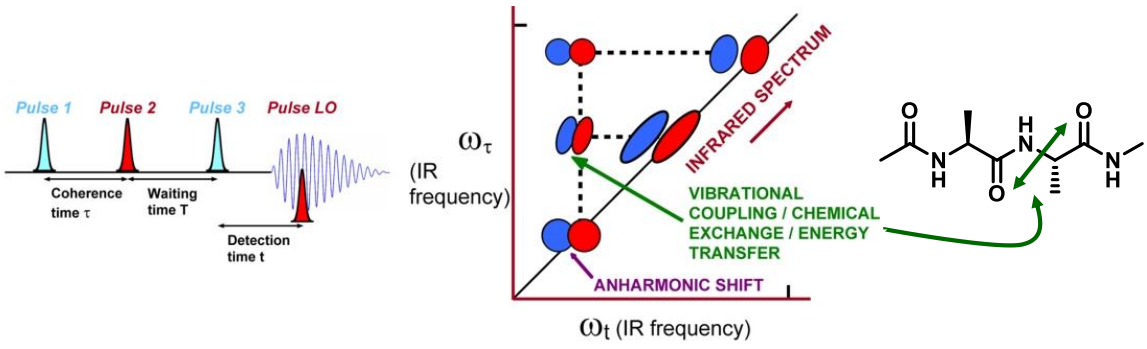

Figure 1.1. Two-Dimensional Infrared Spectroscopy Technique

controllable time delays to generate an IR spectrum containing additional cross-peaks. The cross-peaks found within the spectrum are related to the vibrational coupling between two similar harmonic oscillators. The intensity of the signals arising from the vibrational coupling are sensitive to both distance and orientation and in the cases of amide coupling within a peptide, the signals can be translated into phi/psi angles.[17-18] The two-dimensional IR technique is capable of operating on a picosecond timescale; as such, multiple snapshots can be collected and translated into dynamic information as to how the peptide folding process is progressing in solution at specific time points.

Phototriggering: A Technique to Explore Peptide/Protein Conformational Change

Phototriggering comprises a method that builds a macrocyclic constraint into the peptide structure such that the constrained peptide takes on a new ground state and confines the peptide into a narrow distribution of conformations. Additionally, the macrocyclic constraint must be photolabile such that laser-induced photolysis will break the constraint on an ultrafast timescale permitting the peptide to refold to new ground state configurations. One of the earliest examples of phototriggering was conducted by Hochstrasser and DeGrado.[19-20] These efforts employed bis-aryl disulfides to initiate the conformational change in the dynamics of peptides. The bis-aryl disulfide phototrigger underwent photolysis at 270 nm to sever the disulfide bond and expose two sulfur-centered radicals, permitting the peptide to refold into a new configuration (Figure 1.2).[19] A number of challenges were presented in this experiment. First the hydrophobic nature of the aryl groups could affect the folding process. Second, the sulfur centered radicals can react with the

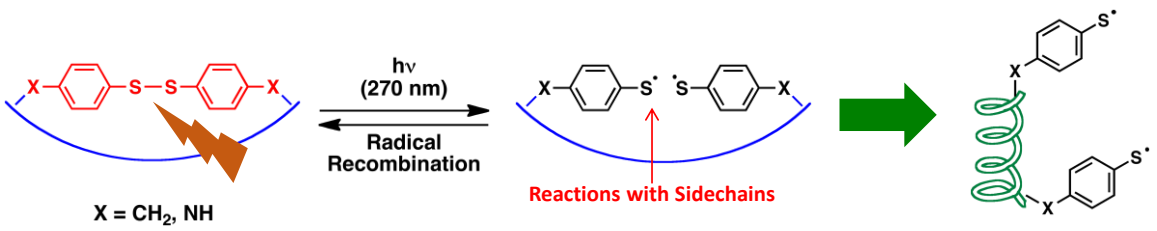

Figure 1.2. Disulfide Bond Photolysis to Initiate Conformational Dynamics

peptide and/or undergo geminate recombination. Lastly, the 270 nm wavelength used to sever the disulfide bond is not compatible with tryptophan and tyrosine residues in the peptide. The information gained from these experiments were used by Hochstrasser and Smith to design an improved phototrigger. The design of an optimal phototrigger for the study of ultrafast folding processes would possess the following properties: 1) fragment rapidly on the femto- to picosecond time scale; 2) undergo fragmentation with a high photoproduct yield upon flash photolysis; 3) constrain the peptide within a narrow, well-defined distribution of conformations; 4) produce photofragmentation products that are nonreactive and do not interfere with the conformational changes or the monitoring techniques; and 5) undergo fragmentation with visible wavelengths to ensure maximum biocompatibility.[21]

Early Work on *s*-Tetrazine Photofragmentation

The *s*-tetrazine molecule possesses the photochemical properties of an ideal phototrigger. The photofragmentation of *s*-tetrazine was initially described by Smith and Hochstrasser.[22] Molecules of *s*-tetrazine were shown to undergo absorption of an ultraviolet (UV) photon at 327 nm to generate an excited state that collapses rapidly to form two

nitriles and nitrogen gas (Figure 1.3). Further experiments at low temperature revealed, that it was possible to use crystals of *s*-tetrazine in natural isotope abundance and tune a laser to selectively photolyze all of the lighter isotope material, leaving an enriched

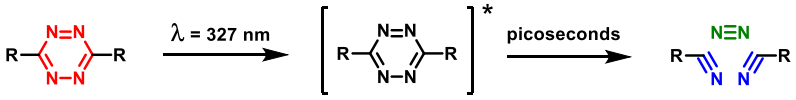

Figure 1.3. Photofragmentation of *s*-Tetrazine

sample with the heavier isotopes.[23-25] This experiment demonstrated that the *s*-tetrazine photolysis reaction mechanism did not contain radical intermediates. Now, given the favorable photochemical properties of *s*-tetrazine, the question arises; how to introduce tetrazine into peptides? The effect of carbon substituents at the 3,6-positions were shown to increase the number of vibrational modes for relaxation of the tetrazine excited state, and as a result, increased the fluorescent lifetimes leading to poor photoproduct yields. The effect of a heavy atom, such as sulfur, however had not been examined and as such might help retain the vibrational energy within the excited state of *s*-tetrazine to promote a better photoproduct yield.

Synthesis of Dichlorotetrazine

To address the question, could sulfur substitution on *s*-tetrazine improve the photochemical outcome, we turned to dichlorotetrazine (**5**, Scheme 1.1). The synthesis of dichlorotetrazine had previously been described,[26-27] beginning from guanidine hydrochloride and heating at reflux with hydrazine precipitated triaminoguanidine hydrochloride (**1**) as a

white amorphous solid (mp 233-237 ºC). The solid **1** was then reacted with two equivalents of acetylacetone which spontaneously formed a bis-pyrazole hydrazine intermediate. Heating the latter leads to an intermediate which forms a dimer and precipitated as a light yellow amorphous solid of dihydrotetrazine **2** (mp 147-149 ºC). After the oxidation of **2** with NO_2 gas, the red the tetrazine core **3** (mp 224-226 ºC) is obtained as a solid following evaporation of the solvent. The pyrazoles of **3** are then displaced with hydrazine resulting in the

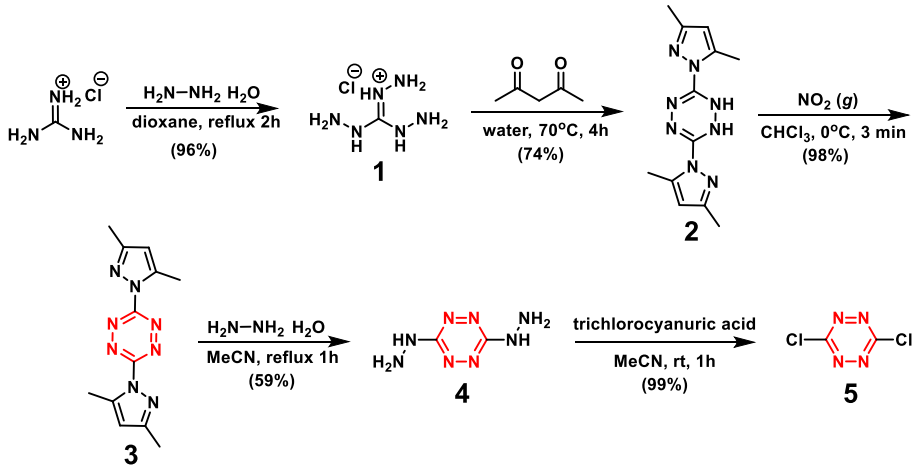

Scheme 1.1. The Synthesis of Dichlorotetrazine

precipitation of dihydrazinyl-s-tetrazine (**4**) as a fine, amorphous powder. Notably, **4** was tested by differential scanning calorimetry and thermogravimetric analysis (DSC-TGA) and shown to undergo an exothermic decomposition above 120 ºC in the presence of air; **CAUTION:** must be used when forming and isolating this compound. Finally, **4** was oxidized with trichloroisocyanuric acid to furnish dichlorotetrazine (**5**) as a red, solid (m.p. 147-150 ºC) in a 41% yield over the five steps.

Preparation of Bis-Cysteine-S,S-Tetrazine and Photophysical Evaluation

To prepare a 3,6-sulfur substituted *s*-tetrazine, a graduate student Joel Courter initially treated dichlorotetrazine (**5**) with two equivalents of cysteine **6**, protected as the methyl ester and acetyl amide, in pyridine and methylene chloride to furnish the model *S,S*-tetrazine compound **7** (Scheme 1.2).[28] Photochemical evaluation of **7** was then conducted

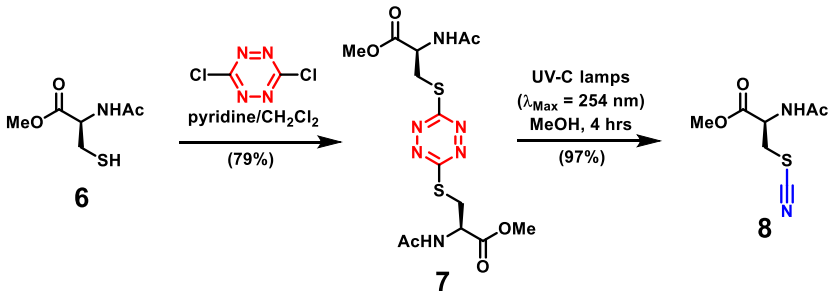

Scheme 1.2. Synthesis and Photolysis of Bis-Cysteine-S,S-Tetrazine

via flash photolysis coupled with transient IR spectroscopy. The experiment consisted of a single flash pulse at 410 nm to release the *s*-tetrazine constraint and the evolution of the thiocyanate absorbance was observed at 2163 cm^{-1} by transient IR on the picosecond time-scale (Figure 1.3).[29] The thiocyanate transient absorbance growth of **8** was plotted at specific time points to determine the formation of thiocyanate time constant of 177 ps with an 11% yield of **8**. Experiments conducted at 355 nm flash pulse doubled the yield to 22%, thus the dicysteine *S,S*-tetrazine **7** represented a new class of compounds that held considerable potential as an ultrafast phototrigger.

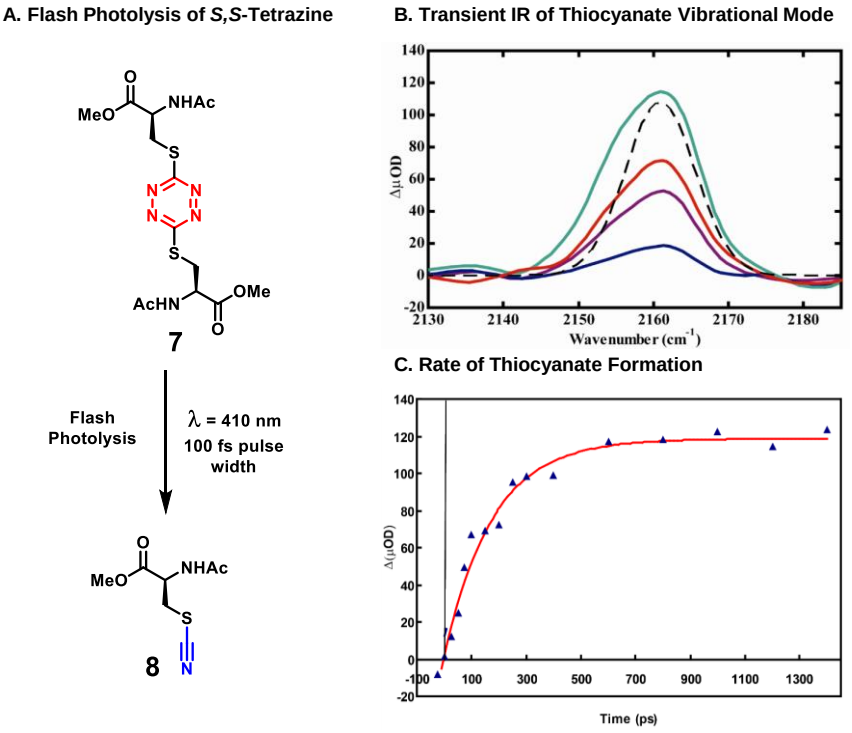

Figure 1.3. Photochemical Evaluation of the S,S-Tetrazine Phototrigger

Preparation of a *S,S*-Tetrazine Kinked Helix Near Equilibrium

To achieve the goal of inserting the *s*-tetrazine phototrigger within larger peptides to explore the helix-coil transition, studies were initiated to construct peptides containing the *s*-tetrazine constraint within the alanine-rich peptide **9** (Figure 1.4), a system which adopts

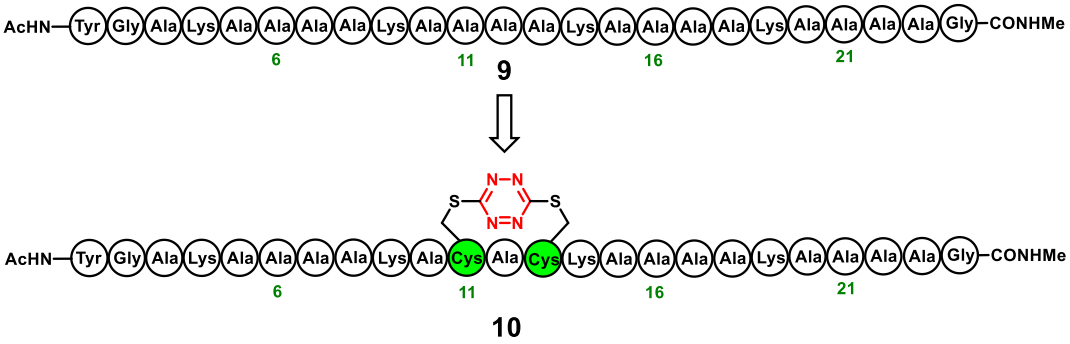

Figure 1.4. Design of a Helical System Perturbed by the s-Tetrazine Chromophore

an α-helical structure in the ground state. Reasoning that the introduction of the *s*-tetrazine moiety within the middle of a 24-residue peptide via insertion between two cysteine residues would permit both the *N*- and *C*-terminal segments of the peptide to adopt an α-helical conformation, while the amino acids near the cysteine residues would form a kinked conformation due to the geometric constraint enforced by the incorporated *s*-tetrazine phototrigger. Photolysis would then release the constraint imposed *s*-tetrazine phototrigger, permitting the peptide to undergo refolding, the exact nature of which had not previously been explored. To this end, the two alanine residues at the tenth and twelfth positions were selected to be replaced with the cysteine residues required to incorporate the *s*-tetrazine, giving rise to **10** (Figure 1.4) as the synthetic target.

Synthesis of Tripeptide Linchpins Containing s-Tetrazine

The first attempt to construct **10**, conducted by postdoctoral fellow Mohannad Abdo, entailed the solid-phase synthesis of the full-length peptide, followed by selective removal of the cysteine protection groups and addition of dichlorotetrazine. After cleavage from the resin support, a complex mixture was observed and no product was obtained from the reaction. Undeterred, we identified that dichlorotetrazine could be introduced into shorter tripeptides employing solid-phase peptide synthesis.[30] To this end, tripeptides were prepared by solid-phase peptide synthesis containing the two requisite cysteine residues (CAC) with the sulfhydryls protected with mono-methoxytrityl (Mmt) groups (Scheme 1.3). Suitable conditions for the selective deprotection of the Mmt, specifically 2% trifluoroacetic acid provided the free sulfhydryls without cleaving the peptide from the solid-support.

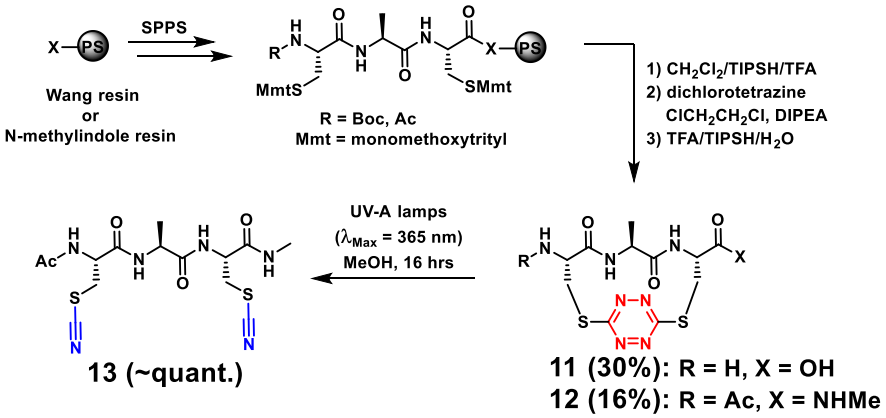

Scheme 1.3. Solid-Phase Synthesis of S,S-Tetrazine Containing Tripeptide Linchpins

The sulfhydryls were next reacted with dichlorotetrazine, and following cleavage from resin, the macrocycles (**11** and **12**) were obtained. To test the photochemical ring opening of the incorporated *s*-tetrazine constraint, peptide **12** was irradiated in a methanol solution under UV-A lamps in a Rayonet photoreactor to provide near quantitative conversion to the dithiocyanate peptide **13** (Scheme 1.3). A series of natural amino acids were incorporated within the tripeptide and were evaluated to demonstrate the compatibility of other side chains with the developed solid-phase peptide synthesis conditions. To this end peptides **14-20** were prepared by the same method (Scheme 1.4). Only arginine displayed additional reactivity after removal of the guanidium protection group. With the ability to prepare various *s*-tetrazine peptide macrocycles now in hand, this synthetic method can also be employed to introduce isotope labels into the peptide backbone. The isotope-enriched amino acids were incorporated into the peptide sequence by the same solid-phase peptide synthesis protocol; dichlorotetrazine insertion gave **21** and **22** (Scheme 1.4). Importantly, the IR signals of the isotopically enriched $^{13}C{=}^{18}O$ amide peptides **21-22** are shifted out of the main amide I band region, given the change in the zero point of the molecular vibration,

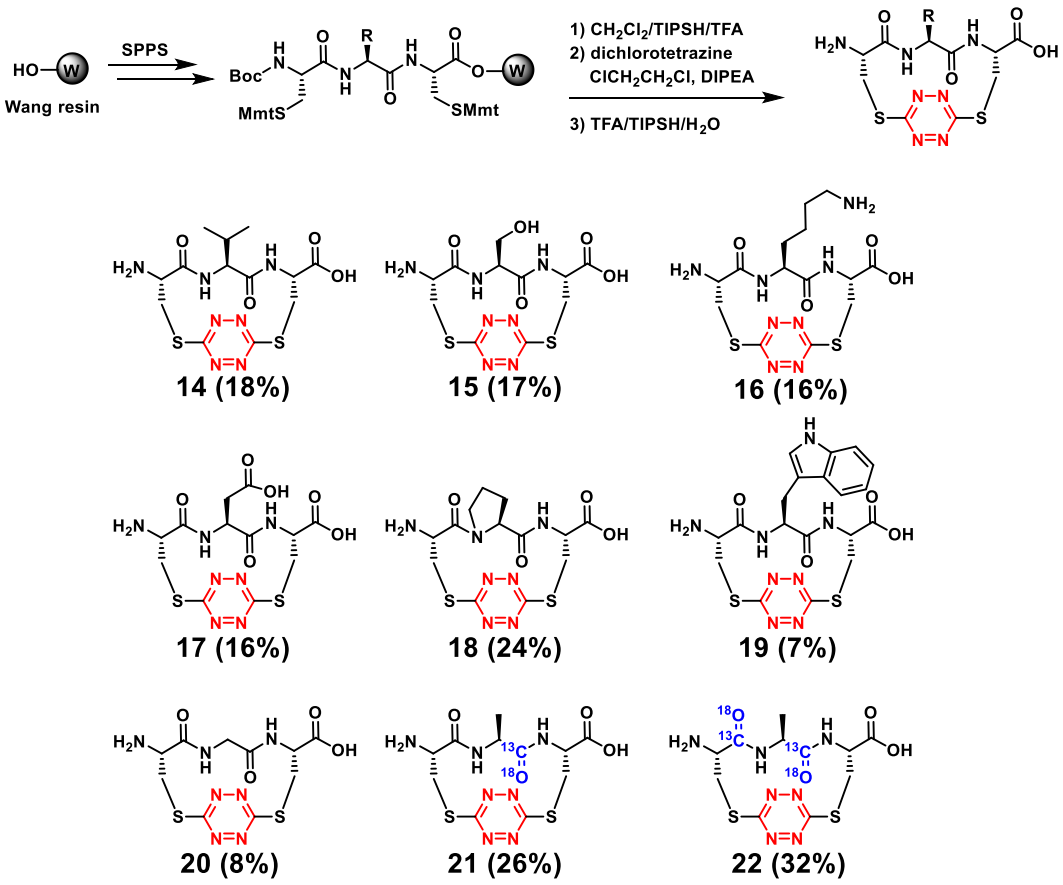

Scheme 1.4. Tetrazine Tripeptide Linchpins Prepared by Solid-Phase Synthesis

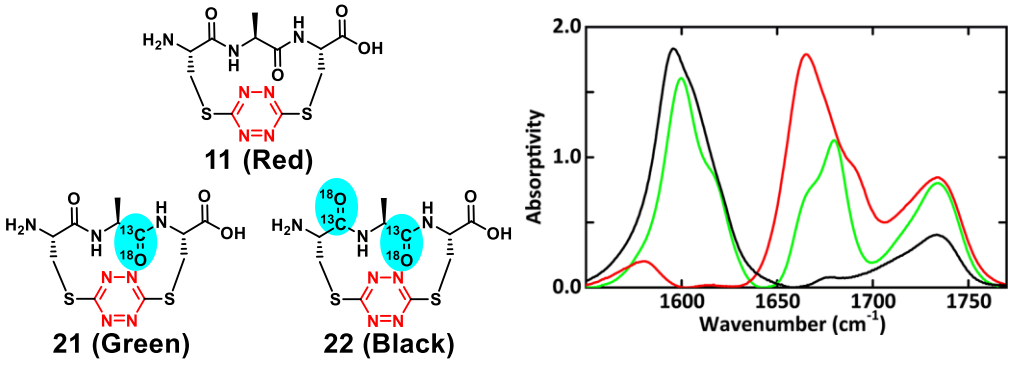

Figure 1.5. Infrared Shift of Isotopically Labeled Amides

and can thus be observed independently from the rest of the peptide backbone (Figure 1.5). The isotope labeling feature permits the monitoring of picosecond structural transitions within the amide backbone by 2D IR without interference from the remaining amide signals of **10** following photochemical release.

A Solution-Phase Fragment Coupling Strategy to Access a Kinked Helix (10)

To prepare kinked helix **10** from the tripeptide linchpins (Figure 1.6), a solution-phase fragment union strategy was developed.[31] This approach first required an orthogonal protection group strategy to differentiate the *N*-terminus of the linchpin **11** from the lysine side-chains of either fragment. The Boc- protection group and the removal thereof was demonstrated to be compatible with the tetrazine ring during the synthesis of the linchpins.

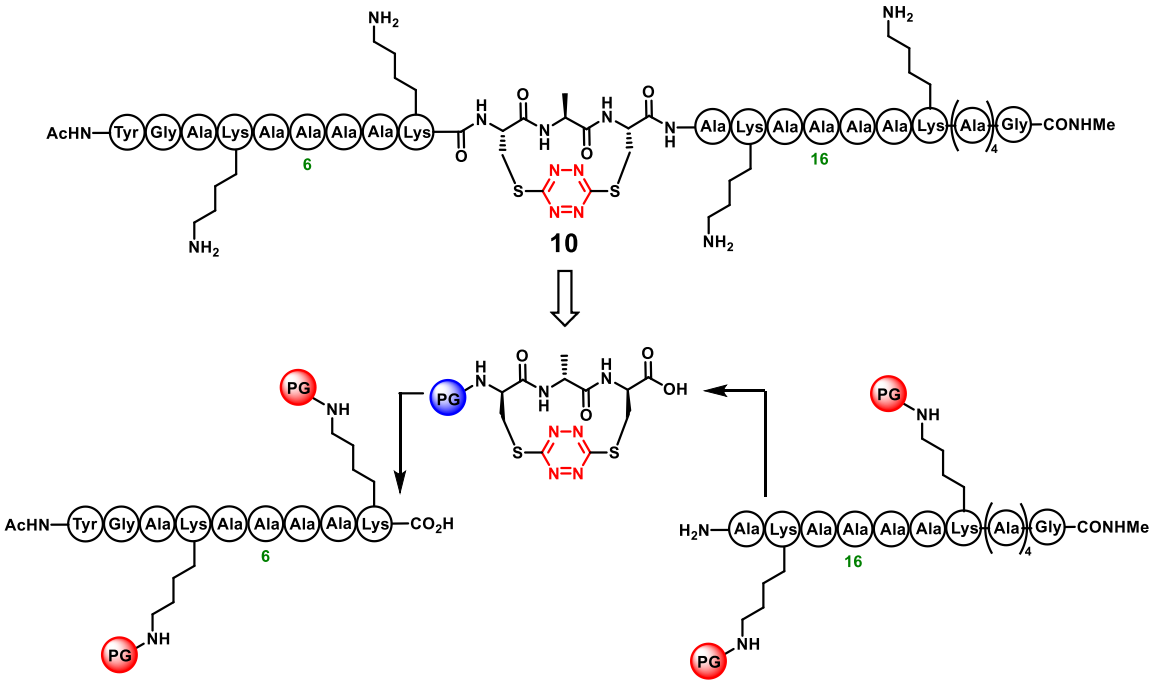

Figure 1.6. Retrosynthesis of a Kinked Helix 10 Arising From a Three-Fragment Union

Evaluation of known deprotection conditions that are orthogonal to Boc were not compatible with the *S,S*-tetrazine phototrigger. Notably, the basic conditions used to remove the Fmoc-group were found to react with the tetrazine peptides. Interesting reactivity with the tetrazine chromophore was observed upon application of reductive conditions employed to remove the Cbz-protection group in peptide **7**. Importantly, treatment with Pd/C and hydrogen gas led to the reduction of the *s*-tetrazine ring to the dihydrotetrazine congener **23**. When the colorless solution of the reduced product **23** was exposed to air, **23** underwent oxidation back to the red starting material **7** (Scheme 1.5).

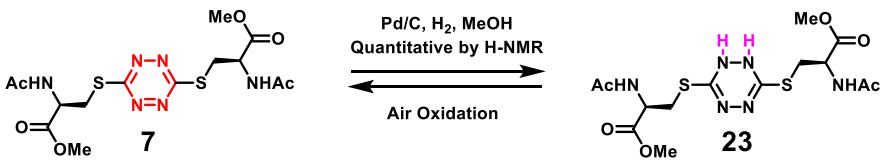

Scheme 1.5. Reduction of the s-Tetrazine Chromophore

To test the conditions for Cbz removal, model peptide **24** was prepared. Treatment of **24** under the identical conditions outlined in Scheme 1.5, reduced the *s*-tetrazine ring; but did not lead to efficient removal of the Cbz group. Forging a new strategy, Cbz is known

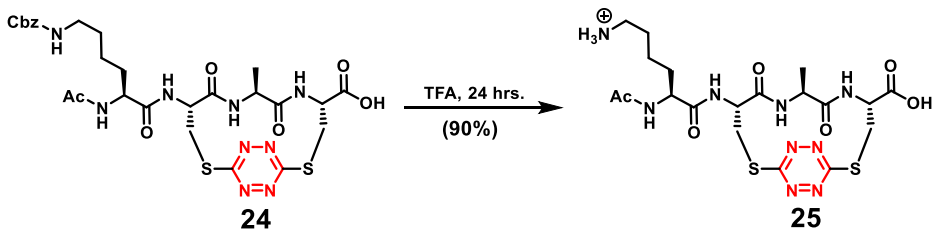

Scheme 1.6. Benzyl Carbamate Removal with Concentrated Trifluoroacetic Acid

to be mildly unstable under strongly acidic conditions. To this end, stirring **24** in a solution of neat TFA (Scheme 1.6) was found to drive off carbon dioxide over the course of 24 hours to furnish **25** with efficient removal of the Cbz group and importantly without affecting the tetrazine chromophore.

Turning next to the construction of the full-length peptide **10** containing the *s*-tetrazine ring, a solution-phase fragment union protocol was developed by post-doctoral fellow Mohannad Abdo. With the use of the Cbz protecting group validated, the synthesis of the target **10** was planned to arise via union of three fragments **26, 27** and **28** (Scheme 1.7). The appropriate linchpin **26** was prepared via Boc protection of the *N*-terminus of **11** (from Scheme 1.3). The protected *C*- and *N*-terminal peptide fragments **27** and **28** in turn were

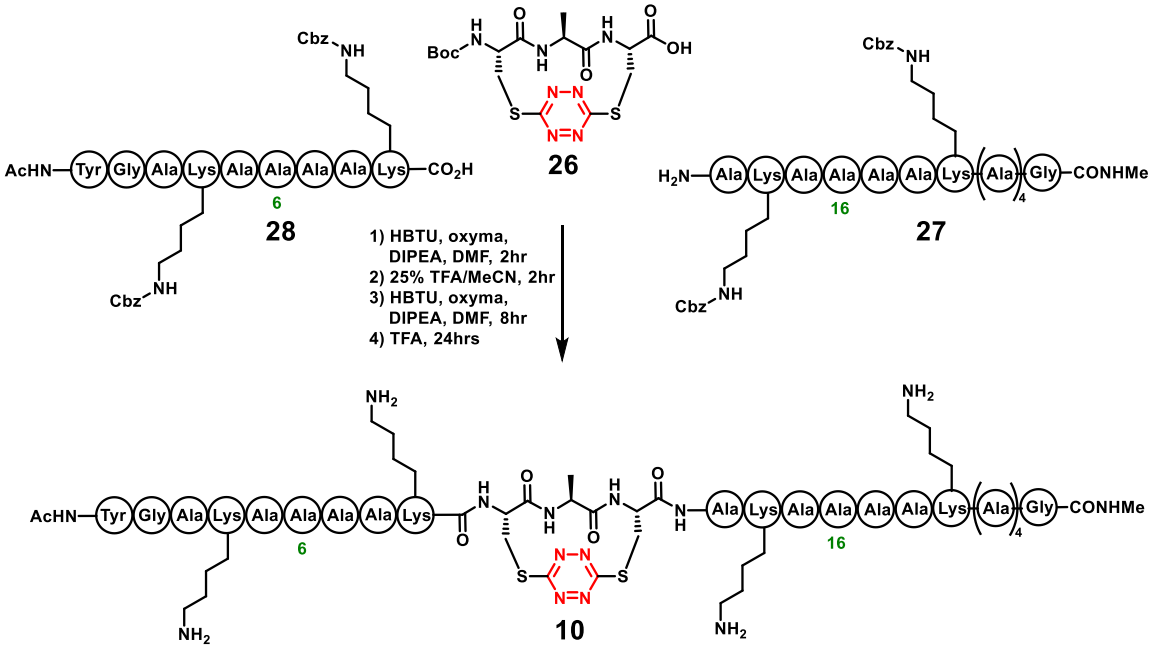

Scheme 1.7. Solution-Phase Fragment Coupling of the *s*-Tetrazine Kinked Helix 10

constructed via solid-phase peptide synthesis employing *N*-methyl indole and 2-chlorotrityl resins, respectively. After activation of linchpin **26** with the coupling agent, HBTU, the free amine of peptide **27** was coupled. Then, following purification and removal of the Boc protecting group, the resulting peptide was attached to the activated peptide fragment **28**. Global deprotection was then achieved by treatment with neat TFA to furnish target peptide **10** in an 11% yield over four steps after final HPLC purification (Scheme 1.7).

To monitor the picosecond structural transitions within specific regions of the amide backbone by 2D IR following the photochemical release of *s*-tetrazine within **10**, the amide stretching modes at specific locations along the peptide construct required differentiation by isotopic editing of the amides. Specifically, we sought to incorporate the $^{13}C{=}^{18}O$ double label at three defined positions along the peptide backbone. The solution phase

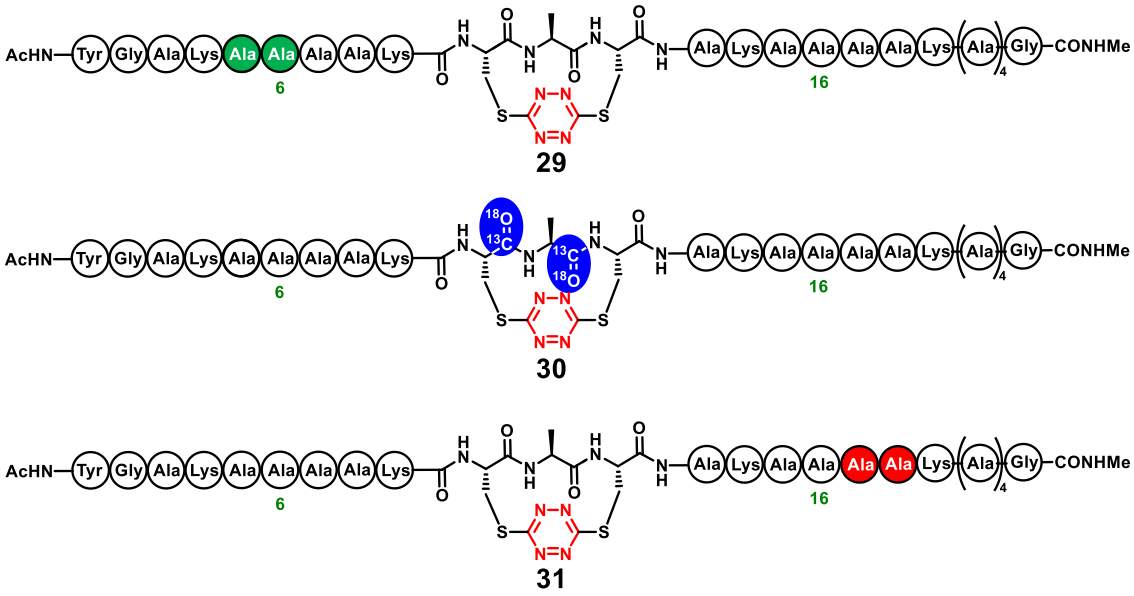

Figure 1.7. Isotopically Enriched Amides Within the Constrained Helices

fragment coupling strategy (Scheme 1.7) was used to prepare labeled peptides **29-31** (Figure 1.7). Peptide **30** would permit measurement of the kinked region while the backbone dynamics distal to the *s*-tetrazine phototrigger could be monitored through the two $^{13}C=^{18}O$-Ala units introduced within **29** or **31** specifically at amino acid locations 5-6 and 17-18, respectively.

2D IR Observation of Non-Equilibrium Folding Dynamics of a Kinked Helix

The isotopically enriched helical peptides **29-31**, constrained with the tetrazine photo-triggering cross-link, were then used to explore the ultrafast, non-equilibrium folding dynamics of the kinked helix.[32] Transient 2D IR spectroscopy was used to record structural snapshots of the bond distances and bond angles during formation of a single helical turn of the kinked helix upon photorelease of the tetrazine chromophore (Figure 1.8). The results with the isotopically labeled variant peptides **29**-**31** proved structurally distinct. When **10** is isotopically edited with $^{13}C=^{18}O$ at residues Cys10 and Ala11 (*i.e.***30**), both

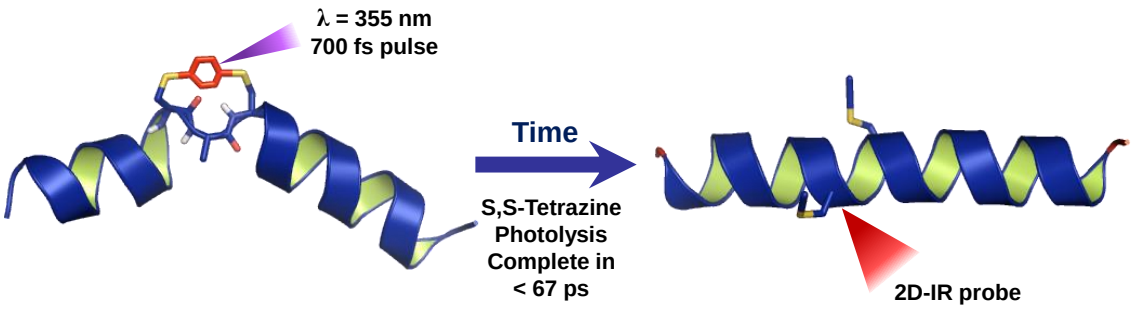

Figure 1.8. Non-Equilibrium Folding Dynamics Observed

amide backbone vibrations are isotopically down-shifted 60 cm^{-1}, which strongly reduces their coupling with those of the other carbonyls. The location, polarization, and line width

of the isotopically shifted amide I band was then used to determine structural parameters in two picosecond snapshots, recorded over a nanosecond range of delays. To examine the site-specific structural changes upon photorelease, the two labeled peptides (**29** and **31**) were also examined. The amide I modes involving **29** and **31** each with a pair of residues spatially separated by approximately one helix turn from the kink revealed equivalent diagonal 2D IR trace spectra through all optical delay times, thereby implying that these residues do not undergo any significant structural change as a result of the photolysis. On the other hand, the transient 2D IR spectrum of peptide **30** containing the labeled pair within the *s*-tetrazine distorted region, exhibits very different spectra and responses to photolysis.

Specifically, the isotopically labeled region of **30**, located around 1,600 cm^{-1}, exhibits significant photolysis-induced changes in peak position and spectral width, which are most evident from the 2D IR diagonal traces. A frequency upshift of 7.5 cm^{-1} occurs over the first 300 ps after photolysis of **30**, followed by a slight decrease to a fixed value (3 cm^{-1} up-shifted) after 500 ps. The 2D IR spectral width of the diagonal 2D IR traces of this band increases by 5 cm^{-1} from the starting constrained configuration and then decreases until about 500 ps delay, whereupon a constant value is reached. The spectral width was fit to exponential decay with a time constant of 97 ± 7 ps indicating rotation about the psi angle to recover the helical structure.

In summary, the design, synthesis and validation of peptides containing the *s*-tetrazine phototrigger in conjunction with 2D IR has permitted acquisition of the non-equilibrium

picosecond snapshots of helix relaxation. The constrained peptide **10** is believed to be located somewhere on the downhill side of the free energy barrier towards the complete helix. Upon release of the constraint, the 2D IR spectra provided a glimpse into the conformational reorganization that occurs as the peptide proceeds toward equilibrium. These experiments reveal key motions along the folding coordinate as the peptide reorganized toward the full α-helical conformation which importantly does not involve movements that push the kink along the chain toward the ends of the peptide. Moreover, the peptide also does not irreversibly unfold before proceeding toward the native helical conformation. Rather, the central region, where the small perturbation to the helical structure had been enforced by the constraint undergoes a local structural change following photorelease. The data collected during the acquisition permits the visualization of the fastest structural changes for **10**, as the peptide proceeds toward the equilibrium ensemble in response to release of the phototrigger. Although the propagation times for helices have been estimated from experiments to be on the order of tens of nanoseconds, the structural movements observed in these experiments suggest that propagation times after nucleation are on the order of hundreds of picoseconds. Moreover, the simulated equilibrium time autocorrelations of the angle between the dipoles, the distance between the two dipoles, and the dihedral angles all agree well with the observed parameters, suggesting the conformational kinetics are well described by linear response theory.[33]

References for Chapter 1

1. McCammon, J. A.; Gelin, B. R.; Karplus, M. Nature **1977**, 267, 585.
2. Henzler-Wildman, K. A.; Lei, M.; Thai, V.; Kerns, S. J.; Karplus,M.; Kern, D. Nature **2007**, 450, 913.
3. Henzler-Wildman, K.; Kern, D. Nature 2007, 450, 964.
4. Smock, R. G.; Gierasch, L. M. Science 2009, 324, 198.
5. Frauenfelder, H.; Sligar, S. G.; Wolynes, P. G. Science 1991, 254, 1598.
6. Brooks, C. L.; Gruebele, M.; Onuchic, J. N.; Wolynes, P. G. *Proc. Natl. Acad. Sci. U.S.A.* **1998**. 95, 11037.
7. Wolynes, P. G.; Eaton, W. A.; Fersht, A. R. *Proc. Natl. Acad. Sci. U.S.A.* **2012**, 109, 17770.
8. Anfinrud P, Schotte F. *Science*. **2005**. 309, 1192-1193.
9. Cho HS, Dashdorj N, Schotte F, Graber T, Henning R, Anfinrud P. *Proc Natl Acad Sci U S A*. **2010**. 107, 7281-7286.
10. Sborgi, L.; Verma, A.; Sadqi, M.; Alba, E.; Muñoz, V. *Methods Mol. Biol.* **2013**, 932, 205.
11. Serrano, A.L.; Waegele, M.M.; Gai, F. *Protein Science*. **2012**, 21, 157-170.
12. Thompson, P. A.; Eaton, W. A.; Hofrichter, J. *Biochemistry*, **1997**, 36, 9200–9210.
13. Thompson, P. A.; Muñoz, V.; Jas, G. S.; Henry, E. R.; Eaton, W. A.; Hofrichter, J. *J. Phys. Chem. B*, **2000**, 104, 378–389.
14. Brooks, C. L. *J. Phys. Chem.* **1996**, 100, 2546–2549.
15. Asplund, M. C.; Zanni, M. T.; Hochstrasser, R. M. *Proc. Natl. Acad. Sci.* **2000**, *97*, 8219.
16. Adapted with permission from the National Academy of Sciences: Hochstrasser, R. M. *Proc. Natl. Acad. Sci.*, **2007**, 104, 14190-14196. Copyright (2007) National Academy of Sciences, U.S.A.
17. Remorino, A.; Korendovych, I. V.; Wu, Y.; DeGrado, W. F.;Hochstrasser, R. M. Science **2011**, 332, 1206.
18. Remorino, A.; Hochstrasser, R. M. Acc. Chem. Res. **2012**, 45,1896.

19. H. S. M. Lu, M. Volk, Y. Kholodenko, E. Gooding, R. M.Hochstrasser,W. F. DeGrado, J. Am. Chem. Soc. **1997**, 119, 7173
20. M. Volk, Y. Kholodenko, H. S. M. Lu, E. A. Gooding, W. F.DeGrado, R. M. Hochstrasser, J. Phys. Chem. B. **1997**, 101, 8607
21. Volk, M. Eur. J. Org. Chem. **2001**, 2605.
22. King, D. S.; Denny, C. T.; Hochstrasser, R. M.; Smith, A. B., III. *J. Am. Chem. Soc.* **1977**, 99, 271-273.
23. Hochstrasser, R. M.; King, D. S.; Smith, A. B., III. *J. Am. Chem. Soc.* **1977**, 99 3923–3933.
24. Dellinger, B.; King, D. S.; Hochstrasser, R. M.; Smith, A. B., III. *J. Am. Chem. Soc.* **1977**, *99*, 3197.
25. Dellinger, B.; King, D. S.; Hochstrasser, R. M.; Smith, A. B., III. *J. Am. Chem. Soc.* **1977**, *99*, 7138.
26. M. D. Coburn, G. A. Buntain, B.W. Harris, M. A. Hiskey, K. Y. Lee, D. G. Ott, J. Heterocycl. Chem. **1991**, 28, 2049.
27. M. D. Helm, A. Plant, J. P. A. Harrity, Org. Biomol. Chem. **2006**, 4, 4278.
28. Tucker, M. J., Courter, J. R., Chen, J., Atasoylu, O., Smith, A. B. and Hochstrasser, R. M. *Angew. Chem. Int. Ed.* **2010**, 49, 3612–3616.
29. Tucker, M. J.; Abdo, M.; Courter, J. R.; Chen, J. X.; Smith, A. B., III; Hochstrasser, R. M. J. Photochem. Photobiol. A. **2012**, 234, 156–163.
30. Abdo, M.; Brown, S. P.; Courter, J. R.; Tucker, M. J.; Hochstrasser, R. M.; Smith, A. B., III. *Org. Lett.* **2012**, 14, 3518-3521.
31. Courter, J. R.; Abdo, M.; Brown, S. B.; Tucker, M. J.; Hochstrasser, R. M.; Smith, A. B., III. *J. Org. Chem.* **2014**. 79, 759-768.
32. Tucker, M. J.; Abdo, M.; Courter, J. R.; Chen, J. X.; Brown, S. P.; Smith, A. B., III; Hochstrasser, R. M. *PNAS*. **2013**, 110, 17314.
33. Ishikawa, H.; Kwak, K.; Chung, J. K.; Kim, S.; Fayer, M. D. *PNAS*. **2008**. 105, 8619-8624.

Experimental for Chapter 1

Reaction Equipment. Solid-phase syntheses were carried out in peptide synthesis reaction vessels (25 or 50 mL) with coarse porosity fritted glass support and Teflon stopcocks. Photolysis experiments were performed in a Rayonet^{TM} Srinivasan-Griffin Photoreactor (The Southern New England Ultraviolet Company) using either UV-A lamps (part # LZC-UVA) or UV-B lamps (part # LZC-UVB) purchased from Luzchem.

Chromatography. Prep-scale reverse-phase chromatography was conducted with a Gilson 215 liquid handler/injector fitted with Gilson 333/334 binary HPLC pumps and UV/vis dual wavelength detector (model 156) and Trilution software. The chromatographies were carried out on a Waters XBridge Prep BEH 130 C18 5µm OBD 19 × 100mm column (part # 186003587). The eluent was acetonitrile (HPLC grade) and Millipore water with 0.1% trifluoroacetic acid buffer unless otherwise noted and gradients specific to the compound.

Instruments Used for Spectral Data. ^{1}H NMR, ^{13}C NMR and 2D NMR spectra were recorded on a Bruker Avance III equipped with either a 5 mm dual inverse probe or 5 mm DCH CryoProbe. The analytical LC-MS analyses were conducted using a Waters 2767 sample manager, consisting of a Waters 2525 binary gradient HPLC connected to a diode array detector and a Waters Micromass ZQ mass spectrometer with electro-spray ionization. The LC-MS samples were analyzed as solutions in water or acetonitrile, prepared at 0.15 – 0.20 mg/mL concentration. The LC-MS chromatography was carried out on an Atlantis–C18 column (4.6 ×50 mm; 5 µm) with linear gradients of 0.05% formic acid in acetonitrile and 0.05% formic acid water. High resolution mass spectrometry was obtained

on Waters LC-TOF mass spectrometer (model LCT-XE Premier) using electrospray ionization in positive or negative mode, depending upon the analyte. MALDI-MS spectra were collected with a Bruker Ultraflex III TOF/TOF matrix-assisted laser desorption/ionization mass spectrometer. All FTIR spectra were taken on a Nicolet 6700 FTIR spectrometer or PerkinElmer FTIR (model Spectrum BX).

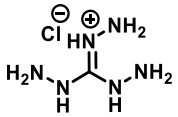

1

Triaminoguanidine hydrochloride (1). A 250 mL round bottom flask was charged with guanidine hydrochloride (14.70 g, 153.9 mmol) and suspended in 1,4-dioxane (80 mL). With magnetic stirring, hydrazine hydrate (25.2 mL, 508 mmol, 3.3 equiv) was added, after one minute, the solid had dissolved and the solution was refluxed for 2.0 hours during which time a white, solid precipitated. The contents were cooled to ambient temperature, vacuum filtered, and the solid washed with 1,4-dioxane (2 × 50 mL). The solid was dried *in vacuo* for 16 hours to yield 20.76 g (96%) of triaminoguanidine hydrochloride, as a crystalline white solid. ^{13}C NMR (126MHz, D_2O) δ = 159.7.

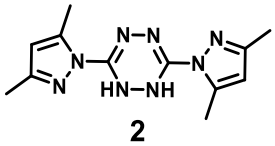

2

A 1L, three necked flask was set-up with a reflux column and mechanical stirred. To the flask was added triaminoguanidine hydrochloride (14.06 g, 100.0 mmol) and dissolved in water (150 mL). Next, with mechanical stirring, acetylacetone (20.0 g, 200 mmol, 2 equiv)

was added dropwise from an additional funnel at a rate such that the exothermic reaction did not rise above ca.40 ^{o}C. After complete addition of the reagent, the solution was stirred at ambient temperature for 15 minutes and then heated to 80 ^{o}C for 3.5 hours during which time a light yellow solid formed and the solution turned dark orange. The contents were diluted with water (100 mL) then cooled to ca. 5 ^{o}C, the solid was collected by vacuum filtration and washed with ice water (3 × 100 mL) until the orange color was removed. The material was dried *in vacuo* for 16 hours to yield 10.00 g (74%) of *bis*-dimethylpyrrazolyldihydrotetrazine as faint yellow, amorphous powder. ^{1}H NMR (500MHz, $CDCl_3$) δ = 8.07 (s, 2 H), 5.96 (s, 2H), 2.48 (s, 6 H), 2.21 (s, 6 H). ^{13}C NMR (126MHz, $CDCl_3$) δ = 150.1, 145.9, 142.4, 110.0, 13.9, 13.6.

3

A 125 mL Erlenmeyer flask was charged with *bis*-dimethylpyrrazolyldihydrotetrazine (10.00 g, 36.7 mmol) and dissolved in $CHCl_3$ (75 mL) then cooled to 0^{o}C in an ice bath. Next, NO_2 gas was generated by dissolving, in portions, copper wire (4.66 g, 73.4 mmol, 2 equiv) in concentrated nitric acid (50 mL) contained in a separate Erlenmeyer flask. The red gas that evolved was pushed with nitrogen gas, through glass tubing and bubbled through the chloroform solution which turned dark red upon addition, the reaction was continued until the solution became saturated with NO_2 evident by the red gas evolving from the chloroform solution (ca. 3 min). The solution was transferred to a separatory funnel washed with saturated $NaHCO_3$ (3 × 25 mL) followed by brine (2 × 25 mL) and dried

over $MgSO_4$. The filtrate was stripped under reduced pressure to yield 9.72 g (98%) of *bis*-dimethylpyrrazolyltetrazine a red, amorphous powder. ^1H NMR (500MHz, $CDCl_3$) δ = 6.16 (s, 2 H), 2.68 (s, 6 H), 2.36 (s, 6 H). ^{13}C NMR (126MHz, $CDCl_3$) δ = 159.4, 154.5, 143.8, 112.0, 14.7, 13.9.

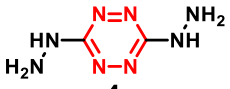

4

CAUTION: The dihydrazinyltetrazine product was found to undergo exothermic decomposition above 120 ºC when analyzed by DSC-TGA under air and ramping the temperature at 5º/minute. No decomposition was observed when dihydrazinyltetrazine was held at 80ºC under air for 60 minutes. As a precaution an inert atmosphere is highly recommended to prevent any oxidation during the course of the reaction.

Dihydrazinyltetrazine (4). A 250 mL, two-necked flask was charged with *bis*-dimethylpyrrazolyltetrazine (9.72 g, 36.0 mmol) and suspended in acetonitrile (75 mL), a reflux condenser was attached and the contents placed under a nitrogen atmosphere. Next, hydrazine hydrate (3.57 mL, 72.0 mmol, 2.05 equiv) was added neat with magnetic stirring. The flask was placed in an oil bath, pre-heated to 70 ºC for 75 minutes, a red precipitate formed and the reaction solution became faint red (almost colorless). The contents were cooled in an ice bath and the red solid collected by vacuum filtration and dried under vacuum for 15 min to yield 3.02 g (59%) of dihydrazinyltetrazine as a red amorphous powder. The product was carried immediately to the next step.

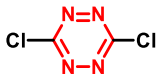

5

Dichlorotetrazine (5). A 100 mL round bottom flask, was charged with dihydrazinyltetrazine (2.95 g, 20.8 mmol) and suspended in acetonitrile (40 mL) then cooled in an ice bath. Trichloroisocynanuric acid (9.89 g, 42.6 mmol, 2.05 equiv) was dissolved in acetonitrile (30 mL) and added dropwise over 15 minutes. The ice bath was removed and the contents stirred at room temperature for 1.0 hour, the color of the solution changed from red to orange. The reaction was vacuum filtered, the white solid was rinsed with acetonitrile (2 × 5 mL) and the filtrate was collected and evaporated (70 torr, bath temperature 22°C) to give a red-orange solid. The crude material was dissolved in CH_2Cl_2 (15 mL) and filtered through a pad of celite (3.5 cm diameter × 8 cm length), the column was eluted with dichloromethane until the solution eluent ran colorless. The solvent was stripped under reduced pressure (100 torr, bath temperature 22°C) to yield 3.10 g (99%) of dichlorotetrazine as a waxy, orange solid. ^{13}C NMR (126MHz, $CDCl_3$) δ = 168.3.

The material can be further purified by sublimation; heating the product in a subliminator at 70°C under a nitrogen atmosphere.

Procedures for Manual Solid-Phase Peptide Synthesis

Resin Washing Procedures. Resin washing was conducted with the indicated solvent and was allowed to contact the resin for 30 seconds during each wash. The solvent was pushed through the frit using an "air push" apparatus made from a 15 mL disposable syringe and a 14/20 septum, or nitrogen gas was used in cases when an inert atmosphere is a requirement.

General Procedures for the Resin Loading

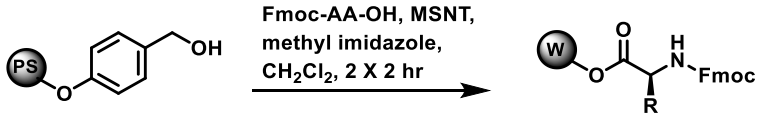

Wang Resin Amino Acid Loading. Wang resin (0.22 mmol) was placed in a peptide synthesis vessel and the resin was swelled in CH_2Cl_2 (10 mL) for 1.0 hour. The solvent was drained and a pre-mixed solution consisting of Fmoc-AA-OH (0.88 mmol, 4 equiv), MSNT (0.88 mmol, 4 equiv) and methyl imidazole (0.66 mmol, 3 equiv) dissolved in CH_2Cl_2 (5 mL) was added to the resin. The contents were gently rocked for 2.0 hours, then drained and the resin washed with CH_2Cl_2 (3 × 5 mL). The procedure was repeated and the resin carried on to the next step.

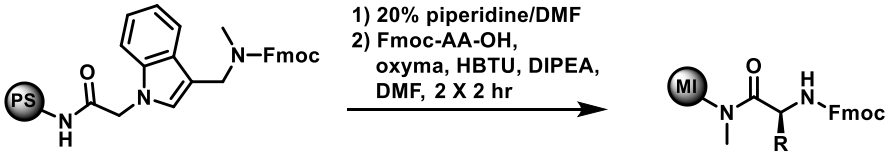

***N*-Methyl Indole AM Resin Amino Acid Loading.** *N*-Methyl indole resin (0.22 mmol) was placed in a peptide synthesis vessel and the resin was swelled in CH_2Cl_2 (10 mL) for

1.0 hour. The solvent was drained and the resin was washed with DMF (3 × 6 mL) then treated with 20% piperidine/DMF (2 × 6 mL) allowing the solution to contact the resin for 10 minutes. The resin was washed with DMF (3 × 5 mL), then a pre-mixed solution consisting of Fmoc-AA-OH (1.1 mmol, 5 equiv), HBTU (1.1 mmol, 5 equiv), oxyma (1.1 mmol, 5 equiv) and DIPEA (2.2 mmol, 10 equiv) dissolved in DMF (5 mL) was added to the resin. The contents were rocked gently for 1.0 hour, then drained and the resin washed with DMF (3 × 5 mL). The coupling procedure was repeated and the resin carried on to the next step.

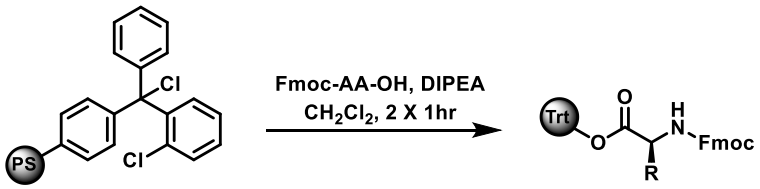

2-Chlorotrityl Chloride Resin Amino Acid Loading. 2-Chlorotrityl chloride resin (0.40 mmol) was placed in a peptide synthesis vessel and the resin was swelled in CH_2Cl_2 (10 mL) for 1 h. The solvent was drained and the resin was then treated with a pre-mixed solution of Fmoc-AA-OH (0.48 mmol, 1.2 equiv), and DIPEA (1.6 mmol, 4 equiv) dissolved in CH_2Cl_2 (5 mL) was added to the resin. The contents were rocked gently for 1 h, then drained and the resin washed with DMF (3 × 5 mL). The coupling procedure was repeated and the resin carried on to the next step.

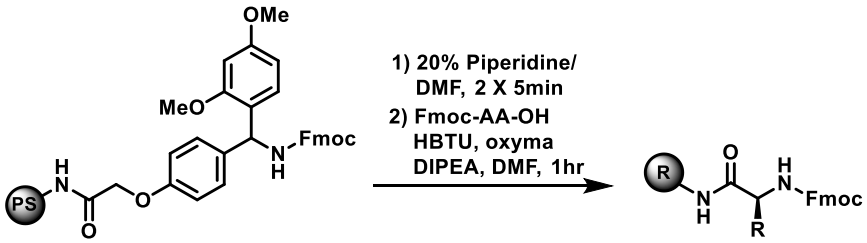

Rink Resin Amino Acid Loading. Rink Novagel resin (0.10 mmol) was placed in a peptide synthesis vessel and the resin was swelled in CH_2Cl_2 (10 mL) for 1 h. The solvent was drained and the resin was washed with DMF (3 × 6 mL) then treated with 20% piperidine/DMF (2 × 6 mL) allowing the solution to contact the resin for 10 minutes. The resin was washed with DMF (5 × 6 mL) and a pre-mixed solution of Fmoc-protected amino acid (0.50 mmol, 5 equiv), HBTU (190 mg, 0.5 mmol, 5 equiv), oxyma (71 mg, 0.5 mmol, 5 equiv) and DIPEA (174 µL, 1.0 mmol, 10 equiv) dissolved in DMF (4 mL) was added to the resin. The contents were rocked gently for 1 h, then drained and the resin washed with DMF (3 × 6 mL).

General Procedure for Manual Solid-Phase Peptide Synthesis

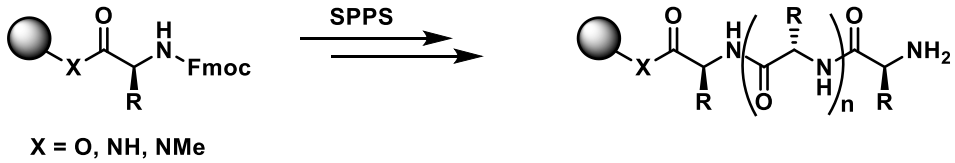

Solid-Phase Peptide Synthesis (SPPS). The resin-bound Fmoc-amino acid (0.1 mmol) was washed with DMF (3 × 5 mL) and then treated with a solution of 20% piperidine/DMF (2 × 6 mL) allowing each treatment to contact the resin for 5 minutes. The resin was washed with DMF (5 × 6 mL), then a pre-mixed solution of Fmoc-protected amino acid (0.5 mmol, 5.0 equiv), HBTU (190 mg, 0.5 mmol, 5.0 equiv), oxyma (71 mg, 0.5 mmol, 5.0 equiv)

and DIPEA (174 μL, 1.0 mmol, 10.0 equiv) dissolved in DMF (4 mL) was added to the resin. The contents were rocked gently for 1 h, then drained and the resin washed with DMF (3 × 5 mL). The Fmoc deprotection procedure was repeated followed by the coupling of the next amino acid in the sequence to synthesize the desired peptide.

General Procedure for Peptide Cleavage and Global Deprotection

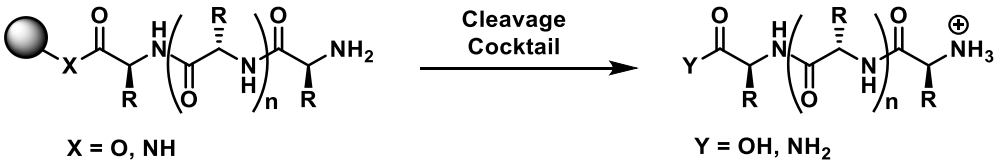

Cleavage Cocktail A: TFA/EDT/TIPSH/water (92.5: 2.5: 2.5: 2.5) Peptides with Cys

Cleavage Cocktail B: TFA/thioanisole/EDT/water (87.5: 5: 5: 2.5) Peptides with Cys & Trp, Arg

Cleavage Cocktail C: TFA/thioanisole/EDT/TIPSH/water (87.5:5:2.5:2.5:2.5) Peptides with Cys & Met

The resin-bound peptide (~0.1 mmol) was pre-swelled in CH_2Cl_2 for 30 minutes and then treated with cleavage cocktail A, B or C (7 mL) and stirred under a nitrogen atmosphere for 4 hours. The filtrate was collected and additional cleavage cocktail (3 × 1 mL) was used to wash the resin. The pooled filtrates were condensed (ca. 1 mL) and Et_2O (15 mL) was added to precipitate the peptide. The white precipitate was collected by vacuum filtration and the solids wash with additional Et_2O. The crude peptide was dried *in vacuo* overnight and purified by reverse-phase high-pressure liquid chromatography (HPLC).

Preparation of ^{13}C Enriched Cysteine Amino Acids for SPPS

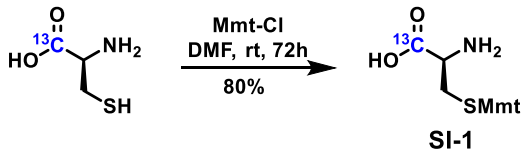

SI-1

A 25 mL round bottom flask was charged with labeled L-cysteine-1-^{13}C (0.52g, 4.3 mmol) and monomethoxytrityl chloride (1.98g, 6.4 mmol, 1.5 equiv) then suspended in DMF (6 mL) and stirred for 72 hours. The product was precipitated out of solution by addition of aqueous NaOAc (1.2M, 25 mL) and the solid collected by vacuum filtration. The crude product was recrystallized from acetone (20 mL, heated to 50°C for 30 minutes) concentrated to half the volume and cooled in an ice bath to yield 1.36g (80%) of **SI-1** as a white solid: ^1H NMR (500 MHz, DMSO-d_6) δ 7.34-7.19 (m, 12H), 6.89 (d, J = 9.0, Hz, 2H), 3.74 (s, 3H), 2.98 (dt, J = 9.0, 4.5 Hz, 1H), 2.60 (ddd, J = 12.5, 4.0, 3.0 Hz, 1H), 2.43 (ddd, J = 12.0, 9.0, 2.0 Hz, 1H); ^{13}C NMR (125 MHz, DMSO-d_6) δ 169.1, 158.3, 145.3, 136.7, 131.0, 129.6, 128.6, 127.3, 113.9, 66.2, 55.8, 54.0 (d, J = 50 Hz), 34.2; HRMS (ES) *m/z* 417.1319 [$(M+Na)^+$; calcd for $C_{22}{}^{13}CH_{23}NO_3NaS$: 417.1330].

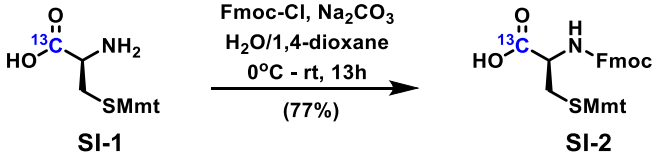

SI-1 **SI-2**

The *S*-protected cysteine-1-^{13}C (1.35g, 3.4 mmol) was transferred to a 100 mL round bottom flask and dissolved in water (35 mL) and 1,4-dioxane (10 mL). The solution was cooled to 0°C and solid sodium carbonate (0.91g, 8.5 mmol, 2.5 equiv) was added followed by the dropwise addition of Fmoc-Cl dissolved in 1,4-dioxane (20 mL) over 5 minutes.

The reaction was stirred for 3 hours at 0°C and then 10 hours at ambient temperature. The solvent was concentrated and an aqueous solution of 5% $KHSO_4$ was added until the mixture reached pH 2. The contents were then extracted with EtOAc (4 × 25 mL) and the pooled organics were dried over Na_2SO_4, then stripped to give a brown oil which solidified into a white solid upon standing overnight. The crude material was purified by silica-gel chromatography using an isocratic 5% MeOH/CH_2Cl_2 eluent to yield 0.81g (77%) of **SI-2** as white foam: ^{1}H NMR (500 MHz, $CDCl_3$) δ 7.77 (t, *J* = 6.5, 2H), 7.61 (t, *J* = 6.5, 2H), 7.42-7.40 (m, 6H), 7.32-7.26 (m, 8H), 7.22-7.19 (m, 2H), 6.80 (d, *J* = 9.0 Hz, 2H), 5.20 (d, *J* = 8.0 Hz, 1H), 4.45-4.37 (m, 2H), 4.33-4.28 (m, 1H), 4.24 (t, *J* = 7.0 Hz, 1H), 3.76 (s, 3H), 2.75 (bs, 2H); ^{13}C NMR (125 MHz, $CDCl_3$) δ 174.9, 158.4, 156.0, 144.6, 141.4, 136.4, 130.9, 129.5, 128.2, 127.9, 127.3, 127.0, 125.2, 120.1, 113.5, 67.4, 67.0, 55.4, 53.0 (d, *J* = 58 Hz), 47.2, 33.7; HRMS (ES) *m/z* 639.2003 [(M+Na)$^+$; calcd for $C_{37}{}^{13}CH_{33}NO_5NaS$: 639.2001].

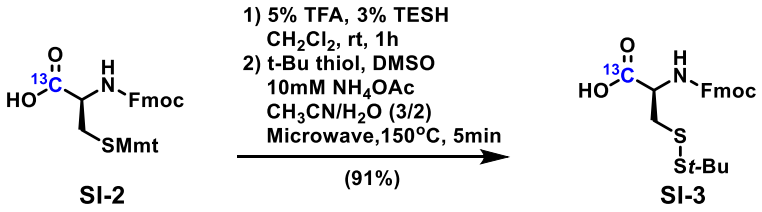

SI-2 SI-3

SI-3: Fmoc-Cysteine(S*t*-Bu)-OH (1-^{13}C). A 50 mL round bottom flask was charged with Fmoc-Cysteine(Mmt)-OH (1-^{13}C) (0.60g, 0.98 mmol) in 95:5:3 CH_2Cl_2/TFA/TES solution (20 mL). The mixture was stirred at room temperature for 1h under a nitrogen atmosphere. The solvent was evaporated under reduced pressure, and the crude residue was washed three times with toluene and after each washing it was evaporated to dryness. The solid

residue was transferred to a sintered funnel and washed twice with pentane. The remaining residue was transferred to a microwave vial (2-5 mL) then dissolved in 2.5 mL of buffer containing 10 mM NH_4OAc in acetonitrile/water (3:2). 2-Methyl-2-propanethiol (1.1 mL, 9.8 mmol) and 0.75 mL DMSO were added, and the reaction mixture was irradiated for 5 min at 150°C. After TLC had indicated complete consumption of the starting material, the reaction mixture was concentrated and extracted with brine and CH_2Cl_2. The organic layer was dried over Na_2SO_4, filtered, and concentrated *in vacuo*. The crude material was purified by silca-gel chromatography using an isocratic 3% MeOH/CH_2Cl_2 eluent to yield 0.38 g (91%) of **SI-3** as white foam: ^{1}H NMR (500 MHz, $CDCl_3$) δ 7.76 (d, *J* = 8.0 Hz, 2H), 7.62 (d, *J* = 7.5 Hz, 2H), 7.40 (t, *J* = 7.5 Hz, 2H), 7.32 (t, *J* = 7.5 Hz, 2H), 5.71 (d, *J* = 7.5 Hz, 1H), 4.73-4.68 (m, 1H), 4.44-4.36 (m, 2H), 4.26 (t, *J* = 7.5 Hz, 1H), 3.28 (dt, *J* = 13.5, 4.5 Hz, 1H), 3.19 (dd, *J* = 13.5, 5.5 Hz, 1H), 1.33 (s, 9H); ^{13}C NMR (125 MHz, $CDCl_3$) δ 175.0, 156.0, 143.8, 141.3, 127.8, 127.2, 125.3, 120.1, 67.5, 53.8 (d, *J* = 60 Hz), 48.4, 47.1, 42.1, 29.9; HRMS (ES) *m/z* 433.1347 [$(M+H)^+$; calcd for $C_{21}{}^{13}CH_{26}NO_4S_2$: 433.1337].

General Procedures for the Preparation of ^{18}O Enriched Amino Acids

The ^{18}O enrichment of ^{13}C enriched Fmoc-Ala-OH and Fmoc-Cys(S*t*-Bu) A 25 mL tear drop flask equipped with a stirring bar was charged with ~ 500 mg of ^{13}C isotopically enriched amino acid. The amino acid was dissolved in 3 mL of a hot 1:1 dioxane and 97% ^{18}O enriched water which was 0.25M in HCl. The solution was stirred under reflux and under nitrogen for 12 h before it was concentrated *in vacuo*. LC-MS analysis was conducted to determine the isotopic enrichment of the amino acid residues and the procedure was repeated if necessary to obtain an ^{18}O enrichment level of 95% or higher.

General Procedure for Introduction of Dichlorotetrazine to Resin-Bound Peptide

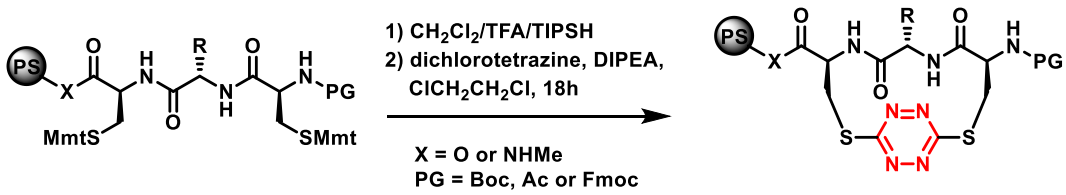

The resin-bound peptide (0.22 mmol) was swelled in CH_2Cl_2 (10 mL) for 1.0 hour. The peptide synthesis vessel was set-up under an inert atmosphere by connecting it to a two-neck round bottom flask fitted with a septum, such that the resin was kept under a blanket of nitrogen and could also be bubbled through the bottom of the frit to agitate the resin. The solvent was drained and a pre-mixed solution of CH_2Cl_2/TIPSH/TFA [(92.5:5.0:2.5 for loaded Wang resin, 6 mL)/ (95:4:1 for loaded *N*-methyl indole AM resin, 6 mL)] was added to the resin and the orange solution agitated for 3 minutes, the contents were drained and the resin washed with CH_2Cl_2 (10 mL). The procedure was repeated 4 additional times until the reaction solution went clear suggesting the monomethoxytrityl groups had been completely removed. The resin was washed with 10% DIPEA/$ClCH_2CH_2Cl$ (3 × 5 mL). To the resin was added a solution of dichlorotetrazine (0.24 mmol, 1.1 equiv) in $ClCH_2CH_2Cl$ (5 mL) followed by the addition of DIPEA (0.5 mL) neat. The peptide vessel was wrapped in foil to exclude ambient light and the contents were gently rocked for 18 hours. The filtrate was drained and the resin washed with CH_2Cl_2 (3 × 5 mL), MeOH (3 × 5 mL) and CH_2Cl_2 (3 × 5 mL).

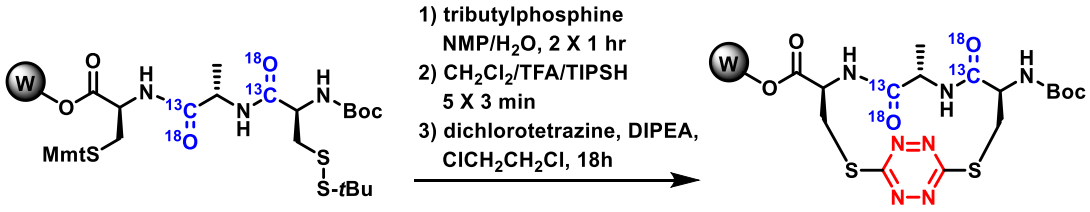

Modified *S,S*-Tetrazine Tethering Protocol for Synthesis of 22. The resin-bound peptide **6** (0.22 mmol) was swelled in CH_2Cl_2 (10 mL) for 1.0 hour. The peptide synthesis vessel was set-up under an inert atmosphere such that the resin was kept under a blanket of nitrogen and could also be bubbled through the bottom of the frit to agitate the resin. The solvent was drained and a pre-mixed solution of tributylphosphine (2.23 g, 11.0 mmol) in NMP/H_2O (9:1, 6 mL) was added to the resin and the solution agitated for 1 h, the contents were drained and the resin washed with CH_2Cl_2 (10 mL) and the procedure was repeated one additional time. Afterwards, a pre-mixed solution of CH_2Cl_2/TIPSH/TFA (92.5:5.0:2.5, 6 mL) was added to the resin and the orange solution agitated for 3 minutes, the contents were drained and the resin washed with CH_2Cl_2 (10 mL). The procedure was repeated 4 additional times until the reaction solution went clear suggesting the monomethoxytrityl groups had been completely removed. The resin was washed with 10% DIPEA/$ClCH_2CH_2Cl$ (3 × 5 mL). To the resin was added a solution of dichlorotetrazine (0.24 mmol, 1.1 equiv) in $ClCH_2CH_2Cl$ (5 mL) followed by the addition of DIPEA (0.5 mL) neat. The peptide vessel was wrapped in foil to exclude ambient light and the contents were gently rocked for 18 hours. The filtrate was drained and the resin washed with CH_2Cl_2 (3 × 5 mL), MeOH (3 × 5 mL) and CH_2Cl_2 (3 × 5 mL).

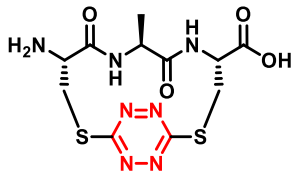

11

Compound 11 was purified by reverse-phase chromatography (gradient 5 – 30% organic over 10 minutes) to give 24.6 mg (30.0%) of **11** as an orange amorphous powder after lyophilization. HRMS (ES) *m/z* 374.0699 [$(M+H)^+$; calcd for $C_{11}H_{16}N_7O_4S_2$: 374.0705]; IR (ATR) 1644 (s), 1531 (m), 1410 (m), 1245 (s), 1202 (m), 1144 (m); ^{1}H NMR (500 MHz, DMSO-d_6) δ 8.78 (d, *J* = 8.5 Hz, 1H), 8.66 (d, *J* = 6.5 Hz, 1H), 8.26 (brs, 3H), 4.80 (ddd, *J* = 6.5, 4.5, 2.0 Hz, 1H), 4.73 (dd, *J* = 16.0, 3.0 Hz, 1H), 4.54 (dd, *J* = 15.0, 4.5 Hz, 1H), 4.32 (t, *J* = 3.0 Hz, 1H), 4.21 (dq, *J* = 8.5, 7.0 Hz, 1H), 3.55 (dd, *J* = 15.0, 2.0 Hz, 1H), 3.50 (dd, *J* = 16.0, 3.0 Hz, 1H), 1.03 (d, *J* = 7.0 Hz, 3H); ^{13}C NMR (125 MHz, DMSO-d_6) δ 171.2, 170.8, 170.7, 169.5, 164.7, 51.7, 51.1, 47.6, 30.4, 30.0, 19.7.

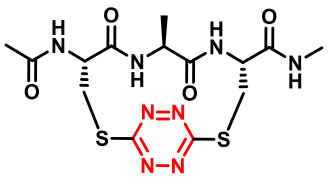

12

Compound 12 was purified by reverse-phase chromatography (gradient 10 – 80% organic over 12 minutes) to give 14.7 mg (15.6%) of **12** as an orange amorphous powder after lyophilization. HRMS (ES) *m/z* 429.1145 [$(M+H)^+$; calcd for $C_{14}H_{21}N_8O_4S_2$: 429.1127]; IR (ATR) 1647 (m), 1542 (w), 1410 (w), 1377 (w), 1067 (s); ^{1}H NMR (500 MHz, DMSO-d_6) δ 8.50 (d, *J* = 7.5 Hz, 1H), 8.47 (d, *J* = 9.0 Hz, 1H), 8.03 (d, *J* = 7.5 Hz, 1H), 7.99 (q, *J* = 4.5 Hz, 1H), 4.77 (dt, *J* = 7.0, 3.5 Hz, 1H), 4.66 (ddd, *J* = 6.5, 4.5, 2.0 Hz, 1H), 4.48 (dd,

J = 15.0, 4.5 Hz, 1H), 4.41 (dd, *J* = 15.0, 2.5 Hz, 1H), 4.16 (dq, *J* = 8.5, 7.0 Hz, 1H), 3.44 (overlapping dd, *J* = 14.5, 2.0 Hz, 1H), 3.32 (dd, *J* = 15.0, 3.5 Hz, 1H), 2.63 (d, *J* = 4.5 Hz, 3H), 1.89 (s, 3H), 1.03 (d, *J* = 7.0 Hz, 3H); ^{13}C NMR (125 MHz, DMSO-d_6) δ 171.6, 171.0, 170.5, 169.2, 168.9, 167.3, 51.4, 50.9, 47.4, 32.9, 30.2, 26.0, 22.5, 19.8.

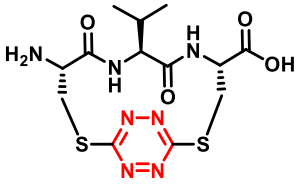

14

Compound 14 was purified by reverse-phase chromatography (gradient 5 – 30% organic over 9 minutes) to give 16.2 mg (18.4%) of **14** as an orange amorphous powder after lyophilization: HRMS (ES) *m/z* 402.1011 [$(M+H)^+$; calcd for $C_{13}H_{20}N_7O_4S_2$: 402.1018]; IR (ATR) 3292 (w, br), 2974 (w), 1644 (s), 1537 (m), 1411 (m), 1391 (m), 1242 (m), 1203 (w), 1144 (w), 1052 (w), 893 (w) cm^{-1}; ^{1}H NMR (500 MHz, D_2O) δ 4.69 (dd, *J* = 15.1, 4.7 Hz, 1H), 4.53 (dd, *J* = 4.0, 2.6 Hz, 1H), 3.87 (d, *J* = 8.8 Hz, 1H), 3.61 (dd, *J* = 16.3, 4.3 Hz, 1H), 3.60 (dd, *J* = 14.9, 2.2 Hz, 1H), 1.86-1.79 (m, 1H), 0.82 (d, *J* = 6.6 Hz, 6H); ^{13}C NMR (125 MHz, D_2O) δ 174.2, 172.3, 171.6, 169.3, 166.4, 59.1, 51.2, 31.7, 30.8, 30.6, 18.1, 18.0.

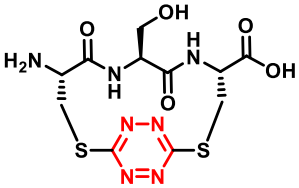

15

Compound 15 was purified by reverse-phase chromatography (gradient 5 – 30% organic over 9 minutes) to give 14.5 mg (16.9%) of **15** as an orange amorphous powder after lyophilization: HRMS (ES) *m/z* 390.0656 [$(M+H)^+$; calcd for $C_{11}H_{16}N_7O_5S_2$: 390.0654]; IR (ATR) 3309 (m, br), 1651 (s), 1646 (s), 1635 (s), 1558 (s), 1540 (s), 1418 (m), 1249 (s), 1202 (w), 1138 (w), 1058 (w), 894 (w) cm^{-1}; ^1H NMR (500 MHz, D_2O) δ 4.66 (overlapping dd, *J* = 14.9, 4.5 Hz, 1H), 4.65 (overlapping m, 1H), 4.54 (t, *J* = 3.1 Hz, 1H), 4.30 (t, *J* = 6.6 Hz, 1H), 3.68 (dd, *J* = 11.5, 6.2 Hz, 1H), 3.61 (dd, *J* = 16.2, 3.8 Hz, 1H), 3.58 (d, *J* = 11.6, 1H), 3.56 (dd, *J* = 11.6, 7.0 Hz, 1H); ^{13}C NMR (125 MHz, D_2O) δ 174.39, 172.43, 169.57, 169.35, 166.56, 61.79, 54.59, 53.91, 51.45, 30.90, 30.04.

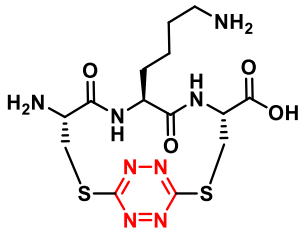

16

Compound 16 was purified by reverse-phase chromatography (gradient 5 – 30% organic over 9 minutes) to give 14.4 mg (15.7%) of **16** as an orange amorphous powder after lyophilization: HRMS (ES) *m/z* 431.1306 [$(M+H)^+$; calcd for $C_{14}H_{23}N_8O_4S_2$: 431.1284]; IR (ATR) 3262 (w, br) 3083 (w, br), 1670 (s), 1642 (s), 1540 (m), 1418 (w), 1395 (w), 1245 (m), 1197 (s), 1138 (s), 894 (w) cm^{-1}; ^1H NMR (500 MHz, D_2O) δ 4.87 (d, *J* = 4.0, 1.5 Hz, 1H), 4.76 (overlapping, 1H), 4.68 (dd, *J* = 15.2, 4.8, 1H), 4.50 (t, *J* = 3.2 Hz, 1H), 4.16 (t, *J* = 7.5 Hz, 1H), 3.63 (dd, *J* = 15.1, 1.6 Hz, 1H), 3.61 (dd, *J* = 16.2, 4.0 Hz, 1H), 2.91 (t, *J* = 7.5 Hz, 2H), 1.71-1.58 (m, 2H), 1.54-1.36 (m, 2H), 1.28-1.18 (m, 2H); ^{13}C NMR (125

MHz, D_2O) δ 173.1, 172.3, 171.8, 169.7, 166.2, 53.0, 52.7, 51.4, 39.2, 32.4, 30.5, 30.4, 26.3, 21.8.

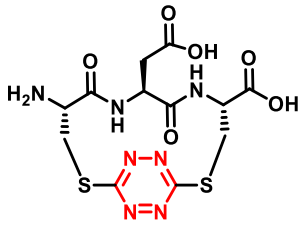

17

Compound 17 was purified by reverse-phase chromatography (gradient 5 – 30% organic over 9 minutes) to give 14.4 mg (15.7%) of **17** as an orange amorphous powder after lyophilization: HRMS (ES) *m/z* 418.0602 [$(M+H)^+$; calcd for $C_{12}H_{16}N_7O_6S_2$: 418.0604]; IR (ATR) 3300 (w, br), 1654 (s), 1556 (m), 1541 (m), 1404 (m), 1242 (s), 1200 (m), 1143 (w), 1053 (w), 894 (w) cm^{-1}; ^1H NMR (500 MHz, D_2O) δ 4.74 (dd, *J* = 15.9, 2.4 Hz, 1H), 4.68 (dd, *J* = 14.7, 4.3 Hz, 1H), 4.65 (dd, *J* = 4.3, 1.2 Hz, 1H) 4.60 (dd, *J* = 9.0, 5.3 Hz, 1H), 4.46 (dd, *J* = 3.8, 2.7 Hz, 1H), 3.59 (dd, *J* = 16.2, 4.2 Hz, 1H), 3.57 (dd, *J* = 14.6, 1.4 Hz, 1H), 2.74 (dd, *J* = 16.0, 5.4 Hz, 1H), 2.59 (dd, *J* = 16.0, 9.1 Hz, 1H); ^{13}C NMR (125 MHz, D_2O) δ 175.83, 175.55, 173.88, 172.09, 170.91, 167.80, 55.65, 52.61, 51.55, 39.43, 32.22, 31.74.

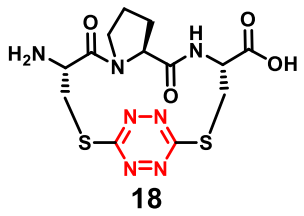

18

Compound 18 was purified by reverse-phase chromatography (gradient 5 – 30% organic over 9 minutes) to give 21.4 mg (24.3%) of **18** as an orange amorphous powder after lyophilization: HRMS (ES) *m/z* 400.0857 [$(M+H)^+$; calcd for $C_{13}H_{18}N_7O_4S_2$: 400.0862]; IR (ATR) 1652 (s), 1506 (m), 1241 (s), 1195 (m), 1134 (m), 1055 (w), 896 (w) cm^{-1}; ^1H NMR (500 MHz, D_2O) δ 4.67 (dd, *J* = 4.0, 2.5 Hz, 1H), 4.48 (d, *J* = 16.0 Hz, 1H), 4.40 (br t, *J* =5.0, 1H), 3.79 (dd, *J* = 10.0, 3.0 Hz, 1H), 3.77 (dd, *J* = 9.0, 2.5 Hz, 1H) 3.68 (m, 2H), 3.62 (dd, *J* = 15.5, 5.5 Hz, 1 H), 3.59 (dd, *J* = 15.2, 2.2 Hz, 1H), 2.41-2.31 (m, 1H), 2.11-2.04 (m, 1H), 1.96-1.91 (m, 2H); ^{13}C NMR (125 MHz, D_2O) δ 175.0, 174.7, 173.5, 171.0, 168.4, 61.5, 56.0, 49.4, 49.3, 32.0, 31.2, 30.5, 25.7.

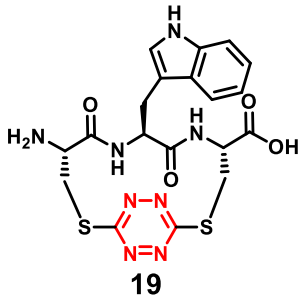

19

Compound 19 was purified by reverse-phase chromatography (gradient 5 – 30% organic over 9 minutes) to give 7.5 mg (7.0%) of **19** as an orange amorphous powder after lyophilization: HRMS (ES) *m/z* 489.1133 [$(M+H)^+$; calcd for $C_{19}H_{21}N_8O_4S_2$: 489.1127]; IR (ATR) 3302 (w, br), 1641 (s), 1541 (m), 1529 (m), 1457 (w), 1416 (m), 1242 (s), 1200 (w), 1055 (w), 896 (w) cm^{-1}; ^1H NMR (500 MHz, D_2O/CD_3OD) δ 7.53 (d, *J* = 7.8 Hz, 1H), 7.34 (d, *J* = 8.2 Hz, 1H), 7.10 (t, *J* = 7.5 Hz, 1H), 7.02 (t, *J* = 7.5 Hz, 1H), 5.35 (s, 1H), 4.72 (dd, *J* = 14.8, 4.4 Hz, 1H), 4.37 (t, *J* = 7.6 Hz, 1H), 4.35 (t, *J* = 3.2 Hz, 1H),

4.20 (dd, *J* = 4.0, 2.5 Hz , 1H), 3.54 (dd, *J* = 16.0, 4.1 Hz, 1H), 3.48 (dd, *J* = 14.8, 2.0 Hz, 1H), 3.12 (dd, *J* = 13.9, 8.1 Hz, 1H), 3.01 (dd, *J* = 14.2, 6.8 Hz, 1H).

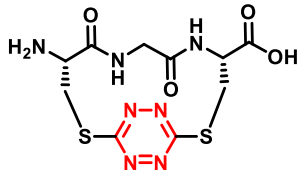

20

Compound 20 was purified by reverse-phase chromatography (gradient 5 – 30% organic over 9 minutes) to give 6.5 mg (8.0%) of **20** as an orange amorphous powder after lyophilization: HRMS (ES) *m/z* 360.0352 [$(M+H)^+$; calcd for $C_{10}H_{14}N_7O_4S_2$: 360.0549]; IR (ATR) 3055 (m, br), 1651 (s), 1538 (m), 1413 (m), 1396 (m), 1238 (s), 1199 (s), 1139 (s), 958 (m), 892 (m) cm^{-1}; ^1H NMR (500 MHz, D_2O) δ 4.72 (dd, *J* = 16.4, 2.3 Hz, 1H), 4.66 (dd, *J* = 15.2, 4.6 Hz, 1H), 4.51 (app t, *J* = 3.3 Hz, 2H), 4.03 (d, *J* = 15.6 Hz, 1H), 3.63 (d, *J* = 16.3 Hz, 1H), 3.62 (d, *J* = 16.3 Hz, 1H), 3.45 (d, *J* = 15.6 Hz, 1H); ^{13}C NMR (125 MHz, D_2O) δ 173.3, 172.2, 169.7, 169.1, 166.7, 53.2, 51.1, 42.2, 30.5, 30.3.

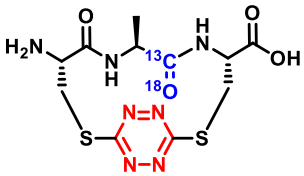

21

Compound 21 was purified by reverse-phase chromatography (gradient 5 – 30% organic over 10 minutes) to give 21.5 mg (26%) of **21** as an orange amorphous powder after lyophilization: HRMS (ES) *m/z* 377.0786 [$(M+H)^+$; calcd for $C_{10}{}^{13}CH_{16}N_7O_3{}^{18}OS_2$: 377.0781]; IR (ATR) 1676 (s), 1594 (s), 1546 (w), 1530 (w), 1416 (w), 1244 (m), 1202

(s), 1138 (s); ^{1}H NMR (500 MHz, DMSO-d_6) δ 8.77 (d, J = 8.5 Hz, 1H), 8.65 (dd, J = 6.5, 3.5 Hz, 1H), 8.33 (d, J = 5.0 Hz, 1H), 8.28 (d, J = 5.0 Hz, 1H), 4.84-4.81 (m, 1H), 4.74 (dd, J = 15.5, 3.0 Hz, 1H), 4.55 (dd, J = 14.5, 4.5 Hz, 1H), 4.35-4.31 (m, 1H), 4.24-4.18 (m, 1H), 3.54 (brd, J = 14.5 Hz, 1H), 3.50 (dd, J = 16.0, 3.0 Hz, 1H), 1.03 (dd, J = 7.0, 4.0 Hz, 3H); ^{1}H NMR (500 MHz, D_2O) δ 4.83 (dq, J = 5.0, 2.5 Hz, 1H), 4.75 (J = 15.5, 3.0 Hz, 1H), 4.68 (dd, J = 15.0, 4.5 Hz, 1H), 4.48 (dd, J = 3.5, 3.0 Hz, 1H), 4.22 (dq, J = 7.0, 4.0 Hz, 1H), 3.62 (dd, J = 15.0, 2.0 Hz, 1H), 3.61 (dd, J = 15.0, 4.0 Hz, 1H), 1.23 (dd, J = 7.0, 4.0 Hz, 3H); ^{13}C NMR (125 MHz, D2O) δ 172.7 172.2, 171.7, 169.1, 165.3, 52.5, 50.9, 48.2 (d, J = 54 Hz), 30.0, 29.7, 17.8.

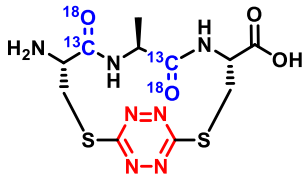

22

Compound 22 was purified by reverse-phase chromatography (gradient 5 – 30% organic over 10 minutes) to give 26.7 mg (32%) of **22** as an orange amorphous powder after lyophilization: HRMS (ES) *m/z* 380.0843 [$(M+H)^+$; calcd for $C_9{}^{13}C_2H_{16}N_7O_2{}^{18}O_2S_2$: 380.0857]; IR (ATR) 1677 (m), 1574 (s), 1413 (m), 1242 (s), 1202 (m), 1144 (m), 1055 (w); ^{1}H NMR (500 MHz, DMSO-d_6) δ 8.76-8.69 (m, 1H), 8.57-8.52 (m, 1H), 4.78-4.74 (m, 1H), 4.72 (brd, J = 15.5 Hz, 1H), 4.56 (dd, J = 15.0, 4.0 Hz, 1H), 4.33-4.29 (m, 1H), 4.27-4.20 (m, 1H), 3.54 (brd, J = 15.0 Hz, 1H), 3.54-3.50 (m, 1H), 1.05 (dd, J = 7.0, 4.0 Hz, 3H); ^{1}H NMR (500 MHz, 1:9 D2O/H_2O) δ 8.75 (dd, J = 8.5, 3.5 Hz, 1H), 8.27 (t, J = 5.0 Hz, 1H), 4.59-4.55 (m, 1H), 4.38 (q, J = 3.5 Hz, 1H), 4.16-4.09 (m, 1H), 3.53-3.47 (m,

1H), 1.13 (dd, *J* = 7.0, 4.5 Hz, 3H); ^{13}C NMR (125 MHz, 1:9 D2O/H_2O) δ 177.2, 174.1, 172.7 (d, *J* = 2 Hz), 170.2, 165.9 (d, *J* = 2 Hz), 53.7, 51.5 (d, *J* = 54 Hz), 48.9 (d, *J* = 54 Hz), 30.8, 30.3, 18.3.

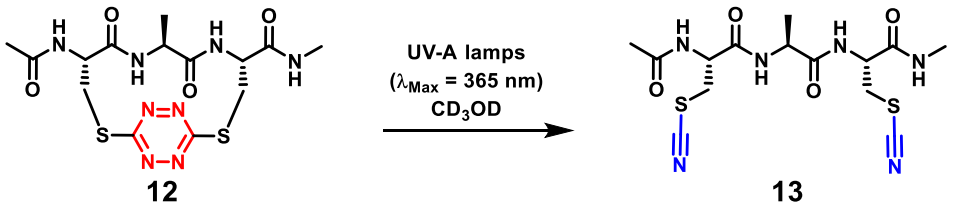

12 13

Compound 13. A solution of tetrazine peptide **12** (2.0 mg) was dissolved in CD_3OD (500 μL) and transferred to an NMR tube. The contents were suspended in a Rayonet photoreactor at a distance of about 5 cm from eight Hitachi FL8BL-8 UV-A (λ_{Max} = 365 nm) lamps. The solution was irradiated for 4 hours and the solution became colorless, an indication that the sample had reached complete conversion. Analysis by H-NMR showed quantitative conversion to furnish **13**: HRMS (ES) *m/z* 423.0870 [(M+Na)$^+$; calcd for $C_{14}H_{20}N_6O_4NaS_2$: 423.0885]; ^{1}H NMR (500 MHz, DMSO-d_6) δ 8.48 (d, *J* = 7.0 Hz, 1H), 8.41 (d, *J* = 8.0 Hz, 1H), 8.27 (d, *J* = 8.0 Hz, 1H), 8.01 (q, *J* = 4.5 Hz, 1H), 4.64 (dt, *J* = 8.0, 4.5 Hz, 1H), 4.49 (dt, *J* = 7.5, 5.5 Hz, 1H), 4.24 (pent, *J* = 7.0 Hz, 1H), 3.41 (dd, *J* = 13.5, 5.5 Hz, 1H), 3.24 (dd, *J* = 13.5, 7.5 Hz, 1H), 3.18 (dd, *J* = 13.5, 8.5 Hz, 1H), 2.61 (d, *J* = 4.5 Hz, 3H), 1.90 (s, 3H), 1.25 (d, *J* = 7.0 Hz, 3H); ^{13}C NMR (500 MHz, DMSO-d_6) δ 172.4, 170.2, 169.1, 168.8, 113.3, 113.2, 52.6, 52.3, 49.2, 35.5, 35.3, 26.0, 22.7, 17.6.

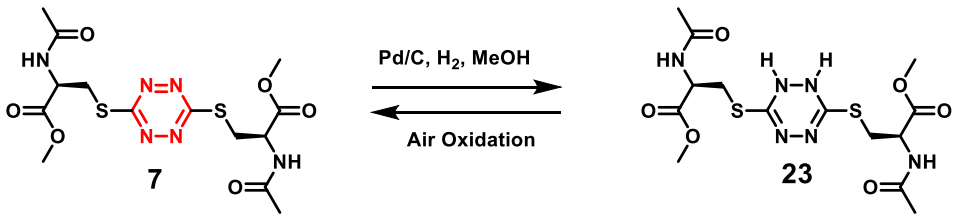

7 23

Compound 23. A 10 mL tear drop flask equipped with a stir bar was charged with a solution of **7** (15.0 mg, 0.035 mmol) in methanol (5 mL). A spatula tip of 10% palladium on carbon (50% wet with water) was added to the solution. The heterogeneous mixture was flushed with hydrogen gas using a balloon and then stirred under a hydrogen gas environment for 5 min. The mixture was then filtered through a pad of silica gel and the filtrate concentrated *in vacuo* to afford, without any required purification, 14.9 mg (98%) of **23** as a colorless oil: HRMS (ES) *m/z* 435.1129 [$(M+H)^+$; calcd for $C_{14}H_{23}N_6O_6S_2$: 435.1121]; IR (CH_2Cl_2) 3047 (s), 2985 (s), 2306 (m), 1745 (s), 1679 (s), 1623 (m), 1510 (s); ^{1}H NMR (500 MHz, CD_3OD) δ 4.69 (dd, *J* = 8.0, 4.5 Hz, 1H), 3.73 (s, 3H), 3.46 (dd, *J* = 14.0, 4.5 Hz, 1H), 3.22 (dd, *J* = 14.0, 8.0 Hz, 1H), 1.99 (s, 3H); ^{1}H NMR (500 MHz, DMSO-d_6) δ 8.89 (s, 1H), 4.43 (d, *J* = 7.5 Hz, 1H), 4.89 (ddd, *J* = 9.0, 7.5, 5.0 Hz, 1H), 3.63 (s, 3H), 3.33 (dd, *J* = 13.5, 5.0 Hz, 1H), 3.06 (dd, *J* = 13.5, 9.0 Hz, 1H), 1.86 (s, 3H); ^{13}C NMR (125 MHz, CD_3OD) δ 173.5, 172.3, 151.8, 54.0, 53.2, 33.2, 22.5; ^{13}C NMR (125 MHz, DMSO-d_6) δ 170.7, 169.3, 149.4, 52.1, 51.5, 31.2, 22.2.

Compound 7 (from oxidation of 23). To a 10 mL tear drop flask charged with **23** (5.2 mg, 0.012 mmol) was added methanol (5 mL). The solution was allowed to stand exposed to air for 8 h after which the solution, which turned from colorless to orange, was concentrated *in vacuo* and then chromatographed on silica gel using 5% methanol/ethyl acetate as the eluent to give 5.0 mg (97%) of **7** as an orange oil: ^{1}H NMR (500 MHz, CD_3OD) δ 4.89 (dd, *J* = 8.5, 5.0 Hz, 1H), 4.00 (dd, *J* = 14.0, 5.0 Hz, 1H), 3.77 (s, 3H), 3.50 (dd, *J* = 14.0, 8.5 Hz, 1H), 1.97 (s, 3H); ^{13}C NMR (125 MHz, CD_3OD) δ 173.7, 173.6, 172.1, 53.3, 52.8, 32.7, 22.4.

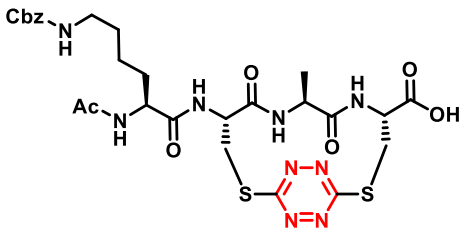

24

Compound 24. Prepared by the general SPPS protocol, initially from 0.11 mmol loaded Wang resin and was purified by reverse-phase chromatography (gradient 10 – 80% organic over 10 min) to give 11.9 mg (16%) of **24** as an orange amorphous powder after lyophilization: HRMS (ES) *m/z* 700.1962 [(M+Na)$^+$; calcd for $C_{27}H_{35}N_9O_8NaS_2$: 700.1948].

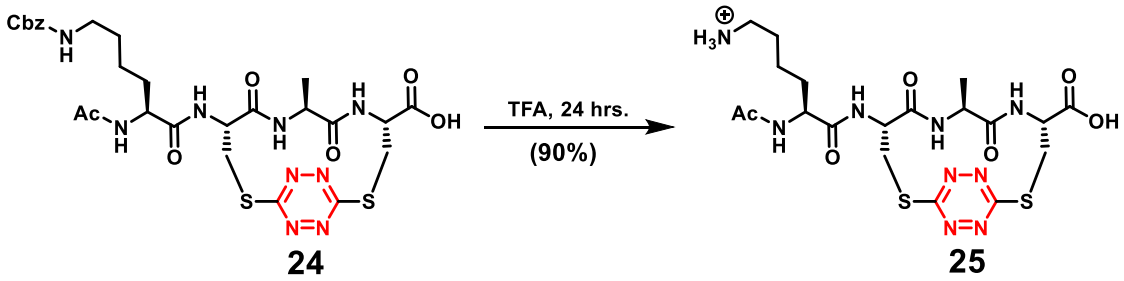

24 **25**

Compound 25. To a 10 mL tear-drop flask charged with **24** (2.0 mg, 0.0030 mmol) was added a solution of TFA (3mL). After stirring for 24 h, completion of the reaction was observed by LC-MS and the solution was concentrated under reduced pressure. The resulting residue was taken into water (1 mL) and then purified by reverse-phase chromatography (gradient 5% – 45% organic over 10 min) to give 1.5 mg (90%) of **25** as an orange amorphous powder after lyophilization: HRMS (ES) *m/z* 544.1777 [(M+H)$^+$; calcd for $C_{19}H_{30}N_9O_6S_2$: 544.1760]; ^{1}H NMR (500 MHz, DMSO-d_6) δ 8.54 (d, J = 6.9 Hz, 1H), 8.48 (d, J = 8.5 Hz, 1H), 8.18 (d, J = 7.9 Hz, 1H), 7.83 (d, J = 6.7 Hz, 1H), 7.74 (s, 4H), 4.74 (ddd, J = 6.6, 4.9, 3.2 Hz, 2H), 4.54 (ddd, J = 14.3, 10.0, 3.7 Hz, 2H), 4.26 (td, J = 8.5, 4.9

Hz, 1H), 4.22 – 4.12 (m, 1H), 3.52 (dd, *J* = 14.8, 2.1 Hz, 1H), 3.37 (dd, *J* = 15.2, 3.5 Hz, 1H), 1.88 (s, 3H), 1.52 (dt, *J* = 9.5, 4.7 Hz, 2H), 1.33 (q, *J* = 7.7 Hz, 2H), 1.24 (s, 2H), 1.00 (d, *J* = 6.8 Hz, 3H). ^{13}C NMR (126 MHz, DMSO) δ 171.3, 171.1, 170.8, 170.7, 170.5, 169.4, 166.8, 52.4, 51.6, 50.9, 47.4, 32.3, 30.9, 30.3, 26.5, 22.4, 22.3, 19.7.

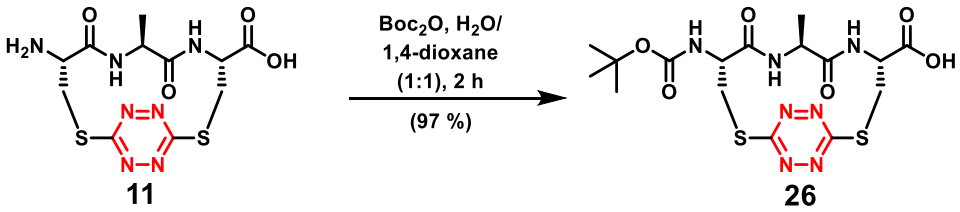

11 26

Compound 26. A 25 mL round bottom flask was charged with **11** (27.0 mg, 0.072 mmol) and $NaHCO_3$ (15.1 mg, 0.180 mmol, 2.5 equiv) then dissolved in water (2.0 mL). A pre-mixed solution of Boc-anhydride (23.7 mg, 0.109 mmol, 1.5 equiv) dissolved in 1,4-dioxane (2.0 mL) was added dropwise over 15 minutes (slow addition of Boc_2O was found to give better yields than adding in one portion) with stirring. After 2.0 hours, completion of the reaction was observed by LC-MS and the reaction solution was purified by reverse-phase chromatography (gradient 10 – 80% organic over 10 minutes) to give 33.1 mg (97.0%) of **26** as an orange amorphous powder after lyophilization. HRMS (ES) *m/z* 474.1232 [$(M+H)^+$; calcd for $C_{16}H_{24}N_7O_6S_2$: 474.1230]; IR (ATR) 3310 (w), 1720 (m), 1666 (s), 1645 (s), 1535 (m), 1508 (m), 1238 (s), 1207 (m), 1166 (s), 1054 (w), 894 (m); ^{1}H NMR (500 MHz, DMSO-d_6) δ 8.41 (d, *J* = 8.0 Hz, 1H), 8.23 (bs, 1H), 6.38 (d, *J* = 6.5 Hz, 1H), 4.55-4.49 (m, 4H), 4.15 (pent, *J* = 7.0 Hz, 1H), 3.54 (dd, *J* = 15.5, 3.0 Hz, 1H), 3.35 (overlapping d, *J* = 15.0, 1H), 1.39 (s, 9H), 1.01 (d, *J* = 7.0 Hz, 3H); ^{13}C NMR (125

MHz, DMSO-d_6) δ 171.1, 170.6, 170.4, 167.2, 163.19, 154.31, 78.6, 52.3, 51.9, 47.5, 32.7, 30.9, 28.1, 19.7.

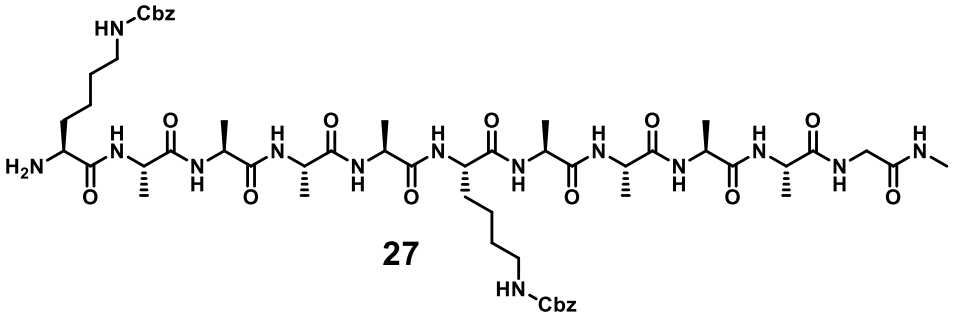

27

Compound 27. Prepared by SPPS, initially from 0.25 mmol loaded methyl indole AM resin and purified by reverse-phase chromatography (gradient 5 – 60% organic over 10 min) to give 116.1 mg (37%) of **27** as a white amorphous powder after lyophilization: HRMS (ES) *m/z* 1252.6707 [$(M+H)^+$; calcd for $C_{58}H_{90}N_{15}O_{16}$: 1252.6690]; MALDI-TOF *m/z* 1274.399 [$(M+Na)^+$; calcd for $C_{58}H_{89}N_{15}O_{16}Na$: 1274.6510].

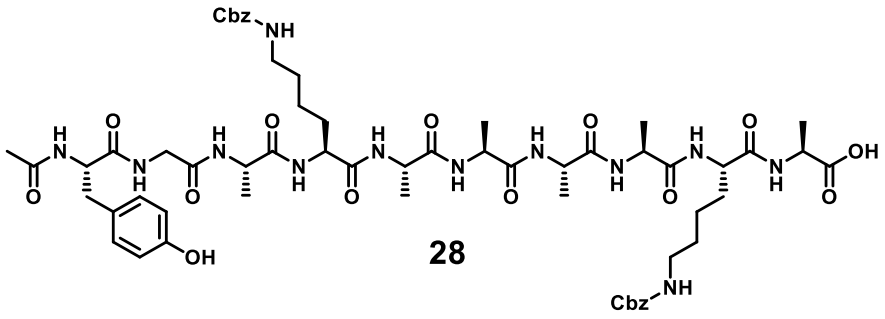

28

Compound 28. Prepared by SPPS, initially from 0.25 mmol loaded 2-chlorotrityl chloride resin and purified by reverse-phase chromatography (gradient 10 – 70% organic over 10 min) to give 109.1 mg (38%) of **28** as a white amorphous powder after lyophilization: HRMS (ES) *m/z* 1160.5630 [$(M+H)^+$; calcd for $C_{56}H_{78}N_{11}O_{16}$: 1160.5628]; MALDI-TOF *m/z* 1182.469 [$(M+Na)^+$; calcd for $C_{56}H_{77}N_{11}O_{16}Na$: 1182.5448].

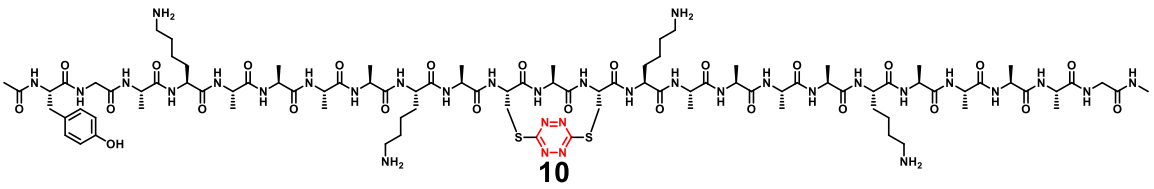

10

Compound 10. To a 10 mL tear-drop flask containing Peptide (30.8 mg, 0.019 mmol) in DMF (2.5 mL) was added dropwise a pre-mixed solution of **I-36** (22.3 mg, 0.019 mmol, 1.0 equiv), Oxyma (3.0 mg, 0.021 mmol, 1.1 equiv), HBTU (8.0 mg, 0.021 mmol, 1.1 equiv) and DIPEA (8.4 µL, 0.048 mmol, 2.5 equiv) in DMF (1.5 mL). After stirring for 8 h, the reaction solution was concentrated under reduced pressure. To the resulting residue was added neat TFA (4 mL). After stirring for 24 h, the solution was concentrated under reduced pressure, taken into acetonitrile/water (1:1), and then purified by reverse-phase chromatography (gradient 5 – 35% organic over 10 min) to give 10.5 mg (25%) of **I-4** as an amorphous powder after lyophilization: HRMS (ES) *m/z* 2213.1260 [$(M+H)^+$; calcd for $C_{93}H_{154}N_{33}O_{26}S_2$: 2213.1184]; MALDI-TOF *m/z* 2213.598 [$(M+H)^+$; calcd for $C_{93}H_{154}N_{33}O_{26}S_2$: 2213.1184].

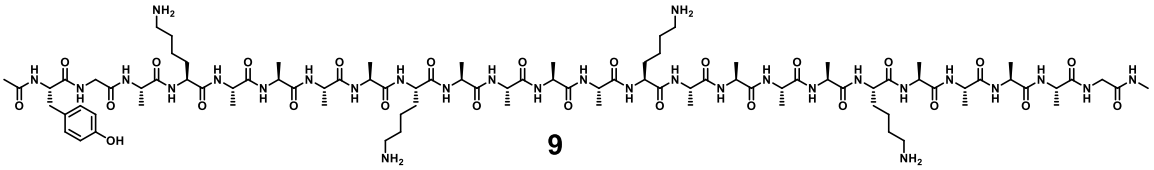

9

Compound 9. Prepared by SPPS, initially from 0.050 mmol loaded methyl indole AM resin and purified by reverse-phase chromatography (gradient 5 – 35% organic over 10 min) to give 13.7 mg (13%) of **9** as a white amorphous powder after lyophilization: HRMS (ES) *m/z* 2093.1575 [$(M+Na)^+$; calcd for $C_{91}H_{155}N_{29}O_{26}Na$: 2093.1596]; MALDI-TOF *m/z* 2071.014 [$(M+H)^+$; calcd for $C_{92}H_{156}N_{29}O_{26}$: 2071.1776].

CHAPTER 2. Stapling and Unstapling Peptides/Proteins with *s*-Tetrazine

Introduction

Modulation of peptide and protein conformation comprises one of the principal determinates of biofunction and molecular recognition.[1] Throughout the late 1970s and 1980s, pioneers in the field such as Hirschmann[2-3] , Hruby[4-5] , and Kessler[6-7] used conformational constraints within natural peptide hormones to lock the active conformations of these structures resulting in improved bioactivity and bioavailability compared to the natural products. These studies demonstrated the active conformation was much more than the simple two-dimensional linear sequence of amino acids, and began to establish the relationship between the overall three-dimensional peptide structure and function. Towards this end, macrocyclization has become an effective tactic to increase proteolytic stability, vary polarity and improve the overall drugability of peptides.[8-10]

Inevitably the rational design of bioactive peptides now seeks to recapitulate the three-dimensional structures that naturally occur in proteins such as, turns, β-sheets and helices (Figure 2.1). The ability to predict and prepare these structures holds the promise

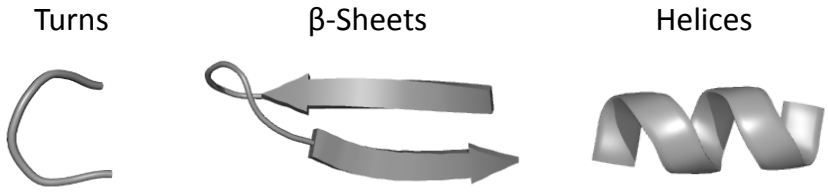

Figure 2.1. Design of Peptides to Mimic Bioactive Structures

toward the development of the next generation of peptide based therapeutics. In moving forward, we will evaluate some of the methods used to restrict peptide conformation.

Disulfide Bonds: Covalent Conformational Restraints Used in Nature

One of the most prevalent covalent modification of peptides and proteins is the disulfide bond, second only to the peptide bond itself. Indeed, nature uses this linkage to induce conformational restrictions for peptides/proteins to stabilize the overall three-dimensional structure.[11] The secondary structure of proteins is important, not only for biofunction and molecular recognition, but also for reducing the exposure of vulnerable residues to proteases. Peptides however are highly susceptible to proteolytic degradation; therein lies one of the main disadvantages of peptides as therapeutics. However, bioactive natural product peptides, such as the antimicrobial defensin peptides, the cysteine knot peptides, and small venom-derived peptides like the conotoxins, have all evolved with multiple disulfide bonds presumably to restrict the conformation and circumvent problems associated degradation. Nature's valuable lesson of constraining the structure of a peptide sequence with disulfides, in turn, renders a more compacted and rigid framework that reduces the exposure of the peptide sequence toward proteolytic degradation.

Peptide Stapling: Synthetic Macrocyclization Constraints

Synthetic macrocyclization strategies have been developed to generate constrained peptides with enhanced stability by tethering two side-chains within the peptide. The macrocyclization strategies that are used to induce and to stabilize the secondary structure of a peptide conformation comprises a tactic known as "stapling". Although stapling protocols

have been developed for constructing β-sheets and turns,[12] much more attention has been focused on stapling α-helices given that α-helices are the largest class of protein secondary structures and in turn have a major role in protein-protein interactions. Early synthetic examples of stapling tactics used to mimic α-helices were designed and prepared by inserting either a lactam or disulfide bridge. For example, studies at Hoffmann-La Roche on human growth hormone-releasing factor (GFP), linked the side-chains of the aspartic acid 8 and lysine 12 residues and found the peptide demonstrated improved potency and significant helical character in an aqueous solution.[13] Later, Taylor and co-workers, applied this tactic for the construction of short peptide sequences, linking the side chains of glutamic acid and lysine *i*, *i* + 4 residues to form a lactam (Figure 2.2).[14-15] This technique demonstrated that short sequences of amino acids retained helical conformation, however the

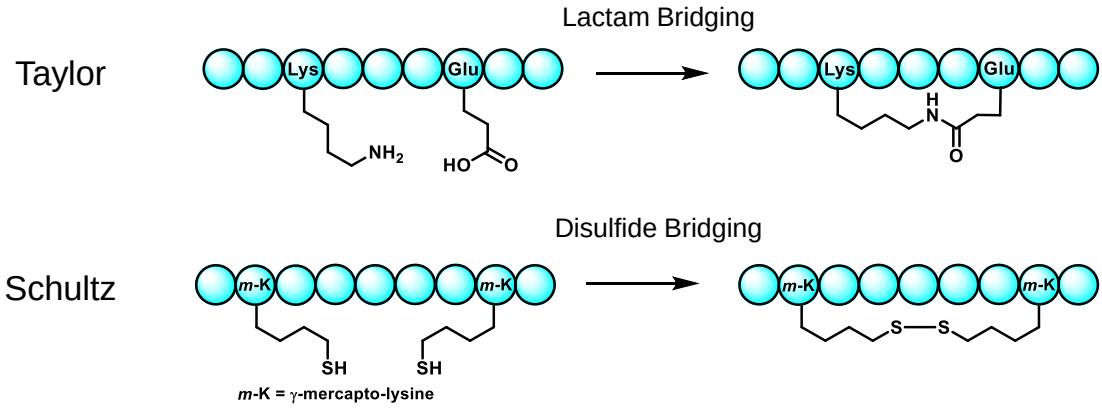

Figure 2.2. Early Peptide Stapling Tactics

lactam bridge proved highly sensitive to the position within the peptide. For example, when the placement of lysine and glutamic acid residues were reversed in the same sequence, no helical content was observed. Schultz and co-workers later reported the synthesis of short

peptides that were designed to bridge the *i*, *i* +7 residues through a single intramolecular disulfide bond (Figure 2.2) to stabilize two turns of an α-helical peptide.[16] Although the results demonstrated the utility of using disulfide bonds to stabilize helical conformations in short peptides, disulfides have both multiple conformations that can affect the nature of the staple and are not stable in the intracellular environment of the cytosol. While these studies began to demonstrate the importance of stapling tactics to stabilize peptide conformations, a major advancement in the field came with the advent of all-hydrocarbon stapling.

All Hydrocarbon Peptide Stapling

The first example of hydrocarbon stapling was carried out by Blackwell and Grubbs employing allylic serine ethers, spaced in an *i*, *i* + 4 fashion, within a peptide followed by macrocyclization via ring-closing metathesis to form a stabilized helix (Figure 2.3).[17]

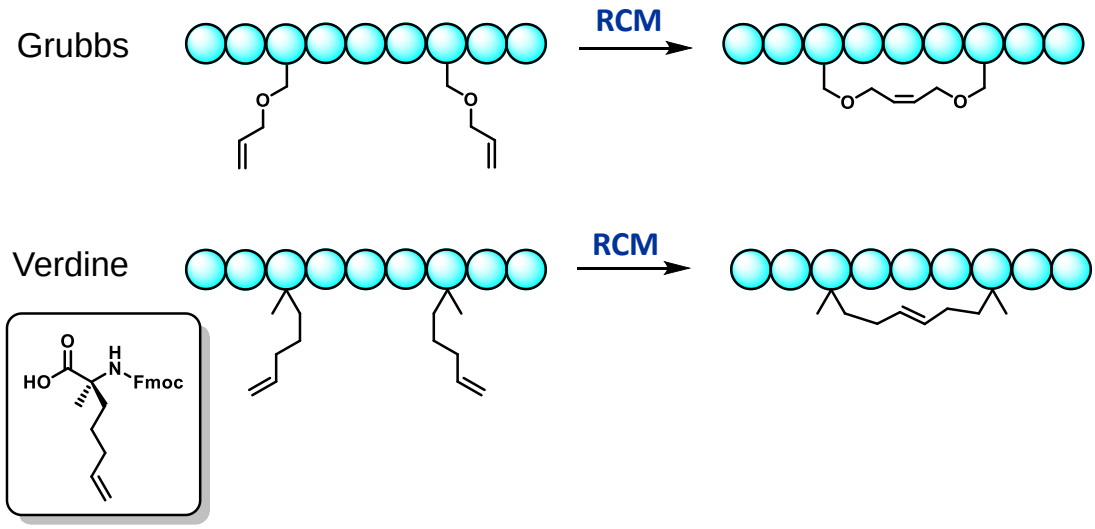

Figure 2.3. First Examples of Helix-Stabilization by Macrocyclization

Verdine and co-workers recognized the significance of this discovery and began preparing new α,α-disubstituted amino acids containing an olefin side-chain (Figure 2.3).[18] After optimizing both the linker length and the stereochemical configuration, the requisite unnatural residues were introduced into peptides by solid-phase peptide synthesis, then macrocyclization with ring-closing metathesis afforded the stapled peptides with increased helicity. This strategy has now reduced to practice the ability to not only to stabilize helical structures, but also the induction of unstructured peptides into their respective helical conformations. All-hydrocarbon stapling provides the ability to predict a helical structure from the linear sequence of amino acids by using crystal structures of protein-protein interactions and, in turn, has permitted the rational design of bioactive peptides endowed with many of the favorable properties of the protein. In many cases, these stapled peptides show improved potency, resistance to proteolytic degradation and improved cellular absorption, opening the potential to target intracellular processes.

Alternative Tactics of Peptide Stapling

An expanding repertoire of peptide stapling techniques has started to emerge.[19] These tactics can be split into two categories (Figure 2.4); first is an intramolecular stapling strategy, which employs the functionality of side-chains within the peptide to form the macrocycle. On the other hand, a bicomponent strategy can be used to link the side-chains of peptides combined with an exogenous component to bridge the peptide into a macrocyclic conformation. While both strategies have been effective for the construction of stapled peptides, these tactics do not permit the removal of the inserted staple (*i.e.* unstapling) without significantly disrupting the peptide structure.

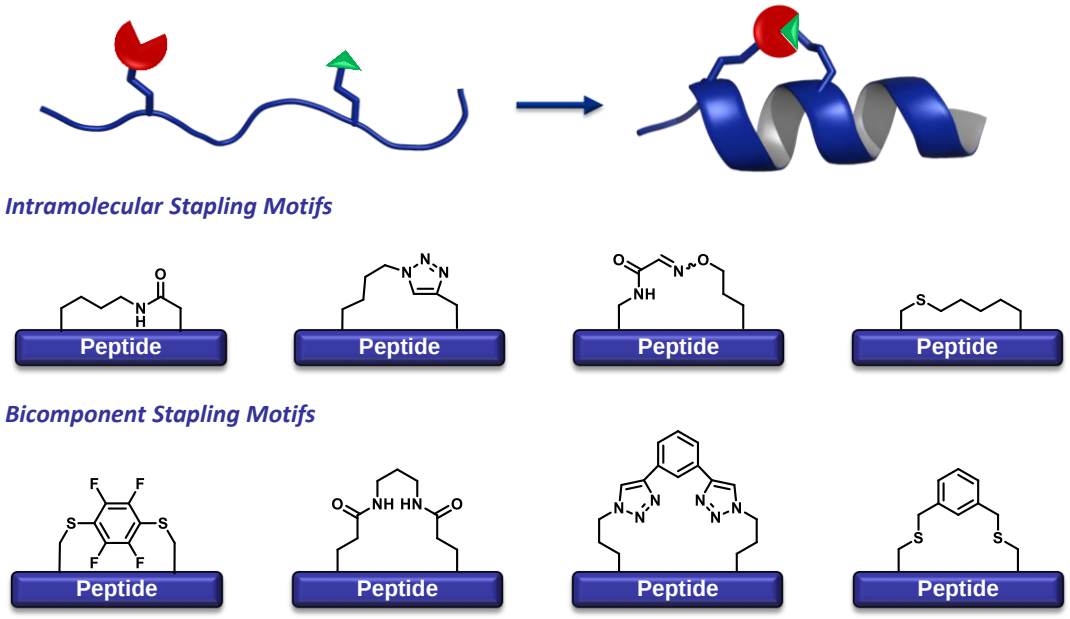

Figure 2.4. Tactics Developed for Peptide Stapling

Nature's Example of Peptide Unstapling

The value of stapled peptides has been well established by the number of reported bio-active stapled peptides, featuring high potency and predictable properties. However within this dissertation a question that must be asked is: what is the value of peptide unstapling? In chapter 1 we presented the release of restricted conformations to permit kinetic measurements for ultrafast structural transitions within peptides. Another advantage of manipulating conformation *in situ* may hold a valuable pharmacological role. Turning to an example from nature, β-defensin (Figure 2.5) is a 20-residue peptide stapled by three disulfide bonds that is produced by epithelial cells throughout the body. This stapled peptide has evolved to stand guard between you and the microbial world. However, initial biological testing of β-defensin has indicated the stapled conformation to be a poor antibiotic against both Gram positive and negative bacteria. It was later discovered that upon treatment of

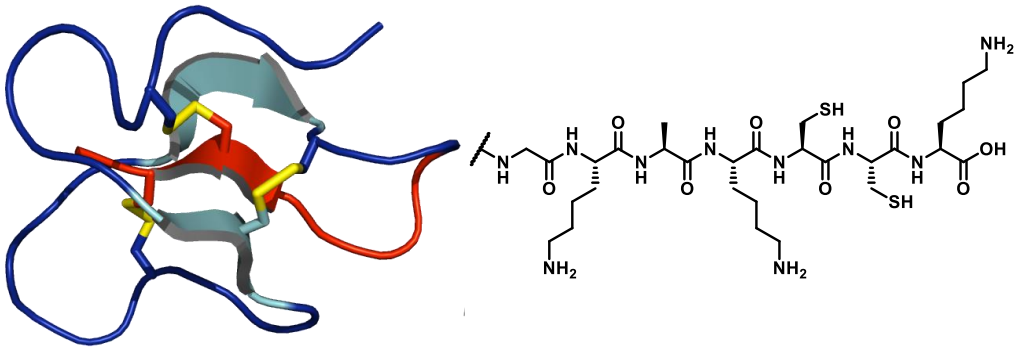

Figure 2.5. β-Defensin Employs Unstapling to Release Active Pharmacophore

β-defensin with thioredoxin reductase results in reduction of the disulfide bonds, effectively unstapling the peptide, which in turn changes the conformation and reveals a potent antibiotic.[20] It was subsequently determined that the pharmacophore of the molecule was contained within the center of the stapled conformation (last 7 C-terminal residues, Figure 2.5), thus rendering it inactive toward bacteria. However, when the antibacterial properties are required, nature has evolved an unstapling mechanism to release the active component.

Unstapling: Development of the *s*-Tetrazine Stapling and Unstapling Protocol

Given the critical role of conformation in peptides and proteins, our focus shifts to *s*-tetrazine: The question asked is, can *s*-tetrazine be used as a stapling motif? Additional questions include: can conditions be developed that permit dichlorotetrazine introduction into unprotected peptides under aqueous conditions? Also of importance, what are the limitations of the ring sizes that could be formed or the amino acid side chain compatibility? And most important, as a peptide staple, would *s*-tetrazine permit restricted peptides to be photochemically unstapled?

A Model System for the Development of s-Tetrazine Stapling and Unstapling

In pursuit of suitable conditions that would permit the incorporation of dichlorotetrazine into unprotected peptides, a model compound **32** (Scheme 2.1) was designed to contain many of the reactive side-chains found within peptides and was prepared by standard Fmoc-based solid-phase peptide synthesis.[21] A series of solvents, denaturants and pH levels were investigated for the reaction of peptide **32** with dichlorotetrazine to form **33**.

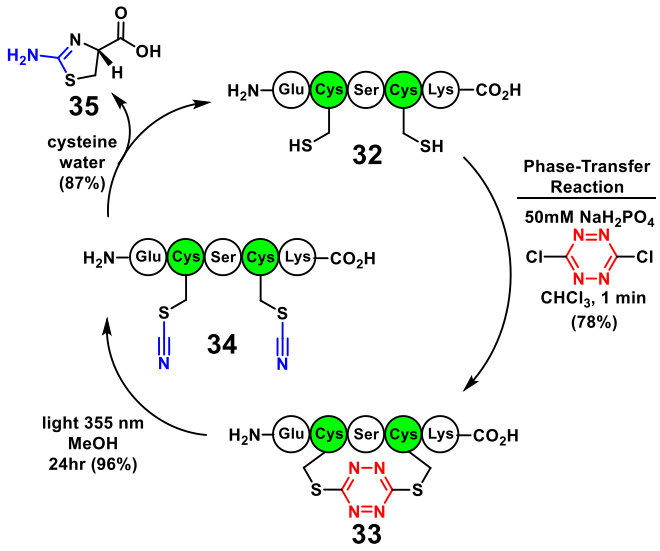

Scheme 2.1. Stapling, Unstapling and Regeneration of the Native Peptide

Separation of the phases containing the two reactants was discovered to permit excellent chemoselective control for the sulfhydryl addition into the highly electrophillic dichlorotetrazine. Mild acidic conditions (pH 5) provided the best chemoselective control in the reaction; lower pH slowed the rate of tetrazine transfer while **33** revealed instability with pH enviroments that were greater than pH 9. Denaturants were also investigated; the addition of guanidine hydrochloride, often used to denature peptides, did not affect the

yield of the model reaction and thus was not included in the phase-transfer cocktail to assist the purification efficiency. A denaturant, such as guanidine hydrochloride, however may play a more significant role in breaking the secondary structure and minimizing aggregation when exploring larger peptide systems. The addition of a reducing agent to the reaction solution to prevent disulfide formation was also considered, however *tris*(2-carboxyethyl)phosphine (TCEP) reacted with dichlorotetrazine during the course of the reaction. In addition t*ris*(2-carboxyethyl)phosphine (TCEP) will also reduce *S,S*-tetrazine motif to the *S,S*-dihydrotetrazine congener and thus was not used in the reaction. In the event that disulfide bond formation becomes problematic, immobilized TCEP can be used to reduce the disulfide and then removed by filtration just prior to the addition of dichlorotetrazine. The best phase-transfer protocol employed peptide **32** with the conditions listed in Scheme 2.1 to provide **33** with minimal side-products and in good yield after purification. Following isolation, **33** was subjected to steady-state irradiation under UV-A lamps to remove the tetrazine chromophore and thus releasing the restricted conformation affording the dithiocyanate peptide **34** in near quantitative yield.

Next a mild protocol to remove the nitriles from the thiocyanate groups in **34** was developed to regenerate the native disulfhydryl peptide **32** (Scheme 2.1). Early studies by Catsimpoolas[22-23] and Patchorn[24] had demonstrated respectively cyanylation of cysteine using an activated arylthiocyanate, and cleavage of the disulfide of cystine with sodium cyanide; both furnished the thiazolamine product **35** (Figure 2.5). These observations suggested that the nitriles could be removed via intramolecular cyclization with cysteine, en-

visioned to be mechanistically analogous to a native-chemical ligation[25] (Figure 2.6). Indeed, treatment of peptide **34** with cysteine in pH 8 buffer regenerated peptide **32** along with thiazolamine **35** (Scheme 2.1) readily isolated from the reaction mixture.

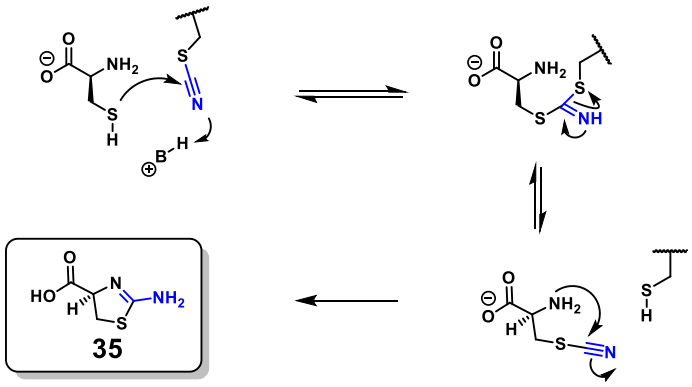

Figure 2.6. Proposed Mechanism of Nitrile Removal from the Thiocyanates

s-Tetrazine Stapling Compatibility with Various Peptide Substrates

Encouraged by the results of the model study, we next explored the incorporation of dichlorotetrazine into a variety of peptide substrates employing various spacing between the cysteine residues while also testing the compatibility all of the coded amino acids. To this end, stapled tetrazine macrocycles **36-43** were prepared (Scheme 2.2) employing the developed protocol and then isolated after reverse-phase chromatography. Minor amounts of disulfide and dimeric products were separated from the reaction mixture while oligimeric products became increasing problematic as the ring sizes of the peptides became larger; however separation of the desired monomer was achieved in every case. Minor amounts of oxidation of the methionine side chain was observed. Additionally, previous solid-phase peptide synthesis of tetrazine peptides containing the arginine side-chain had

resulted in decomposition (Scheme 1.4). Pleasingly, both peptides containing methionine and arginine side-chains were stable to this protocol with *s*-tetrazine in solution after isolation under buffered conditions.

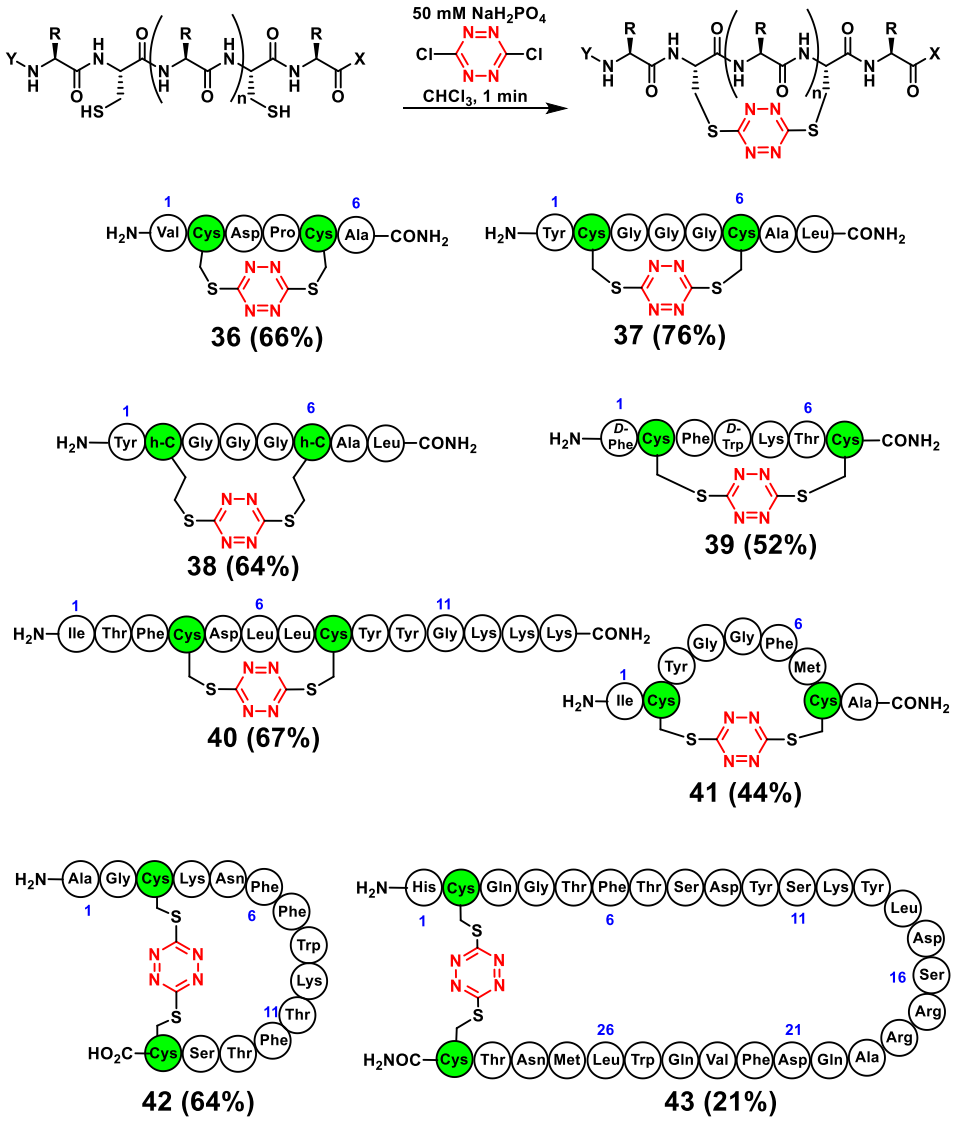

Scheme 2.2. *s*-Tetrazine Stapled Peptides Prepared by Phase-Transfer Conditions

Photochemical Unstapling of *s*-Tetrazine Stapled Peptides

Pleasingly, the photochemical release of the *s*-tetrazine staple under steady-state irradiation proved feasible. First, tetrazine peptides **36-38** were subjected to the identical conditions employed in Scheme 2.1; however only small amounts of product were observed in these cases. Next, a screen for optimal photochemical conditions entailed a variety of solvents, additives and wavelengths. Unfortunately, photochemical side-products were still observed in the crude reactions mixtures. However, in the best case scenario methanol was used as the solvent and UV-B lamps (λ_{Max} = 312 nm) as the light source. Under these conditions, the unstapled products **44-46** could be separated from the complex mixtures, with yields ranging from 25-46% (Scheme 2.3). Undeterred, we next investigated the effect of the reaction temperature and the relationship towards the formation of side-products. To

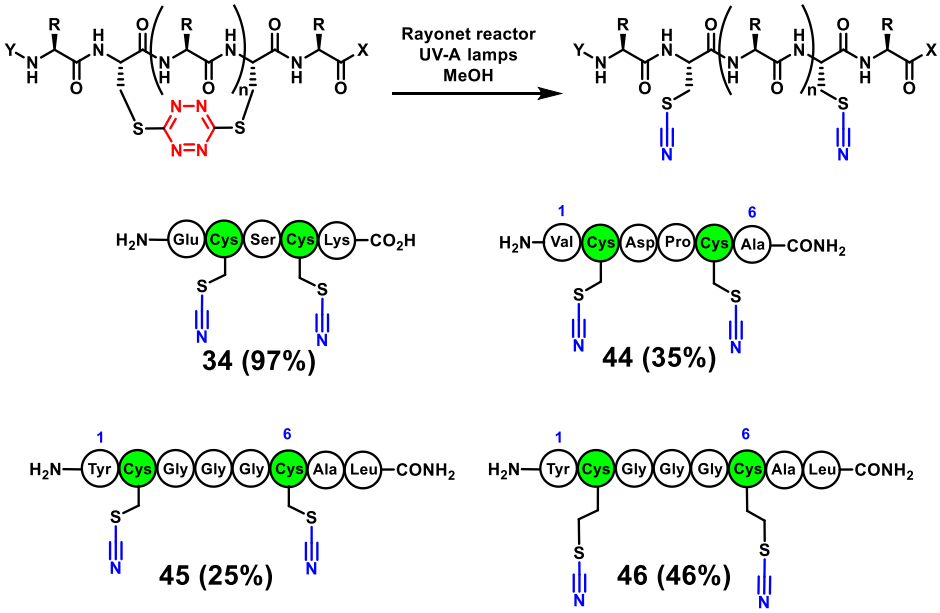

Scheme 2.3. Photochemical Unstapling Under Initial Conditions

control the temperature of the reaction within the Rayonet photoreactor, an apparatus was built from a glass bottle and connected to a circulating chiller (Figure 2.7). Then **37** was dissolved in methanol, the solution transferred to a sealed microwave vial and transferred to the apparatus with the contents submersed in the cooling

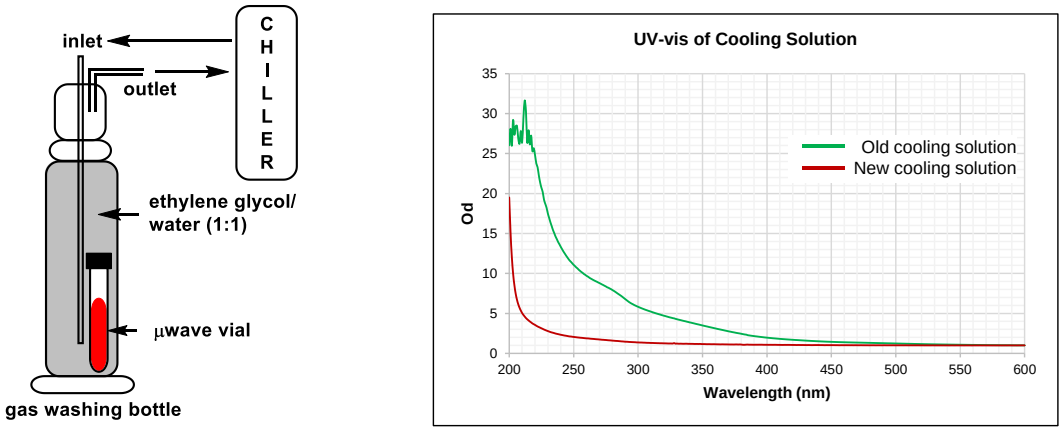

Figure 2.7. (A) Apparatus employed to Conduct Temperature Controlled Photolysis (B) UV-vis of Different Cooling Solutions

solution. The reactant **37** was irradiated under UV-B lamps at 1°C for seven days to furnish **45** in 85% yield by LC-MS. Encouraged by the result, that the reaction proceeded without the formation of side-products, although the conditions required one week to reach completion. Analysis of the cooling solution by UV-vis indicated strong absorbance at lower wavelengths. Comparison with newly prepared cooling solution suggested an algae was preventing the transmission of light into the sample (Figure 2.7). The cooling solution was changed and the identical reaction was performed again. Now the starting material **37** was consumed after only four hours providing **45** albeit present within a complex mixture. Isolation afforded **45** in 36% yield after purification. Increasing the transmission of light into

the reaction had now resulted in additional side products! While restricting the transmission of light with algae revealed that the reaction was capable of forming **45** as a single product, the results suggested a least two possible photochemical mechanisms were occurring with reaction conditions B (Scheme 2.4). Postulating that one mechanism involved a triplet-

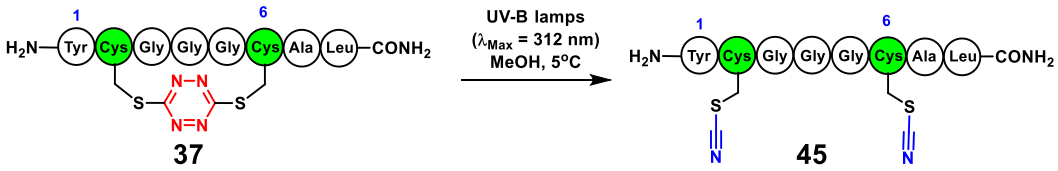

Conditions	Cooling Solution	Time	Yield
A	contained algae	7 days	85%
B	new ethylene glycol/water	4 hours	36%

Scheme 2.4. Temperature Controlled Photolysis

state radical leading to the formation of the side-products; while another led to the formation of **45** which does not contain long-lived radical intermediates. The latter was also supported by the photophysical experiments described in Chapter 1. Reasoning that oxygen gas would suppress side-reactions arising from a triplet-state radical, solutions containing peptides **36-38, 40, 42** were sparged with oxygen prior to photochemical irradiation. Under these conditions exclusive formation of the unstapled peptides **44-48** (Scheme 2.5) occurred when the photolysis was conducted with UV-B lamps in the presence of oxygen. For peptides containing tryptophan and methionine residues (*cf.* **39, 41, 42**), additional reactivity was observed under the oxygen conditions; nonetheless the dithiocyanate counterpart **48** is provided as an example that could be isolated in 38% yield after purification. In

the end, conditions were defined that permitted the tetrazine macrocycle to be readily unstapled photochemically *in situ* to yield the unconstrained linear dithiocyanate peptides **44-48**, which were in turn converted to their native structures employing cysteine for nitrile removal (Figure 2.6).

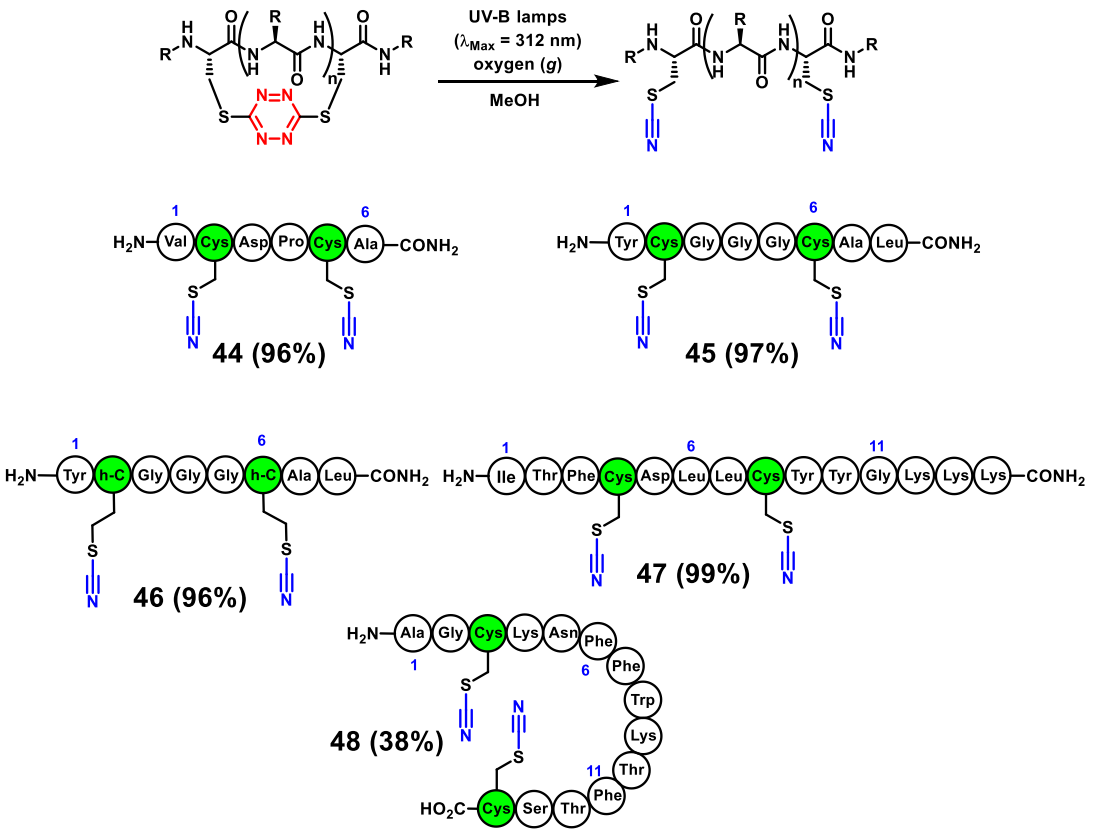

Scheme 2.5. Oxygenated Photolysis and Effective Unstapling of s-Tetrazine

Stapling Peptides with Proximal Lysine Residues

Given the successful completion of the initial goals with regards to stapling and unstapling peptides with *s*-tetrazine, the question we now ask: can the side chains of other amino acids be used to staple peptides and, in turn, would those structures undergo photochemical

unstapling? Envisioning a strategy that would employ unprotected peptides containing only a single cysteine sulfhydryl followed by introduction of *s*-tetrazine would generate *Cl,S*-tetrazine peptides. Importantly, changing the nature of the buffer, the *Cl,S*-tetrazine peptides, might be inclined to undergo macrocyclization with the amino group of a proximal lysine side-chain to form an *S,N*-tetrazine stapled peptide. By seeking to isolate the *Cl,S*-tetrazine product, this strategy could also be used for macrocyclization strategies with other peptide side-chains and/or provide access to peptide/protein *S,S*-tetrazine conjugates via a separate cysteine residue of a different molecule. Our focus thus turned to stapling and unstapling employing proximal lysine side chains.

An investigation was initiated to determine suitable conditions that would permit unprotected peptides, containing a single cysteine residue, to be functionalized with *s*-tetrazine in aqueous buffer, thus arriving at the *Cl,S*-tetrazine peptide. A model peptide **49** was constructed by manual Fmoc-based solid-phase peptide synthesis (SPPS) and evaluated under several conditions. First, treatment of **49** with the aforementioned biphasic protocol resulted in the formation of symmetrical homodimer. As such, the conditions were changed to a monophasic system. To this end, peptide **49** was dissolved in a pH 5 monosodium phosphate buffer. In a separate flask three equivalents of dichlorotetrazine was dissolved in acetonitrile. Upon adding the aqueous solution of peptide to the acetonitrile solution, and stirring for one minute, **50** was obtained in 71% yield after reverse-phase chromatography (Scheme 2.6). Notably, the *Cl,S*-tetrazine peptide **50** is stable in the presence of protonated amines and in acidic buffers (< pH 6). With **50** in hand, conditions to effect

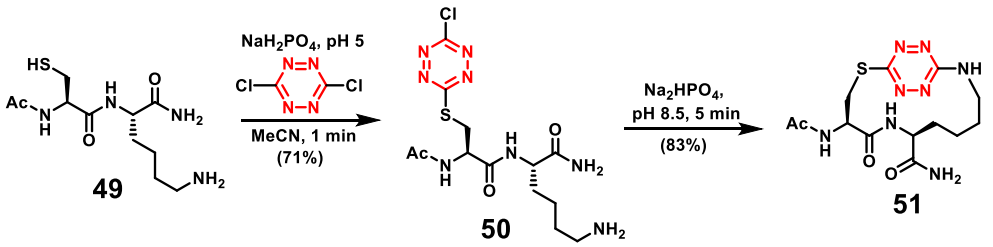

Scheme 2.6. Synthesis of *Cl,S*-Tetrazine Peptide 50 and *S,N*-Tetrazine Peptide 51

macrocyclization with the proximal lysine side-chain were examined by changing the pH of the buffer. Evaluation of a tris-buffer system at pH 8.5 was not compatible, finding that the amine of the tris buffer reacted with tetrazine faster than the lysine side-chain. The buffer system was therefore changed to a phosphate buffer (pH 8.5). After stirring for five minutes **51** resulted with minimal reactivity toward the buffer/solvent. During the course of this reaction some *S,N*-dimer had also formed. The reaction was therefore conducted at a lower concentration (500 μM) of the peptide substrate **50.** These conditions facilitated the optimal addition of the lysine side-chain into tetrazine to furnish **51** in 83% yield after purification by reverse-phase chromatography. Thus, the model system **49** supports the strategy of using the *Cl,S*-tetrazine intermediate **50** to gain access to the *S,N*-tetrazine macrocycle **51** with the amino side-chain of lysine.

Unstapling the *S,N*-Tetrazine Peptide 51

Turning our attention to the photochemical unstapling of **51**, questions had arisen regarding the effect of the nitrogen atom on the photochemical properties of the tetrazine chromophore. The previously developed photochemical conditions for unstapling *S,S*-tetrazine peptides were applied to a solution of **51** in methanol and sparged with oxygen gas prior to irradiation with UV-B lamps (Scheme 2.7). The reaction resulted in a complex

mixture of products. Analysis by proton NMR and LC-MS suggested formation of a methanol adduct as one of the products. Speculating that the cyanamide functionally of **52** may not be stable in nucleophilic solvents, we turned to water as a solvent to trap potentially the envisioned cyanamide as the urea. A second reaction was conducted with **51** dissolved in water [100μM], in a heavy-walled Pyrex tube and sparged with oxygen gas. The contents

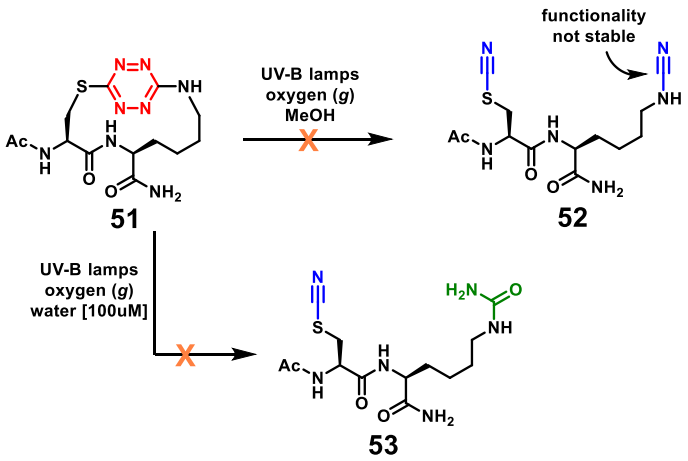

Scheme 2.7. Photochemical Unstapling of *S,N*-Tetrazine Peptide 51

were then irradiated with a single UV-B lamp to restrict the transmission of light into the sample. After four days, **51** was consumed with only one major product observed in the solution. LC-MS analysis indicated the mass of the product to be similar to **53** (M + H, m/z = 359), however after comparing the NMR spectra of the product from the photolysis with an authentic sample of **53**, prepared by solid-phase peptide synthesis, found that the two samples did not match. It is clear that the addition of a nitrogen atom to the *s*-tetrazine ring

affects the photochemical properties of the molecule. Transient absorption and phosphorescence measurements will need to be conducted to further elucidate the photophysics of these molecules. Such work is outside the scope of this thesis.

Bioconjugate Reaction Exploiting the s-Tetrazine Staple

A significant advantage of the *s*-tetrazine staple is the reactivity of the incorporated tetrazine to introduce probes via inverse electron demand Diels-Alder reactions.[26] To demonstrate this feature, fluorescein dye **54** was prepared and combined with stapled peptide **42** to obtain a diastereomeric mixture of the fluorescein labeled peptide **55** (Scheme 2.8). Thus, tetrazine staples hold the promise of a dual role: confining peptide conformation and introducing photophysical and other potential probes.[27-29]

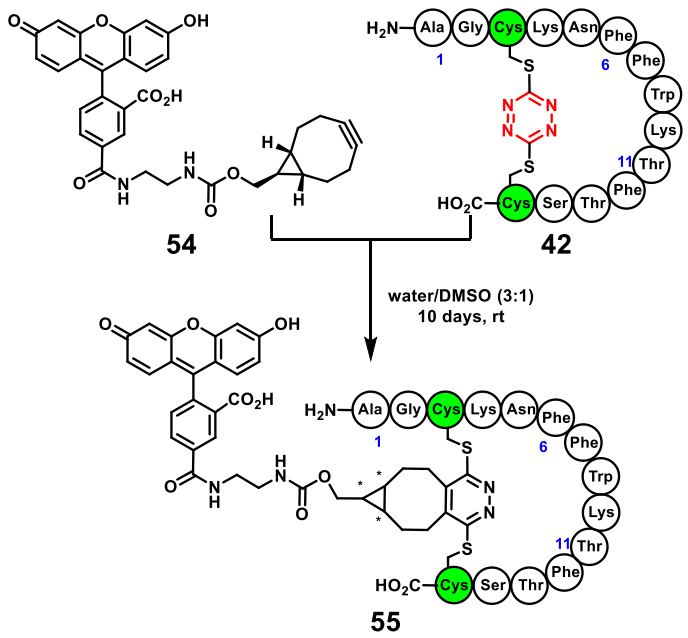

Scheme 2.8. *s*-Tetrazine Stapled Peptides Provide Effective Bioconjugate Handle

Stapling and Unstapling the Protein Thioredoxin with *s*-Tetrazine

The tetrazine stapling and unstapling protocol was next extended to proteins. Thioredoxin (**Trx**) was selected as a model protein, which contains a single, solvent exposed disulfide bond. The biphasic protocol used to staple peptides was ineffective for thioredoxin due to the formation of insoluble forms of the protein upon mixing with organic solvent. A new protocol was thus developed for thioredoxin employing a monophasic aqueous buffer. The new procedure entailed first reduction of the thioredoxin disulfide bond with immobilized TCEP, which was then removed by filtration. The reduced thioredoxin, in a pH 5 acetate buffer, was then stirred with a pre-mixed solution of dichlorotetrazine in dimethyl sulfoxide (acetate buffer/dimethyl sulfoxide; 50:1) with an overall concentration of protein at 20 μM (Scheme 2.9). After one minute, **56** was formed as

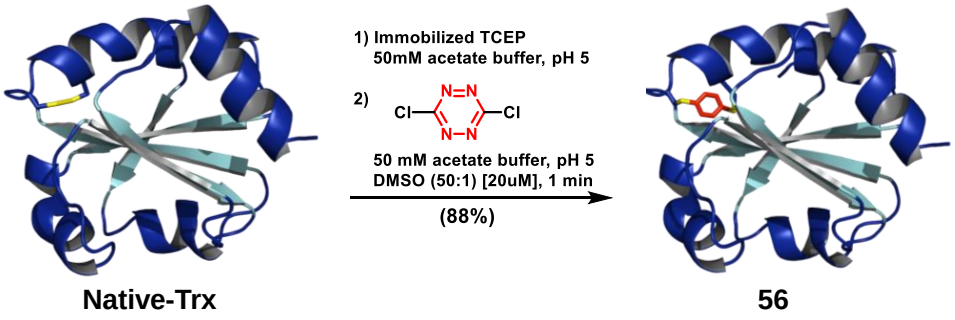

Scheme 2.9. Stapling the Protein Thioredoxin with s-Tetrazine

indicated by MALDI-TOF-MS (m/z = 11757.782). Purification was achieved with a desalting column. The Bradford assay is a protocol that quantifies microgram quantities of protein by measuring an absorbance shift upon binding of coomassie blue dye complexed

to the protein.[30] The Bradford method determined an 88% yield for the reaction, while reverse-phase C4-LC-MS chromatography indicated 90% purity for the sample, thus illustrating that the stapling of thioredoxin with *s*-tetrazine proceeds with high efficiency to furnish **56**.

With the **56** in hand, *in situ*, photolysis under an ambient atmosphere with UV-B lamps was conducted to effect unstapling of the *s*-tetrazine adduct (Scheme 2.10). After one hour MALDI-TOF-MS revealed the loss of N_2, but also partial loss of nitrile groups from the thiocyanates. To completely remove the nitriles, a solution of cysteine was added. After four hours the reaction solution was removed via centrifugal filtration. Addition of Ellman's reagent then furnished the disulfide bond of the protein **57**, again as observed by MALDI-TOF-MS. Bradford's method revealed a 73% yield for the reaction with C4-LC-MS chromatograms indicating a 52% purity for the regenerated protein **57**.

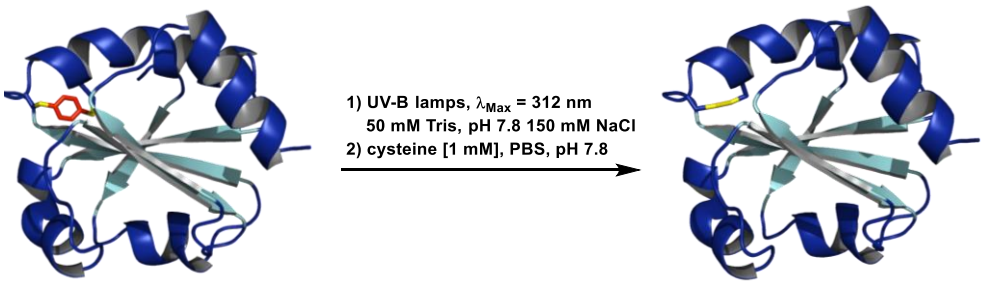

Scheme 2.10. Unstapling the Protein Thioredoxin Containing s-Tetrazine with UV-B Lamps

To interrogate the regenerated protein as the native form, bioactivity measurements were conducted. Evaluation of the enzymatic activity for the thioredoxin compounds was

examined using insulin as the substrate and dithiothreitol as the electron donor system (Figure 2.8). In this assay, dithiothreitol reduces thioredoxin and the reduced protein then

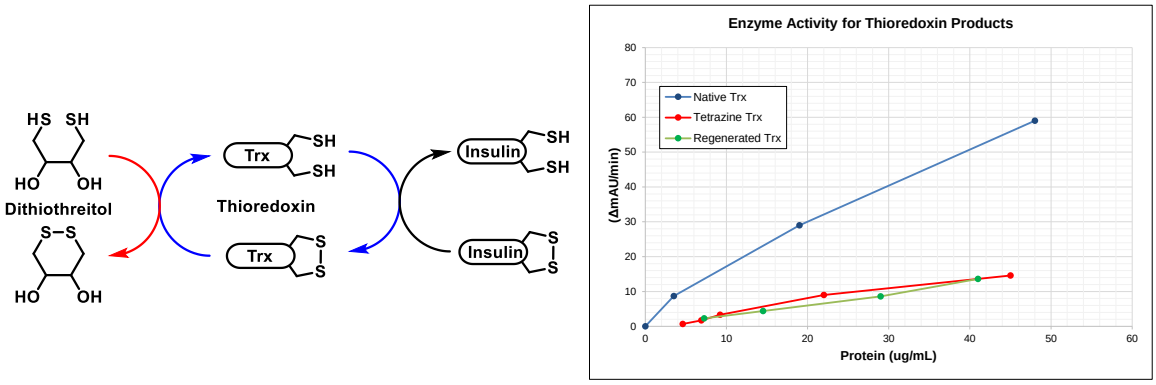

Figure 2.8. Bioactivity Measurement for Regenerated Thioredoxin Resulting from UV-B Photolysis

reduces the disulfide bonds of insulin. The reduction of insulin is monitored at 650 nm by an increase in turbidity for the solution. The bioactivity measurements involve a change in absorbance at 650 nm per minute as a function of protein concentration again determined by the Bradford method. The regenerated protein **57** did not show substantial increase in the catalytic turnover for the reduction of insulin when compared to the **56**. However, the regenerated protein **57** does remain reactive towards electrophiles such as dichlorotetrazine when resubjected to the described stapling conditions (Scheme 2.9). In addition, native thioredoxin, without incorporation of *s*-tetrazine, was treated with the identical photochemical conditions used to unstaple **56** (Scheme 2.11) only to find similar loss of biological activity. This finding suggested that the photochemical conditions were not compatible with this biological system.

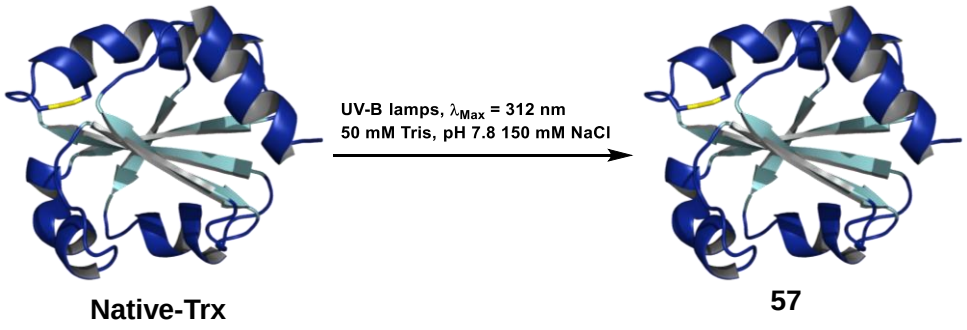

Scheme 2.11. Control Reaction for the Photolysis of Thioredoxin with UV-B Lamps

New Photochemical Conditions for Unstapling *s*-Tetrazine Thioredoxin

New photochemical conditions were developed to permit the unstapling and regeneration of the native protein thioredoxin. Reasoning that the loss of biological activity was due, in part, to the higher energy wavelengths of the UV-B lamps (λ_{Max} = 312 nm), we turned to laser-induced photolysis using a Nd:YAG flashlamp with a 355 nm wavelength. In addition to the lower energy wavelength, the flashlamp contains a delay between each pulse, which may permit relaxation of other possible excited states prior to a subsequent excitation pulse. To this end, *s*-tetrazine thioredoxin (**56**) was dissolved in degassed 10 mM PBS, 100 mM NaCl, pH 7 at an overall concentration of 10 μM, and irradiated with the 355 nm flashlamp (Scheme 2.12). After one hour, MALDI-TOF-MS did not detect **56.** Importantly, a new mass corresponding to the loss of nitrogen gas was observed suggesting thioredoxin containing two thiocyanates had been formed. The reaction solution was then treated with 10 mM cysteine in 500 mM phosphate buffer system (pH 7.8) to achieve a 1 mM overall concentration of cysteine and a 9 μM concentration for the protein which was allowed to stand at 5ºC for 16 hours. The reaction solution was then removed by centrifugal

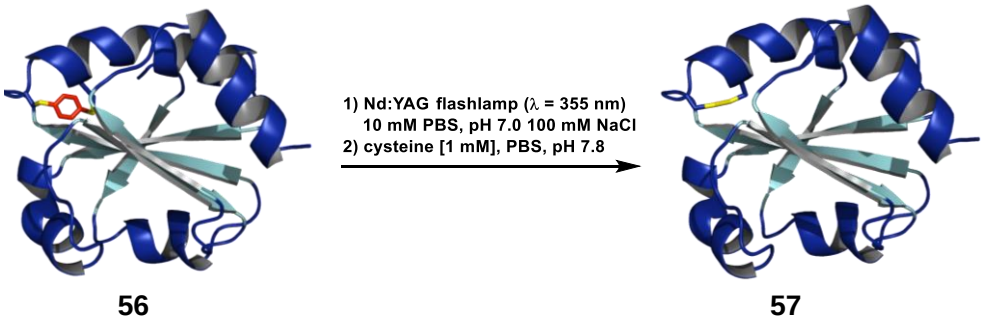

Scheme 2.12. Biocompatible Unstapling Conditions with Laser-Induced Photolysis

filtration and analyzed by MALDI-TOF-MS to find both the loss of the nitriles from the thiocyanates and the molecular mass of regenerated thioredoxin protein.

Bioactivity measurements were then conducted to evaluate **57** resulting from the 355 nm flashlamp photolysis experiment. The insulin reduction assay was conducted, as described in Figure 2.6, with native thioredoxin, **56** and **57** from Scheme 2.12. The protein concentrations were determined by the Bradford method with the assays run in triplicate. Analysis of the data revealed that although the bioactivity of **57** was significantly less than

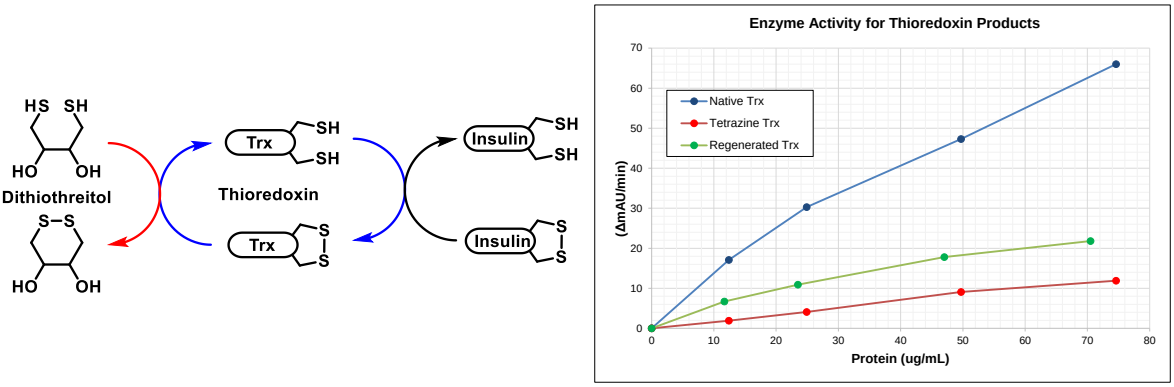

Figure 2.9. Bioactivity Measurement for Regenerated Thioredoxin Resulting from Laser-Induced Photolysis

that of the native thioredoxin, **57** did however display an increase in activity when compared to protein containing tetrazine **56** (Figure 2.9). Pleasingly, this result indicates that some of the native protein was regenerated with the flashlamp conditions for photolysis. This encouraging result demonstrates that these conditions are at least in part compatible with biological systems.

To summarize, conditions have developed and validated for the incorporation of *s*-tetrazine employing cysteine sulfhydryl groups of *unprotected* peptides and the protein thioredoxin. The biphasic reaction enables the construction of macrocyclic peptides, with a wide range of functionally and ring topology, bridging from one to 27 amino acid residues adjoining cysteines. Importantly, the stapled conformations can be released photochemically to their thiocyanate counterparts, and in turn the resulting thiocyanates removed to regenerate the native peptide. To the best of our knowledge *s*-tetrazine comprises the first example of a readily removable peptide staple. Finally, the stapling and unstapling protocol has been extended to include thioredoxin as an example of a protein with an incorporated *s*-tetrazine construct that can also serve a useful role in conjugation strategies.

References for Chapter 2

1. Bock, J. E.; Gavenonis, J.; Kritzer, J. A. *ACS Chem. Biol.* **2013**. 8, 488-499.
2. Veber, D. F.; Holly, F. W.; Nutt, R. F.; Bergstrand, S. J.; Brady, S. F.; Hirschmann, R.; Glitzer, M. S.; Saperstein, R. Nature 1979, 280, 512.
3. Veber, D. F., Freidinger, R. M., Perlow, D. S., Paleveda, W. J., Holly, F. W., Strachan, R. G., Nutt, R. F., Arison, B. H., Homnick, C., Glitzer, M. S., Saperstein, R., and Hirschmann, R. *Nature*. **1981**, 292, 55−58.
4. Hruby, V**.** *Life Sciences*, **1982**, 31, 189-199.
5. Hruby, V. J.; Al-Obeidi, F.; Kazmierski, W. Biochem. J. 1990, 268, 249.
6. Kessler, H.; Holzemann, Liebigs Ann. Chem. **1981**, 2028.
7. Kessler, H. Angew. Chem., Int. Ed. 1982, 21, 512.
8. Marsault, E.; Peterson, M. L. *J. Med. Chem.* **2011**, 54, 1961-2004.
9. White, C. J.; Yudin, A. K. *Nature Chemistry.* 2011, 3, 509-524.
10. Walensky, L. D.; Bird, G. H. *J. Med. Chem.* **2014**, 57, 6275-6288.
11. Gongora-Benítez, M.; Tulla-Puche, J.; Albericio, F. *Chem. Rev.* **2014**, 114, 901−926
12. Pelay-Gimeno, M.; Glas, A.; Koch, O.; Grossmann, T. N. *Angew. Chem. Int. Ed.* **2015**, 54, 8896-8927.
13. Felix, A. M.; Heimer, E. P.; Wang, C.-T.; Lambros, T. J.; Fournier, A.; Mowles, T. F.; Maines, S.; Campbell, R. M.; Wegrzynski, B. B.; Toome, V.; Fry, D.; Madison, V. S. *Int. J. Pept. Protein Res.* **1988**, 32, 441-454.
14. Osapay, G.; Taylor, J. *J. Am. Chem. Soc.* **1990**, 112, 6046-6051
15. Osapay, G.; Taylor, J. *J. Am. Chem. Soc.* **1992**, 114, 6966-6973
16. Jackson, D. Y.; King, D. S.; Chmielewski, J.; Singh, S.; Schultz, P. G. *J. Am. Chem. Soc.* **1991**, *113*, 9391-9392.
17. Blackwell, H. E.; Grubbs, R. H. *Angew. Chem. Int. Ed.* **1998**, 37, 3281-3284.
18. Schafmeister, C. E.; Po, J.; Verdine, G. L. *J. Am. Soc. Chem.* **2000**, 122, 5891-5892.
19. Lau, Y.H.; de Andrade, P.; Wu, Y.; Spring, D.R. *Chem. Soc. Rev*. **2015**, 44, 91-102
20. Schroeder, B. O.; Wu, Z.; Nuding, S.; Groscurth, S.; Marcinowski, M.; Beisner, J.; Buchner, J.; Schaller, M.; Stange, E. F.; Wehkamp, J. *Nature*. **2011**. 469, 419-423

21. Brown, S.P.; Smith A. B., III. *J. Am. Chem. Soc.*, **2015**, *137*, 4034–4037.
22. Catsimpoolas, N.; Wood, J. L. *J. Biol. Chem*. **1964**, 239, 4132
23. Catsimpoolas, N; Wood, J. L. *J. Biol. Chem.* **1966**, 241, 1790.
24. Degani, Y.; Neumann, H.; Patchorn, A. *J. Am. Chem. Soc*. **1970**, 92, 6969.
25. Dawson, P.E.; Muir, T.W.; Clark-Lewis, I.; Kent, S.B.H. *Science*. **1994**. 266, 776 – 779.
26. Carboni, R.A.; Lindsey, R.V. *J. Am. Chem. Soc.* **1959**, 81, 4342.
27. Blackman, M.L.; Royzen, M.; Fox, J.M. *J. Am. Chem. Soc.* **2008**. 130, 13518-13519.
28. *Selvaraj, R.; Fox, J. M. Curr. Opin. Chem. Biol.* ***2013****, 17, 753-760.*
29. *Wu, Z., Liu, S., Hassink, M., Nair, I., Park, R., Li, L., Todorov, I., Fox, J. M., Li, Z., Shively, J. E., Conti, P. S., Kandeel, F. J. Nucl. Med.* ***2013****, 54, 244-251.*
30. Bradford, M. M. *Anal. Biochem*. **1976**. 72, 248-254.

Experimental for Chapter 2

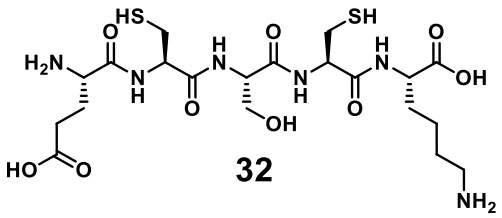

Peptide 32. was constructed by SPPS from 1.0 mmol loaded 2-chloro-chlorotrityl resin. Removal of the peptide from resin was conducted with cocktail A (20 mL) following the general cleavage method. The peptide was purified by reverse-phase HPLC (5 - 15% organic over 5 min) to give 360 mg (45% •2 TFA salt form) of a white amorphous powder after lyophilization: HRMS (ES) found *m/z* 569.2067 [$(M+H)^+$; calcd for $C_{28}H_{37}N_6O_9S_2$: 569.2063]; ^{1}H NMR (500 MHz, D_2O) δ ppm 1.38 - 1.48 (m, 2 H) 1.68 (quin, *J* = 7.3 Hz, 2 H) 1.72 - 1.81 (m, 1 H) 1.85 - 1.94 (m, 1 H) 2.19 (q, *J* = 7.3 Hz, 2 H) 2.55 (t, *J* = 7.3 Hz, 2 H) 2.90 - 3.02 (m, 6 H) 3.89 (t, *J* = 4.9 Hz, 2 H) 4.14 (t, *J* = 6.5 Hz, 1 H) 4.32 (dd, *J* = 8.9, 5.2 Hz, 1 H) 4.52 (t, *J* = 5.4 Hz, 1 H) 4.58 (t, *J* = 6.2 Hz, 1 H) 4.61 (t, *J* = 6.30 Hz, 1 H); ^{13}C NMR (126MHz, D_2O) δ 176.6, 176.2, 171.6, 171.5, 171.4, 169.4, 61.1, 55.8, 55.7, 55.6, 53.4, 52.4, 39.3, 30.3, 29.4, 26.3, 26.1, 25.5, 25.4, 22.2**;** IR (KBr, cm^{-1}) 3425 (br), 3286 (br), 3077 (br), 2950 (br), 1682 (s), 1628(s), 1535 (m), 1429 (m), 1207 (s), 1132 (s).

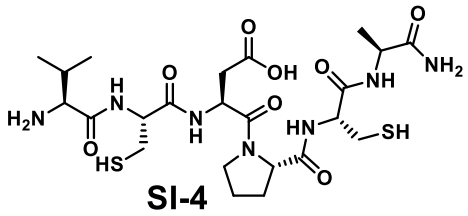

Peptide SI-4. was constructed by SPPS from 0.10 mmol loaded Rink amide resin. Removal of the peptide from resin was conducted with cocktail A following the general cleavage method. The peptide was purified by reverse-phase HPLC (5 - 35% organic over 12 min) to give 46.4 mg (65% • TFA salt form) of a white amorphous powder after lyophilization: HRMS (ES) Found *m/z* 606.2378 [$(M+H)^+$; calcd for $C_{23}H_{40}N_7O_8S_2$: 606.2380]; ^{1}H NMR (500MHz ,DMSO-d_6) δ 8.55 (br. s., 1 H), 8.52 (d, *J* = 7.3 Hz, 2 H), 8.08 (d, *J* = 7.3 Hz, 1 H), 7.74 (d, *J* = 7.5 Hz, 1 H), 7.06 (s, 2 H), 7.02 (s, 2 H), 4.78 (q, *J* = 6.9 Hz, 1 H), 4.44 (dd, *J* = 5.4, 11.3 Hz, 1 H), 4.27 (dd, *J* = 3.8, 8.5 Hz, 1 H), 4.23 (dd, *J* = 4.8, 8.1 Hz, 1 H), 4.21 (dd, *J* = 4.8, 8.3 Hz, 1 H), 4.11 (quin, *J* = 7.2 Hz, 1 H), 3.71 (t, *J* = 6.3 Hz, 2 H), 3.55 (d, *J* = 5.5 Hz, 1 H), 2.82 (d, *J* = 4.6 Hz, 1 H), 2.83 (dd, *J* = 4.8, 13.7 Hz, 1 H), 2.76 (br. s., 1 H), 2.77 (dd, *J* = 8.5, 15.0 Hz, 1 H), 2.75 (br. s., 1 H), 2.71 (dd, *J* = 7.1, 16.4 Hz, 1 H), 2.42 (dd, *J* = 6.9, 16.2 Hz, 1 H), 2.11 - 2.00 (m, 2 H), 1.99 - 1.92 (m, 1 H), 1.92 - 1.84 (m, 2 H), 1.23 (d, *J* = 7.1 Hz, 3 H), 0.92 (d, *J* = 6.7 Hz, 3 H), 0.89 (d, *J* = 6.7 Hz, 3 H); ^{13}C NMR (126 MHz, DMSO-d_6) δ 174.1, 171.9, 171.7, 169.2, 168.9, 167.9, 60.2, 57.2, 55.5, 54.9, 48.3, 47.8, 47.0, 35.6, 29.9, 29.1, 26.3, 25.8, 24.5, 18.4, 18.0, 17.7; IR (KBr, cm^{-1}) 3332(br), 3067(m), 2974(m), 1664(vs), 1525(m), 1451(w), 1200(m), 1132(w).

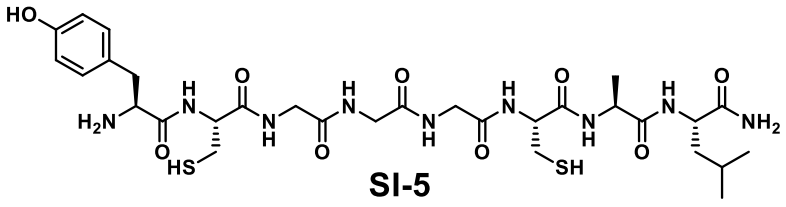

SI-5

Peptide SI-5. was constructed by SPPS from 0.10 mmol loaded Rink amide resin. Removal of the peptide from resin was conducted with cocktail A following the general cleavage

method. The peptide was purified by reverse-phase HPLC (5 - 35% organic over 15 min) to give 39.2 mg (46% • TFA salt form) of a white amorphous powder after lyophilization: HRMS (ES) Found *m/z* 742.3011 [$(M+H)^+$; calcd for $C_{30}H_{48}N_9O_9S_2$: 742.3016]; ^{1}H NMR (500MHz ,DMSO-d_6) δ = 9.37 (br. s., 1 H), 8.82 (d, *J* = 7.7 Hz, 1 H), 8.31 (br. t, *J* = 5.6 Hz, 2 H), 8.22 (d, *J* = 7.1 Hz, 1 H), 8.18 (t, *J* = 5.0 Hz, 1 H), 8.10 (d, *J* = 7.1 Hz, 2 H), 7.73 (d, *J* = 8.1 Hz, 1 H), 7.23 (s, 1 H), 7.05 (d, *J* = 8.1 Hz, 2 H), 6.97 (s, 1 H), 6.71 - 6.67 (m, *J* = 8.1 Hz, 2 H), 4.49 (dd, *J* = 6.7, 13.7 Hz, 1 H), 4.41 (dd, *J* = 7.3, 13.1 Hz, 1 H), 4.23 (dd, *J* = 7.1, 14.3 Hz, 1 H), 4.19 (dd, *J* = 8.1, 15.7 Hz, 1 H), 4.04 (t, *J* = 5.9 Hz, 1 H), 3.85 (dd, *J* = 5.7, 16.6 Hz, 1 H), 3.77 (d, *J* = 5.4 Hz, 6 H), 3.75 (dd, *J* = 5.5, 17.0 Hz, 1 H), 3.01 (dd, *J* = 5.2, 14.3 Hz, 1 H), 2.85 - 2.74 (m, 4 H), 2.75 - 2.65 (m, 1 H), 2.40 (t, *J* = 8.4 Hz, 1 H), 1.58 (quind, *J* = 6.6, 13.3 Hz, 1 H), 1.45 (t, *J* = 7.2 Hz, 2 H), 1.22 (d, *J* = 7.1 Hz, 3 H), 0.87 (d, *J* = 6.7 Hz, 3 H), 0.82 (d, *J* = 6.5 Hz, 3 H); ^{13}C NMR (126MHz ,DMSO-d_6) δ 174.0, 171.7, 169.5, 169.3, 169.2, 169.0, 168.9, 168.3, 156.6, 130.5, 124.7, 115.4 (2C), 55.1, 54.9, 53.6, 50.9, 48.7, 42.0, 42.0, 42.0, 41.0, 36.2, 26.2, 26.2, 24.2, 23.1, 21.6, 17.6; IR (KBr, cm^{-1}) 3306(br), 2957(m), 1661(vs), 1518(s), 1202(m), 1136(w).

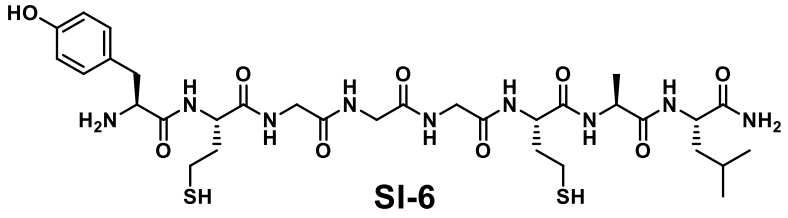

SI-6

Peptide SI-6. was constructed by SPPS from 0.10 mmol loaded Rink amide resin. Removal of the peptide from resin was conducted with cocktail A following the general cleavage method. The peptide was purified by reverse-phase HPLC (5 - 35% organic over 15 min)

to give 43.8 mg (50% • TFA salt form) of a white amorphous powder after lyophilization: HRMS (ES) Found *m/z* 770.3336 [(M+H)$^+$; calcd for $C_{40}H_{487}N_7O_7S_2$: 770.3336]; ^{1}H NMR (500 MHz, DMSO-d_6) δ 9.33 (s, 1H), 8.67 (d, *J* = 8.0 Hz, 1H), 8.18 (t, *J* = 5.8 Hz, 1H), 8.14 (q, *J* = 5.5 Hz, 2H), 8.09 (d, *J* = 7.2 Hz, 1H), 8.06 – 7.98 (m, 3H), 7.69 (d, *J* = 8.4 Hz, 1H), 7.22 (s, 1H), 7.03 (d, *J* = 8.5 Hz, 2H), 6.94 (s, 1H), 6.69 (d, *J* = 8.5 Hz, 2H), 4.47 (ddd, *J* = 8.2, 5.3 Hz, 1H), 4.38 (ddd, *J* = 8.3, 5.1 Hz, 1H), 4.28 – 4.13 (m, 2H), 4.02 – 3.93 (m, 1H), 3.83 (dd, *J* = 16.6, 5.8 Hz, 1H), 3.79 – 3.68 (m, 4H), 2.99 (dd, *J* = 14.2, 5.4 Hz, 1H), 2.79 (dd, *J* = 13.8, 8.5 Hz, 1H), 2.68 (s, 0H), 2.48 – 2.40 (m, 2H), 2.37 (t, *J* = 8.0 Hz, 1H), 2.29 (t, *J* = 8.0 Hz, 1H), 2.08 – 1.74 (m, 4H), 1.58 (dt, *J* = 13.4, 6.7 Hz, 1H), 1.45 (dd, *J* = 8.4, 6.2 Hz, 2H), 1.21 (d, *J* = 7.1 Hz, 3H), 0.88 (d, *J* = 6.6 Hz, 3H), 0.83 (d, *J* = 6.5 Hz, 3H); ^{13}C NMR (126 MHz, DMSO) δ 173.9, 171.7, 170.7, 170.5, 169.1, 168.9, 168.8, 168.1, 156.5, 130.4, 124.7, 115.3, 53.6, 51.7, 51.5, 50.8, 48.4, 42.0, 41.9, 41.0, 36.8, 36.5, 36.1, 24.2, 23.0, 21.6, 20.3, 20.2, 17.6; IR (KBr, cm^{-1}) 3309(br), 2956(m), 1662(vs), 1515(s), 1202(m), 1136(w).

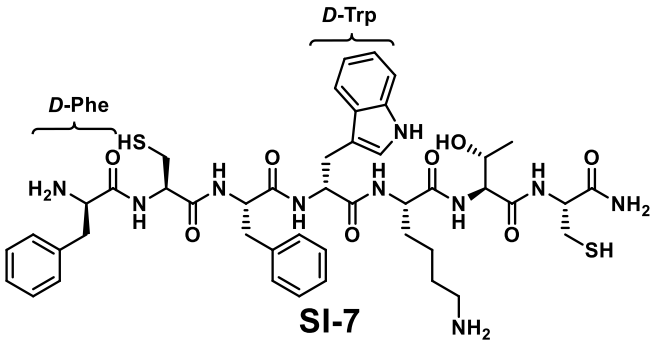

SI-7

Peptide SI-7. was constructed by SPPS from 0.10 mmol loaded Rink amide resin. Removal of the peptide from resin was conducted with cocktail B following the general cleavage method. The peptide was purified by reverse-phase HPLC (5 - 60% organic over 12 min)

to give 45.6 mg (44% • TFA salt form) of a white amorphous powder after lyophilization: HRMS (ES) Found *m/z* 933.4111 [$(M+H)^+$; calcd for $C_{45}H_{61}N_{10}O_8S_2$: 933.4115]; ^{1}H NMR (500 MHz, DMSO-d_6) δ 10.81 (s, 1H), 8.63 (d, *J* = 8.0 Hz, 1H), 8.33 (d, *J* = 8.3 Hz, 1H), 8.28 (d, *J* = 8.1 Hz, 1H), 8.17 (d, *J* = 8.0 Hz, 1H), 8.15 (s, 2H), 7.99 (d, *J* = 8.0 Hz, 1H), 7.85 (d, *J* = 8.0 Hz, 1H), 7.71 (s, 2H), 7.66 (d, *J* = 7.9 Hz, 1H), 7.39 (s, 1H), 7.36 – 7.23 (m, 5H), 7.15 (d, *J* = 2.4 Hz, 1H), 7.11 (dt, *J* = 4.9, 1.7 Hz, 2H), 7.06 – 7.01 (m, 3H), 7.01 – 6.94 (m, 1H), 4.68 (ddd, *J* = 8.4, 5.8 Hz, 1H), 4.54 (ddd, *J* = 8.6, 4.3 Hz, 1H), 4.42 (q, *J* = 6.5 Hz, 1H), 4.36 (dp, *J* = 10.5, 5.6, 4.9 Hz, 2H), 4.23 (dd, *J* = 7.9, 4.3 Hz, 1H), 4.17 – 4.10 (m, 1H), 4.03 (dd, *J* = 6.5, 4.5 Hz, 1H), 3.11 – 3.02 (m, 2H), 2.96 (dd, *J* = 14.0, 7.8 Hz, 1H), 2.92 – 2.81 (m, 2H), 2.81 – 2.72 (m, 2H), 2.72 – 2.64 (m, 2H), 2.54 (t, *J* = 7.9 Hz, 1H), 2.29 (t, *J* = 8.5 Hz, 1H), 2.02 (t, *J* = 8.6 Hz, 1H), 1.63 (td, *J* = 13.3, 6.9 Hz, 1H), 1.53 – 1.36 (m, 3H), 1.13 (p, *J* = 7.4 Hz, 2H), 1.05 (d, *J* = 6.3 Hz, 3H); ^{13}C NMR (126 MHz, DMSO) δ 171.8, 171.4, 171.3, 170.3, 169.8, 168.8, 168.0, 137.5, 136.1, 134.8, 129.5, 129.5, 129.2, 128.5, 127.9, 127.2, 127.2, 126.1, 123.9, 120.8, 118.6, 118.1, 111.2, 109.7, 66.3, 58.3, 54.6, 54.5, 54.0, 53.3, 53.2, 52.1, 38.7, 37.3, 37.3, 31.3, 28.7, 26.7, 26.6, 26.1, 22.0, 19.5; IR (KBr, cm^{-1}) 3281(br), 2928(w), 1671(s), 1523(m), 1202(m).

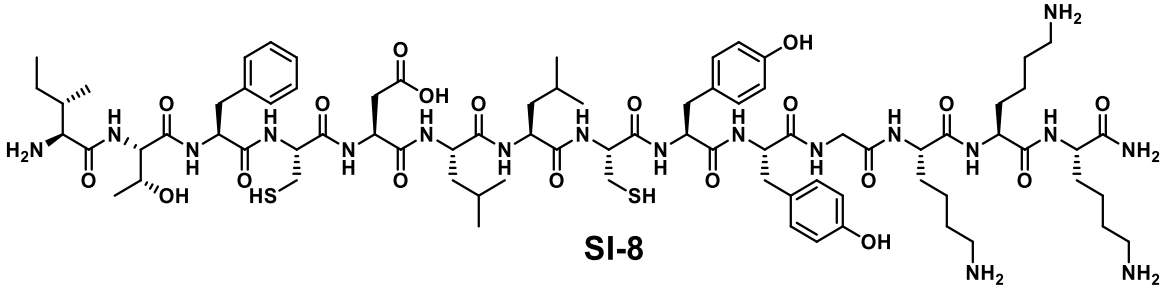

SI-8

Peptide SI-8. was constructed by SPPS from 0.10 mmol loaded Rink amide resin. Removal of the peptide from resin was conducted with cocktail A following the general cleavage

method. The peptide was purified by reverse-phase HPLC [eluent water/MeCN/AcOH (85:10:5) and MeCN (organic) buffered with 0.1%TFA] (5 - 40% organic over 15 min) to give 49.5 mg (23% • 4 TFA salt form) of a white amorphous powder after lyophilization: MALDI-TOF Found *m/z* 1694.004 [$(M+H)^+$; calcd for $C_{79}H_{125}N_{18}O_{19}S_2$: 1693.880]; ^{1}H NMR (500 MHz, DMSO-d_6) δ 12.45 (s, 1H), 9.21 (d, *J* = 15.0 Hz, 2H), 8.43 (d, *J* = 7.5 Hz, 1H), 8.31 (dd, *J* = 8.2, 3.8 Hz, 2H), 8.16 – 7.87 (m, 13H), 7.85 (d, *J* = 7.9 Hz, 2H), 7.81 – 7.62 (m, 13H), 7.39 (s, 1H), 7.25 – 7.18 (m, 4H), 7.18 – 7.12 (m, 1H), 7.06 (s, 1H), 7.01 (d, *J* = 8.5 Hz, 2H), 6.93 (d, *J* = 8.3 Hz, 2H), 6.63 (d, *J* = 8.3 Hz, 2H), 6.60 (d, *J* = 8.5 Hz, 2H), 5.00 (d, *J* = 4.4 Hz, 1H), 4.62 (dq, *J* = 7.9, 4.7 Hz, 1H), 4.57 (q, *J* = 7.1 Hz, 1H), 4.41 (q, *J* = 7.2 Hz, 2H), 4.38 – 4.23 (m, 6H), 4.20 (q, *J* = 7.7 Hz, 1H), 4.18 – 4.08 (m, 1H), 3.93 (q, *J* = 4.9 Hz, 1H), 3.82 – 3.64 (m, 3H), 3.05 (dd, *J* = 14.2, 3.9 Hz, 1H), 2.90 (dd, *J* = 14.0, 3.2 Hz, 1H), 2.82 (t, *J* = 7.1 Hz, 2H), 2.79 – 2.56 (m, 15H), 2.38 (t, *J* = 8.6 Hz, 1H), 2.21 (t, *J* = 8.5 Hz, 1H), 1.79 – 1.55 (m, 7H), 1.56 – 1.47 (m, 11H), 1.47 – 1.37 (m, 5H), 1.37 – 1.23 (m, 3H), 1.24 – 1.19 (m, 1H), 1.05 (d, *J* = 6.3 Hz, 4H), 0.86 (t, *J* = 6.7 Hz, 7H), 0.83 – 0.74 (m, 13H); ^{13}C NMR (126 MHz, DMSO-d_6) δ 173.4 , 172.1 , 171.7 , 171.6 , 171.4 , 171.3 , 170.9 , 170.9 , 170.4 , 169.6 , 168.7 , 167.9 , 155.9 , 155.8 , 137.5 , 130.1 , 130.0 , 129.1 , 128.0 , 126.2 , 118.5 , 114.9 , 114.9 , 66.9 , 57.9 , 56.3 , 55.0 , 54.5 , 54.3 , 53.6 , 52.5 , 52.2 , 52.1 , 51.2 , 49.7 , 40.7 , 40.3 , 39.3 , 39.1 , 38.8 , 38.7 , 38.7 , 36.3 , 31.5 , 31.2 , 26.7 , 26.6 , 26.4 , 24.1 , 24.0 , 23.8 , 23.2 , 23.1 , 22.3 , 22.3 , 21.6 , 21.5 , 19.3 , 14.5 , 11.1; IR (KBr, cm^{-1}) 3285(br), 3080(br), 2960(m), 1676(s), 1634(s), 1516(m), 1203(m), 1137(m).

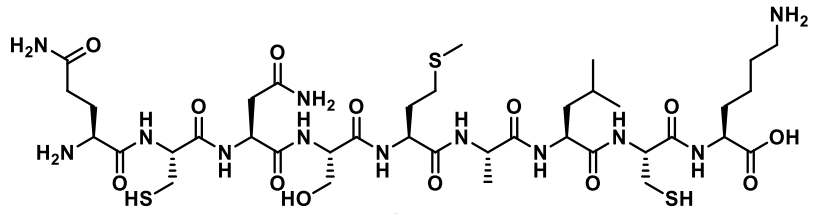

SI-9

Peptide SI-9 was constructed by SPPS from 0.20 mmol loaded 2-chloro-chlorotirtyl resin. Removal of the peptide from resin was conducted with cocktail C following the general cleavage method. The peptide was purified by reverse-phase HPLC (5 - 60% organic over 15 min) to give 124 mg (51% • 2 TFA salt form) of a white amorphous powder after lyophilization: HRMS (ES) Found *m/z* 997.4268 [$(M+H)^+$; calcd for $C_{38}H_{69}N_{12}O_{13}S_3$: 997.4269]; ^{1}H NMR (500 MHz, DMSO-d_6) δ 8.8 (d, *J* = 7.9 Hz, 1H), 8.5 (d, *J* = 7.4 Hz, 1H), 8.2 (s, 3H), 8.2 (d, *J* = 7.6 Hz, 1H), 8.1 (d, *J* = 7.7 Hz, 1H), 8.1 (d, *J* = 6.9 Hz, 1H), 7.9 (d, *J* = 7.1 Hz, 1H), 7.9 (dd, *J* = 8.0, 2.4 Hz, 2H), 7.8 (s, 3H), 7.5 (d, *J* = 26.5 Hz, 2H), 7.0 (d, *J* = 30.5 Hz, 2H), 5.1 (s, 1H), 4.6 (q, *J* = 7.1 Hz, 1H), 4.5 (td, *J* = 7.5, 5.3 Hz, 1H), 4.4 (td, *J* = 7.7, 5.0 Hz, 1H), 4.3 (ddd, *J* = 13.6, 9.1, 4.8 Hz, 1H), 4.3 (d, *J* = 7.6 Hz, 1H), 4.2 – 4.2 (m, 2H), 4.1 (td, *J* = 8.5, 4.7 Hz, 1H), 3.9 (s, 1H), 3.6 (s, 1H), 3.6 (s, 1H), 2.9 – 2.7 (m, 7H), 2.6 (dd, *J* = 15.5, 6.1 Hz, 1H), 2.5 (d, *J* = 1.8 Hz, 10H), 2.5 – 2.4 (m, 3H), 2.3 (t, *J* = 8.6 Hz, 1H), 2.2 (dd, *J* = 9.1, 6.5 Hz, 2H), 2.0 (s, 3H), 2.0 – 1.9 (m, 3H), 1.9 – 1.8 (m, 1H), 1.8 – 1.7 (m, 1H), 1.6 (dt, *J* = 11.3, 5.5 Hz, 2H), 1.6 – 1.5 (m, 2H), 1.5 (t, *J* = 7.3 Hz, 2H), 1.3 (q, *J* = 8.2 Hz, 2H), 1.2 (d, *J* = 7.1 Hz, 3H), 0.9 (d, *J* = 6.5 Hz, 3H), 0.8 (d, *J* = 6.5 Hz, 3H); ^{13}C NMR (126 MHz, DMSO-d_6) δ 173.5, 173.4, 172.1, 172.0, 171.6, 171.3, 171.0, 170.3, 169.7, 169.2, 168.5, 61.4, 55.7, 55.0, 54.7, 52.1, 51.8, 51.8, 51.1, 49.9, 48.4, 40.5, 38.6, 37.0, 31.3, 30.3, 30.3, 29.6, 27.0, 26.6, 26.4, 26.4, 24.1, 23.2, 22.4, 21.5, 17.6,

14.7; IR (KBr, cm^{-1}) 3286(br), 3078(w), 2960(w), 1664(s), 1635(s), 1541(m), 1202(m), 1137(w), 1033(m), 1008(m).

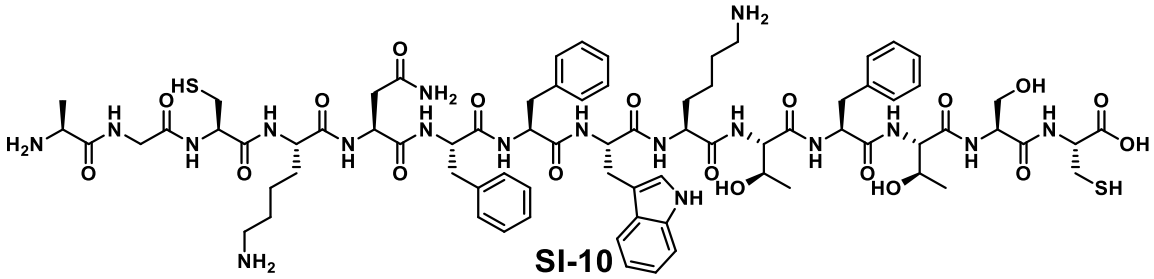

Peptide SI-10. was constructed by automated SPPS from 0.10 mmol pre-loaded Fmoc-Cys(Trt)-Wang resin. Removal of the peptide from resin was conducted with cocktail B following the general cleavage method. The peptide was purified by reverse-phase HPLC (10 - 60% organic over 15 min) to give 38 mg (19% • 3 TFA salt form) of a white amorphous powder after lyophilization: MALDI-TOF Found *m/z* 1639.125 [$(M+H)^+$; calcd for $C_{76}H_{107}N_{18}O_{19}S_2$: 1639.740]; ^{1}H NMR (500 MHz, DMSO-d_6) δ 10.79 (s, 1H), 8.67 (t, *J* = 5.8 Hz, 1H), 8.28 – 8.01 (m, 8H), 8.01 – 7.87 (m, 4H), 7.84 – 7.64 (m, 7H), 7.61 (d, *J* = 7.9 Hz, 1H), 7.47 (s, 1H), 7.32 (d, *J* = 8.0 Hz, 1H), 7.28 – 7.13 (m, 13H), 7.13 – 7.08 (m, 5H), 7.08 – 7.01 (m, 2H), 6.98 (t, *J* = 7.4 Hz, 1H), 6.60 (s, 1H), 5.17 – 5.07 (m, 1H), 4.90 (d, *J* = 5.0 Hz, 1H), 4.71 – 4.62 (m, 1H), 4.57 (q, *J* = 7.4 Hz, 1H), 4.51 (q, *J* = 6.8 Hz, 2H), 4.48 – 4.41 (m, 3H), 4.41 – 4.30 (m, 5H), 4.25 – 4.15 (m, 2H), 4.05 – 3.93 (m, 3H), 3.94 – 3.86 (m, 2H), 3.82 (dd, *J* = 16.8, 5.6 Hz, 1H), 3.72 – 3.54 (m, 4H), 3.50 (s, 1H), 3.18 – 3.11 (m, 2H), 3.11 – 3.05 (m, 2H), 3.03 – 2.93 (m, 3H), 2.93 – 2.75 (m, 7H), 2.75 – 2.62 (m, 7H), 2.45 – 2.39 (m, 1H), 2.36 (dd, *J* = 15.5, 6.3 Hz, 1H), 1.71 – 1.56 (m, 3H), 1.56 – 1.39 (m, 8H), 1.35 (d, *J* = 7.0 Hz, 3H), 1.32 – 1.16 (m, 5H), 1.14 (d, *J* = 6.8 Hz, 1H), 1.04 (d, *J* = 6.3 Hz, 3H), 0.99 (d, *J* = 6.2 Hz, 3H); ^{13}C NMR (126 MHz, DMSO-d_6) δ 171.8, 171.4,

171.4, 171.2, 171.1, 171.0, 170.9, 170.7, 170.5, 169.9, 169.8, 169.7, 169.7, 169.7, 168.4, 137.8, 137.6, 137.6, 136.1, 129.3, 129.3, 129.1, 128.1, 128.0, 128.0, 127.4, 126.2, 126.2, 123.7, 120.9, 118.3, 109.9, 72.5, 70.6, 70.5, 69.8, 66.8, 66.5, 63.1, 61.8, 61.6, 57.9, 57.9, 57.8, 57.8, 55.0, 54.6, 54.1, 53.9, 53.7, 53.4, 52.4, 52.3, 49.6, 48.2, 41.8, 37.4, 37.2, 37.1, 31.3, 31.2, 27.7, 26.7, 26.7, 26.6, 25.6, 22.3, 22.2, 19.4, 19.3, 19.3, 17.3; IR (KBr, cm^{-1}) 3399(br), 3298(br), 3063(w), 2929(w), 1663(s), 1553(m), 1202(w), 1134(w), 1032(w), 1008(w).

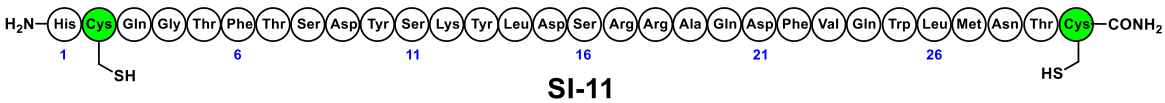

SI-11

Peptide SI-11. was constructed by automated SPPS from 0.10 mmol loaded Rink amide resin. Removal of the peptide from resin was conducted with cocktail B following the general cleavage method. The peptide was purified by reverse-phase HPLC (10 - 60% organic over 20 min) to give 39.6 mg (11% • 4 TFA salt form) of a white amorphous powder after lyophilization: MALDI-TOF Found *m/z* 3600.001 [$(M+H)^+$; calcd for $C_{156}H_{231}N_{45}O_{48}S_3$: 3599.625]; IR (KBr, cm^{-1}) 3306(br), 2933(w), 1655(s), 1541(m), 1202(m).

General Phase-Transfer Protocol for Tetrazine Insertion

A round bottom flask, was charged with unprotected peptide **1** (1 - 1000 µmol) then sealed with a septum and purged with argon. Next, a degassed solution of 50mM (pH ~5) mono-sodium phosphate was added (1 -2 mM concentration of peptide in solution) followed by a solution of dichlorotetrazine (3 equiv) in $CHCl_3$ (equal volume to peptide). The two-phases were stirred vigorously for 1 minute. The mixture was divide between Falcon tubes then transferred to a benchtop centrifuge and further separated at 2500 RPM for 1 minute. The aqueous phase, now orange in color, was collected and each organic layer was ex-tracted with an additional portion of water then transferred to a benchtop centrifuge and separated again at 2500 RPM for 1 minute. All of the aqueous fractions were combined and lyophilized. The crude mixture was then purified by reverse-phase high-pressure liquid chromatography (HPLC) to yield an orange powder after lyophilization.

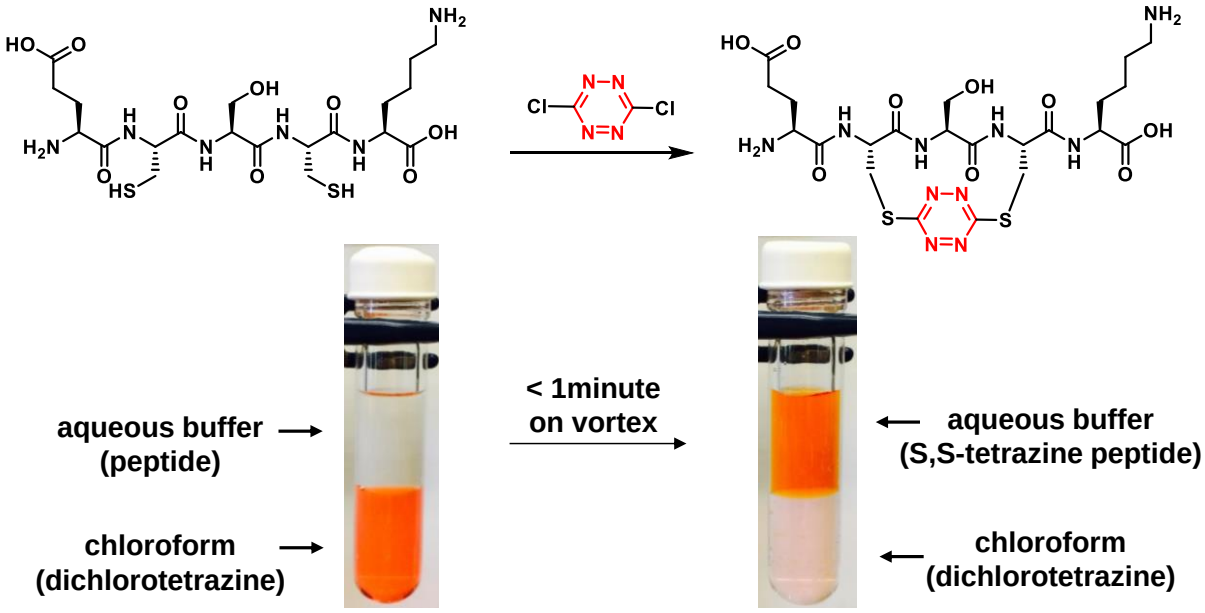

Conditions for the above reaction are different from the general phase-transfer protocol and employ only 1.1 equivalents of dichlorotetrazine to illustrate the colorimetric transfer of tetrazine into the peptide.

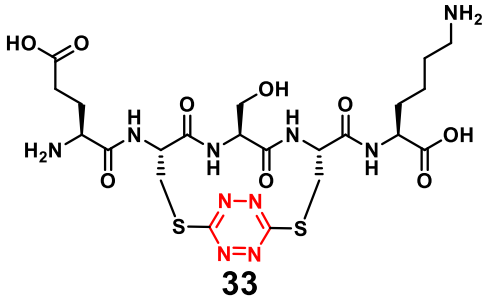

33

Peptide 33. Peptide **1a** (5.7 mg, 10 µmol) was subjected to the general phase-transfer protocol to construct **33**. The crude reaction mixture was purified by reverse-phase HPLC (gradient 5-15% organic over 5 min) to give (5.1 mg, 78%) of an orange powder after lyophilization. HRMS (ES) Found *m/z* 647.2028 $[(M+H)^+$; calcd for $C_{22}H_{35}N_{10}O_9S_2$: 647.2030]; ^{1}H NMR (500 MHz, D_2O) δ ppm 1.36 (quin, *J*=7.80 Hz, 2 H) 1.58 - 1.66 (m, 3

H) 1.68 (q, *J*=7.90 Hz, 2 H) 1.79 (ddd, *J*=13.90, 8.30, 5.50 Hz, 1 H) 1.78 (ddd, *J*=13.25, 8.10, 5.30 Hz, 1 H) 2.07 (q, *J*=7.34 Hz, 2 H) 2.39 (dd, *J*=7.30, 5.10 Hz, 1 H) 2.39 (dd, *J*=9.80, 7.40 Hz, 1 H) 2.93 (t, *J*=7.48 Hz, 9 H) 3.50 (dd, *J*=15.60, 4.06 Hz, 3 H) 3.54 (dd, *J*=18.20, 6.20 Hz, 1 H) 3.57 (dd, *J*=11.30, 7.70 Hz, 1 H) 4.10 (t, *J*=6.52 Hz, 1 H) 4.14 (dd, *J*=8.44, 5.24 Hz, 1 H) 4.20 (dd, *J*=7.10, 6.40 Hz, 1 H) 4.53 (dd, *J*=15.39, 2.99 Hz, 1 H) 4.56 (dd, *J*=15.60, 4.92 Hz, 1 H) 4.80 (t, *J*=3.42 Hz, 1 H) 4.99 (dd, *J*=4.90, 1.90 Hz, 1 H); ^{13}C NMR (126 MHz, Deuterium Oxide) δ 178.6, 178.1, 171.7, 170.6, 170.4, 169.9, 169.1, 169.1, 61.8, 55.0, 53.9, 52.4, 52.2, 51.5, 39.1, 31.4, 31.1, 30.7, 30.2, 26.7, 26.2, 22.1; IR (KBr, cm^{-1}) 3430(br), 3291(br), 3074(br), 2945(br), 1658(s), 1525(m), 1197(s), 1139(m); UV-vis λ_{Max} 278 nm, 419 nm, 507 nm.

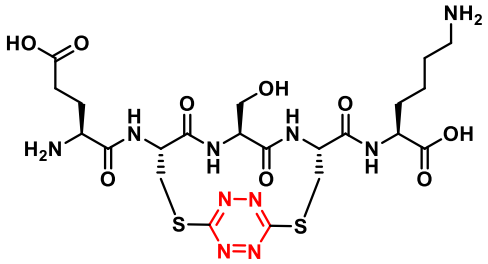

33

(Large Scale) Peptide 33. Peptide **32** (570 mg, 1000 µmol) was subjected to the general phase-transfer protocol to construct **33**. The crude reaction mixture was purified by reverse-phase HPLC (gradient 5-15% organic over 5 min) to give (465 mg, 72 %) of an orange powder after lyophilization. Spectral data was identical to compound **33**.

UV-Vis Spectrum of Peptide 33 [73 µM] in pH 7.8 buffer

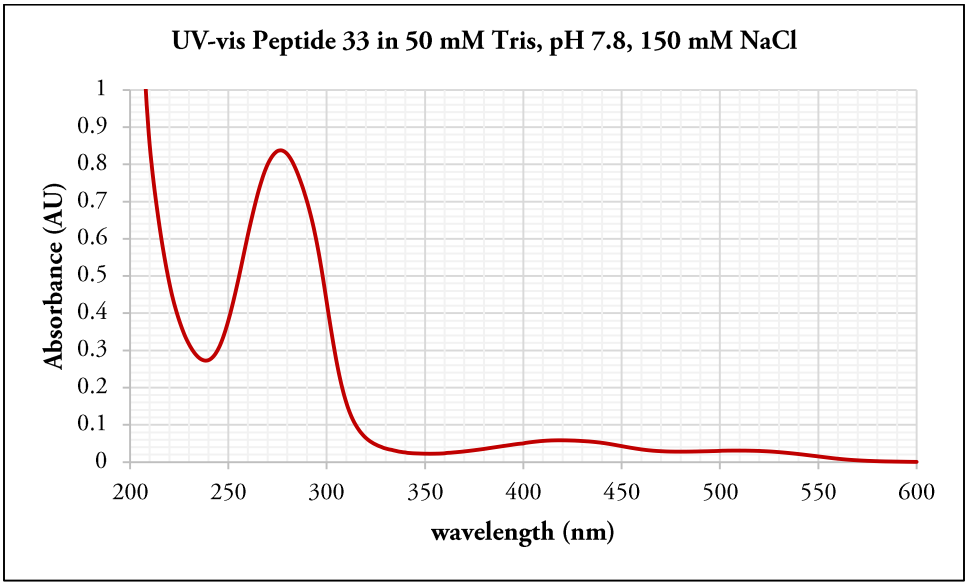

Zoom Region 300 – 600 nm: UV-Vis Spectrum of Peptide 33 [73 µM] in pH 7.8 buffer

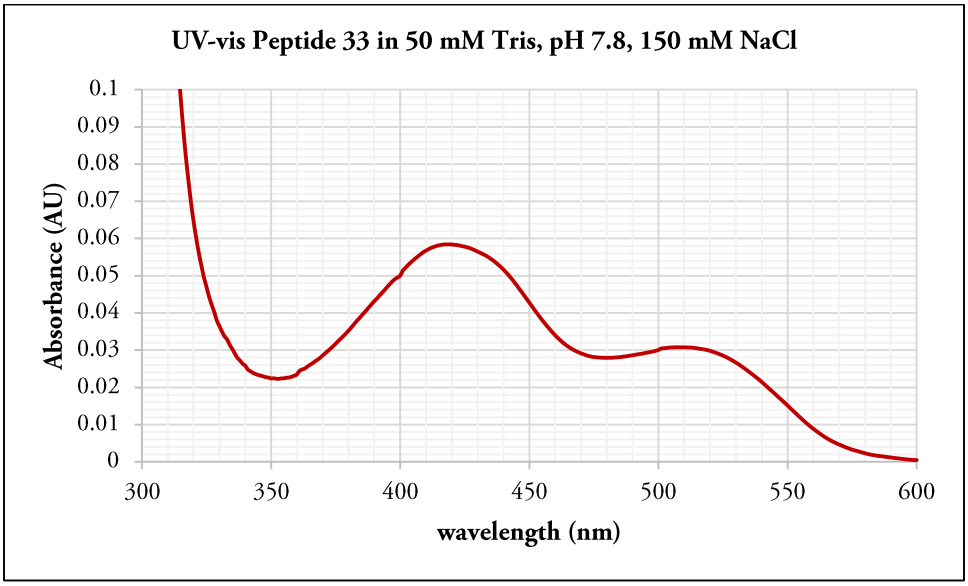

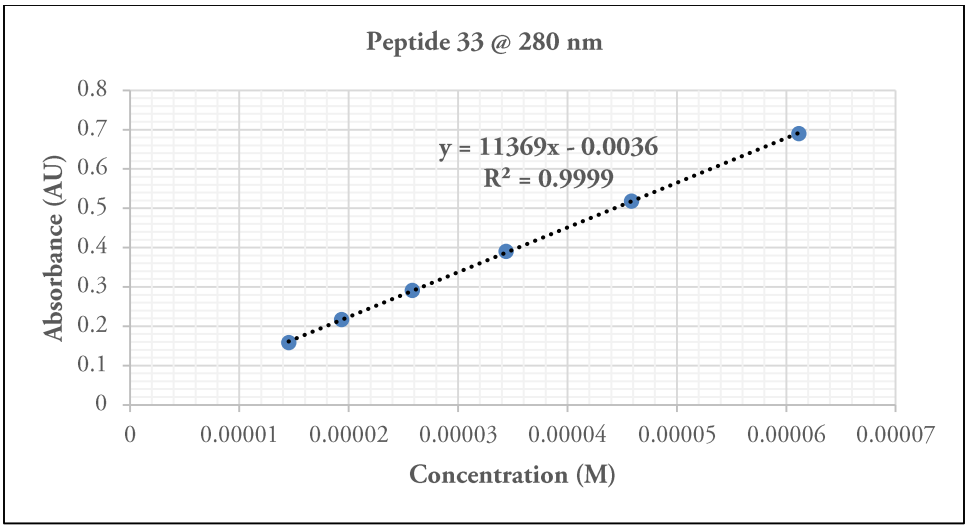
Peptide 33 @ 280 nm
y = 11369x - 0.0036
R² = 0.9999
Absorbance (AU)
Concentration (M)
0.8
0.7
0.6
0.5
0.4
0.3
0.2
0.1
0
0
0.00001
0.00002
0.00003
0.00004
0.00005
0.00006
0.00007

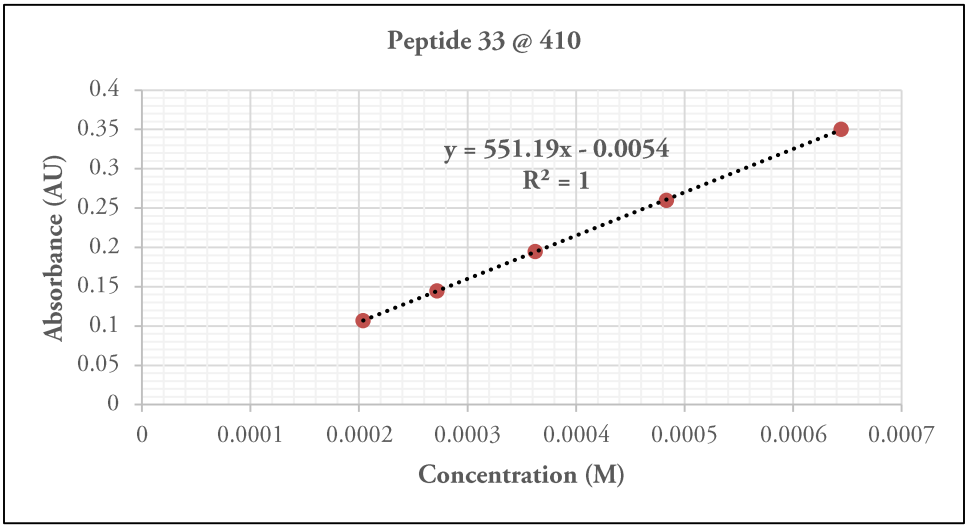
Peptide 33 @ 410
y = 551.19x - 0.0054
R² = 1
Absorbance (AU)
Concentration (M)
0.4
0.35
0.3
0.25
0.2
0.15
0.1
0.05
0
0
0.0001
0.0002
0.0003
0.0004
0.0005
0.0006
0.0007

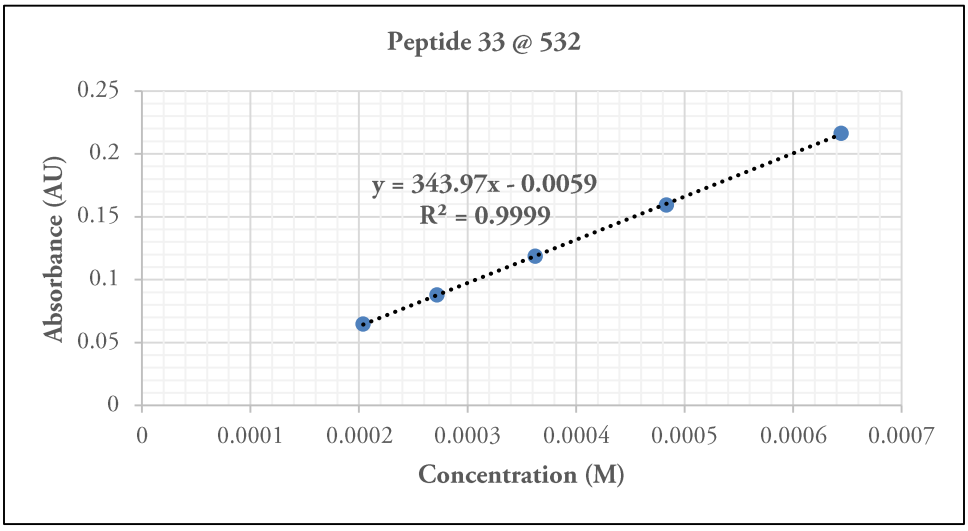
Peptide 33 @ 532
y = 343.97x - 0.0059
R² = 0.9999
Absorbance (AU)
Concentration (M)
0.25
0.2
0.15
0.1
0.05
0
0
0.0001
0.0002
0.0003
0.0004
0.0005
0.0006
0.0007

Table of Stabilty Data for the S,S-Tetrazine Peptide 33

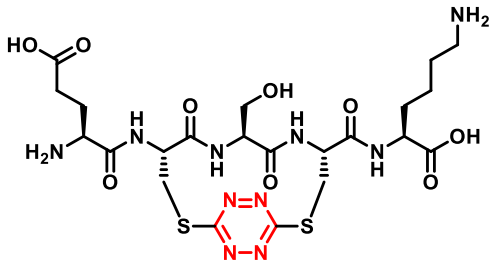

33

Buffer	Stability
100 mM phosphate buffer; pH 5	stable for > 1 week
100 mM phosphate buffer; pH 7	stable for > 1 week
100 mM phosphate buffer; pH 8	stable for > 1 week
100 mM phosphate buffer; pH 10	slowly decomposes half-life ≤ 4 days
100 mM acetate buffer, pH 5	stable for > 1 week
100 mM Tris buffer, pH 7	stable for > 1 week
100 mM Tris buffer pH 9	slowly decomposes half-life ≥ 1 week
100 mM ammonium bicarbonate	stable for > 1 week
citric acid buffer, pH 3	stable for > 1 week
6 M Guanidine HCl, pH 7 PBS	stable for > 1 week
8 M Urea, pH 7 PBS	stable for > 1 week
Storage Conditions	**Storage Period**
ambient temperature	stable for months as a lyophilized powder
elevated temperature	stable after reflux in water (100ºC) for 24 hours
freeze-thaw cycles	stable for 5 cycles of freeze-thaw in buffer
light exposure	stable for >1 week in buffer under fluorescent lights, stable for months as a lyophilized powder
refrigerated temperature	stable for > 1 year when stored as a lyophilized powder in a refrigerator at 10ºC
Organic solvents/Reagents	**Stability**
Methanol	stable for > 1 week
dimethyl sulfoxide	stable for > 1 week
acetonitrile/water (4:1)	stable for > 1 week
glycerol/water (1:1)	stable for > 1 week
trifluoroethanol	stable for > 1 week
trifluoroacetic acid	stable for > 2 days
dimethyl sulfoxide/trimethylamine (9:1)	decomposes
1 mM cysteine in 100 mM Tris buffer, pH 7	turns colorless, mass of **33** increases by 2
1 mM TCEP in 100 mM Tris buffer, pH 7	turns colorless, mass of **33** increases by 2

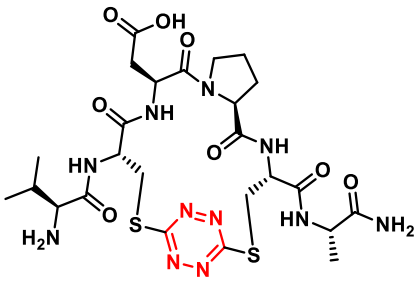

36

Peptide 36. Peptide **SI-4** (14.1 mg, 23µmol) was subjected to the general phase-transfer protocol to construct **36.** The crude reaction mixture was purified by reverse-phase HPLC (gradient 5-30% organic over 10 min) to give (10.5 mg, 67%) of an orange powder after lyophilization.: HRMS (ES) Found *m/z* 684.2341 [$(M+H)^+$; calcd for $C_{25}H_{38}N_{11}O_8S_2$: 684.2346]; ^{1}H NMR (500MHz ,DMSO-d_6) δ = 8.71 (d, *J* = 6.8 Hz, 1 H), 8.46 (d, *J* = 4.5 Hz, 1 H), 8.00 (d, *J* = 7.7 Hz, 1 H), 7.91 (d, *J* = 9.6 Hz, 1 H), 7.43 (s, 1 H), 7.15 (br. s., 3 H), 7.04 (s, 1 H), 4.77 (dd, *J* = 3.4, 6.8 Hz, 1 H), 4.74 (dd, *J* = 2.6, 15.8 Hz, 1 H), 4.69 (dd, *J* = 1.9, 9.0 Hz, 1 H), 4.67 (dd, *J* = 1.9, 9.6 Hz, 1 H), 4.42 - 4.34 (m, 1 H), 4.20 (quin, *J* = 7.2 Hz, 1 H), 4.06 (dd, *J* = 11.2, 14.6 Hz, 1 H), 3.77 (dd, *J* = 5.9, 7.9 Hz, 1 H), 3.66 (d, *J* = 5.1 Hz, 1 H), 3.54 - 3.47 (m, 2 H), 3.44 (dd, *J* = 2.6, 15.4 Hz, 1 H), 3.42 (dd, *J* = 2.8, 10.0 Hz, 1 H), 2.37 (dd, *J* = 2.4, 17.1 Hz, 1 H), 2.19 (dd, *J* = 10.5, 17.3 Hz, 1 H), 2.06 (sxt, *J* = 6.8 Hz, 1 H), 1.99 - 1.88 (m, 2 H), 1.77 (quind, *J* = 6.6, 12.0 Hz, 1 H), 1.71 - 1.62 (m, 1 H), 1.24 (d, *J* = 7.1 Hz, 3 H), 0.93 (d, *J* = 7.1 Hz, 3 H), 0.91 (d, *J* = 6.8 Hz, 3 H); ^{13}C NMR (126 MHz, DMSO) δ 173.8, 171.4, 171.1, 171.1, 171.1, 168.7, 168.4, 167.4, 158.3, 59.6, 57.6, 54.3, 51.2, 48.4, 48.1, 46.4, 34.6, 32.0, 31.0, 30.1, 28.6, 25.0, 18.6, 18.5, 17.6; IR (KBr, cm^{-1}) 3285(br), 3069(br), 1671(s), 1639(s), 1523(m), 1406(w), 1240(m), 1201(m), 1137(m).

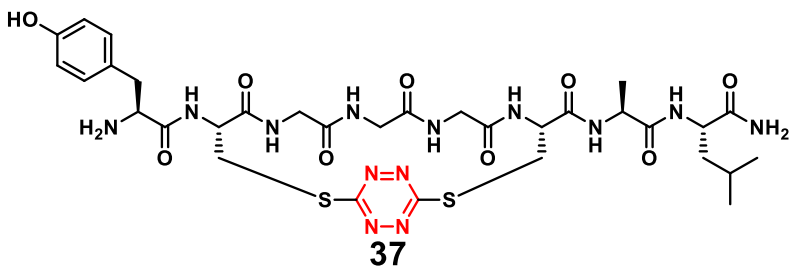

37

Peptide 37. Peptide **SI-5** (15.3 mg, 21µmol) was subjected to the general phase-transfer protocol to construct **37**. The crude reaction mixture was purified by reverse-phase HPLC (gradient 5-40% organic over 15 min) to give (12.9 mg, 76%) of an orange powder after lyophilization: HRMS (ES) Found *m/z* 820.2981 [$(M+H)^+$; calcd for $C_{32}H_{46}N_{13}O_9S_2$: 820.2983]; ^{1}H NMR (500MHz, DMSO-d_6) δ = 9.36 (s, 1 H), 9.16 (d, *J* = 7.3 Hz, 1 H), 8.72 (dd, *J* = 4.1, 7.0 Hz, 1 H), 8.22 (d, *J* = 7.3 Hz, 1 H), 8.19 - 8.15 (m, 3 H), 7.88 (d, *J* = 8.1 Hz, 1 H), 7.84 (d, *J* = 8.3 Hz, 1 H), 7.73 (t, *J* = 5.7 Hz, 1 H), 7.24 (s, 1 H), 7.05 (br. s., 1 H), 7.03 (d, *J* = 8.5 Hz, 2 H), 6.96 (br. s., 1 H), 6.69 (d, *J* = 8.3 Hz, 2 H), 6.51 (s, 1 H), 4.81 - 4.72 (m, 2 H), 4.28 (quin, *J* = 7.2 Hz, 1 H), 4.21 (dt, *J* = 6.0, 8.5 Hz, 1 H), 4.03 (t, *J* = 6.0 Hz, 1 H), 4.00 (dd, *J* = 7.5, 16.2 Hz, 1 H), 3.80 (dd, *J* = 4.1, 10.3 Hz, 1 H), 3.77 (dd, *J* = 6.0, 16.5 Hz, 1 H), 3.71 - 3.55 (m, 4 H), 3.49 (dd, *J* = 3.8, 16.0 Hz, 1 H), 3.02 (dd, *J* = 5.6, 14.3 Hz, 1 H), 2.85 (dd, *J* = 7.5, 13.9 Hz, 1 H), 1.65 - 1.55 (m, 1 H), 1.51 - 1.42 (m, 2 H), 1.25 (d, *J* = 7.1 Hz, 3 H), 0.88 (d, *J* = 6.6 Hz, 3 H), 0.84 (d, *J* = 6.4 Hz, 3 H); ^{13}C NMR (126MHz ,DMSO-d_6) δ = 174.0, 172.2, 171.6, 171.0, 169.2, 169.1, 169.0, 169.0, 168.8, 168.2, 158.1, 156.5, 130.5, 124.6, 115.3, 53.6, 52.6, 52.1, 50.9, 48.6, 42.5, 42.2, 42.1, 40.9, 36.0, 32.0, 31.3, 24.2, 23.0, 21.6, 17.8; IR (KBr, cm^{-1}) 3293(br), 2928(w), 1670(s), 1517(m), 1238(m).

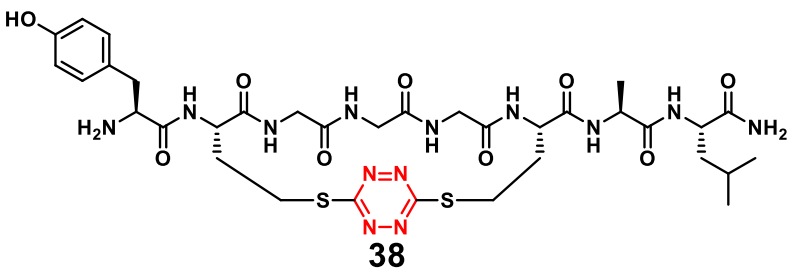

38

Peptide 38. Peptide **SI-6** (16.0 mg, 21 µmol) was subjected to the general phase-transfer protocol to construct **38**. The crude reaction mixture was purified by reverse-phase HPLC (gradient 5-40% organic over 15 min) to give (11.2 mg, 64%) of an orange powder after lyophilization: HRMS (ES) Found *m/z* 848.3286 [$(M+H)^+$; calcd for $C_{34}H_{50}N_{13}O_9S_2$: 848.3296]; ^{1}H NMR (500MHz ,DMSO-d_6) δ = 9.36 (br. s., 1 H), 8.76 (d, *J* = 7.5 Hz, 1 H), 8.31 (t, *J* = 5.4 Hz, 1 H), 8.21 (d, *J* = 6.3 Hz, 1 H), 8.16 - 8.06 (m, 3 H), 8.02 (t, *J* = 5.9 Hz, 1 H), 7.96 (d, *J* = 8.1 Hz, 1 H), 7.77 (d, *J* = 7.7 Hz, 1 H), 7.23 (br. s., 1 H), 7.04 (d, *J* = 7.1 Hz, 2 H), 6.96 (br. s., 1 H), 6.70 (d, *J* = 7.1 Hz, 2 H), 4.59 (t, *J* = 9.0 Hz, 1 H), 4.45 (dd, *J* = 6.9, 15.0 Hz, 1 H), 4.26 (ddd, *J* = 6.5, 7.3, 14.9 Hz, 1 H), 4.20 (dd, *J* = 7.5, 15.9 Hz, 1 H), 4.02 (br. s., 1 H), 3.90 (dd, *J* = 5.9, 16.1 Hz, 1 H), 3.77 (dd, *J* = 5.2, 16.4 Hz, 1 H), 3.74 (dd, *J* = 4.8, 14.9 Hz, 1 H), 3.69 - 3.53 (m, 4 H), 3.41 - 3.33 (m, 2 H), 3.24 (quin, *J* = 7.4 Hz, 2 H), 2.99 (dd, *J* = 5.0, 13.7 Hz, 1 H), 2.83 (dd, *J* = 7.5, 14.1 Hz, 1 H), 2.30 (d, *J* = 7.7 Hz, 1 H), 2.08 (ddd, *J* = 5.4, 8.7, 14.3 Hz, 1 H), 2.04 - 1.91 (m, 2 H), 1.59 (dt, *J* = 6.4, 13.0 Hz, 1 H), 1.51 - 1.38 (m, 1 H), 1.23 (d, *J* = 7.1 Hz, 3 H), 0.87 (d, *J* = 5.4 Hz, 3 H), 0.83 (d, *J* = 5.7 Hz, 3 H); ^{13}C NMR (126MHz ,DMSO-d_6) δ = 174.1, 171.8, 171.7, 171.7, 170.8, 170.5, 169.2, 169.1, 168.8, 168.3, 156.6, 130.5, 124.8, 115.4, 53.7, 51.4, 51.2, 50.8, 48.5, 42.6, 42.3, 42.1, 41.0, 36.1, 31.5, 31.2, 26.4, 26.2, 24.2, 23.1, 21.6, 17.7; IR (KBr, cm^{-1}) 3290(br), 2927(w), 1672(s), 1516(m), 1240(m).

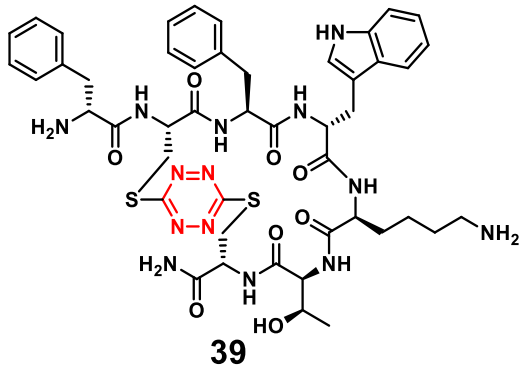

39

Peptide 39. Peptide **SI-7** (11.0 mg, 11.8 µmol) was subjected to the general phase-transfer protocol to construct **39**. The crude reaction mixture was purified by reverse-phase HPLC (gradient 10-60% organic over 15 min) to give 6.2 mg (52%) of an orange powder after lyophilization: HRMS (ES) Found *m/z* 1011.4095 [(M+H)$^+$; calcd for $C_{47}H_{59}N_{14}O_8S_2$: 1011.4082]; ^{1}H NMR (500 MHz, DMSO-d_6) δ 10.87 (s, 1H), 9.07 (d, *J* = 8.3 Hz, 1H), 8.57 (d, *J* = 8.2 Hz, 1H), 8.36 (d, *J* = 8.6 Hz, 1H), 8.30 (d, *J* = 8.6 Hz, 1H), 8.23 (d, *J* = 8.4 Hz, 1H), 8.14 (s, 3H), 7.73 (s, 3H), 7.66 (d, *J* = 7.9 Hz, 1H), 7.50 (d, *J* = 8.1 Hz, 1H), 7.38 (d, *J* = 30.6 Hz, 2H), 7.31 (d, *J* = 8.0 Hz, 1H), 7.30 – 7.28 (m, 4H), 7.28 – 7.21 (m, 2H), 7.17 (d, *J* = 2.4 Hz, 1H), 7.12 – 6.97 (m, 5H), 6.88 (d, *J* = 6.8 Hz, 2H), 6.59 (s, 1H), 4.97 (d, *J* = 4.8 Hz, 1H), 4.84 (td, *J* = 8.8, 4.5 Hz, 1H), 4.70 (dd, *J* = 8.3, 3.4 Hz, 1H), 4.68 – 4.64 (m, 1H), 4.57 (ddd, *J* = 14.2, 8.6, 5.8 Hz, 1H), 4.28 (dt, *J* = 14.3, 8.6, 6.1 Hz, 2H), 4.20 (dd, *J* = 8.2, 4.5 Hz, 1H), 4.15 – 4.07 (m, 1H), 3.86 (q, *J* = 5.3 Hz, 1H), 3.67 – 3.53 (m, 2H), 3.45 (dd, *J* = 14.0, 8.2 Hz, 1H), 3.09 (dt, *J* = 13.9, 5.3 Hz, 3H), 2.88 (ddd, *J* = 19.7, 14.2, 9.2 Hz, 2H), 2.75 – 2.66 (m, 5H), 2.63 (dd, *J* = 13.4, 4.8 Hz, 1H), 1.61 (dq, *J* = 17.3, 5.4 Hz, 1H), 1.54 – 1.38 (m, 3H), 1.27 – 1.07 (m, 3H), 0.96 (d, *J* = 6.3 Hz, 3H); ^{13}C NMR (126 MHz, DMSO-d_6) δ 171.6, 171.4, 171.3, 171.0, 170.0, 169.0, 168.5, 168.4, 157.8, 137.2, 136.2, 134.8, 129.6, 129.3, 128.6, 127.9, 127.2, 127.1, 126.2, 124.1, 121.0, 118.6, 118.3,

111.4, 109.8, 66.9, 57.4, 53.6, 53.5, 53.4, 52.9, 51.4, 50.4, 38.7, 37.9, 37.3, 33.8, 32.0, 30.7, 28.7, 26.6, 22.1, 19.5.

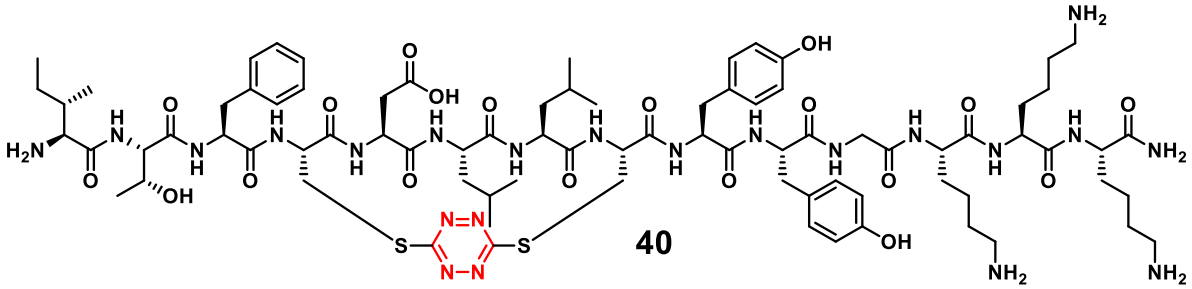

40

Peptide 40. Peptide **SI-8** (17.0 mg, 10μmol) was subjected to the general phase-transfer protocol to construct **40**. The crude reaction mixture was purified by reverse-phase HPLC [eluent water/MeCN/AcOH (85:10:5) and MeCN (organic) buffered with 0.1%TFA] (gradient 0-60% organic over 20 min) to give (11.8 mg, 67%) of an orange powder after lyophilization: MALDI-TOF Found *m/z* 1793.153 [$(M+Na)^+$; calcd for $C_{81}H_{122}N_{22}NaO_{19}S_2$: 1793.860]; ^{1}H NMR (500 MHz, DMSO-d_6) δ 8.93 (s, 1H), 8.63 (d, *J* = 7.2 Hz, 1H), 8.41 (d, *J* = 8.3 Hz, 1H), 8.27 (d, *J* = 7.6 Hz, 1H), 8.23 – 8.12 (m, 6H), 8.12 – 8.05 (m, 1H), 8.01 (s, 7H), 7.95 (s, 3H), 7.89 (d, *J* = 8.0 Hz, 2H), 7.43 (s, 1H), 7.29 – 7.23 (m, 1H), 7.22 (s, 1H), 7.21 (s, 2H), 7.18 – 7.12 (m, 1H), 7.10 (s, 1H), 7.04 (d, *J* = 8.3 Hz, 2H), 6.97 (d, *J* = 8.3 Hz, 2H), 6.65 (d, *J* = 8.0 Hz, 2H), 6.62 (d, *J* = 8.2 Hz, 2H), 4.84 (q, *J* = 6.5 Hz, 1H), 4.73 – 4.63 (m, 2H), 4.59 (dd, *J* = 13.9, 5.9 Hz, 1H), 4.42 (dq, *J* = 15.0, 7.6 Hz, 2H), 4.34 – 4.22 (m, 3H), 4.22 – 4.09 (m, 3H), 3.92 (dd, *J* = 12.5, 6.8 Hz, 3H), 3.81 – 3.68 (m, 3H), 3.02 (dd, *J* = 14.2, 4.3 Hz, 1H), 2.89 (dd, *J* = 34.1, 11.3 Hz, 3H), 2.85 – 2.79 (m, 1H), 2.74 (h, *J* = 6.1 Hz, 8H), 2.66 (dd, *J* = 16.2, 4.8 Hz, 2H), 1.73 – 1.61 (m, 2H), 1.59 – 1.51 (m, 10H), 1.50 – 1.42 (m, 3H), 1.32 (dt, *J* = 15.7, 7.9 Hz, 9H), 1.22 (d, *J* = 6.9 Hz, 1H), 1.05 (d, *J* = 6.1 Hz, 4H), 0.88 (d, *J* = 6.5 Hz, 3H), 0.85 (d, *J* = 6.3 Hz, 3H), 0.83 (d, *J* = 6.5 Hz,

3H), 0.81 (d, *J* = 4.0 Hz, 3H), 0.80 (d, *J* = 3.7 Hz, 4H), 0.78 (d, 3H), 0.75 (d, *J* = 6.4 Hz, 3H); ^{13}C NMR (126 MHz, DMSO-d_6) δ 173.5, 172.1, 171.7, 171.6, 171.4, 171.4, 171.1, 170.9, 170.8, 170.7, 169.2, 169.2, 169.0, 168.7, 167.8, 155.9, 155.8, 137.4, 130.2, 129.2, 128.0, 127.7, 127.5, 126.3, 66.9, 65.8, 58.3, 56.3, 54.5, 54.4 , 53.5 , 52.8 , 52.4 , 52.2 , 51.1 , 50.8 , 49.6 , 42.0 , 38.5 , 37.4 , 36.7 , 36.3 , 36.2 , 31.4 , 30.8, 26.5, 26.5, 26.5, 24.0, 23.9, 23.5, 23.1, 22.3, 22.2, 21.8, 21.5, 21.2, 19.4, 14.5, 11.2; IR (KBr, cm^{-1}) 3412(br), 2963(w), 1668(s), 1517(m), 1238(w), 1203(m), 1134(m), 1033(w), 1009(w).

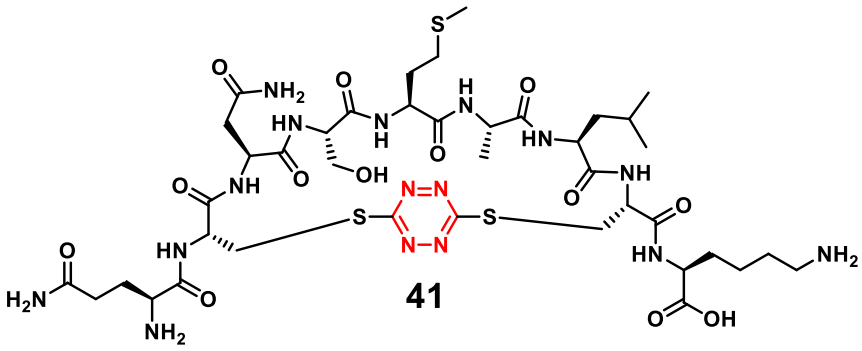

Peptide 41. Peptide **SI-9** (10.0 mg, 10 µmol) was subjected to the general phase-transfer protocol to construct **41**. The crude reaction mixture was purified by reverse-phase HPLC [elutant water/MeCN/AcOH (85:10:5) and MeCN (organic) buffered with 0.1%TFA] (gradient 0-60% organic over 15 min) to give (4.7 mg, 44 %) of an orange powder after lyophilization: HRMS (ES) Found *m/z* 1075.4239 [(M+H)$^+$; calcd for $C_{34}H_{50}N_{13}O_9S_2$: 1075.4236]^{1}H NMR (500 MHz, DMSO-d_6) δ 9.19 (d, *J* = 8.1 Hz, 1H), 8.47 (d, *J* = 7.3 Hz, 1H), 8.41 – 8.28 (m, 5H), 8.22 (d, *J* = 8.1 Hz, 1H), 8.07 (d, *J* = 7.8 Hz, 1H), 8.01 (d, *J* = 5.2 Hz, 1H), 7.99 – 7.89 (m, 3H), 7.66 (s, 2H), 7.59 – 7.48 (m, 2H), 7.08 (s, 1H), 6.98 (s, 1H), 4.82 (ddd, *J* = 13.6, 8.2, 5.0 Hz, 1H), 4.65 (dd, *J* = 14.7, 6.9 Hz, 1H), 4.53 (dd, *J* = 13.7, 6.2 Hz, 1H), 4.28 – 4.05 (m, 6H), 3.86 (dd, *J* = 11.3, 5.8 Hz, 1H), 3.79 – 3.69 (m,

3H), 3.64 (dd, *J* = 14.0, 6.9 Hz, 1H), 2.73 (q, *J* = 6.8 Hz, 2H), 2.67 (dd, *J* = 15.6, 6.5 Hz, 1H), 2.58 (dd, *J* = 15.3, 6.1 Hz, 1H), 2.42 – 2.34 (m, 1H), 2.23 (dd, *J* = 9.2, 6.7 Hz, 2H), 2.01 (s, 4H), 1.94 (q, *J* = 7.4 Hz, 2H), 1.86 – 1.77 (m, 1H), 1.77 – 1.68 (m, 1H), 1.65 – 1.46 (m, 5H), 1.44 – 1.30 (m, 5H), 1.16 (d, *J* = 7.1 Hz, 3H), 0.88 (d, *J* = 6.5 Hz, 3H), 0.83 (d, *J* = 6.5 Hz, 4H); ^{13}C NMR (126 MHz, DMSO-d_6) δ 173.5, 173.1, 172.2, 172.1, 172.0, 171.7, 171.3, 170.9, 170.2, 169.4, 168.8, 168.7, 61.1, 56.0, 52.1, 51.8, 51.8, 51.6, 51.2, 50.2, 48.6, 38.5, 36.8, 32.3, 30.9, 30.4, 30.4, 30.2, 29.9, 27.0, 26.5, 24.2, 23.2, 22.2, 21.5, 17.8, 14.6; IR (KBr, cm^{-1}) 3413(br), 2923(m), 1655(s), 1541(m), 1236(m).

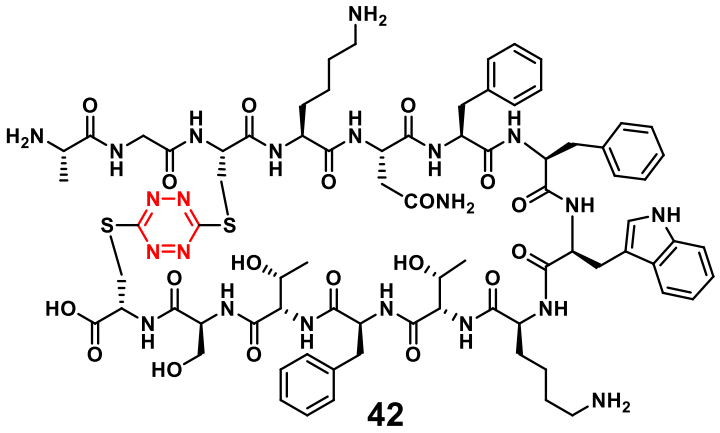

42

Peptide 42. Peptide **SI-10** (8.3 mg, 5.1 µmol) was subjected to the general phase-transfer protocol to construct **42**. The crude reaction mixture was purified by reverse-phase HPLC (gradient 10-60% organic over 15 min) to give (5.5 mg, 63%) of an orange powder after lyophilization: MALDI-TOF Found *m/z* 1717.968 [(M+H)$^+$; calcd for $C_{78}H_{105}N_{22}O_{19}S_2$: 1717.736]. ^{1}H NMR (500 MHz, DMSO-d_6) δ 10.79 (s, 1H), 8.66 (t, *J* = 4.9 Hz, 2H), 8.50 (d, *J* = 6.4 Hz, 2H), 8.43 – 8.37 (m, 1H), 8.33 – 8.26 (m, 1H), 8.20 – 8.16 (m, 5H), 8.12 – 8.06 (m, 1H), 8.05 – 8.01 (m, 5H), 7.93 (d, *J* = 5.2 Hz, 1H), 7.88 – 7.83 (m, 13H), 7.79 – 7.72 (m, 2H), 7.70 – 7.65 (m, 3H), 7.58 (d, *J* = 7.5 Hz, 2H), 7.37 – 7.27 (m, 1H), 7.25 –

7.04 (m, 22H), 7.04 – 6.93 (m, 2H), 5.44 – 5.40 (m, 1H), 5.26 – 5.19 (m, 1H), 5.16 – 5.10 (m, 1H), 4.96 – 4.92 (m, 1H), 4.86 – 4.79 (m, 1H), 4.79 – 4.71 (m, 1H), 4.62 – 4.52 (m, 2H), 4.47 – 4.41 (m, 1H), 4.34 – 4.29 (m, 6H), 4.26 – 4.22 (m, 2H), 4.15 – 4.08 (m, 1H), 3.99 – 3.95 (m, 1H), 3.92 – 3.86 (m, 2H), 3.84 (d, *J* = 5.8 Hz, 1H), 3.81 – 3.73 (m, 1H), 3.62 – 3.58 (m, 3H), 1.69 – 1.65 (m, 3H), 1.57 – 1.39 (m, 3H), 1.36 (t, *J* = 7.2 Hz, 3H), 1.23 (d, *J* = 7.0 Hz, 2H), 1.05 – 0.99 (m, 5H), 0.96 (t, *J* = 6.2 Hz, 3H); ^{13}C NMR (126 MHz, DMSO) δ 176.4, 171.9, 171.7, 171.6, 171.4, 171.2, 171.0, 171.0, 170.9, 170.9, 170.8, 170.1, 169.9, 169.7, 169.4, 168.6, 168.5, 137.8, 137.7, 137.6, 137.5, 136.2, 136.1, 129.2, 129.2, 129.1, 128.9, 128.9, 128.1, 128.1, 127.3, 127.1, 126.3, 123.7, 72.5, 69.8, 67.0, 66.9, 66.5, 65.8, 63.1, 61.8, 61.5, 57.8, 55.2, 55.1, 54.8, 54.0, 53.7, 53.5, 52.7, 52.4, 51.1, 49.6, 48.2, 43.2, 41.8, 38.7, 37.5, 37.2, 37.0, 36.6, 26.7, 26.6, 26.5, 26.5, 22.5, 22.2, 20.5, 19.4, 19.0, 17.3; IR (KBr, cm^{-1}) 3421(br), 2925(m), 1654(s), 1508(m), 1117(m), 1032(s), 1008(s).

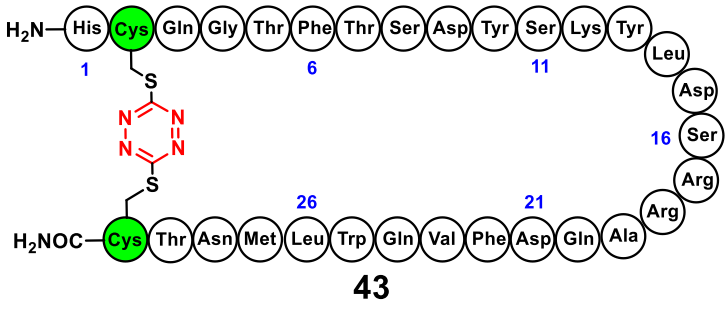

43

Peptide 43. Peptide **SI-11** (7.2 mg, 2 µmol) was subjected to the general phase-transfer protocol with 6M guanidine hydrochloride additive to construct **43**, the salts were removed by dialysis and the crude reaction mixture was purified by reverse-phase HPLC (10 - 60%

organic over 20 min) to give (1.5 mg, 21%) of an orange powder after lyophilization. MALDI-TOF Found *m/z* 3677.277 [$(M+H)^+$; calcd for $C_{158}H_{230}N_{49}O_{48}S_3$: 3677.622].

General Procedure for Unstapling S,S-Tetrazine Peptides Photochemically

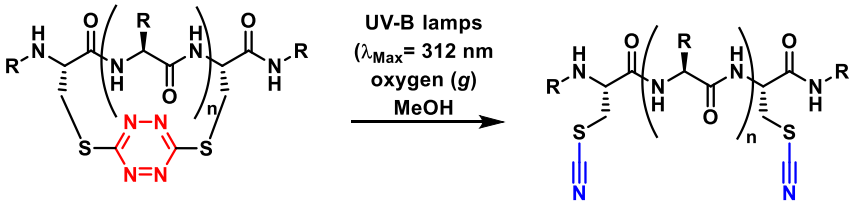

A 10 mL glass vial was charged with a solution of tetrazine stapled peptide in MeOH (1-2 mM). The contents were capped with a septum and sparged with oxygen gas for 15 minutes. The solution was then irradiated in a Rayonet® photoreactor equipped with four (7 watt) UV-B lamps (λ_{Max} = 312 nm) until the solution turned colorless. The MeOH was evaporated *in vacuo*, then redissolved in water and lyophilized to yield a white amorphous powder.

Colormetric Change that Occurs After Irradiation in a Rayonet® Photoreactor

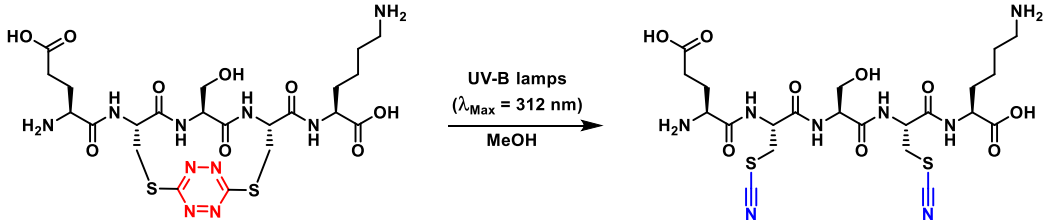

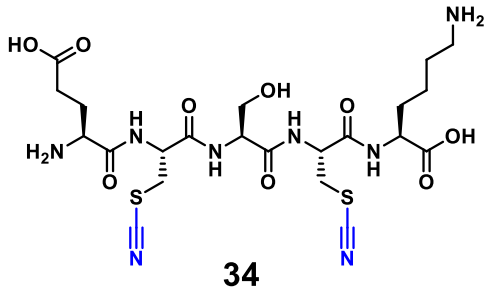

34

Peptide 34. Peptide **33** (10.0 mg, 15 µmol) was subjected to the general photochemical unstapling protocol to yield 9.4 mg (98%). HRMS (ES) Found *m/z* 619.1961 $[(M+H)^+$; calcd for $C_{22}H_{35}N_8O_9S_2$: 619.1963]; ^{1}H NMR (500 MHz, Deuterium Oxide) δ 4.96 (dd, *J* = 7.4, 5.4 Hz, 1H), 4.89 (dd, *J* = 7.9, 5.0 Hz, 1H), 4.61 (t, *J* = 5.6 Hz, 1H), 4.36 (dd, *J* = 8.6, 5.1 Hz, 1H), 4.22 (t, *J* = 6.4 Hz, 1H), 3.93 (d, *J* = 5.7 Hz, 2H), 3.62 (ddd, *J* = 14.2, 5.2, 2.2 Hz, 2H), 3.45 (ddd, *J* = 14.2, 8.8, 7.7 Hz, 2H), 3.03 (t, *J* = 7.6 Hz, 2H), 2.59 (t, *J* = 7.4 Hz, 2H), 2.26 (q, *J* = 7.1 Hz, 2H), 1.93 (ddd, *J* = 13.5, 8.3, 5.1 Hz, 1H), 1.80 (td, *J* = 14.8, 14.2, 8.1 Hz, 1H), 1.72 (pd, *J* = 7.2, 2.2 Hz, 2H), 1.47 (p, *J* = 7.4, 6.8 Hz, 2H); ^{13}C NMR (126 MHz, D_2O) δ 177.7, 177.1, 172.8, 171.3, 171.1, 170.9, 115.4, 115.3, 62.5, 57.0, 54.6, 54.6, 54.5, 53.7, 40.6, 35.7, 35.6, 31.6, 30.5, 27.7, 27.3, 23.5; IR (KBr, cm^{-1}) 3425(br), 3286(br), 3077(br), 2950(br), 2159(w), 1682(s), 1628(s), 1535(m), 1429(m), 1207(s), 1132(s).

Photochemical Unstapling with UV-A Lamps (λ_{Max} = 365 nm)

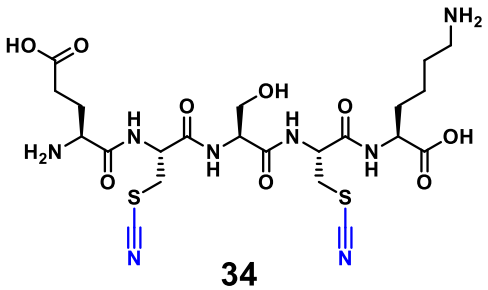

34

Peptide 34. Peptide **33** (15.0 mg, 23 µmol) was dissolved in MeOH (25 mL) and transferred to a thin-walled pyrex tube. The contents were then irradiated in a Rayonet photoreactor with twelve (7 watt) UV-A lamps (λ_{Max}= 365 nm) for 24 hours, during which time the solution turned from red to colorless. The solvent was evaporated then redissolved in water and lyophilized to yield 13.8 mg (96%) of a white amorphous powder. Spectral data was identical to **34** photolyzed with UV-B lamps.

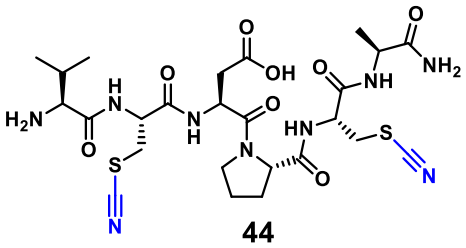

44

Peptide 44. Peptide **36** (1.5 mg, 2.2 µmol) was subjected to the general photochemical unstapling protocol to yield 1.4 mg (96%): HRMS (ES) Found *m/z* 656.2283 [$(M+H)^+$; calcd for $C_{25}H_{38}N_9O_8S_2$: 656.2285]; ^{1}H NMR (500 MHz, DMSO-d_6) δ 8.88 (d, *J* = 7.7 Hz, 1H), 8.84 (d, *J* = 7.9 Hz, 1H), 8.08 (d, *J* = 5.6 Hz, 3H), 7.98 (d, *J* = 8.0 Hz, 1H), 7.76 (d, *J* = 7.5 Hz, 1H), 7.14 (s, 1H), 7.02 (s, 1H), 4.85 (q, *J* = 7.1 Hz, 1H), 4.68 (q, *J* = 7.7 Hz, 1H), 4.51 (td, *J* = 8.6, 4.4 Hz, 1H), 4.29 (dd, *J* = 8.6, 3.6 Hz, 1H), 4.14 (p, *J* = 7.3 Hz, 1H), 3.67

(dt, *J* = 10.8, 5.8 Hz, 4H), 3.55 (dd, *J* = 13.5, 4.6 Hz, 2H), 3.45 (dd, *J* = 13.5, 5.4 Hz, 1H), 3.27 (dd, *J* = 13.3, 9.2 Hz, 1H), 3.20 (dd, *J* = 13.4, 8.1 Hz, 1H), 2.81 (dd, *J* = 16.9, 6.6 Hz, 1H), 2.09 (dt, *J* = 9.2, 4.5 Hz, 2H), 1.95 (tq, *J* = 10.2, 5.9, 5.3 Hz, 2H), 1.89 (dd, *J* = 11.3, 5.0 Hz, 1H), 1.24 (d, *J* = 7.0 Hz, 3H), 0.93 (dd, *J* = 12.7, 6.9 Hz, 6H); ^{13}C NMR (126 MHz, DMSO-d_6) δ 173.6, 172.0, 171.7, 169.2, 168.0, 167.8, 167.6, 113.0, 112.4, 60.2, 57.2, 52.8, 52.1, 48.4, 47.7, 46.9, 35.7, 34.9, 34.9, 29.8, 28.8, 24.2, 18.2, 17.8, 17.3; IR (KBr, cm^{-1}) 3323(br), 3067(m), 2974(m), 2160(w), 1669(s), 1525(m), 1202(m).

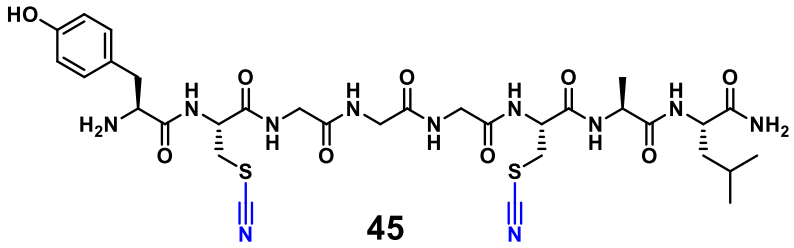

Peptide 45. Peptide **37** (2.8 mg, 3.4 µmol) was subjected to the general photochemical unstapling protocol to yield 2.6 mg (97%): HRMS Found (ES) *m/z* 792.2917 [(M+H)$^+$; calcd for $C_{32}H_{46}N_{11}O_9S_2$: 792.2921]; ^{1}H NMR (500 MHz, DMSO-d_6) δ 9.34 (s, 1H), 9.06 (d, *J* = 8.0 Hz, 1H), 8.52 (t, *J* = 5.7 Hz, 1H), 8.39 (d, *J* = 8.2 Hz, 1H), 8.33 (d, *J* = 7.2 Hz, 1H), 8.19 (dt, *J* = 11.2, 5.8 Hz, 2H), 8.08 (s, 3H), 7.77 (d, *J* = 8.4 Hz, 1H), 7.23 (s, 1H), 7.05 (d, *J* = 8.4 Hz, 2H), 6.96 (s, 1H), 6.71 (d, *J* = 8.4 Hz, 2H), 4.82 – 4.70 (m, 1H), 4.66 (td, *J* = 8.3, 4.7 Hz, 1H), 4.26 – 4.16 (m, 2H), 3.99 (d, *J* = 8.0 Hz, 1H), 3.89 – 3.71 (m, 6H), 3.67 – 3.58 (m, 1H), 3.49 (td, *J* = 13.5, 4.9 Hz, 2H), 3.27 (dd, *J* = 13.5, 7.8 Hz, 1H), 3.22 – 3.17 (m, 1H), 3.04 (dd, *J* = 14.3, 5.0 Hz, 1H), 2.82 (dd, *J* = 14.3, 8.2 Hz, 1H), 1.58 (dt, *J* = 13.5, 6.6 Hz, 1H), 1.45 (t, *J* = 7.2 Hz, 2H), 1.23 (d, *J* = 7.2 Hz, 3H), 0.86 (dd, *J* = 20.4, 6.6 Hz, 6H); ^{13}C NMR (126 MHz, DMSO-d_6) δ 174.4, 171.9, 169.6, 169.5, 168.6,

168.5, 156.8, 130.8, 124.8, 115.6, 113.1, 54.0, 52.5, 52.4, 51.1, 49.1, 41.7, 41.5, 41.4, 41.1, 36.3, 35.6, 35.5, 24.5, 23.3, 21.8, 17.9; IR (KBr, cm^{-1}) 3294(br), 3067(br), 2962(m), 2159(w), 1676(s), 1518(s), 1431(w), 1205(m), 1136(m).

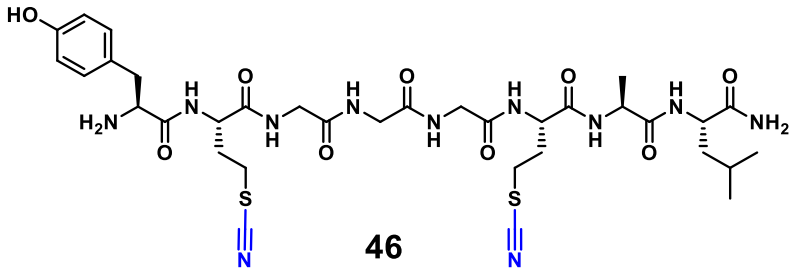

46

Peptide 46. Peptide **38** (3.2 mg, 3.8 µmol) was subjected to the general photochemical unstapling protocol to yield 3.0 mg (96%). HRMS Found (ES) *m/z* 820.3257 [$(M+H)^+$; calcd for $C_{34}H_{50}N_{11}O_9S_2$: 820.3234]; ^{1}H NMR (500 MHz, DMSO-d_6) δ 9.33 (s, 1H), 8.32 (t, *J* = 5.6 Hz, 1H), 8.25 (d, *J* = 7.2 Hz, 1H), 8.22 (d, *J* = 5.7 Hz, 1H), 8.19 – 8.13 (m, 1H), 7.80 (d, *J* = 8.3 Hz, 1H), 7.73 – 7.69 (m, 2H), 7.68 (d, *J* = 5.1 Hz, 1H), 7.29 (s, 1H), 7.02 (d, *J* = 8.1 Hz, 2H), 6.98 (s, 1H), 6.69 (d, *J* = 8.1 Hz, 2H), 6.56 (s, 1H), 4.55 – 4.47 (m, 1H), 4.44 (dd, *J* = 13.5, 8.1 Hz, 1H), 4.33 – 4.16 (m, 2H), 4.13 (t, *J* = 5.4 Hz, 1H), 3.83 (dd, *J* = 16.6, 5.7 Hz, 1H), 3.79 – 3.68 (m, 4H), 3.13 – 2.99 (m, 3H), 2.93 (dd, *J* = 14.5, 4.7 Hz, 1H), 2.82 – 2.65 (m, 1H), 2.21 – 2.10 (m, 1H), 2.10 – 2.04 (m, 1H), 2.04 – 1.92 (m, 2H), 1.69 – 1.53 (m, 2H), 1.44 (dt, *J* = 9.2, 4.5 Hz, 2H), 1.39 – 1.31 (m, 1H), 1.21 (d, *J* = 7.1 Hz, 3H), 0.87 (d, *J* = 6.3 Hz, 3H), 0.83 (d, *J* = 6.6 Hz, 3H); ^{13}C NMR (126 MHz, DMSO) δ 173.9, 171.6, 170.0, 169.1, 168.8, 168.8, 166.9, 156.3, 131.7, 131.5, 130.3, 128.6, 115.2, 112.9, 112.8, 67.4, 50.9, 50.8, 48.4, 42.0, 41.9, 41.0, 38.1, 29.8, 29.8, 28.3, 24.1, 23.2, 23.0, 22.3, 21.5, 17.6, 13.8, 10.8; IR (KBr, cm^{-1}) 3409(br), 2928(w), 2159(w), 1671(s), 1541(m), 1205(m), 1180(w), 1134(w).

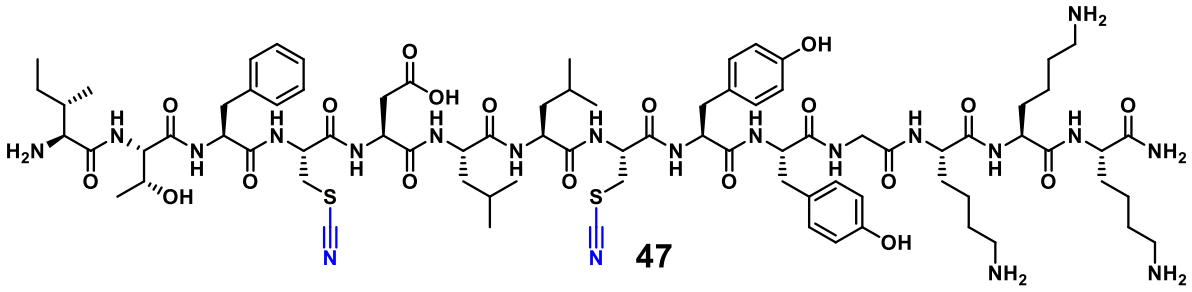

Peptide 47. Peptide **40** (4.0 mg, 2.3 μmol) was subjected to the general photochemical unstapling protocol to yield 3.9 mg (99%): MALDI-TOF Found *m/z* 1743.230 [$(M+H)^+$; calcd for $C_{81}H_{123}N_{20}O_{19}S_2$: 1743.871]; ^{1}H NMR (500 MHz, DMSO-d_6) δ 9.21 (d, *J* = 12.0 Hz, 1H), 8.57 (d, *J* = 7.4 Hz, 1H), 8.32 (d, *J* = 8.3 Hz, 1H), 8.23 – 8.17 (m, 1H), 8.15 (d, *J* = 7.8 Hz, 1H), 8.13 – 8.00 (m, 4H), 7.97 (d, *J* = 7.6 Hz, 1H), 7.92 (d, *J* = 8.1 Hz, 1H), 7.86 (d, *J* = 7.7 Hz, 1H), 7.80 (s, 7H), 7.40 (s, 1H), 7.21 (d, *J* = 6.7 Hz, 3H), 7.16 (d, *J* = 6.3 Hz, 1H), 7.07 (s, 1H), 7.02 (d, *J* = 8.4 Hz, 2H), 6.92 (d, *J* = 8.2 Hz, 2H), 6.64 (d, *J* = 8.1 Hz, 2H), 6.60 (d, *J* = 8.3 Hz, 2H), 5.42 (s, 1H), 5.22 – 5.14 (m, 1H), 5.01 (d, *J* = 4.0 Hz, 1H), 4.66 – 4.57 (m, 3H), 4.55 (t, *J* = 7.0 Hz, 1H), 4.49 (d, *J* = 3.6 Hz, 1H), 4.44 (d, *J* = 6.6 Hz, 1H), 4.43 – 4.38 (m, 1H), 4.37 – 4.24 (m, 3H), 4.23 – 4.17 (m, 1H), 4.17 – 4.09 (m, 1H), 4.03 (q, *J* = 6.8 Hz, 1H), 3.98 – 3.90 (m, 1H), 3.81 – 3.68 (m, 2H), 3.15 (dd, *J* = 13.3, 8.7 Hz, 1H), 3.07 (dd, *J* = 14.5, 3.3 Hz, 1H), 2.91 (d, *J* = 11.3 Hz, 1H), 2.83 (dd, *J* = 13.9, 9.1 Hz, 1H), 2.75 (s, 6H), 2.65 – 2.62 (m, 1H), 1.78 – 1.39 (m, 17H), 1.31 (s, 5H), 1.23 (d, *J* = 6.8 Hz, 3H), 1.05 (d, *J* = 6.3 Hz, 3H), 0.86 (t, *J* = 6.8 Hz, 5H), 0.84 – 0.73 (m, 11H); ^{13}C NMR (126 MHz, DMSO) δ 176.4, 173.5, 171.8, 171.7, 171.6, 171.4, 171.3, 171.2, 170.6, 169.7, 169.2, 168.7, 168.4, 167.9, 167.9, 155.9, 155.8, 137.4, 130.1, 130.1, 129.2, 128.0, 127.7, 127.4, 126.3, 114.9, 114.9, 72.5, 67.0, 65.8, 63.1, 57.9, 56.3, 54.6, 53.6, 52.6, 52.6, 52.3, 52.3, 52.3, 52.2, 52.2, 52.1, 51.2, 51.2, 51.2, 51.1, 49.8, 38.7, 36.3, 31.5, 26.7, 26.6,

24.1, 23.9, 23.2, 23.1, 22.3, 22.2, 21.7, 21.6, 20.5, 19.4, 14.5, 11.1; IR (KBr, cm^{-1}) 3298(br), 3071(br), 2962(m), 2933(m), 2159(w), 1671(s), 1517(m), 1438(m), 1203(s), 1137(m).

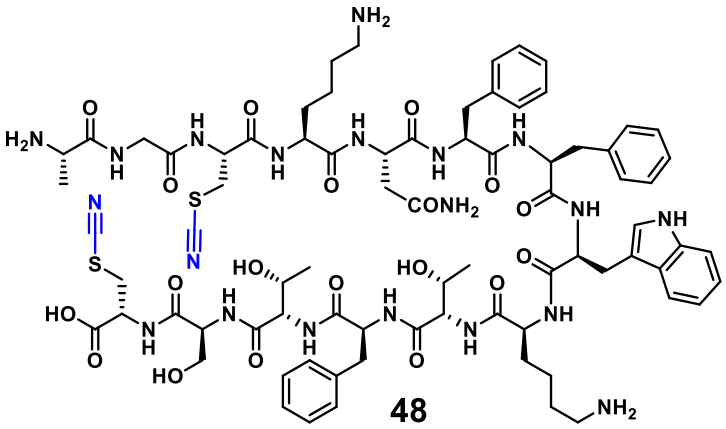

48

Peptide 48. Peptide **42** (8.3 mg, 5.1 µmol) was subjected to the general photochemical unstapling protocol, without sparging with oxygen gas (atmospheric oxygen was not excluded). The crude reaction mixture was purified by reverse-phase HPLC (gradient 10-60% organic over 15 min) to yield 2.1 mg (38%) of a white powder after lyophilization. MALDI-TOF *m/z* 1689.333 [$(M+H)^+$; calcd for $C_{78}H_{105}N_{20}O_{19}S_2$: 1689.730]; ^{1}H NMR (500 MHz, DMSO-d_6) δ 10.77 (s, 1H), 8.67 (t, *J* = 5.7 Hz, 1H), 8.48 (d, *J* = 8.0 Hz, 1H), 8.34 (d, *J* = 8.0 Hz, 1H), 8.21 – 8.01 (m, 6H), 8.01 – 7.86 (m, 5H), 7.86 – 7.65 (m, 6H), 7.61 (d, *J* = 7.9 Hz, 1H), 7.50 – 7.41 (m, 2H), 7.32 (d, *J* = 7.9 Hz, 1H), 7.27 – 7.08 (m, 15H), 7.05 (t, *J* = 7.5 Hz, 1H), 7.00 (d, *J* = 9.7 Hz, 1H), 6.97 (d, *J* = 7.4 Hz, 1H), 4.88 (d, *J* = 4.5 Hz, 1H), 4.72 – 4.60 (m, 1H), 4.57 (d, *J* = 5.8 Hz, 1H), 4.54 – 4.42 (m, 2H), 4.42 – 4.26 (m, 4H), 4.21 (dd, *J* = 8.6, 3.9 Hz, 2H), 4.10 – 3.93 (m, 1H), 3.94 – 3.82 (m, 3H), 3.74 – 3.57 (m, 1H), 3.53 – 3.43 (m, 1H), 3.19 (dd, *J* = 13.7, 8.8 Hz, 2H), 3.14 – 3.06 (m, 1H),

3.03 – 2.95 (m, 2H), 2.94 – 2.88 (m, 1H), 2.88 – 2.76 (m, 2H), 2.71 (t, *J* = 7.3 Hz, 4H), 2.41 – 2.32 (m, 1H), 1.71 – 1.60 (m, 1H), 1.58 – 1.41 (m, 7H), 1.36 (d, *J* = 6.9 Hz, 3H), 1.32 – 1.18 (m, 5H), 1.14 (d, *J* = 6.9 Hz, 1H), 1.04 (d, *J* = 6.2 Hz, 3H), 0.97 (d, *J* = 6.4 Hz, 3H); ^{13}C NMR (126 MHz, DMSO) δ 171.8, 171.3, 171.2, 170.9, 170.8, 170.8, 170.6, 170.5, 170.3, 170.1, 169.8, 169.7, 169.7, 168.6, 168.4, 137.7, 137.6, 137.5, 136.0, 129.2, 129.2, 129.0, 128.0, 127.9, 127.3, 126.1, 126.1, 123.6, 120.8, 118.5, 118.4, 118.2, 116.1, 112.9, 111.2, 109.8, 70.5, 70.4, 66.6, 61.4, 57.9, 57.8, 54.1, 53.9, 53.7, 53.3, 53.3, 52.5, 52.3, 52.3, 49.5, 48.1, 41.8, 38.7, 37.3, 37.3, 37.2, 37.2, 37.2, 37.0, 35.6, 31.1, 26.6, 26.6, 22.1, 22.1, 19.3, 19.3, 17.1; IR (KBr, cm^{-1}) 3424(br), 2933(w), 2159(w), 1671(s), 1632(s), 1526(m), 1204(w), 1136(w).

General Procedure for Nitrile Removal from the Thiocyanates

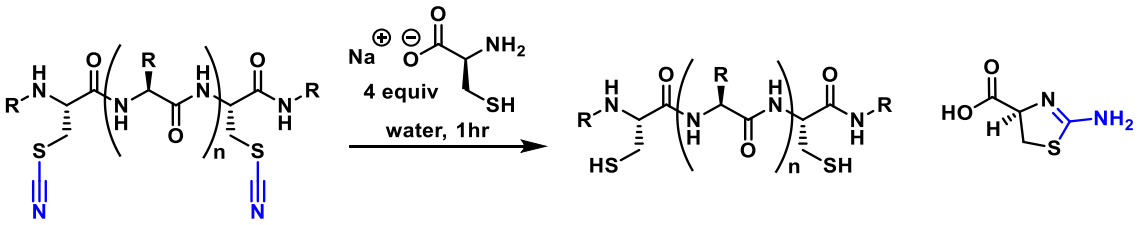

A 13 mm test tube was charged with peptide **3** (1-5 mg) and dissolved in water (1.0 mL). To this solution was added 4 equivalents of a pre-mixed 250 mM solution of sodium cysteine [prepared by dissolving cysteine (121 mg, 1.0 mmol) in 0.25M NaOH (4 mL, 1 equiv)]. The contents were stirred for 1 hour, then formic acid (4-8 equiv) was added and the reaction solution was purified by reverse-phase high-pressure liquid chromatography (HPLC) to yield peptide **1** as a white lyophilized powder and **4** was also separated from the reaction.

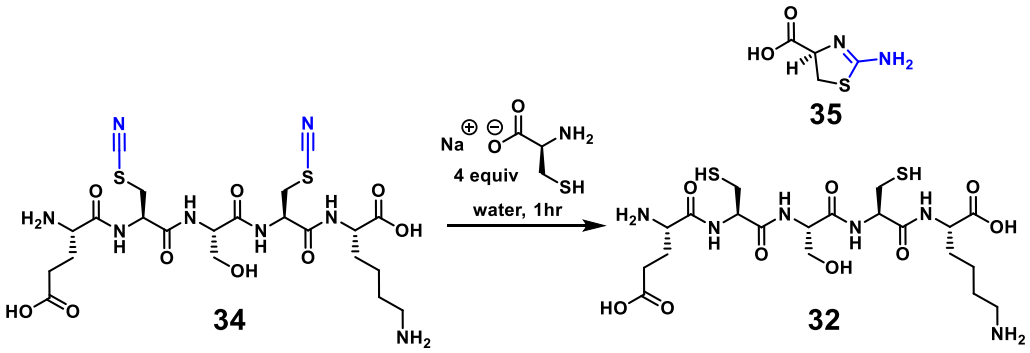

Regeneration of 32. Peptide **34** (6.2 mg, 10.0 μmol) was subjected to the general nitrile removal protocol then purified by reverse-phase HPLC (5 - 15% organic over 5 min) to yield 4.9 mg (87%) of peptide **32** as a white lyophilized powder and 1.3 mg (45%) **35** is also separated from the reaction. Spectral data was identical to **32** prepared by SPPS.

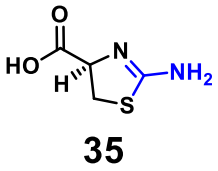

35

(R)-2-amino-4,5-dihydrothiazole-4-carboxylic acid (35): HRMS Found (ES) *m/z* 147.0228 [$(M+H)^+$; calcd for $C_4H_6N_2O_2S$: 147.0228]; ^{1}H NMR (500 MHz, Deuterium Oxide) δ 4.75 (dd, *J* = 8.8, 5.0 Hz, 1H), 3.92 (dd, *J* = 11.3, 8.9 Hz, 1H), 3.69 (dd, *J* = 11.4, 5.0 Hz, 1H); ^{13}C NMR (126 MHz, Deuterium Oxide) δ 175.5, 173.9, 63.8, 34.7; IR (KBr, cm^{-1}) 3153(br), 2980(br), 22840(br), 2347(m), 2281(m), 2222(m), 1638(s), 1588(s), 1442(m), 1392(s), 1290(m).

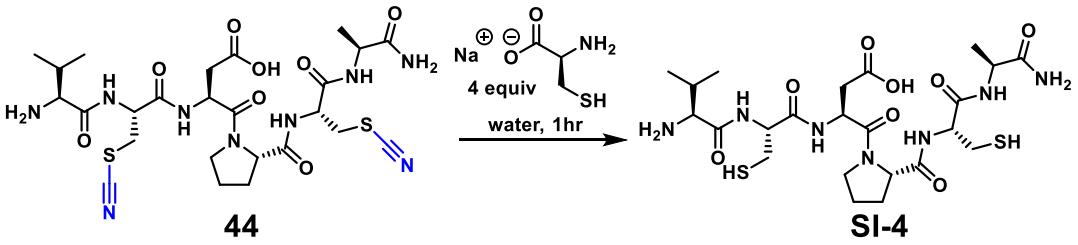

44 SI-4

Regeneration of SI-4. Peptide **44** (1.1 mg, 1.7 μmol) was subjected to the general nitrile removal protocol then purified by reverse-phase HPLC (5 - 35% organic over 12 min) to yield 0.7 mg (68%) of peptide **SI-4** as a white lyophilized powder. Spectral data was identical to **SI-4** prepared by SPPS.

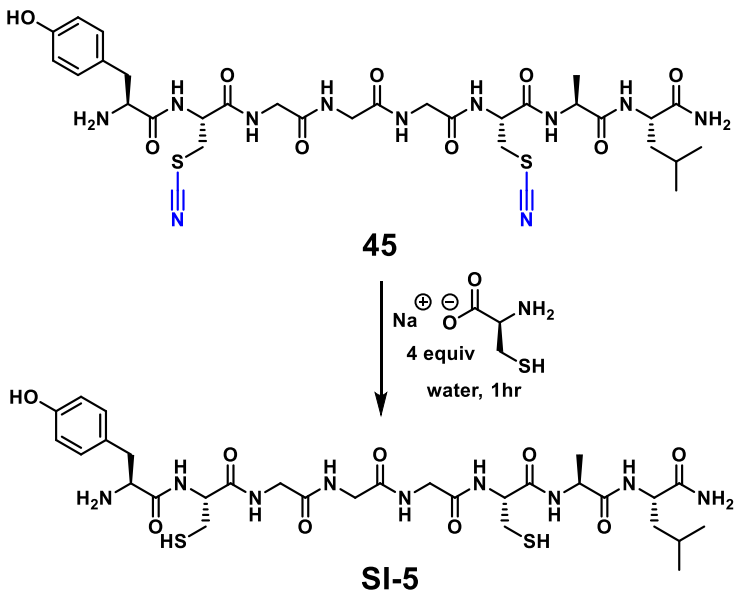

45 SI-5

Regeneration of SI-5. Peptide **45** (1.5 mg, 1.9 μmol) was subjected to the general nitrile removal protocol then purified by reverse-phase HPLC (5 - 60% organic over 12 min) to yield 1.1 mg (78%) of peptide **SI-5** as a white lyophilized powder. Spectral data was identical to **SI-5** prepared by SPPS.

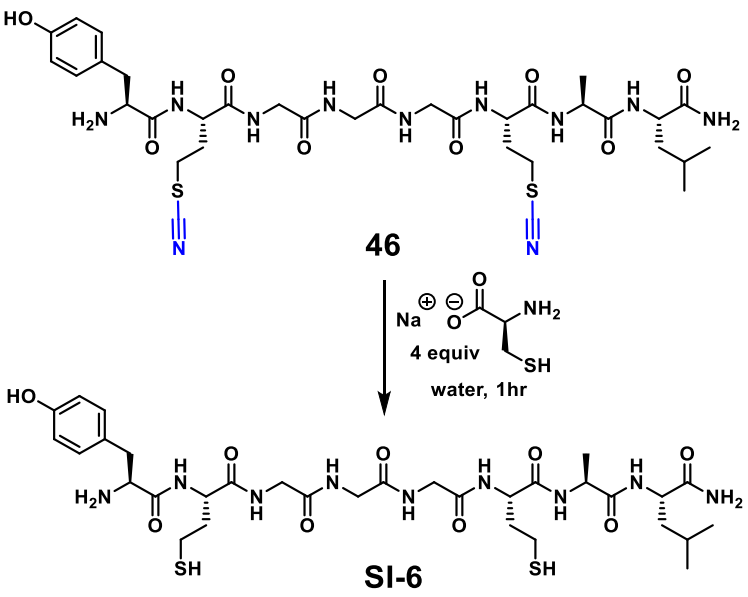

Regeneration of SI-6. Peptide **46** (5.0 mg, 6.1 μmol) was subjected to the general nitrile removal protocol then purified by reverse-phase HPLC (5 - 60% organic over 12 min) to yield 2.7 mg (58%) of peptide **SI-6** as a white lyophilized powder. Spectral data was identical to **SI-6** prepared by SPPS.

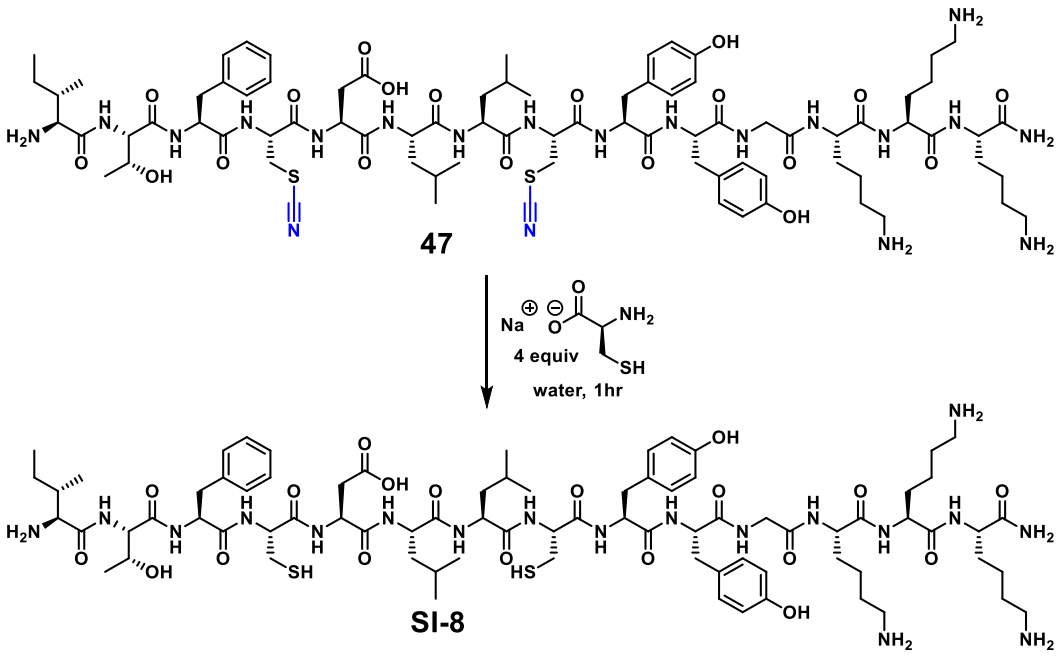

Regeneration of SI-8. Peptide **3e** (1.7 mg, 1.0 μmol) was subjected to the general nitrile removal protocol then purified by reverse-phase HPLC [eluent water/MeCN/AcOH (85:10:5) and MeCN (organic) buffered with 0.1%TFA] (5 - 40% organic over 15 min) to yield 0.9 mg (55%) of peptide **SI-8** as a white lyophilized powder. Spectral data was identical to **SI-8** prepared by SPPS.

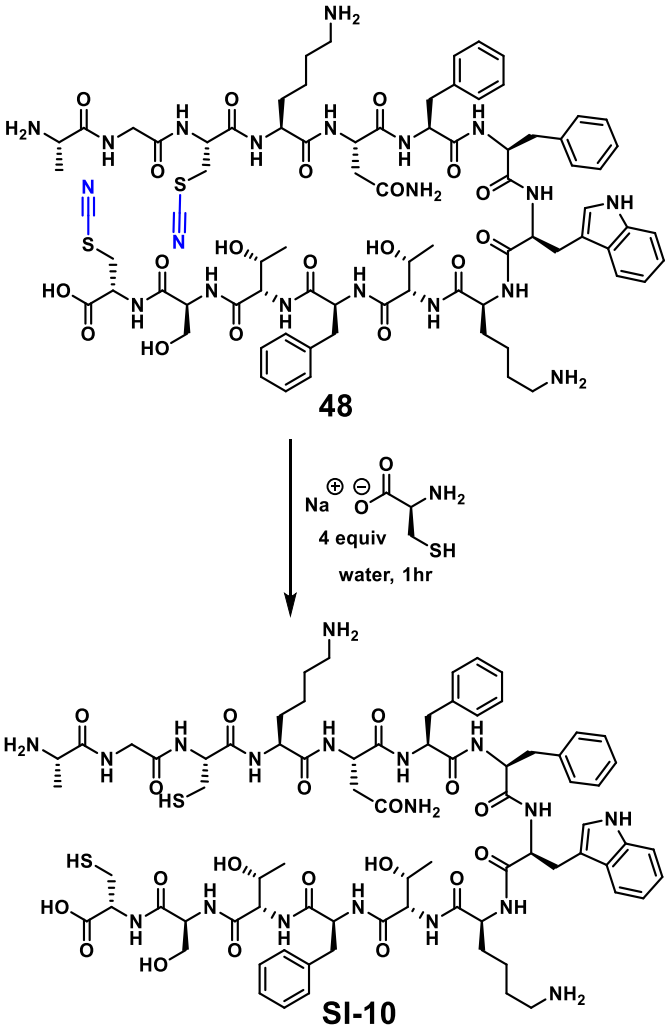

Regeneration of SI-10. Peptide **48** (3.2 mg, 1.9 μmol) was subjected to the general nitrile removal protocol then purified by reverse-phase HPLC (10 - 60% organic over 15 min) to

yield 2.1 mg (68%) of peptide **SI-10** as a white lyophilized powder. Spectral data was identical to **SI-10** prepared by SPPS.

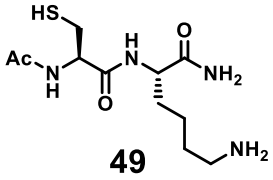

49

Peptide 49. Constructed by SPPS from 0.20 mmol loaded Rink amide resin. Removal of the peptide from resin was conducted with cocktail B following the general cleavage method. The peptide was purified by reverse-phase HPLC (5 - 40% organic over 12 min) and exchanged with 0.1 M HCl to give 27.3 mg (42% • HCl salt form) of a white amorphous powder after lyophilization: HRMS (ES) Found *m/z* 291.3893 [$(M+H)^+$; calcd for $C_{11}H_{23}N_4O_3S$: 291.3895].

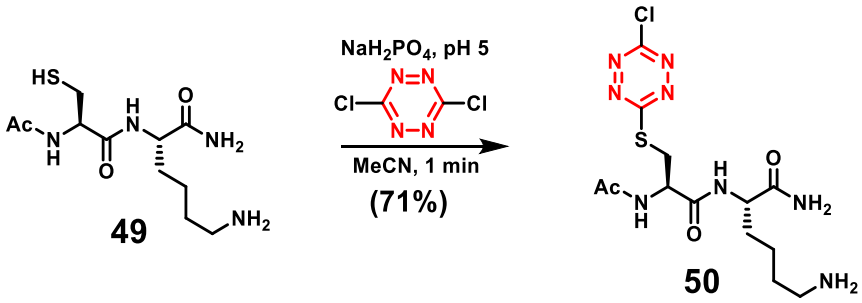

Peptide 50. A 50 mL plastic Flacon tube was charged with peptide **49** (13.7 mg, 0.042 mmol) and dissolved in 10 mM monosodium phosphate buffer (50 mL). To a separate 250 mL round bottom flask was added dichlorotetrazine (19 mg, 0.126 mmol, 3 equiv.) and dissolved in acetonitrile (25 mL). To the solution of dichlorotetrazine was added 10 mM monosodium phosphate buffer (25 mL) immediately followed by the solution of peptide

49 and the contents were stirred for one minute. The reaction solution was frozen in dry ice/acetone bath and lyophilized. The crude product was purified by reverse-phase HPLC (5 - 45% organic over 12 min) and exchanged with 0.1 M HCl to give 13.2 mg (71% • HCl salt form) of **50** as an orange amorphous powder after lyophilization. HRMS (ES) Found *m/z* 405.1217 [$(M+H)^+$; calcd for $C_{13}H_{22}ClN_8O_3S$: 405.1219]; ^{1}H NMR (500 MHz, DMSO-d_6) δ 8.39 (d, *J* = 8.0 Hz, 1H), 8.04 (d, *J* = 8.1 Hz, 1H), 7.74 (s, 3H), 7.31 (s, 1H), 7.06 (s, 1H), 4.70 (q, *J* = 7.3 Hz, 1H), 4.18 (td, *J* = 8.5, 4.9 Hz, 2H), 3.78 (dd, *J* = 13.5, 5.7 Hz, 1H), 3.53 (dd, *J* = 13.5, 7.6 Hz, 1H), 2.75 (d, *J* = 6.3 Hz, 2H), 1.86 (s, 3H), 1.75 – 1.64 (m, 1H), 1.52 (ddd, *J* = 12.6, 8.8, 5.1 Hz, 4H), 1.38 – 1.21 (m, 2H). ^{13}C NMR (126 MHz, DMSO) δ 174.7, 173.0, 169.8, 169.2, 164.9, 52.3, 51.3, 32.0, 31.2, 26.6, 22.4, 22.1.

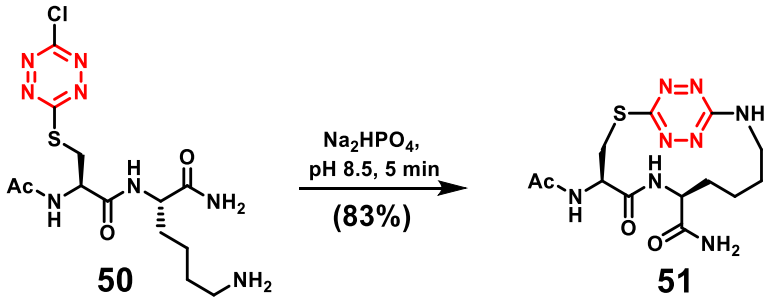

Peptide 51. A 250 mL round bottom flask was charged with peptide **50** (9.6 mg, 0.022 mmol) dissolved in 1 mM monosodium phosphate (40 mL) pH ~5. With vigorous stirring of the solution containing peptide **50** was added 500 mM disodium phosphate (5 mL) to change the pH to ~8.5 and stirring continued for five minutes. Next, 1M HCl (2.2 mL) was added to adjust to pH 6, followed by the addition of MeCN (0.5 mL). The solution was divided into two parts. The solution was transferred to a gravity C_{18}-silica-gel 25 gram column, preequilibrated with water/MeCN (99:1) and 0.1%TFA. The solution was allowed to drain and flushed with water/MeCN (99:1) and 0.1%TFA to remove most of the salts.

The product can be visualized by the red color and was collected by eluting with water/MeCN (1:1) and 0.1%TFA. After all the red material was collected, the column was then equilibrated back to water/MeCN (99:1) and 0.1%TFA and repeated for the other fraction. The fractions containing the product were condensed *in vacuo* to remove the MeCN and lyophilized. The remaining product was purified by reverse-phase HPLC (10 - 60% organic over 12 min) and exchanged with 0.1 M HCl to give 6.7 mg (83%) of **51** as an orange amorphous powder after lyophilization. HRMS (ES) Found *m/z* 369.1451 [$(M+H)^+$; calcd for $C_{13}H_{21}N_8O_3S$: 369.1452]. ^{1}H NMR (500 MHz, DMSO-d_6) δ 8.40 (t, *J* = 6.6 Hz, 1H), 8.22 (d, *J* = 8.6 Hz, 1H), 7.31 (s, 1H), 7.18 (d, *J* = 7.5 Hz, 1H), 7.04 (s, 1H), 4.46 (t, *J* = 8.9 Hz, 1H), 4.05 (dd, *J* = 11.7, 5.5 Hz, 1H), 3.92 (d, *J* = 14.8 Hz, 1H), 3.78 – 3.63 (m, 1H), 3.55 – 3.43 (m, 1H), 3.38 (dd, *J* = 14.8, 9.4 Hz, 1H), 1.88 – 1.74 (m, 1H), 1.65 – 1.54 (m, 1H), 1.54 – 1.44 (m, 1H), 1.40 – 1.29 (m, 1H), 1.11 – 0.96 (m, 2H). ^{13}C NMR (126 MHz, DMSO) δ 172.7, 169.5, 169.1, 162.3, 160.3, 51.9, 51.6, 37.4, 31.4, 31.2, 29.1, 22.6, 20.5.

Synthesis of Bicyclononyne Tethered to a Fluorescein Dye

Compounds SI-12 and SI-13 were prepared according to the following procedures.

5-((2-aminoethyl)carbamoyl)-2-(6-hydroxy-3-oxo-3H-xanthen-9-yl)benzoic acid (SI-12): Gasparini, G.; Bang, E. K.; Molinard, G.; Tulumello, D. V.; Ward, S.; Kelley, S. O.; Roux, A.; Sakai, N.; Matile, S. *J. Am. Chem. Soc.* **2014**, 136, 6069 – 6074.

(1R,8S,9r)-Bicyclo[6.1.0]non-4-yn-9-ylmethyl (4-nitrophenyl) carbonate (SI-13): Schieber, C.; Bestetti, A.; Lim, J. P.; Ryan, Anneke D.; Nguyen, T. L.; Eldridge, R.; White, A. R.; Gleeson, P. A.; Donnelly, P. S.; Williams, S. J.; Mulvaney, P. *Angew. Chem. Int. Ed.* **2012** , 51, 10523 – 10527.

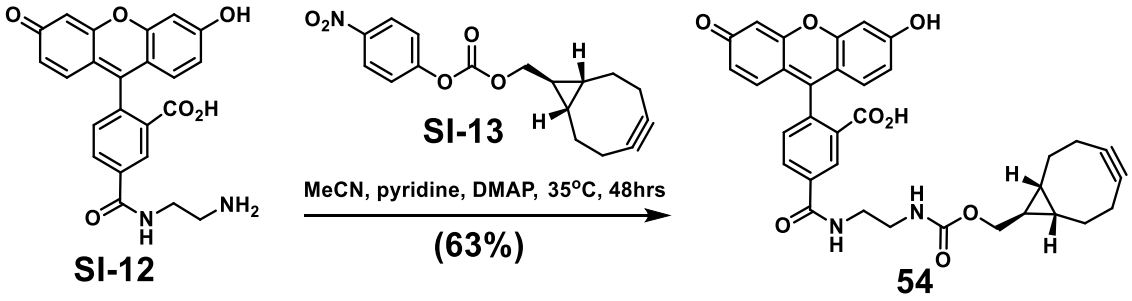

Compound 54. To a 5 mL round bottom flask containing 5-((2-aminoethyl)carbamoyl)-2-(6-hydroxy-3-oxo-3H-xanthen-9-yl)benzoic acid (9.0 mg, 22 μmol) dissolved in MeCN (500 μL) was added bicyclo[6.1.0]non-4-yn-9-ylmethyl (4-nitrophenyl) carbonate (8.3 mg, 26 μmol, 1.2 equiv) in MeCN (250 μL) followed by the addition of pyridine (16 μL, 200 μmol, 10 equiv) and DMAP (2.7 mg, 22 μmol, 1 equiv). The contents were then stirred at 35ºC for 48 hours. The reaction mixture was evaporated and the crude re-dissolved in water/MeCN (7:3, 1000 μL) and purified by reverse-phase HPLC (gradient 10-80% organic

over 15 minutes) to give 8.2 mg (63%) after lyophilization. HRMS (ES) *m/z* 595.2069 [$(M+H)^+$; calcd for $C_{34}H_{31}N_2O_8$: 595.2080]. ^{1}H NMR (500 MHz, Methanol-d_4) δ 8.49 (s, 1H), 8.21 (d, *J* = 8.0 Hz, 1H), 7.34 (d, *J* = 8.0 Hz, 1H), 6.79 (s, 2H), 6.73 (d, *J* = 8.3 Hz, 2H), 6.64 (d, *J* = 8.8 Hz, 2H), 4.15 (d, *J* = 8.2 Hz, 2H), 3.54 (t, *J* = 5.7 Hz, 2H), 3.39 (t, *J* = 6.0 Hz, 2H), 2.19 (d, *J* = 12.8 Hz, 4H), 2.09 (d, *J* = 15.3 Hz, 2H), 1.56 (dd, *J* = 21.8, 9.7 Hz, 2H), 1.36 (dt, *J* = 17.3, 8.6 Hz, 1H), 0.87 (t, *J* = 10.0 Hz, 2H).

Bioconjugation of 54 with s-Tetrazine Peptide 42

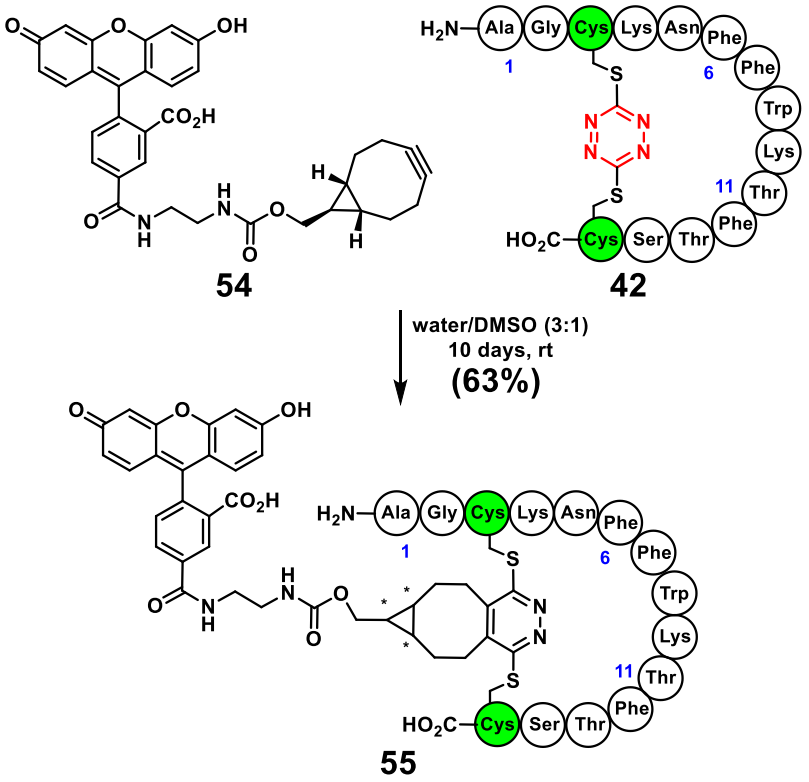

Compound 55. To a 5 mL round bottom flask was added a solution (1.1 mM) of peptide **42** dissolved in water (500 µL) followed by a solution (1.2 mM) of bicyclononyne **54** in DMSO (500 µL). The contents were stirred at room temperature for 4 days and the solvent

removed *in vacuo*. The residue was purified by reverse-phase HPLC (gradient 10-60% organic over 15 min) to give (0.9 mg, 68%) of a yellow-orange powder after lyophilization. MALDI-TOF *m/z* 2283.468 [$(M+H)^+$; calcd for $C_{112}H_{135}N_{22}O_{27}S_2$: 2283.930].

Tetrazine Stapling of the Thioredoxin Protein

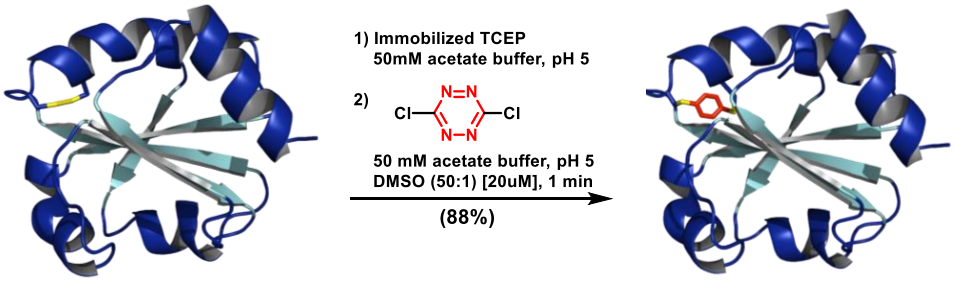

Native-Trx **56**

To a 1.7 mL mini-centrifuge tube containing thioredoxin (0.25 mg, 21 nmol) dissolved in acetate buffer pH 5 (200 mM, 100 µL), was added TCEP immobilized on agrose (300 µL, 8 µmol/mL, 2.4 µmol, 112 equiv); the final buffer concentration was 50 mM. The reaction was stirred at room temperature for 2.0 hours under an argon atmosphere. The contents were kept under a blanket of argon, then filtered through a plastic pipet tip with a cotton plug and rinsed with degassed 50 mM acetate buffer pH 5 (3 × 200 µL). To the pooled filtrates (1.0 mL) in a 1.7 mL mini-centrifuge tube was added a pre-mixed solution of dichlorotetrazine in DMSO (20 µL, 87 nmol, 4 equiv, [0.67 mg/mL]) and stirred for 1 minute. The solution was then transferred to a pre-equilibrated disposable PD-10 desalting column and eluted with 50 mM Tris, pH 7.8, 150 mM NaCl. The fractions containing protein were pooled and stored at 4ºC. Bradford assay (88% yield). MALDI-TOF *m/z* 11757.782

[$(M+H)^+$; 11756.45; calculated for Trx-1 (11675.43 Da) + tetrazine (80.01 Da) + H^+ (1.01)].

Photochemical Unstapling and Regeneration of the Thioredoxin Protein

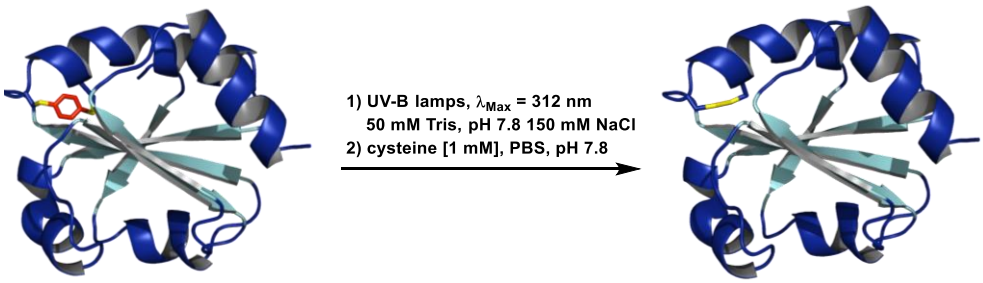

56 **57**

Sample Preparation for Comparison

A sample of tetrazine thioredoxin (0.1 mg, 8 nmol), from the desalting column in 50 mM Tris, pH 7.8, 150 mM NaCl (1000 μL) was divided between two 1.7 mL mini-centrifuge tubes. One sample underwent photolysis and the other used as a comparsion.

Tetrazine Thioredoxin Photolysis

A 1.7 mL mini-centrifuge tube containing tetrazine thioredoxin (0.05 mg, 4 nmol) dissolved in 50 mM Tris, pH 7.8, 150 mM NaCl (500 μL) was suspended in a Rayonet® photoreactor equipped with three UV-B lamps. The contents were irradiated for 1.0 hour, MALDI indicated consumption of the starting material with partial loss of the nitrile groups.

Regeneration of the Protein

To the photolyzed sample dissolved in 50 mM Tris, pH 7.8, 150 mM NaCl (500 µL), was added cysteine (25 µL) of a 20 mM solution in the Tris buffer system and TCEP (25 µL) of a 20 mM solution in the Tris buffer system. The contents were allowed to stand for 4.0 hours and then diluted to 3 mL with the Tris buffer system and transferred for centrifugation in an Amicon centrifugal filter (MWCO 3000, 35º fixed angle rotor @ 7000×G, 30 minutes, 4ºC), the concentrated sample (150 µL) was diluted to 3 mL and repeated. The retenate was collected and diluted to 500µL with the Tris buffer system, then Ellman's reagent [5,5'-dithio-bis-(2-nitrobenzoic acid)] (25 µL of a 20 mM solution in the Tris buffer system) was added and allowed to stand for 6.0 hours. The contents were then diluted to 3 mL with the Tris buffer system and transferred for centrifugation in an Amicon centrifugal filter (MWCO 3000, 35º fixed angle rotor @ 7000×G, 30 minutes, 4ºC). The retenate was collected and diluted to 500 µL with the Tris buffer solution and analyzed by MALDI-TOF and FPLC. Bradford assay (73% yield). MALDI-TOF *m/z* 11676.188 [$(M+H)^+$; 11676.44].

Measurement of Regenerated Thioredoxin Bioactivity

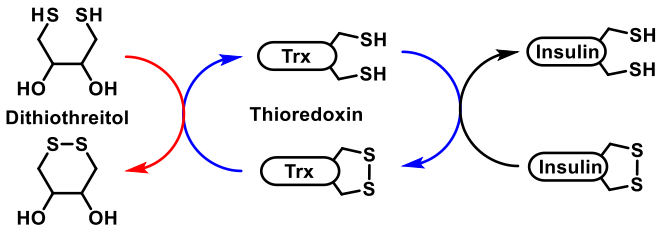

Thioredoxin activity was measured by following the reduction of insulin described by the method of Xianqin Yang and Kesen Ma, *Journal of Bacteriology*, **2010**, 192(5), 1370–1376.

The standard thioredoxin assay mixture, prepared in 200 µL overall volume, contained 50 mM sodium phosphate buffer, pH 7.0, 1 mM EDTA, 0.15 mM human insulin, 1 mM dithiothreitol. The amounts of native thioredoxin *E. coli*, tetrazine thioredoxin, and regenerated thioredoxin were varied, concentrations of protein were determined by Bradford assay. Sample were run in duplicate, the increase in turbity from the reduction of insulin was monitored at 650 nm at 30°C by a Tecan plate reader.

The kinetic curves were baseline corrected by subtracting from insulin reduction by dithiothreitol alone. The corrected slopes from the kinetic data (ΔmAU/min), in the linear region, were plotted as a function of concentration of protein.

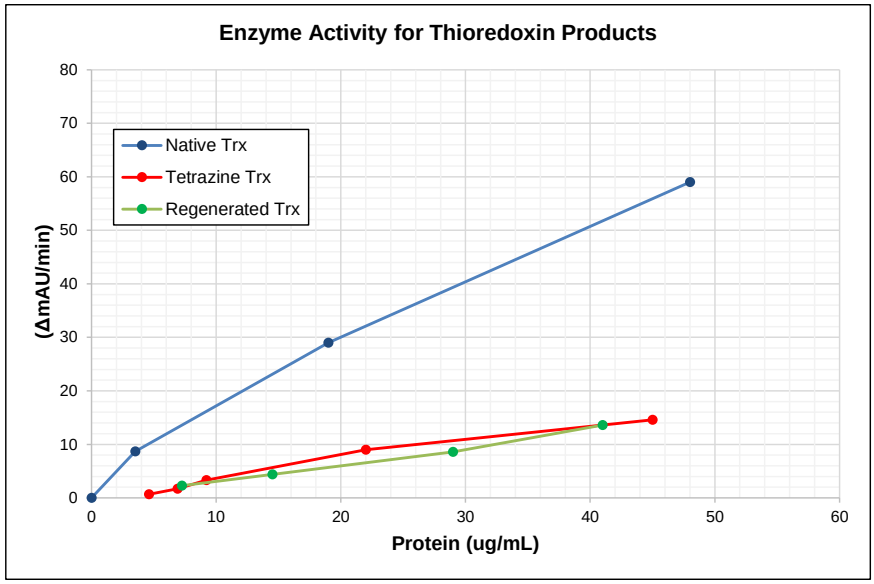

Control Experiment for the Photolysis of Native Thioredoxin

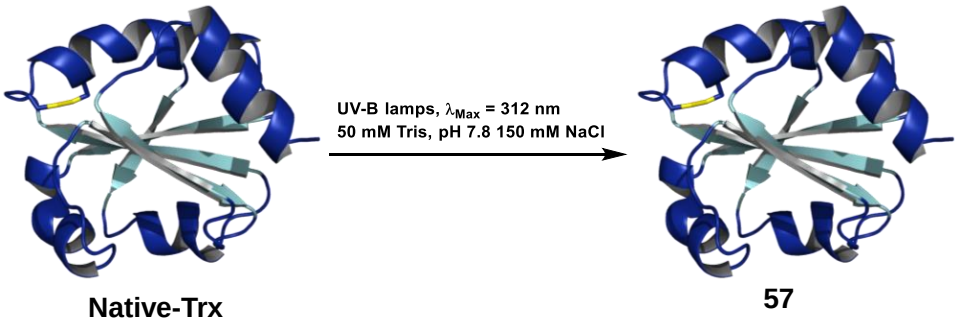

A 1.7 mL mini-centrifuge tube containing native thioredoxin (0.05 mg, 4 nmol) dissolved in 50 mM Tris, pH 7.8, 150 mM NaCl (500 µL) was suspended in a Rayonet® photoreactor equipped with three UV-B lamps. The contents were irradiated for 1.0 hour, MALDI indicated no change in the mass after photolysis. The native thioredoxin and the product from photolysis were analyzed by the insulin reduction bioassay described previously. The product from photolysis showed a significant decrease in activity when compared to the activity of the native protein.

Photochemical Unstapling of 56 with Nd:YAG Flashlamp at 355 nm

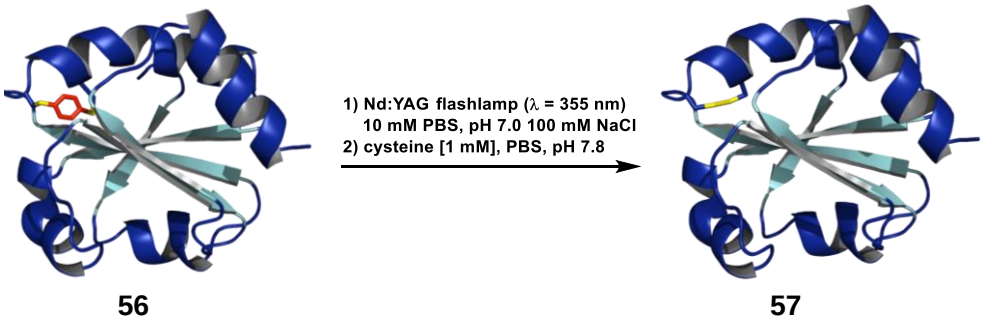

To a 3 mL quartz cuvette was added tetrazine thioredoxin **56** (0.23 mg, 20 nmol) dissolved in 10 mM PBS, pH 7.0, 100 mM NaCl (2000 µL) overall concentration of protein 10µM

and then transferred to a laser setup consisting of a Nd:YAG laser with a 355 nm wavelength. The contents were irradiated for 1.0 hour. MALDI indicated consumption of the starting material. The reaction solution was then treated with 10 mM cysteine in 500 mM phosphate buffer system (pH 7.8) to achieve a 1 mM overall concentration of cysteine and a 9 μM concentration for the protein which was allowed to stand at 5ºC for 16 hours. The reaction solution was then removed by centrifugal filtration and analyzed by MALDI-TOF-MS to find both the loss of the nitriles from the thiocyanates and the molecular mass of regenerated thioredoxin protein. MALDI-TOF *m/z* 11676.188 [$(M+H)^+$; 11676.44].

Bioactivity Measurement for Thioredoxin Resulting from the Flashlamp Conditions

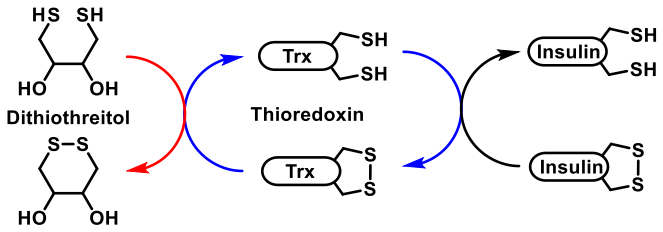

The standard thioredoxin assay mixture, prepared in 200 μL overall volume, contained 50 mM sodium phosphate buffer, pH 7.0, 1 mM EDTA, 0.15 mM human insulin, 1 mM dithiothreitol. The amounts of native thioredoxin *E. coli*, tetrazine thioredoxin, and regenerated thioredoxin were varied, concentrations of protein were determined by Bradford assay. Sample were run in triplicate, the increase in turbity from the reduction of insulin was monitored at 650 nm at 30°C by a Tecan plate reader.

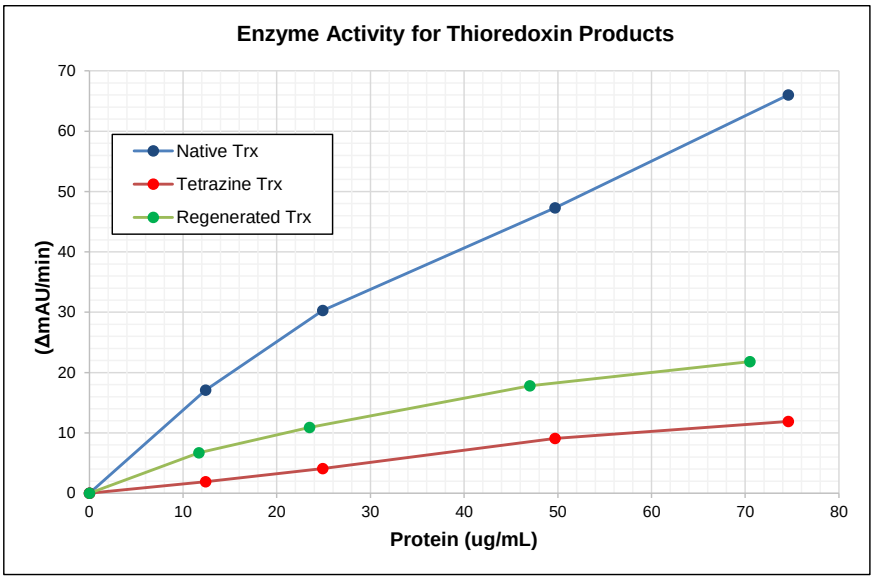

Inverse-Electron Demand Diels-Alder Reaction of Bicyclononyne with Tetrazine Thioredoxin

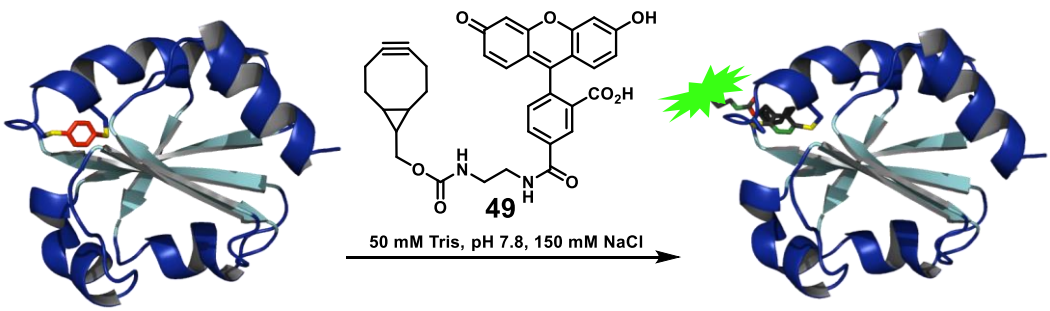

To a 1.7 mL mini-centrifuge tube containing tetrazine thioredoxin (0.05 mg, 4 nmol) dissolved in 50 mM Tris, pH 7.8, 150 mM NaCl (500 µL) was added a solution of **5** (100 µL, 0.024 mg, 40 nmol, 10 equiv) dissolved in the Tris buffer system. The contents were allowed to stand at ambient temperature for 10 days. The contents were next transferred for centrifugation in an Amicon centrifugal filter (MWCO 3000, 35º fixed angle rotor @ 7000×G, 30 minutes, 4ºC), the concentrated sample (150 µL) was diluted to 3 mL with the

Tris buffer and repeated. The reaction was monitored by mass spectrometry, which illustrated the loss of nitrogen and an additional mass equal to **5** . MALDI-TOF *m/z* 12323.622 [$(M+H)^+$; 12322.64; calculated for tetrazine Trx (11755.44) + **5** (594.20 Da) + H^+ (1.01) – N_2 (28.01)].

APPENDIX

Relevant Spectra

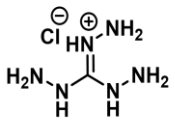

1

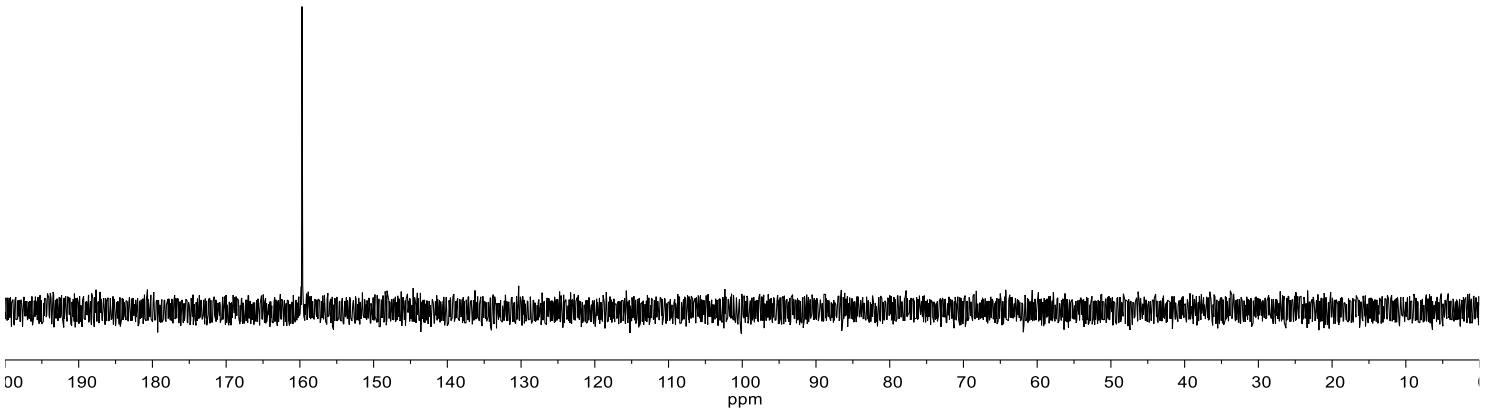

Figure A.1. 125 MHz ^{13}C-NMR Spectrum of Compound 1 in D_2O

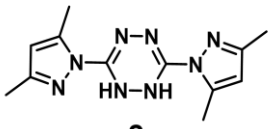

2

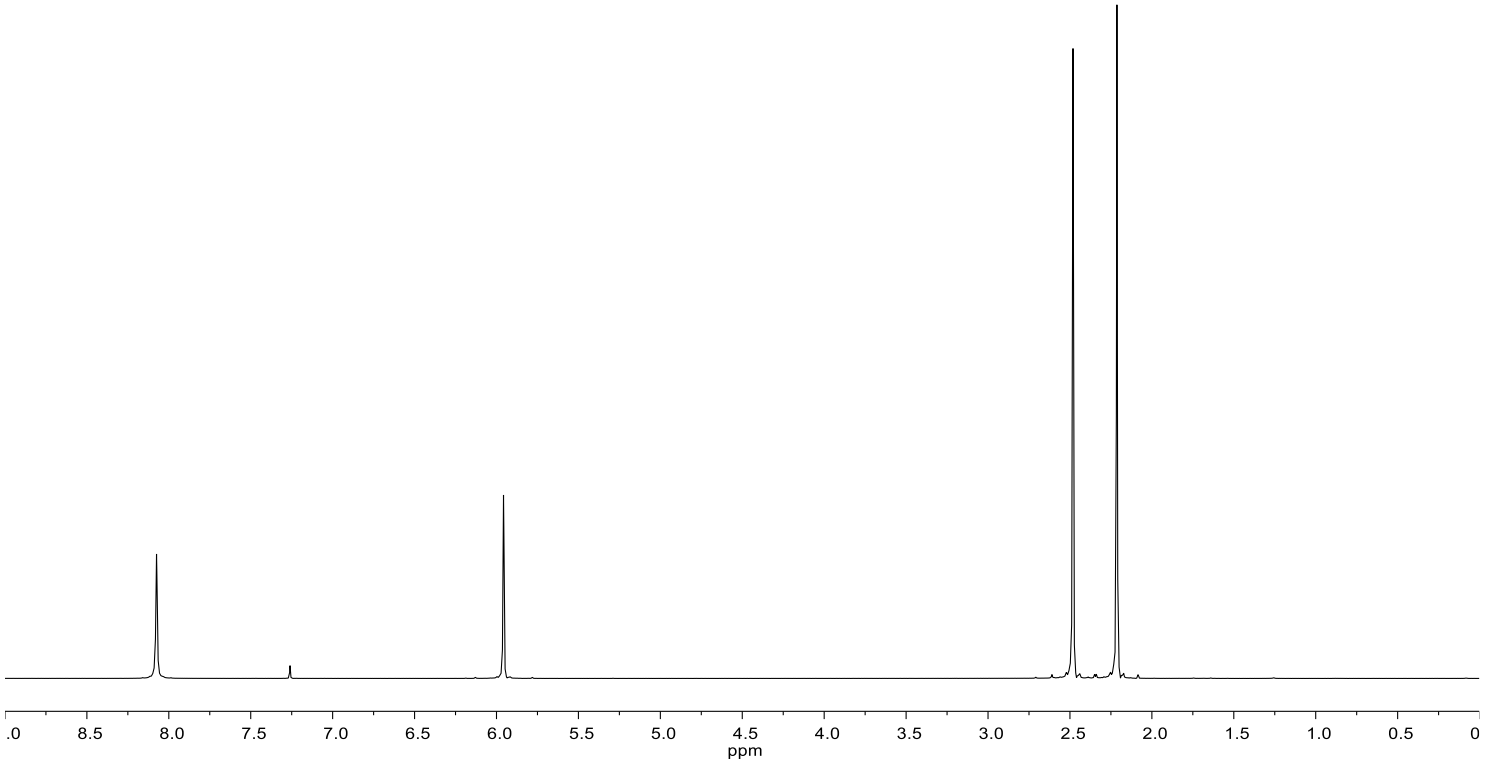

Figure A.2. 500 MHz ^{1}H-NMR Spectrum of Compound 2 in $CDCl_3$

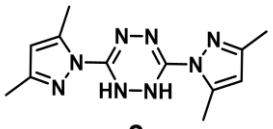

2

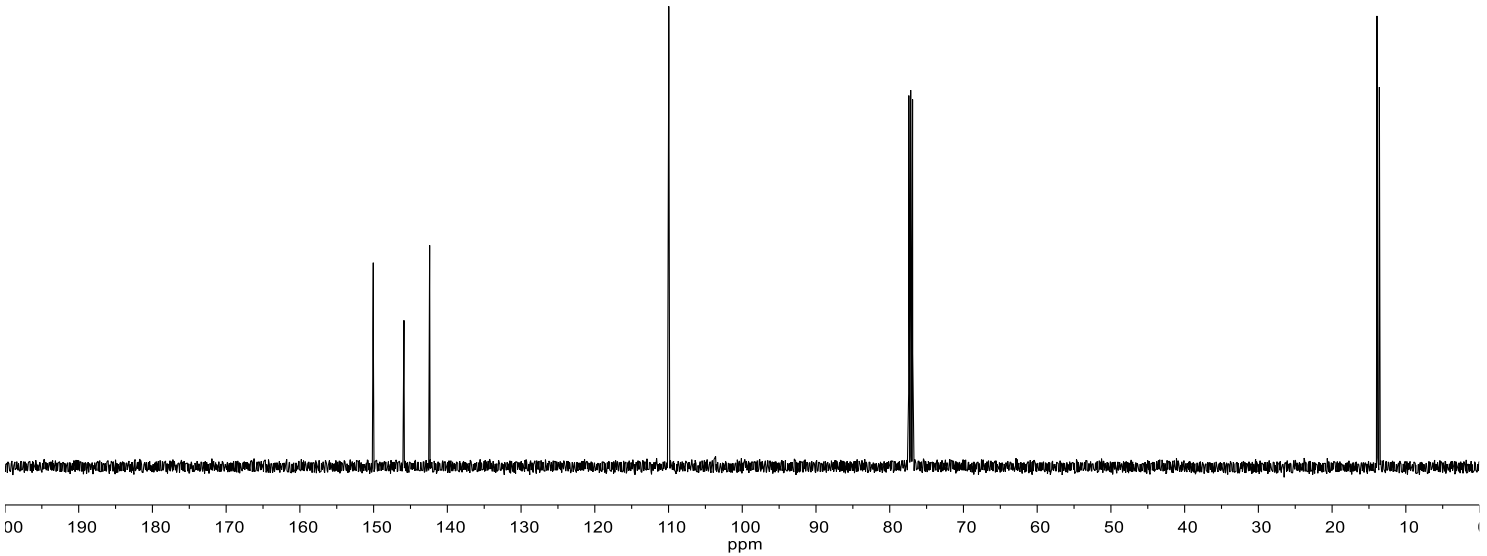

Figure A.3. 125 MHz ^{13}C-NMR Spectrum of Compound 2 in $CDCl_3$

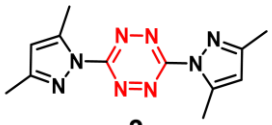

3

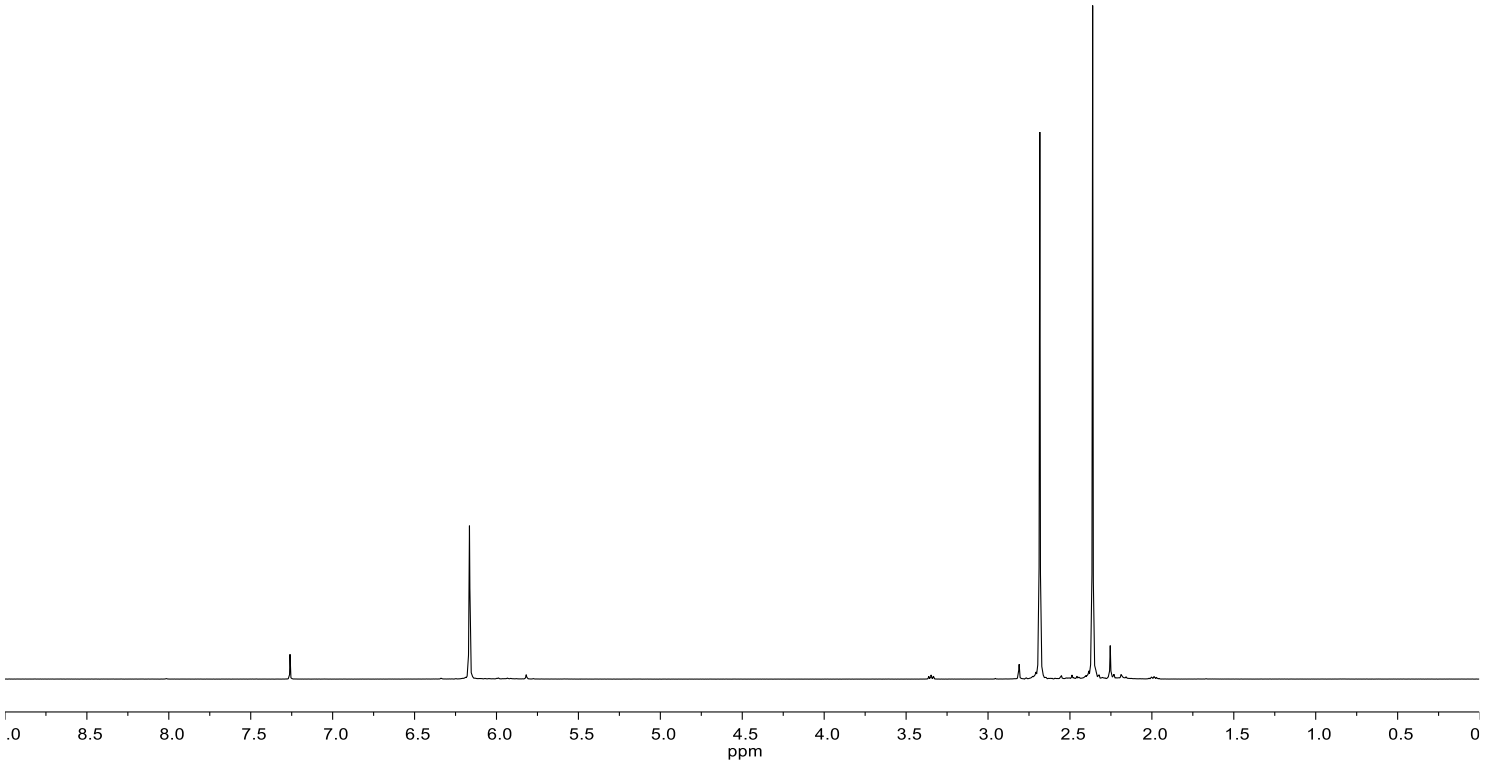

Figure A.4. 500 MHz ^{1}H-NMR Spectrum of Compound 3 in $CDCl_3$

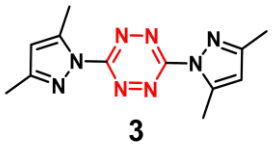

3

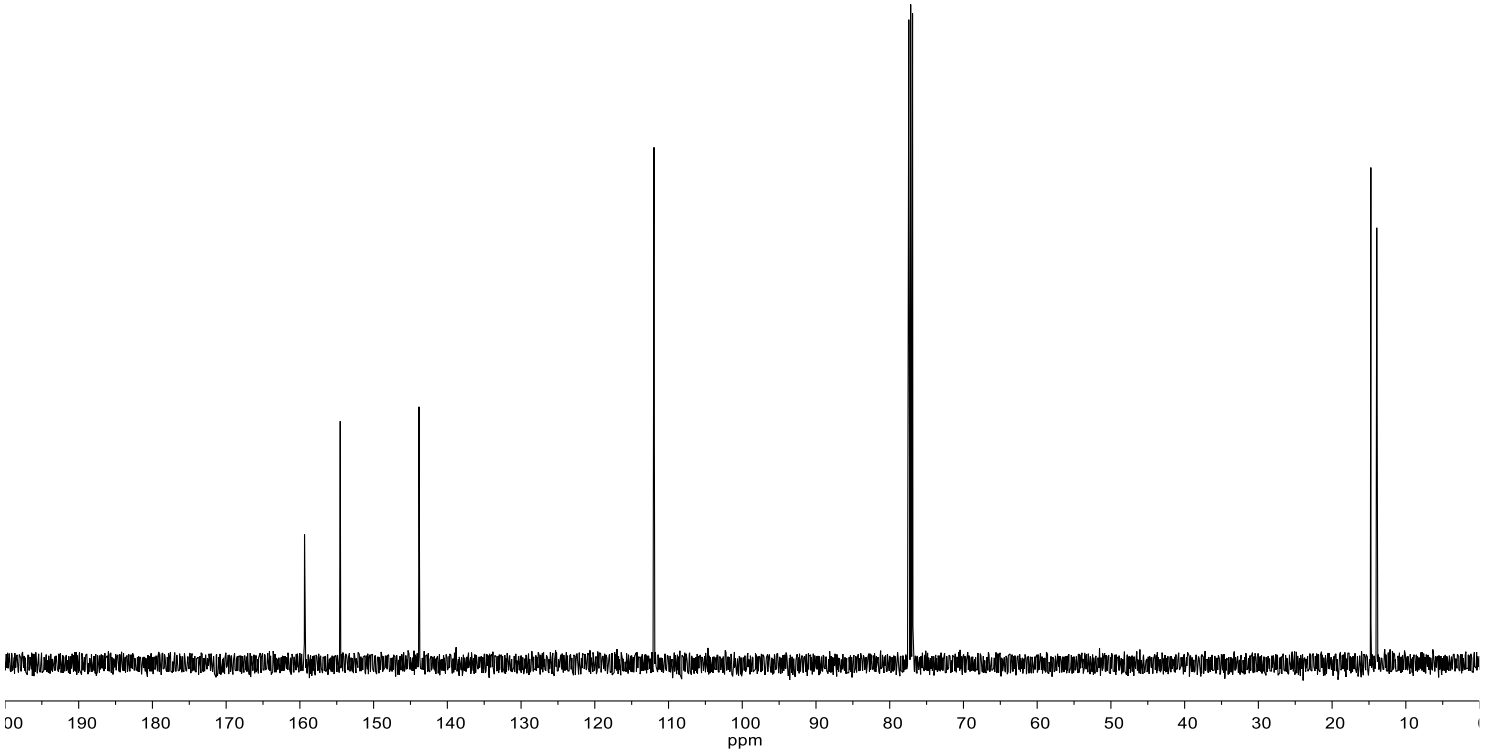

Figure A.5. 125 MHz ^{13}C-NMR Spectrum of Compound 3 in $CDCl_3$

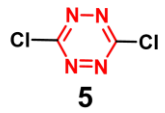

5

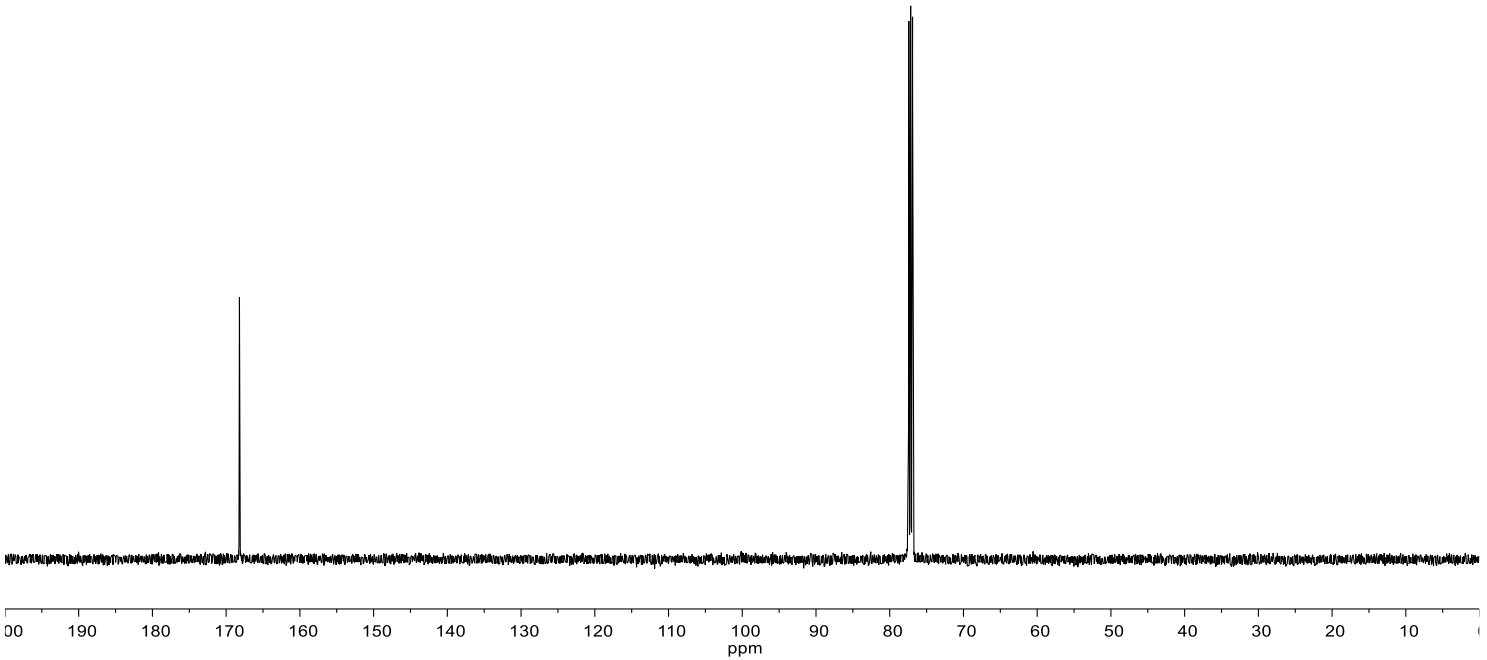

Figure A.6. 125 MHz ^{13}C-NMR Spectrum of Compound 5 in $CDCl_3$

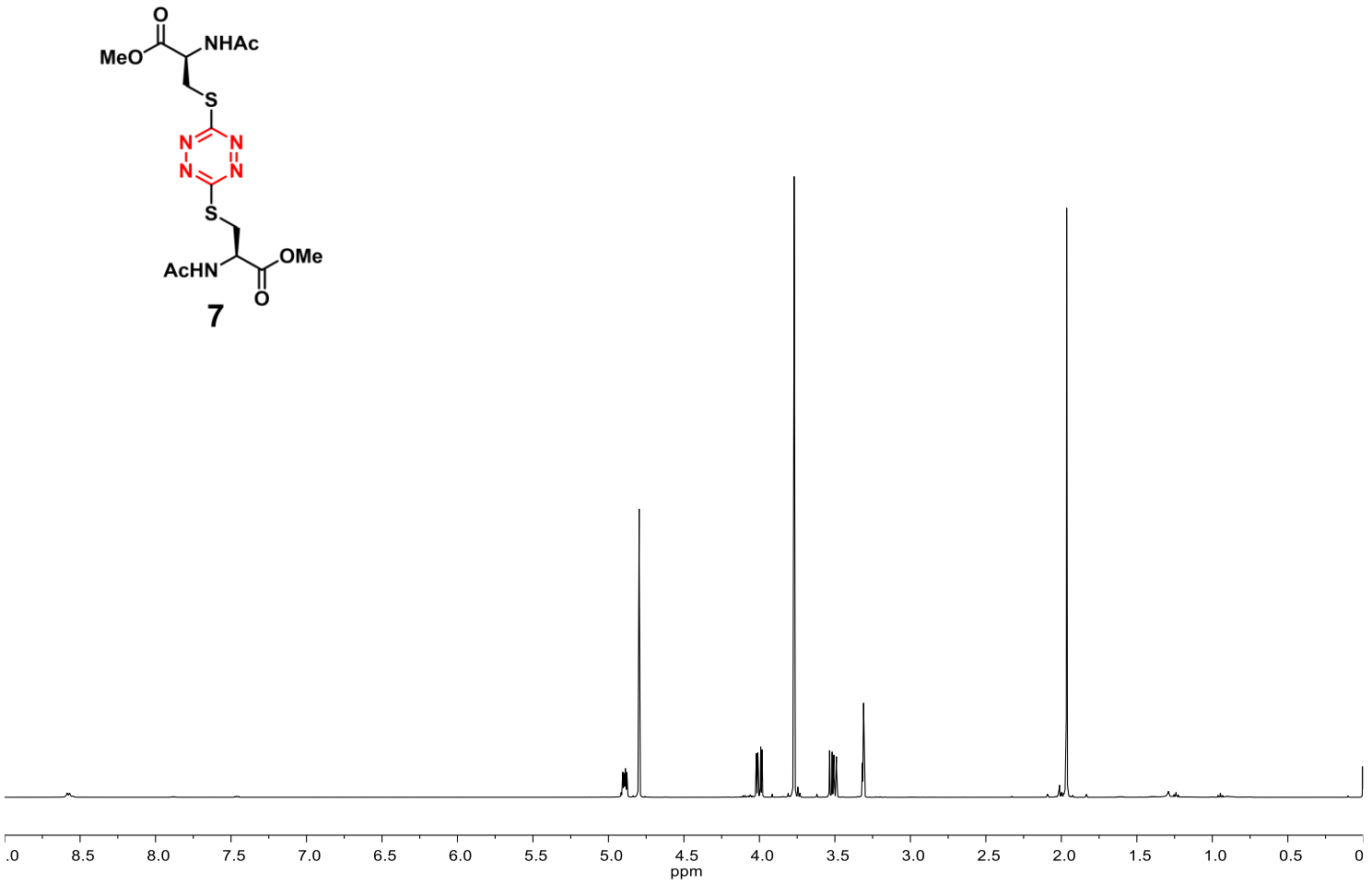

Figure A.7. 500 MHz ^{1}H-NMR Spectrum of Compound 7 in CD_3OD

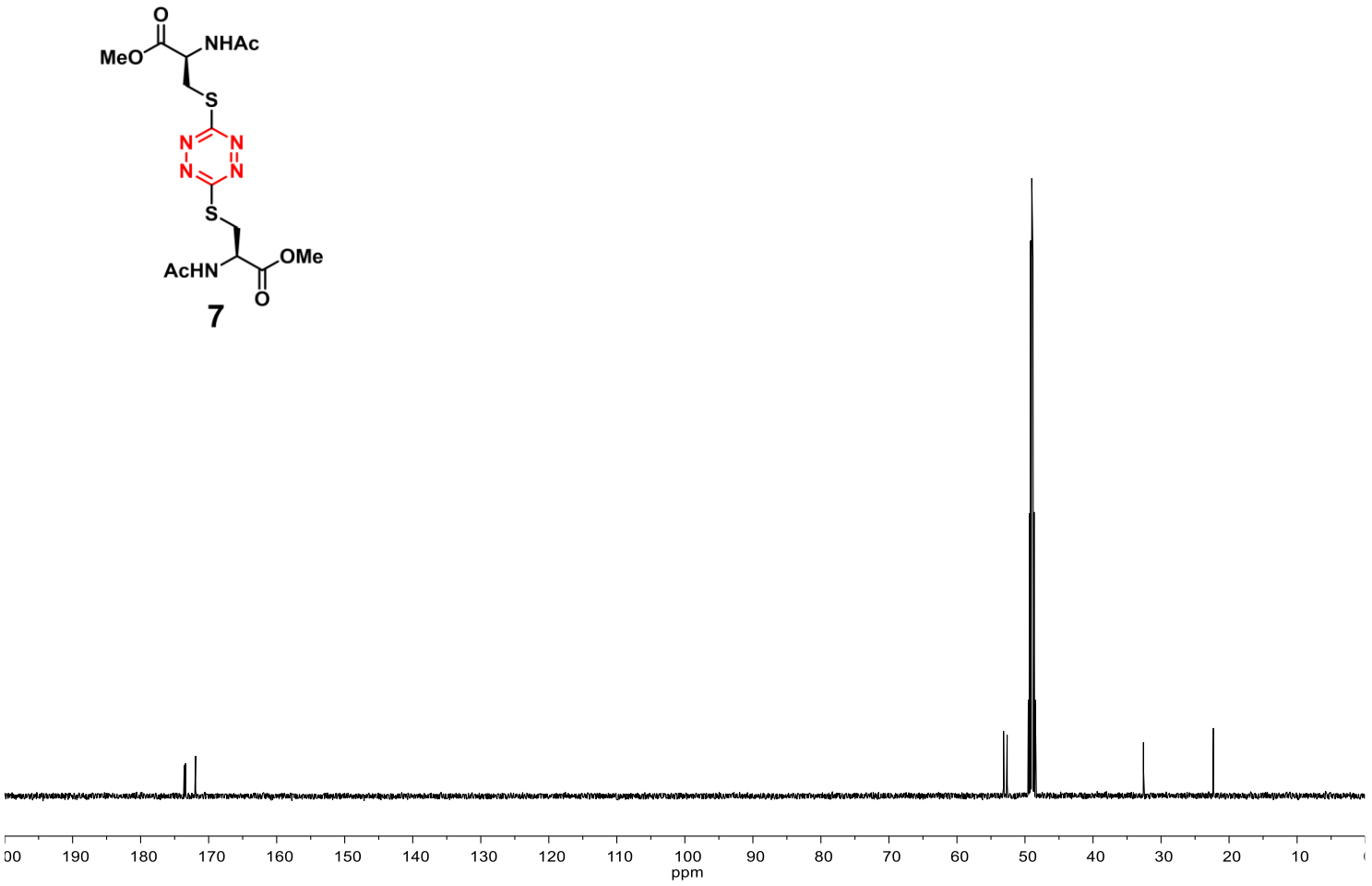

Figure A.8. 125 MHz ^{13}C-NMR Spectrum of Compound 7 in CD_3OD

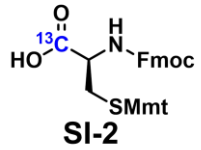

SI-2

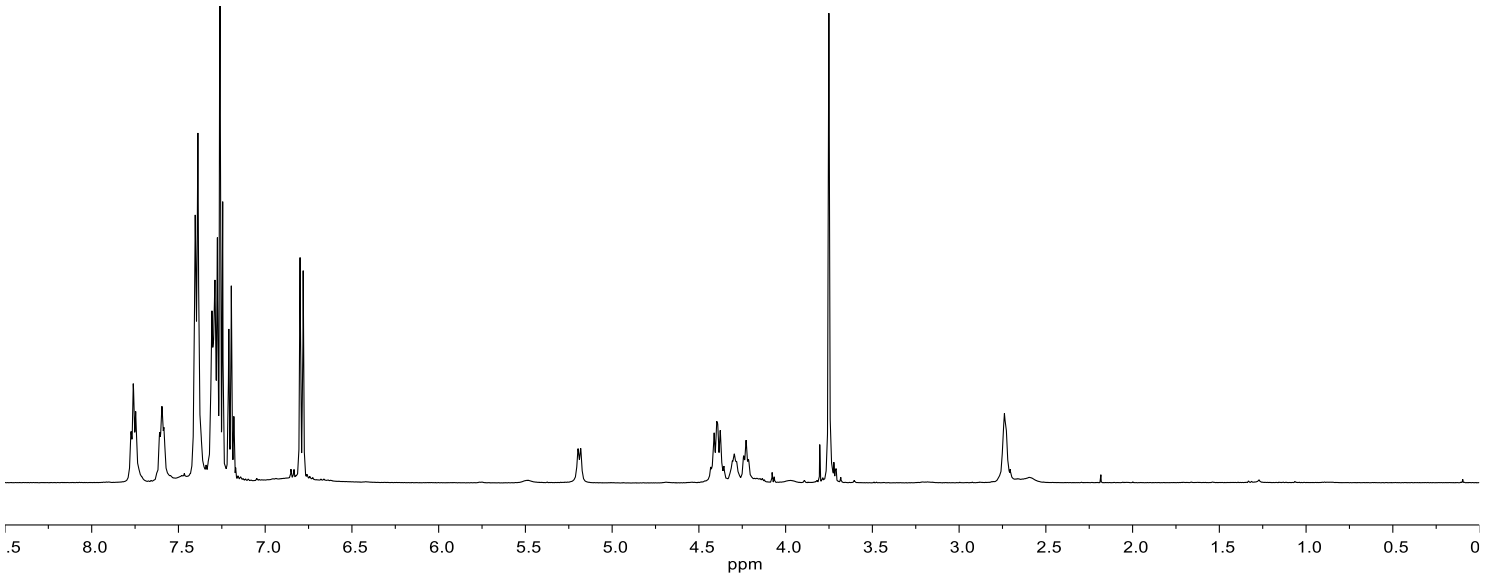

Figure A.9. 500 MHz ^{1}H-NMR Spectrum of Compound SI-2 in $CDCl_3$

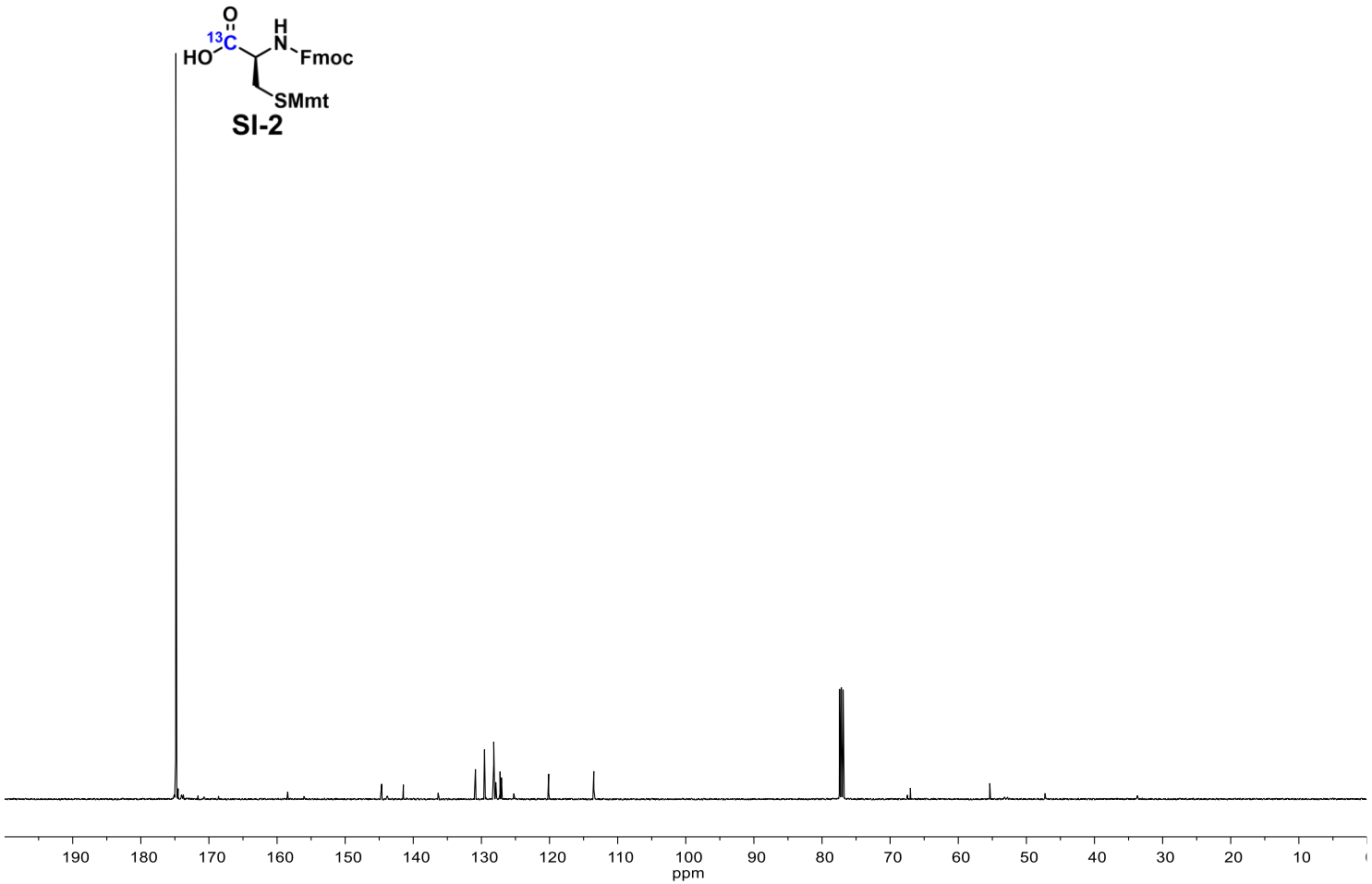

Figure A.10. 125 MHz ^{13}C-NMR Spectrum of Compound SI-2 in $CDCl_3$

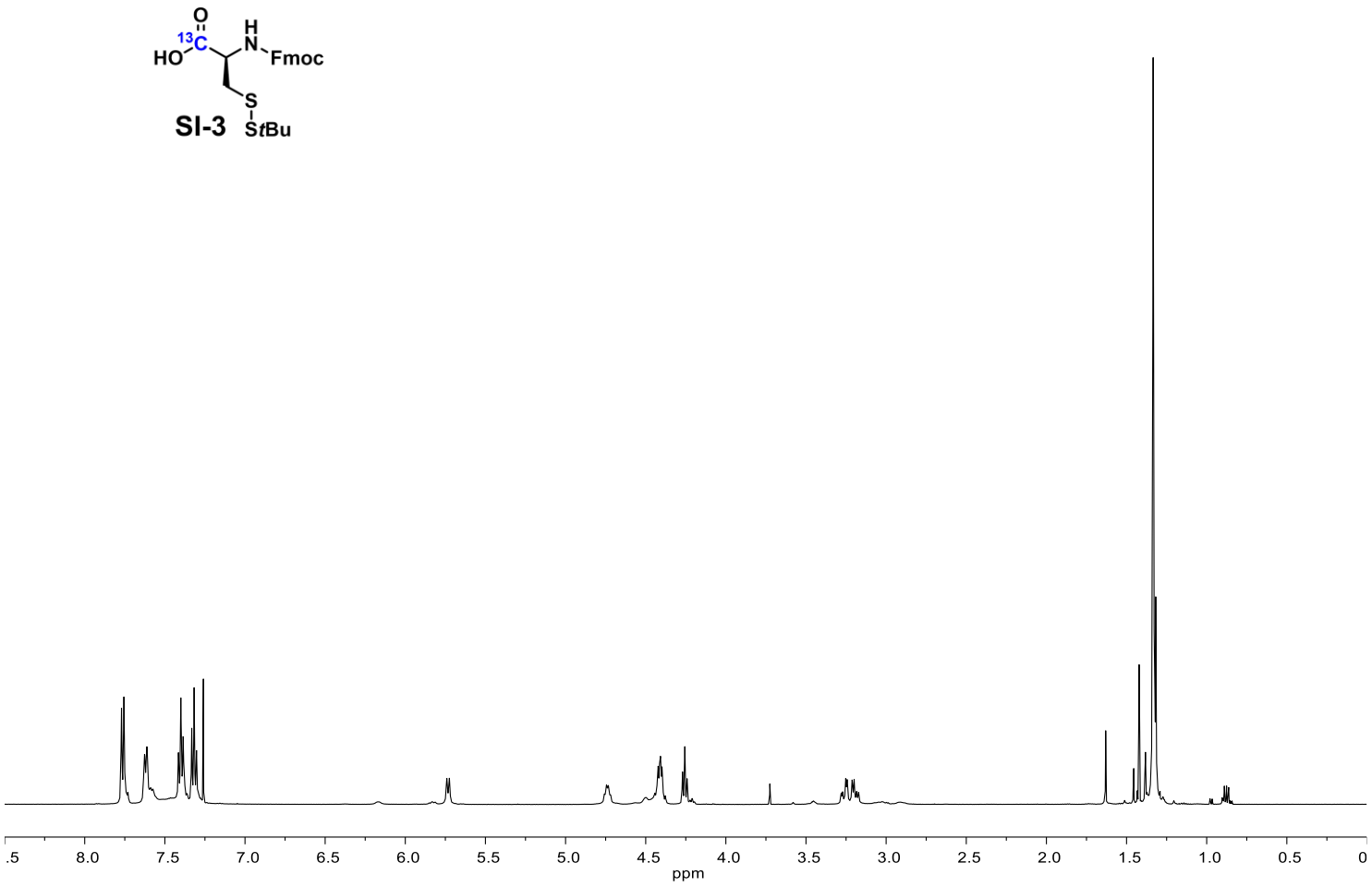

Figure A.11. 500 MHz ^{1}H-NMR Spectrum of Compound SI-3 in $CDCl_3$

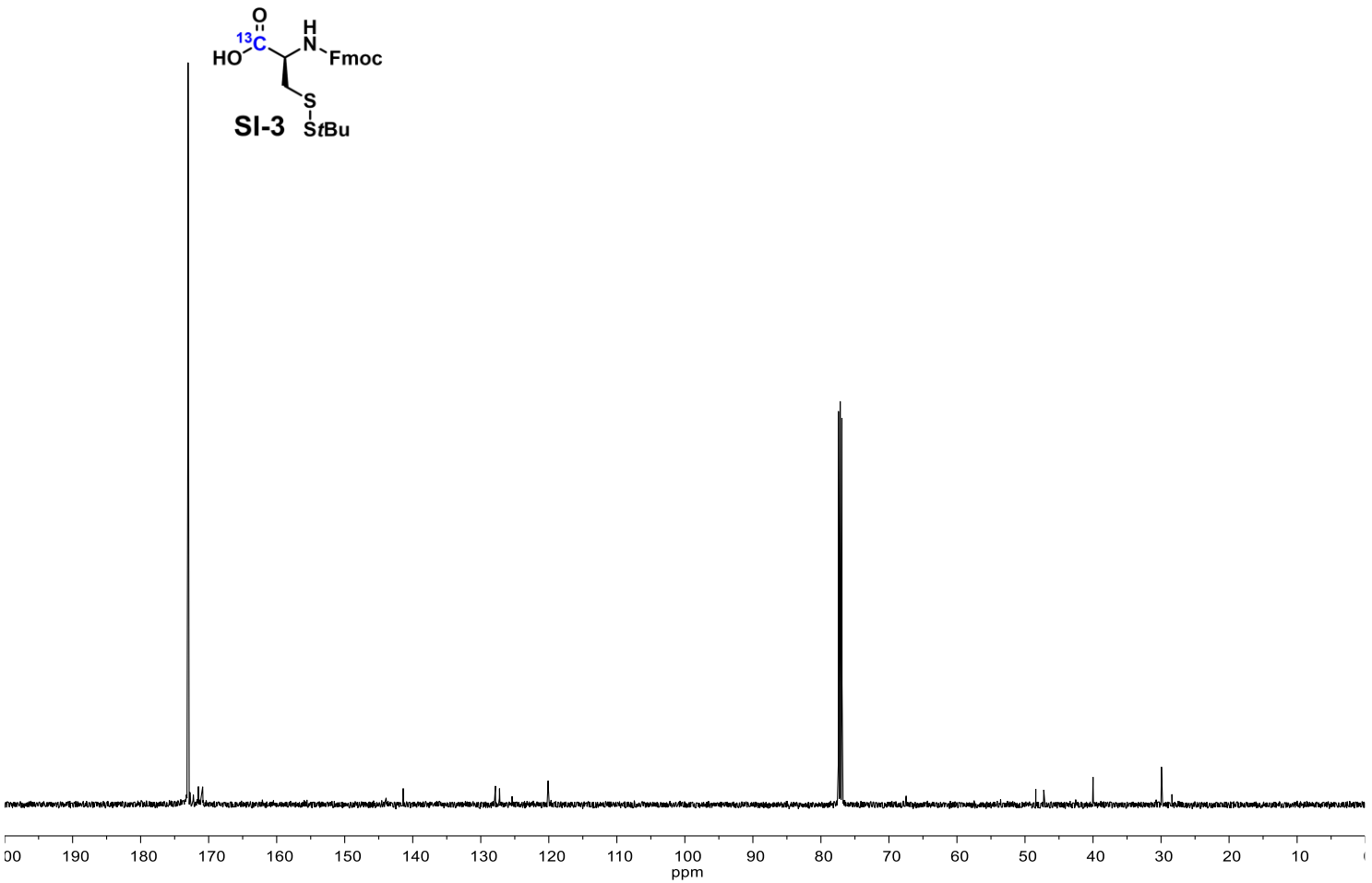

Figure A.12. 125 MHz ^{13}C-NMR Spectrum of Compound SI-3 in $CDCl_3$

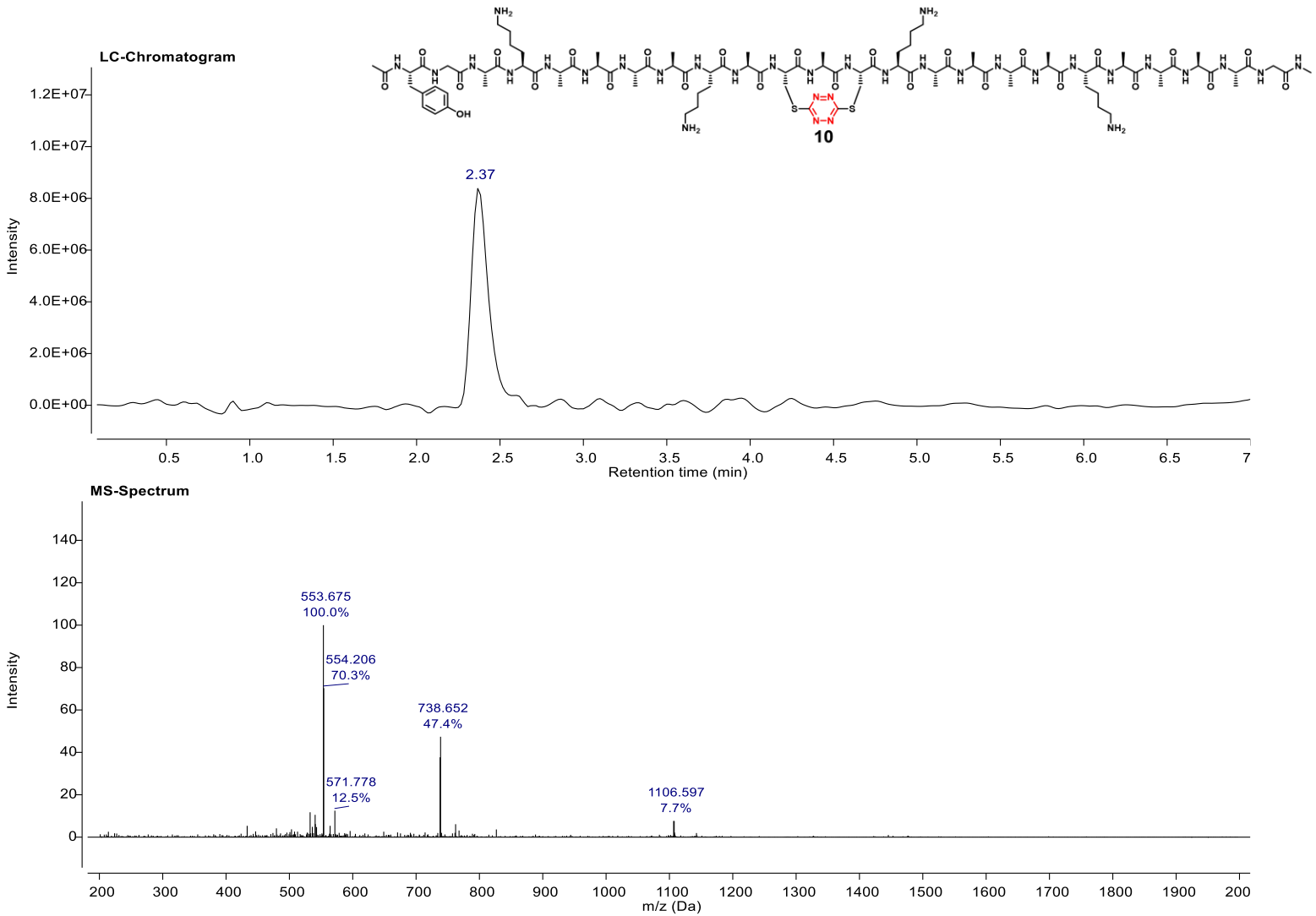

Figure A.13. LC-MS Spectrum of Compound 10 Gradient 5-60 for 7 Minutes

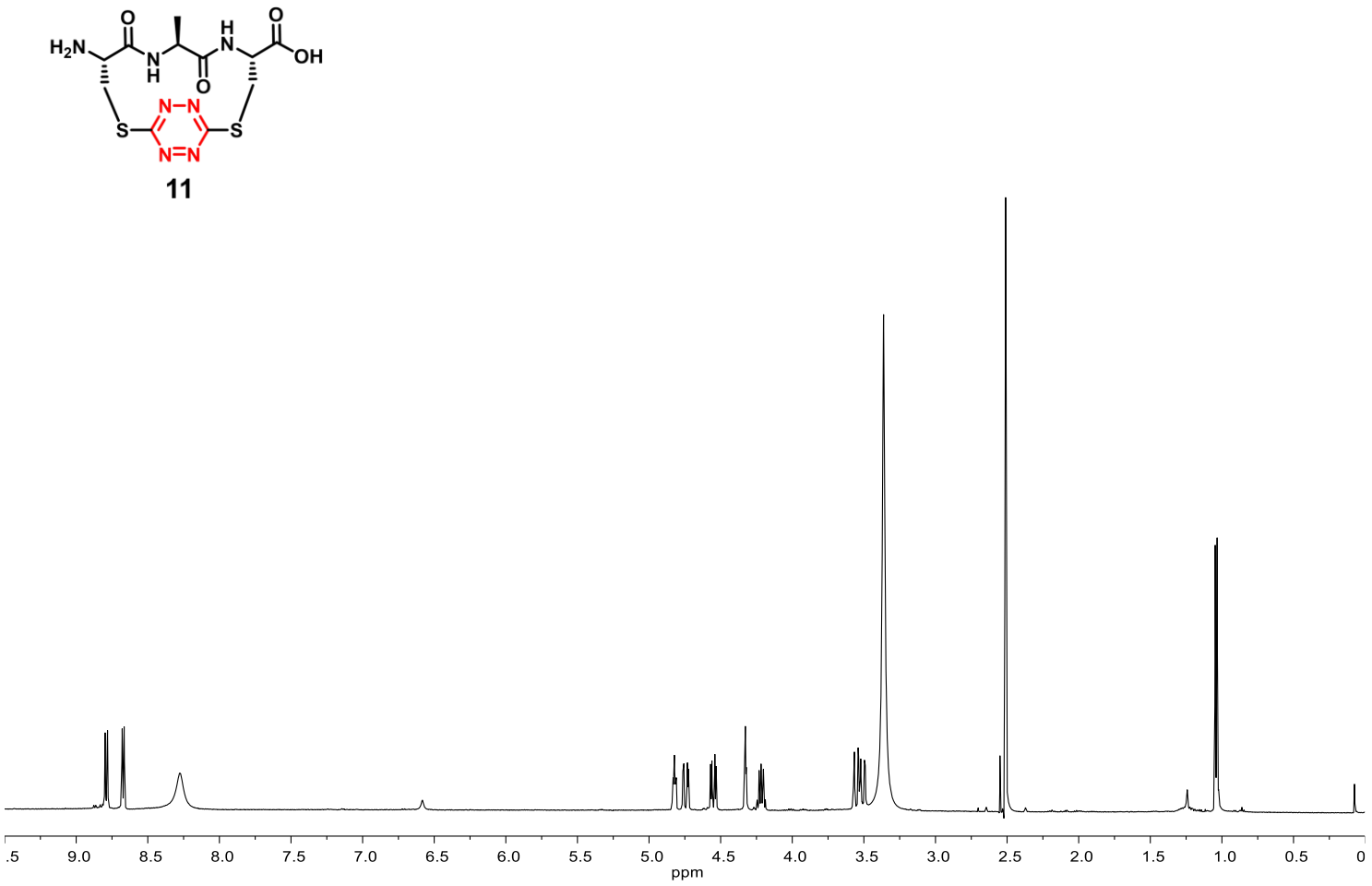

Figure A.14. 500 MHz ^{1}H-NMR Spectrum of Compound 11 in d_6-DMSO

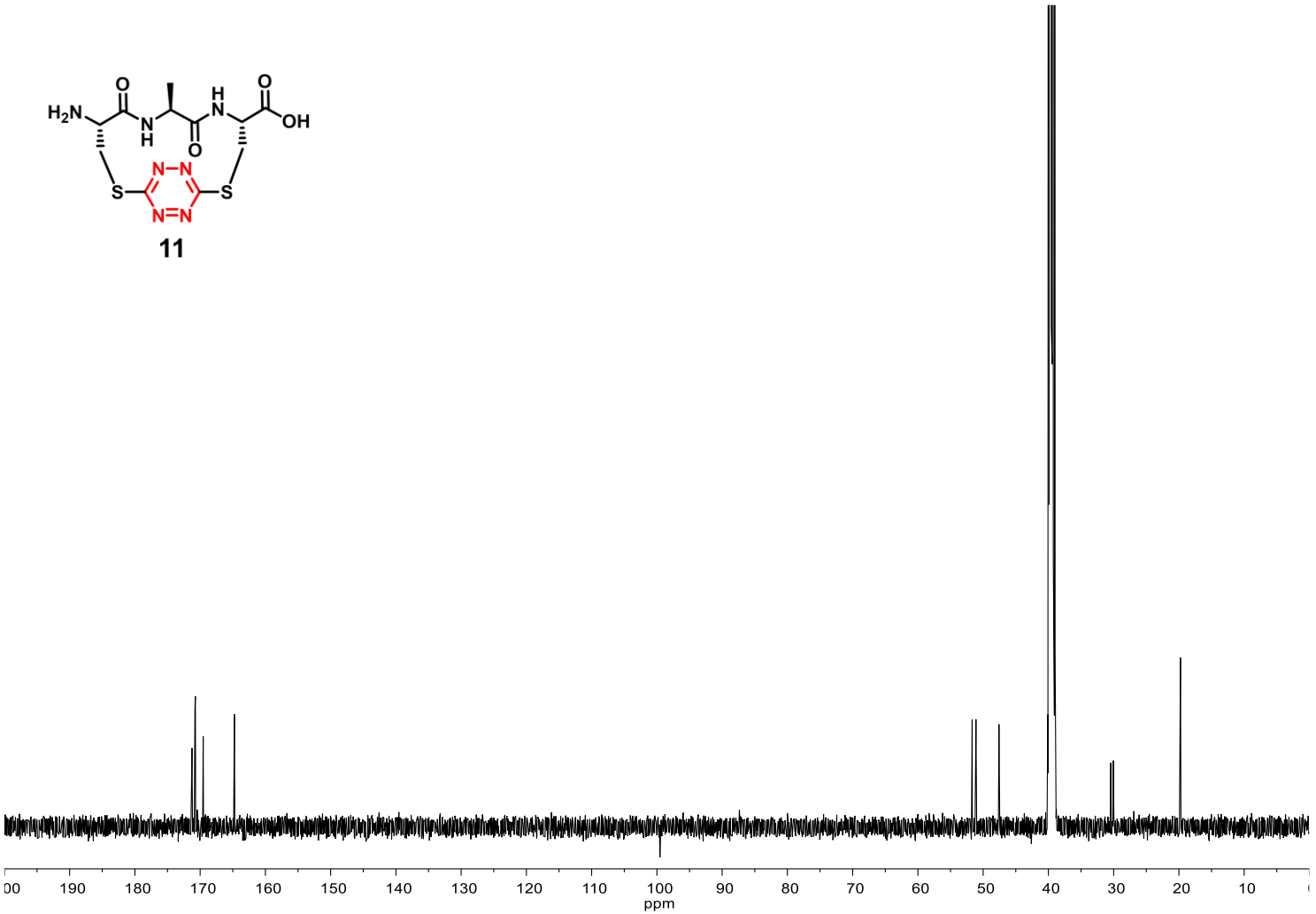

Figure A.15. 125 MHz ^{13}C-NMR Spectrum of Compound 11 in d_6-DMSO

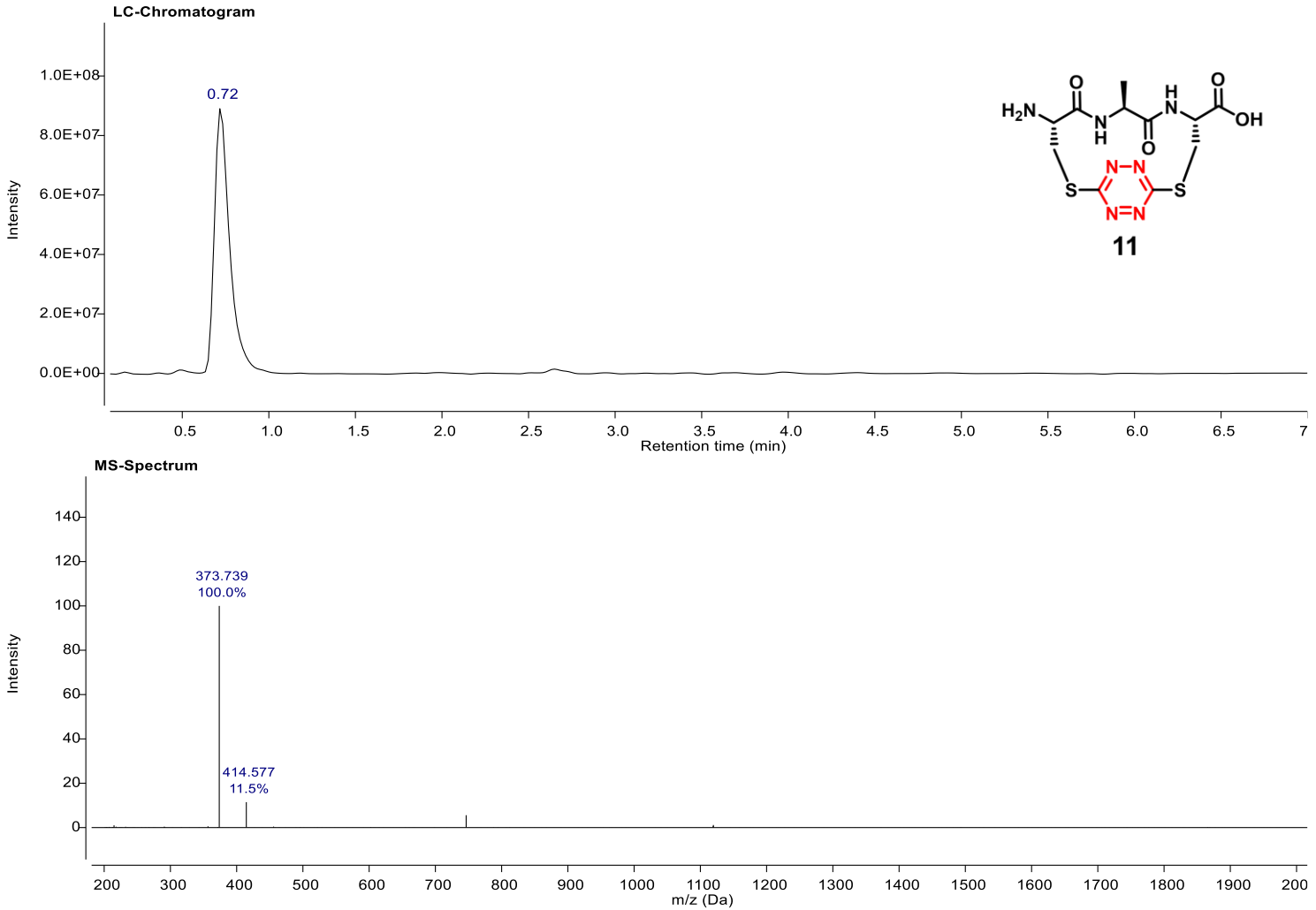

Figure A.16. LC-MS Spectrum of Compound 11 Gradient 5-60 for 7 Minutes

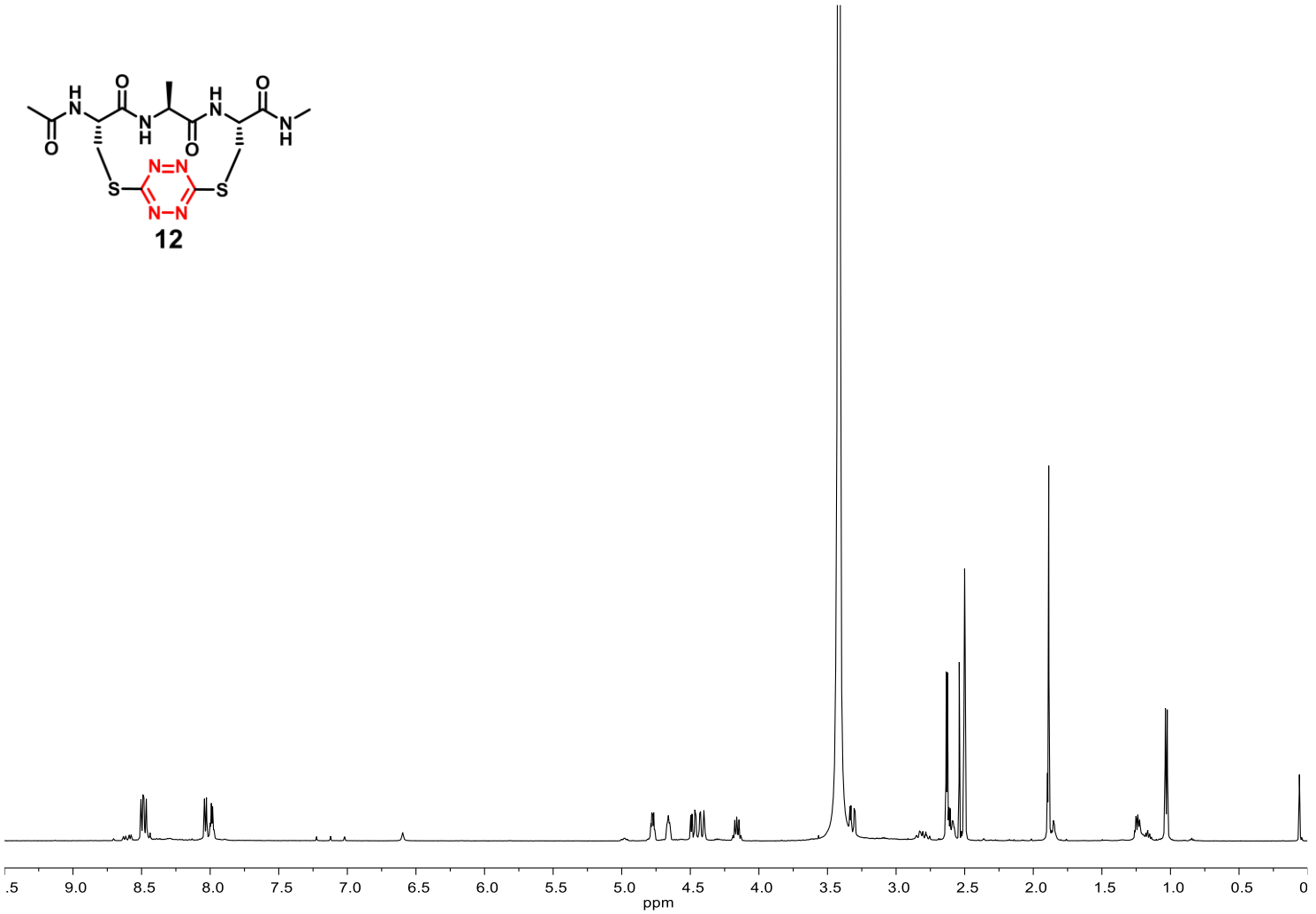

Figure A.17. 500 MHz ^{1}H-NMR Spectrum of Compound 12 in d_6-DMSO

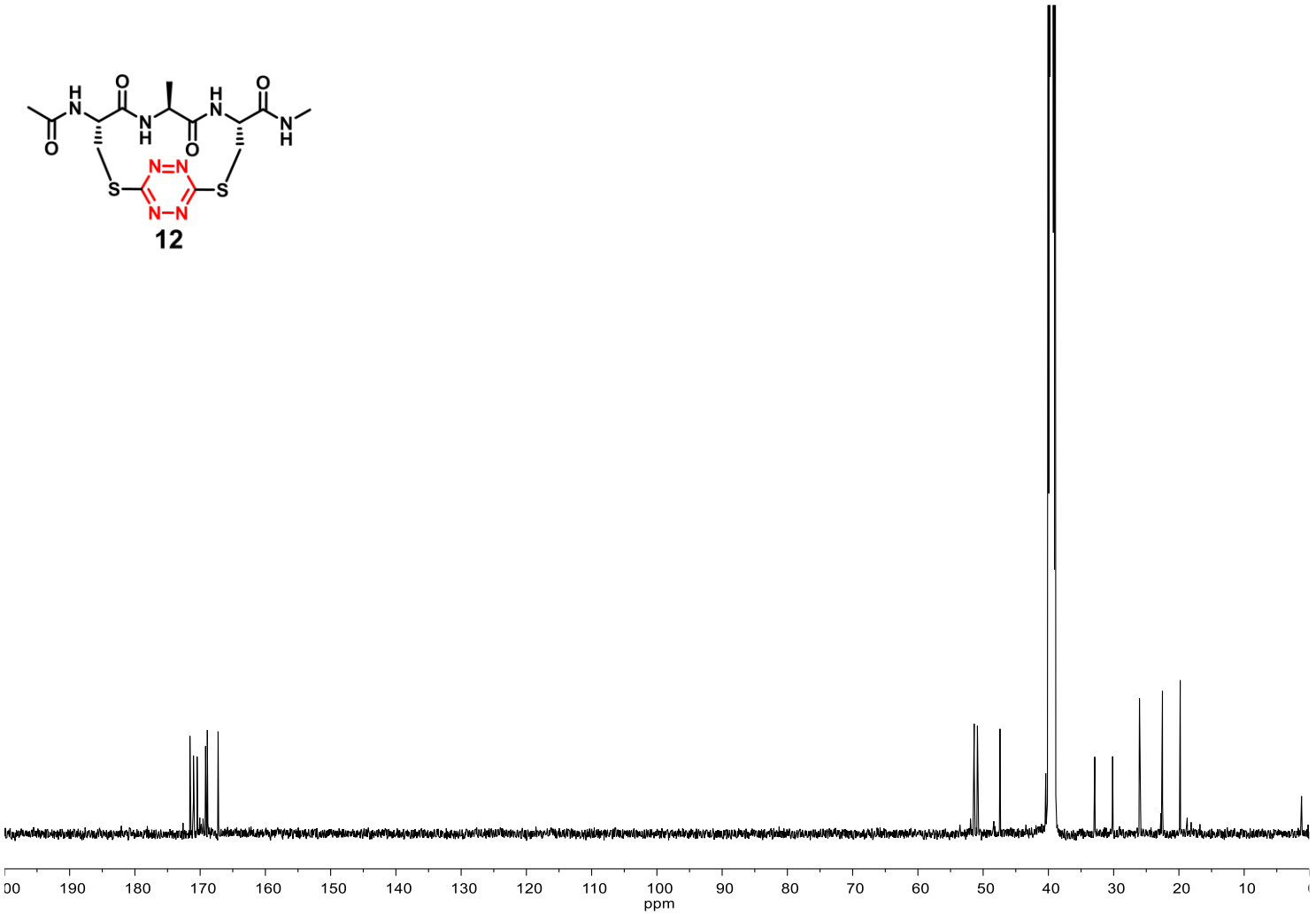

Figure A.18. 125 MHz ^{13}C-NMR Spectrum of Compound 12 in d_6-DMSO

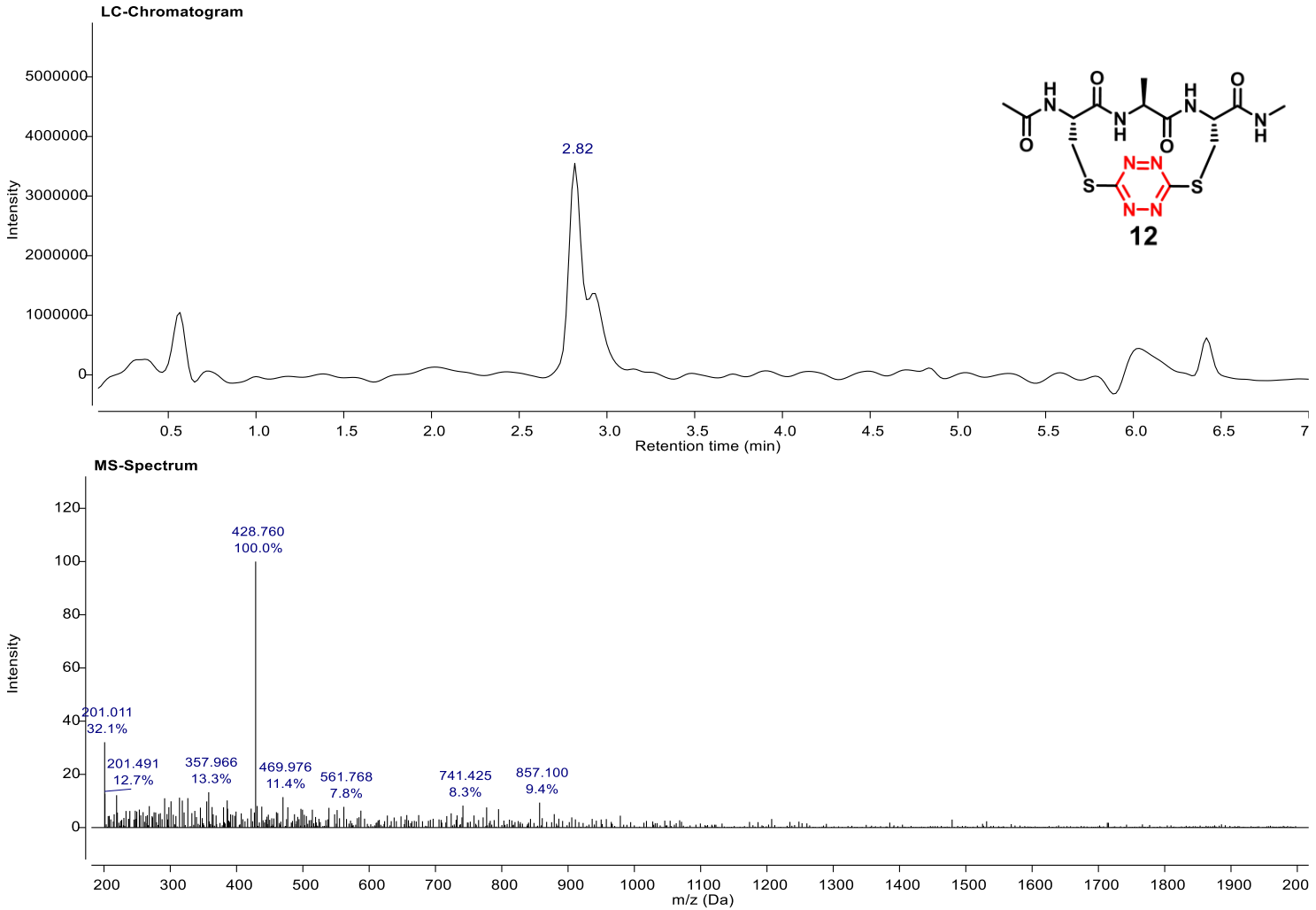

Figure A.19. LC-MS Spectrum of Compound 12 Gradient 5-60 for 7 Minutes

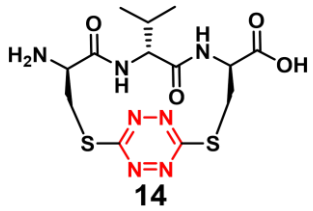

14

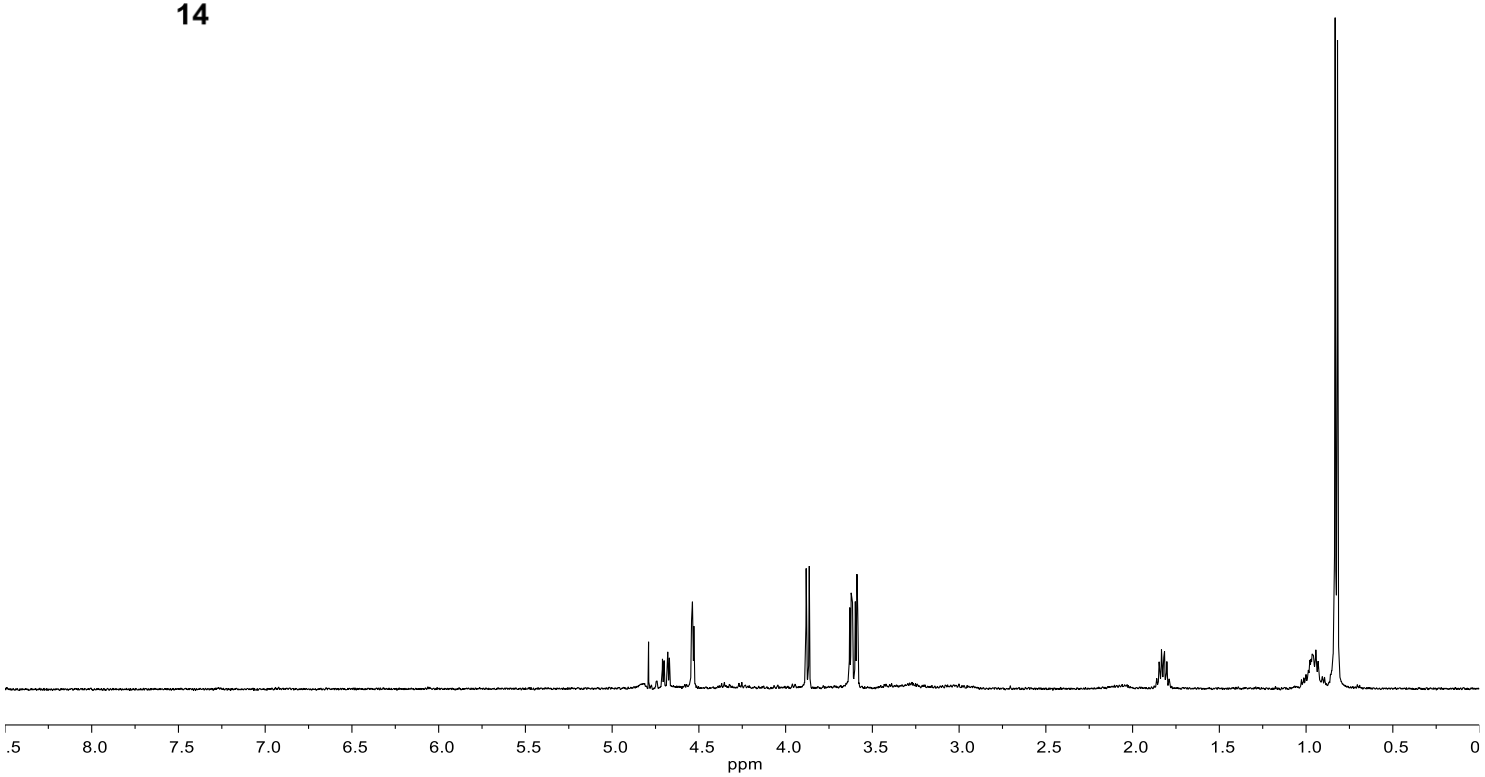

Figure A.20. 500 MHz ^{1}H-NMR Spectrum of Compound 14 in D_2O

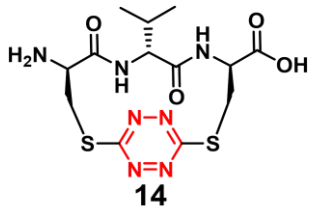

14

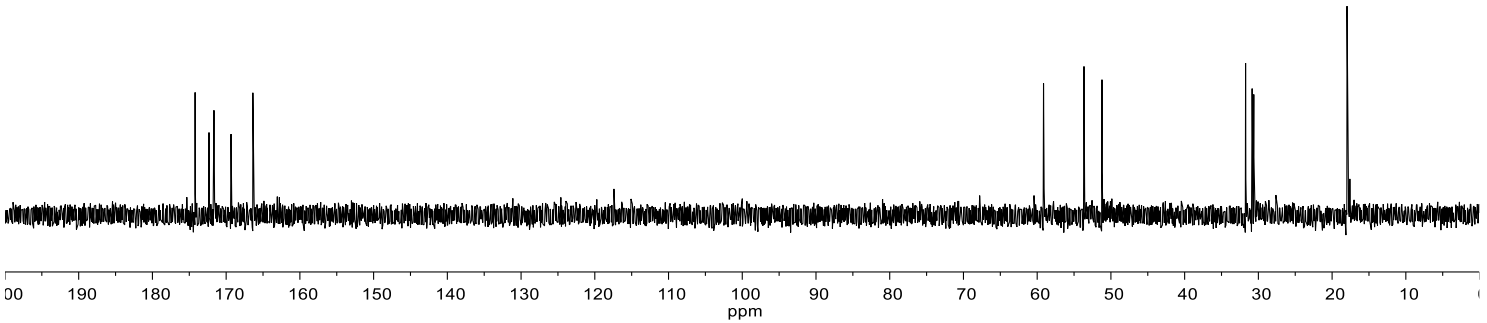

Figure A.21. 125 MHz ^{13}C-NMR Spectrum of Compound 14 in D_2O

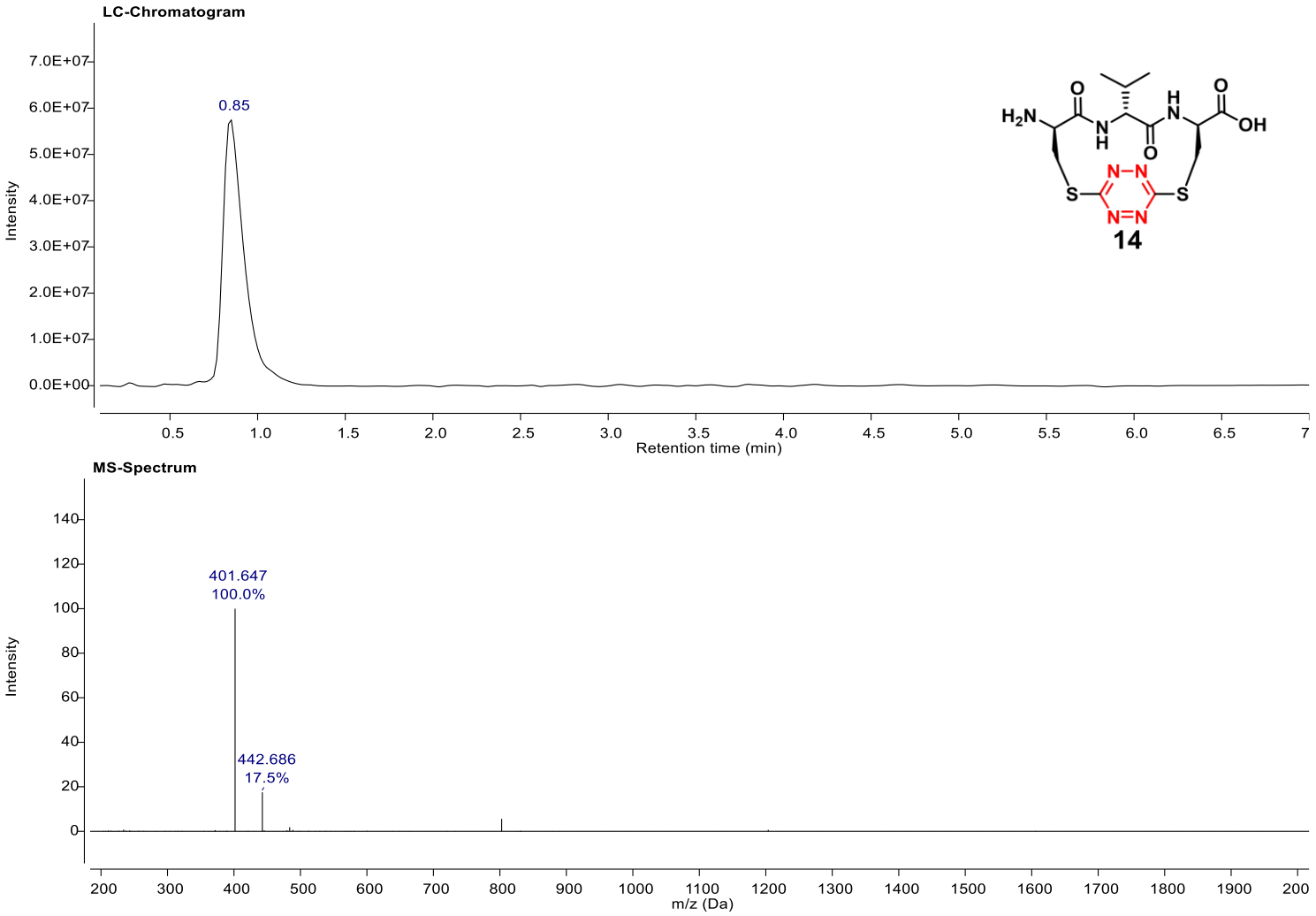

Figure A.22. LC-MS Spectrum of Compound 14 Gradient 5-60 for 7 Minutes

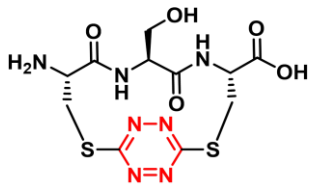

15

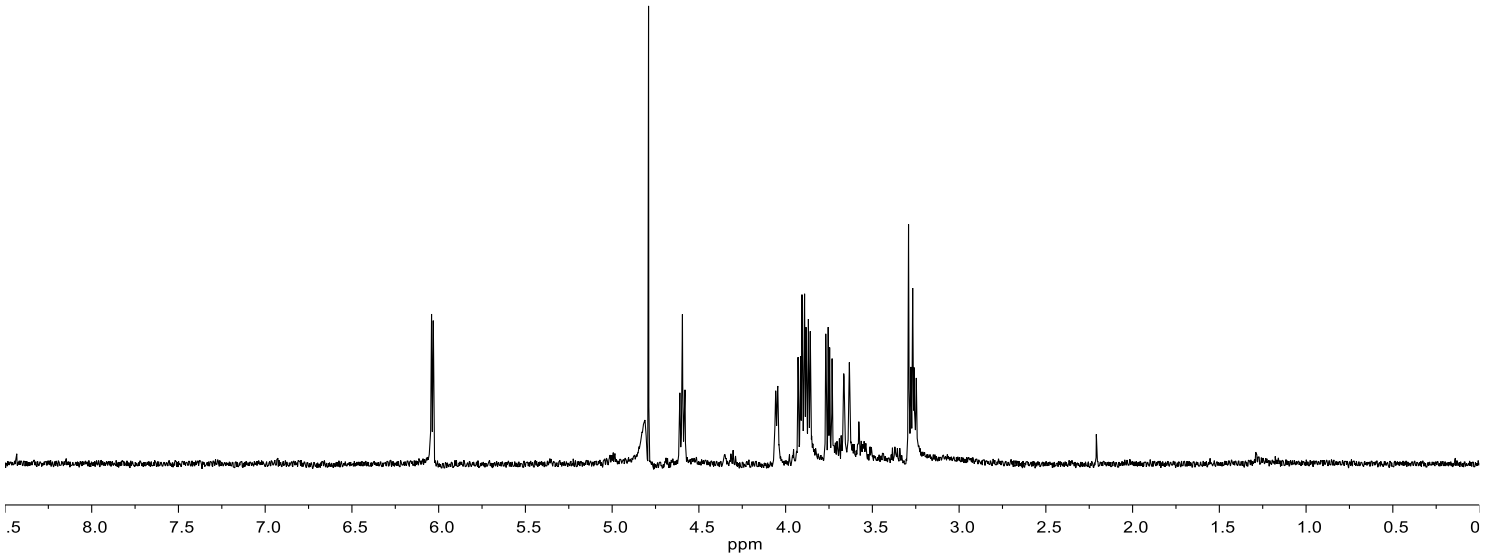

Figure A.23. 500 MHz ^{1}H-NMR Spectrum of Compound 15 in D_2O

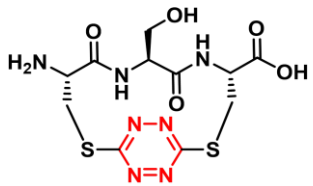

15

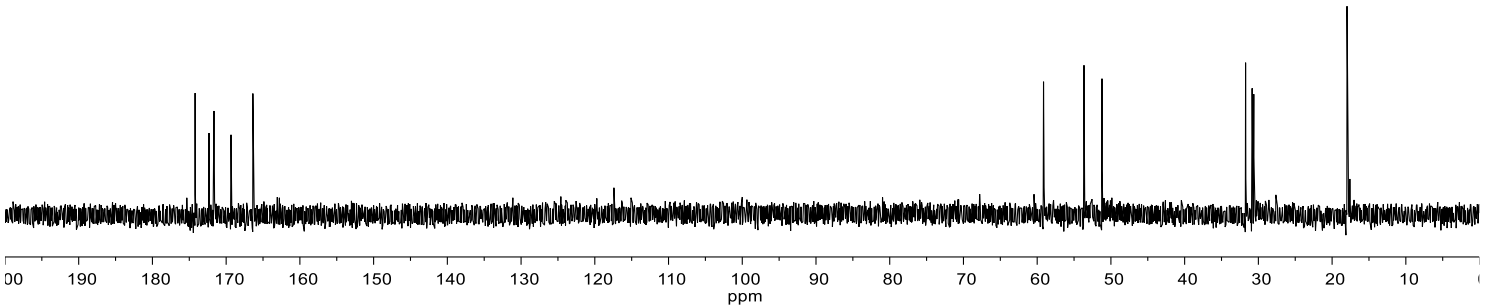

Figure A.24. 125 MHz ^{13}C-NMR Spectrum of Compound 15 in D_2O

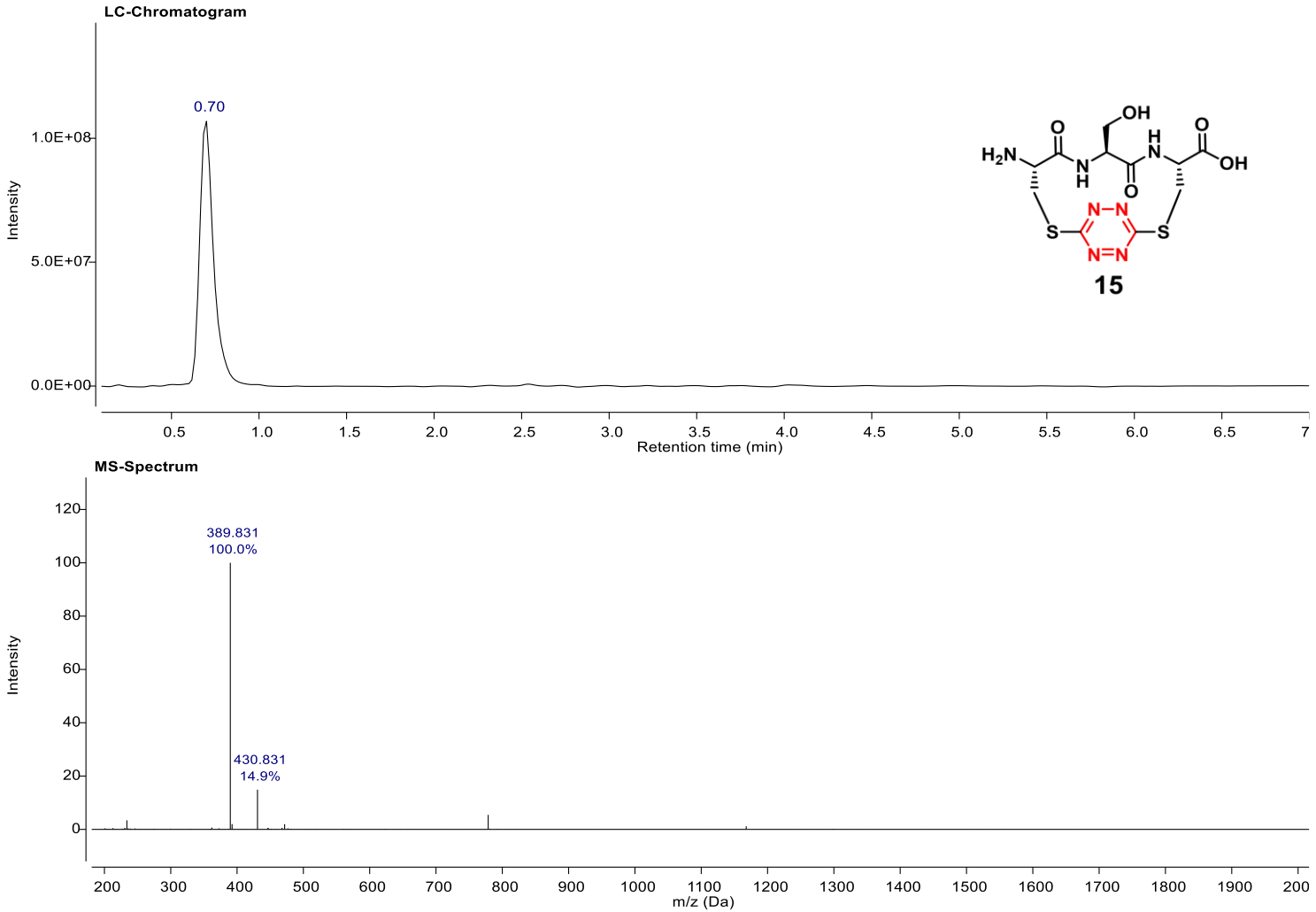

Figure A.25. LC-MS Spectrum of Compound 15 Gradient 5-60 for 7 Minutes

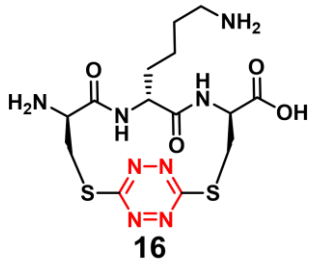

16

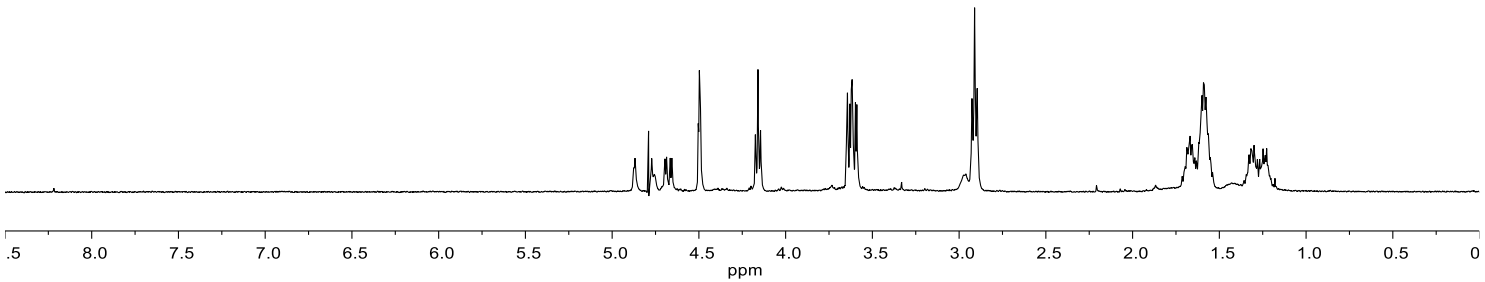

Figure A.26. 500 MHz ^{1}H-NMR Spectrum of Compound 16 in D_2O

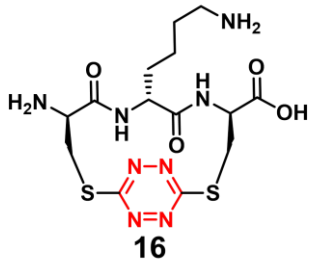

16

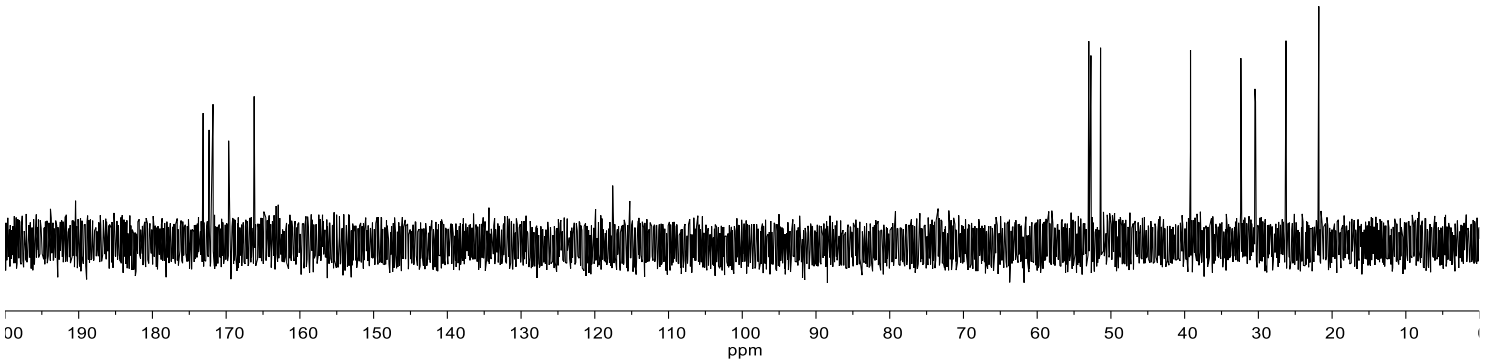

Figure A.27. 125 MHz ^{13}C-NMR Spectrum of Compound 16 in D_2O

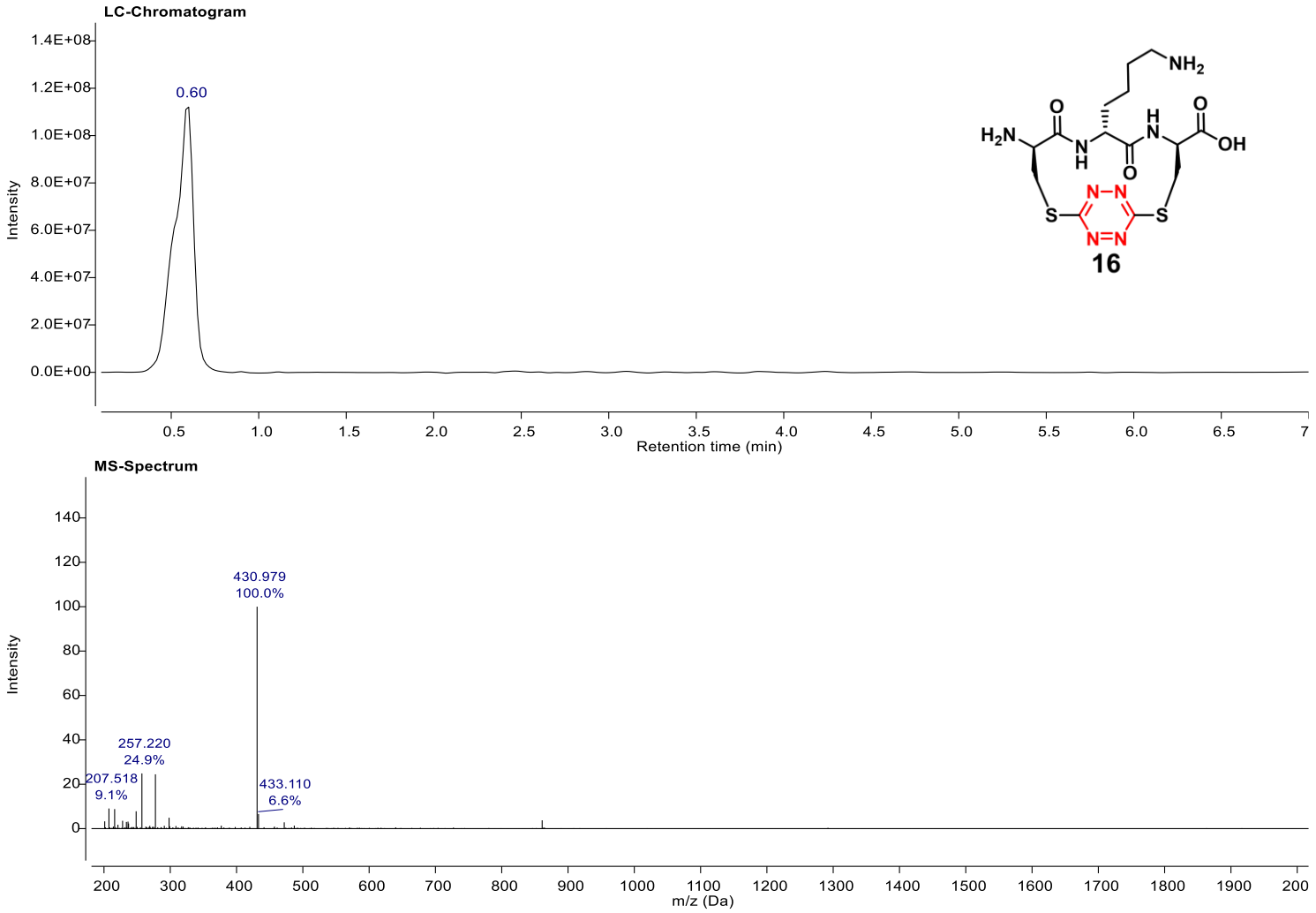

Figure A.28. LC-MS Spectrum of Compound 16 Gradient 5-60 for 7 Minutes

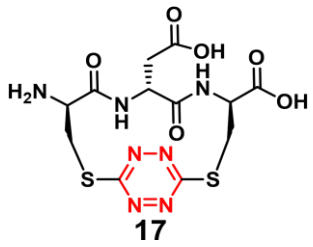

17

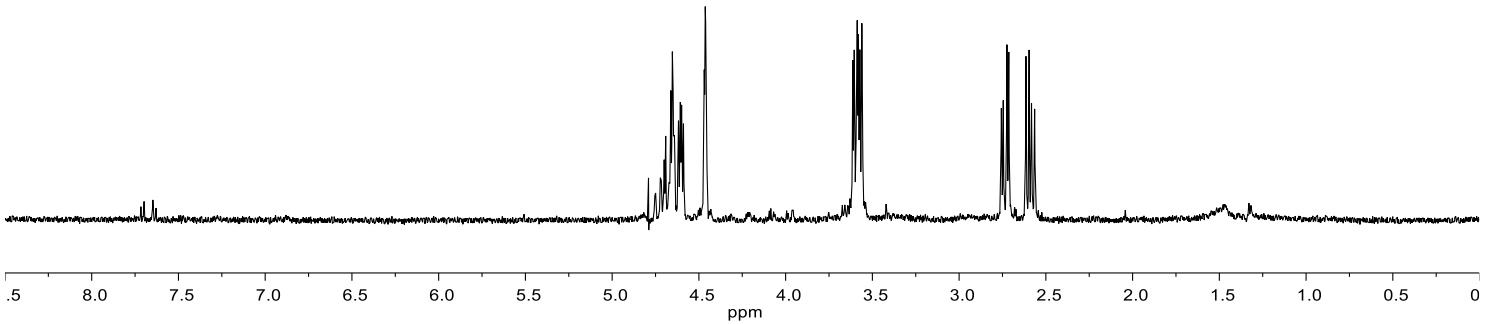

Figure A.29. 500 MHz ^{1}H-NMR Spectrum of Compound 17 in D_2O

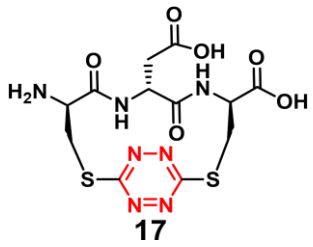

17

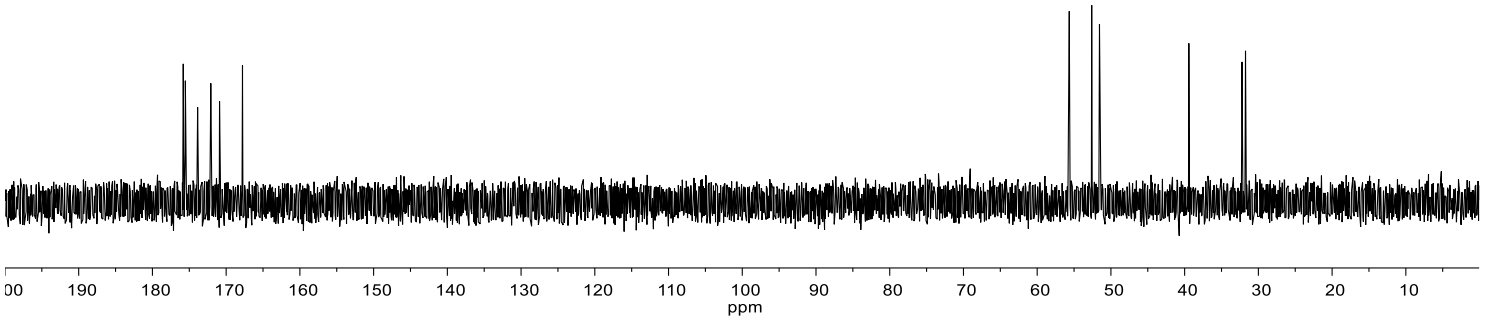

Figure A.30. 125 MHz ^{13}C-NMR Spectrum of Compound 17 in D_2O

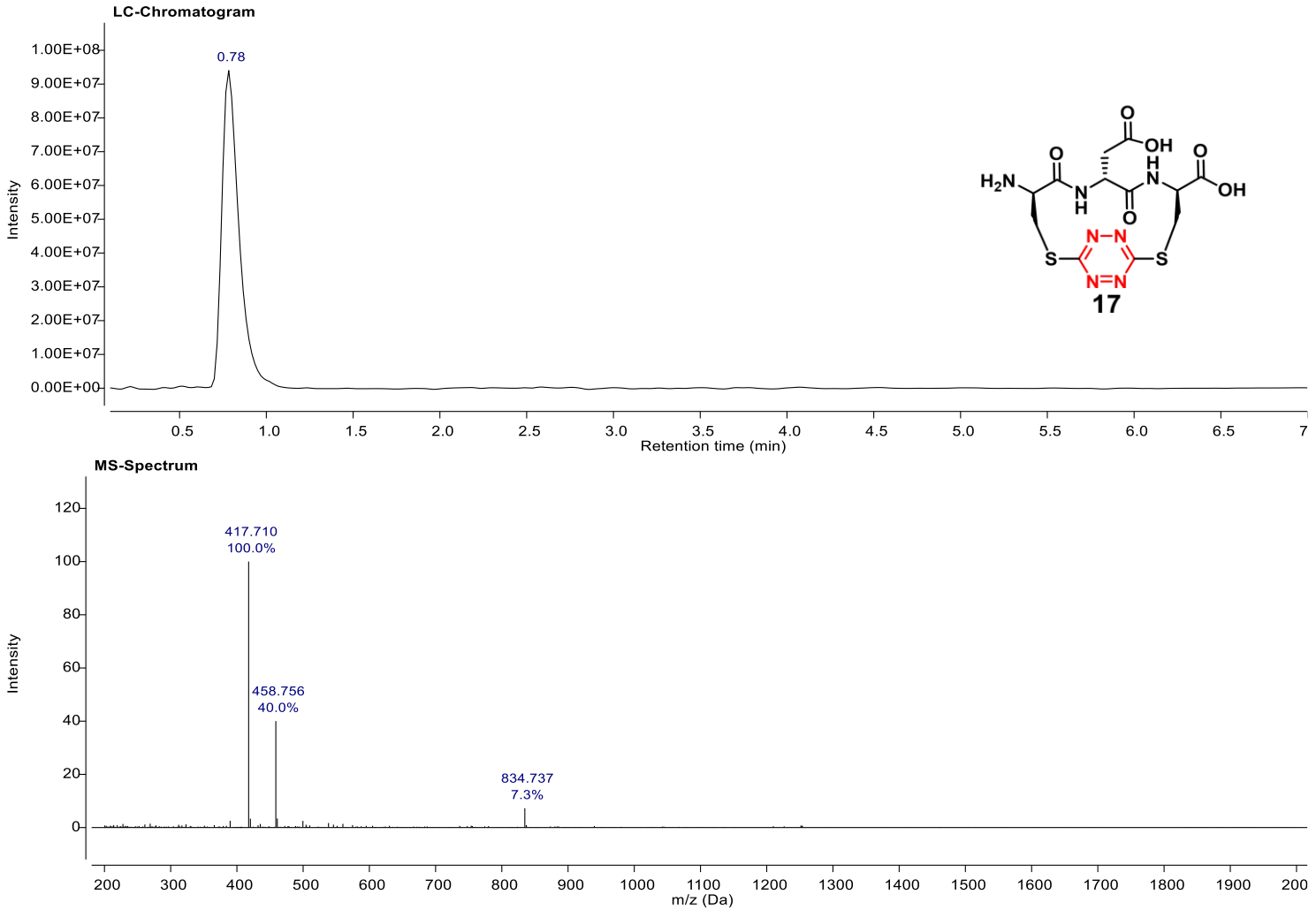

Figure A.31. LC-MS Spectrum of Compound 17 Gradient 5-60 for 7 Minutes

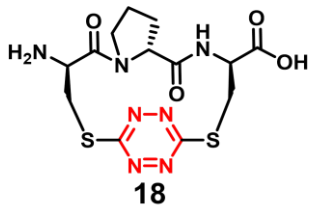

18

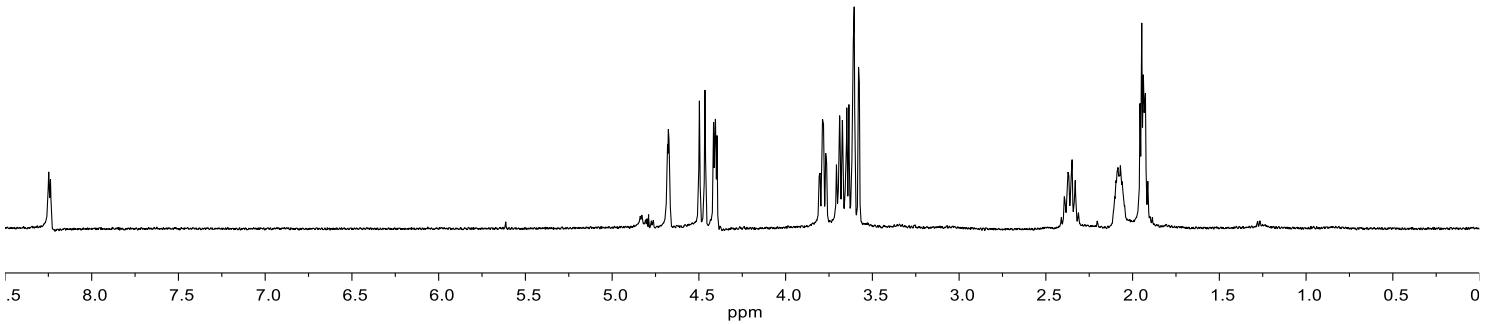

Figure A.32. 500 MHz ^{1}H-NMR Spectrum of Compound 18 in D_2O

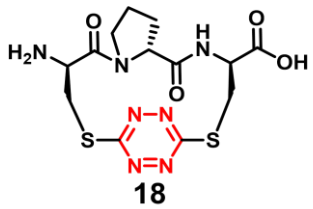

18

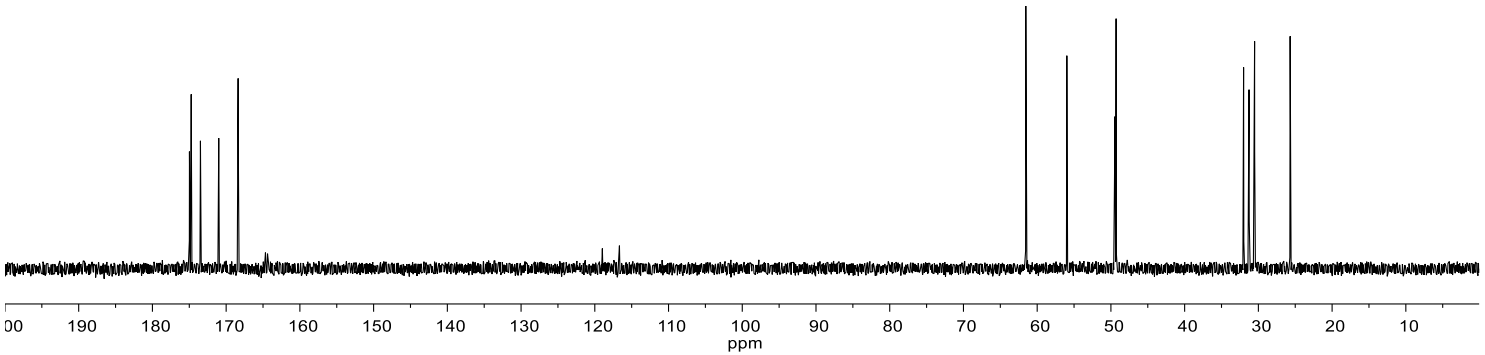

Figure A.33. 125 MHz ^{13}C-NMR Spectrum of Compound 18 in D_2O

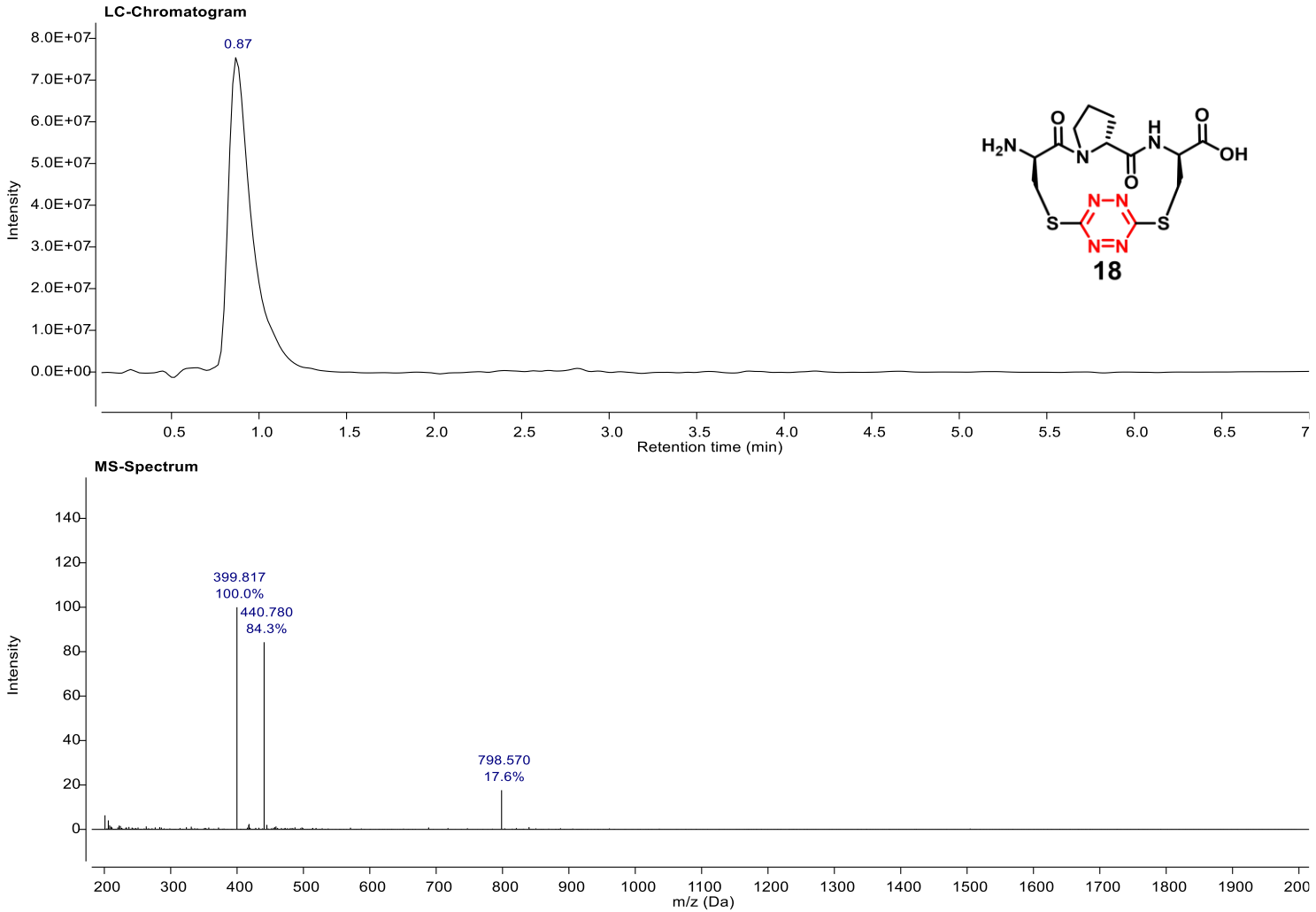

Figure A.34. LC-MS Spectrum of Compound 18 Gradient 5-60 for 7 Minutes

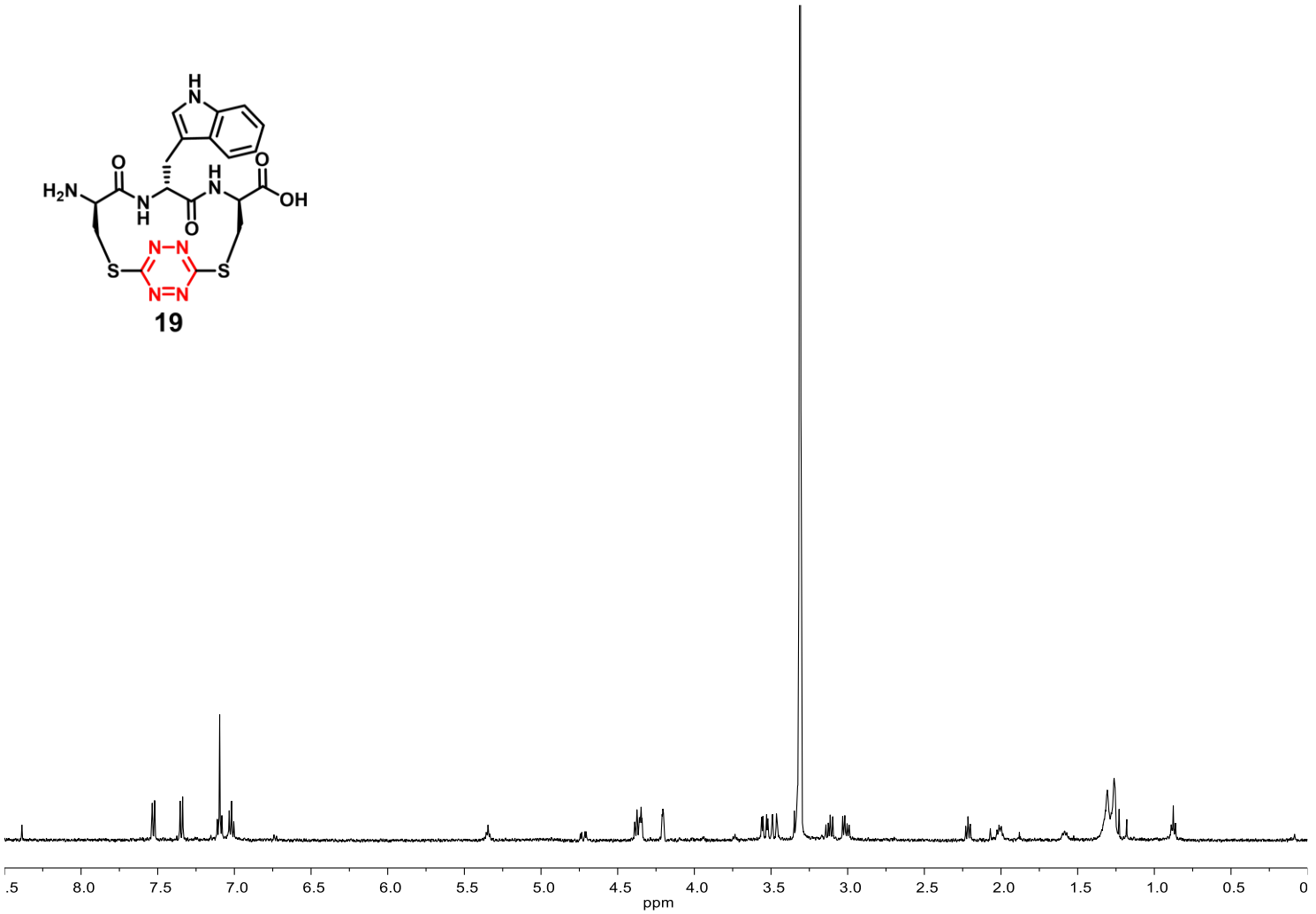

Figure A.35. 500 MHz ^{1}H-NMR Spectrum of Compound 19 in CD_3OD

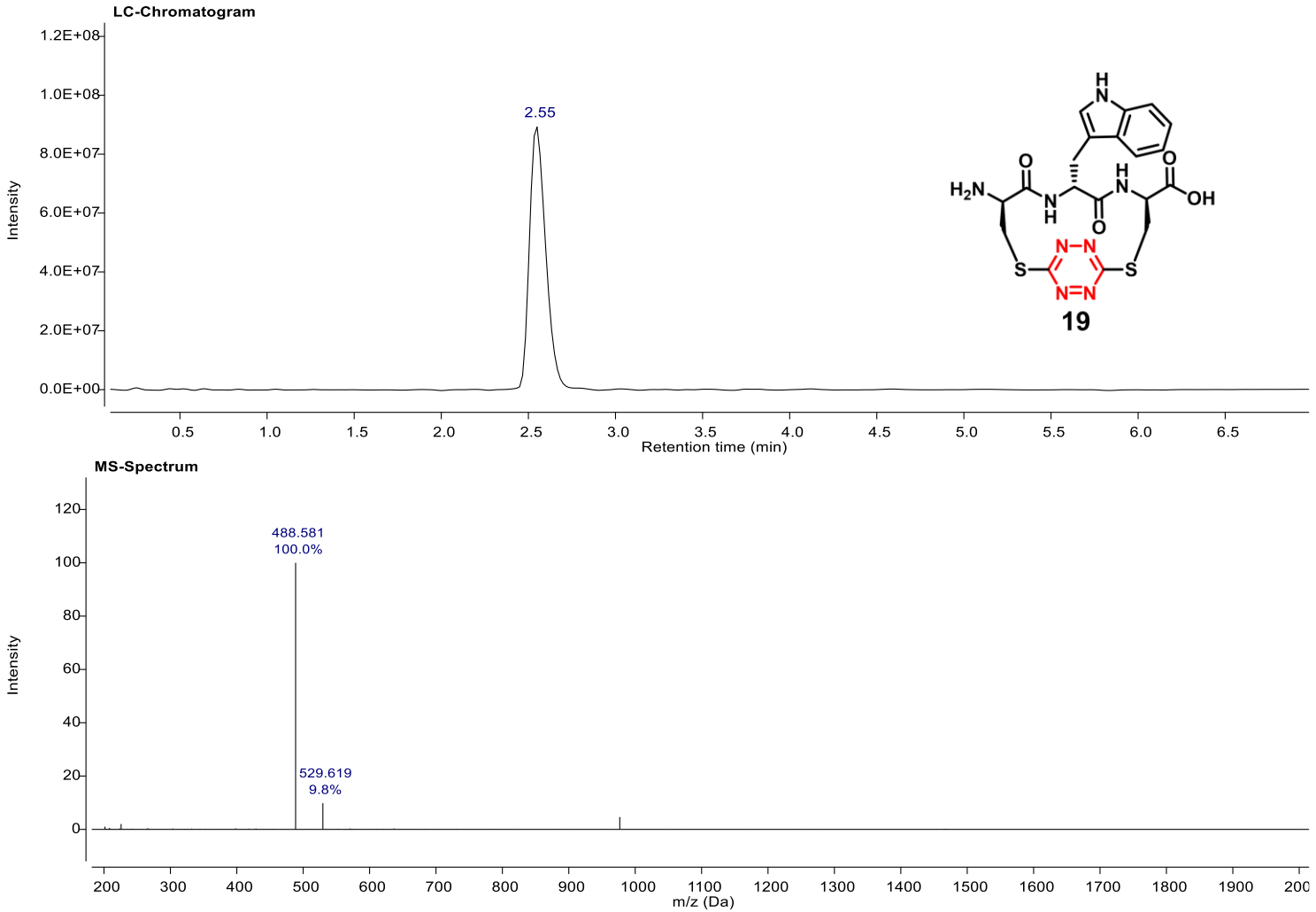

Figure A.36. LC-MS Spectrum of Compound 19 Gradient 5-60 for 7 Minutes

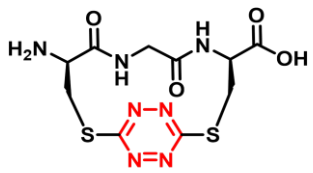

20

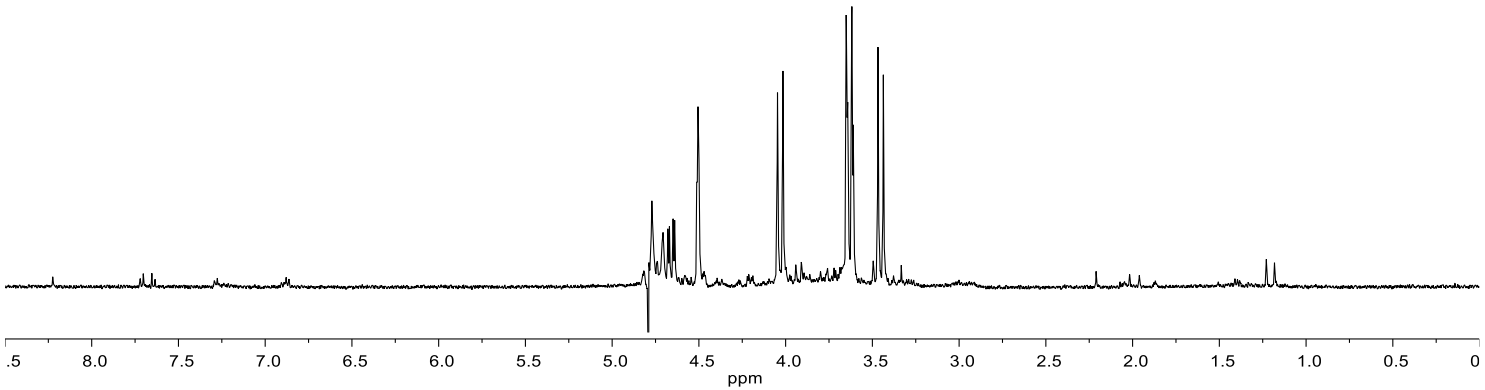

Figure A.37. 500 MHz ^{1}H-NMR Spectrum of Compound 20 in D_2O

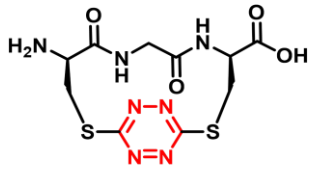

20

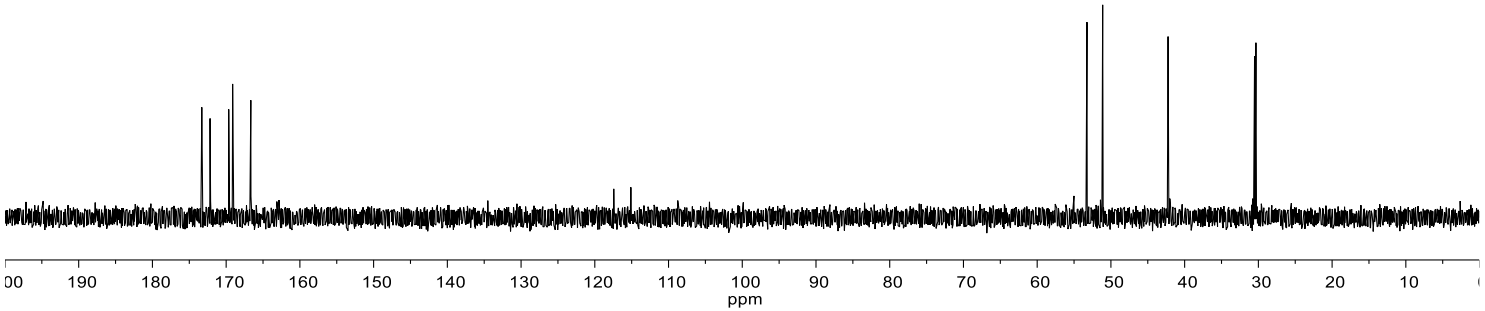

Figure A.38. 125 MHz ^{13}C-NMR Spectrum of Compound 20 in D_2O

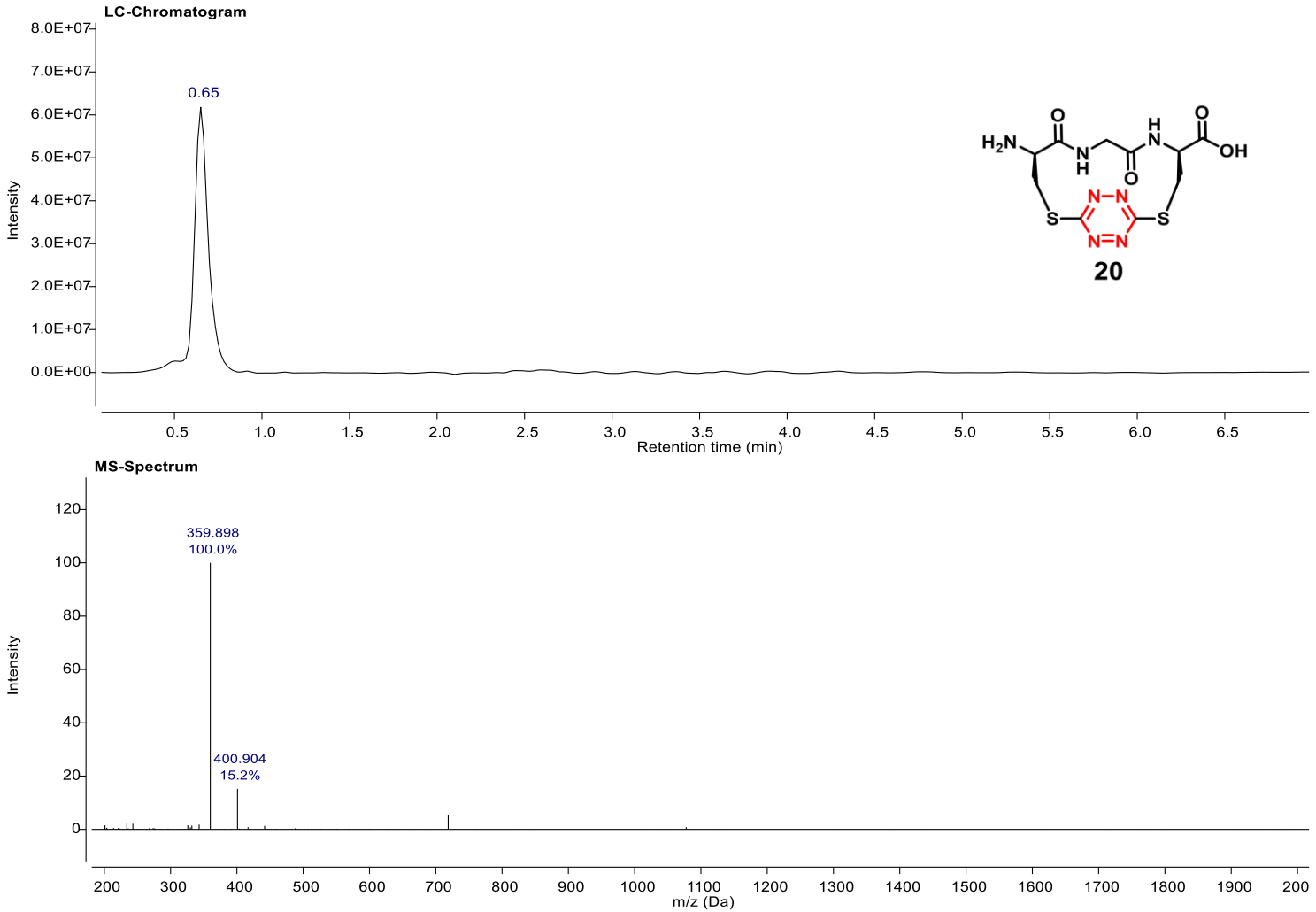

Figure A.39. LC-MS Spectrum of Compound 20 Gradient 5-60 for 7 Minutes

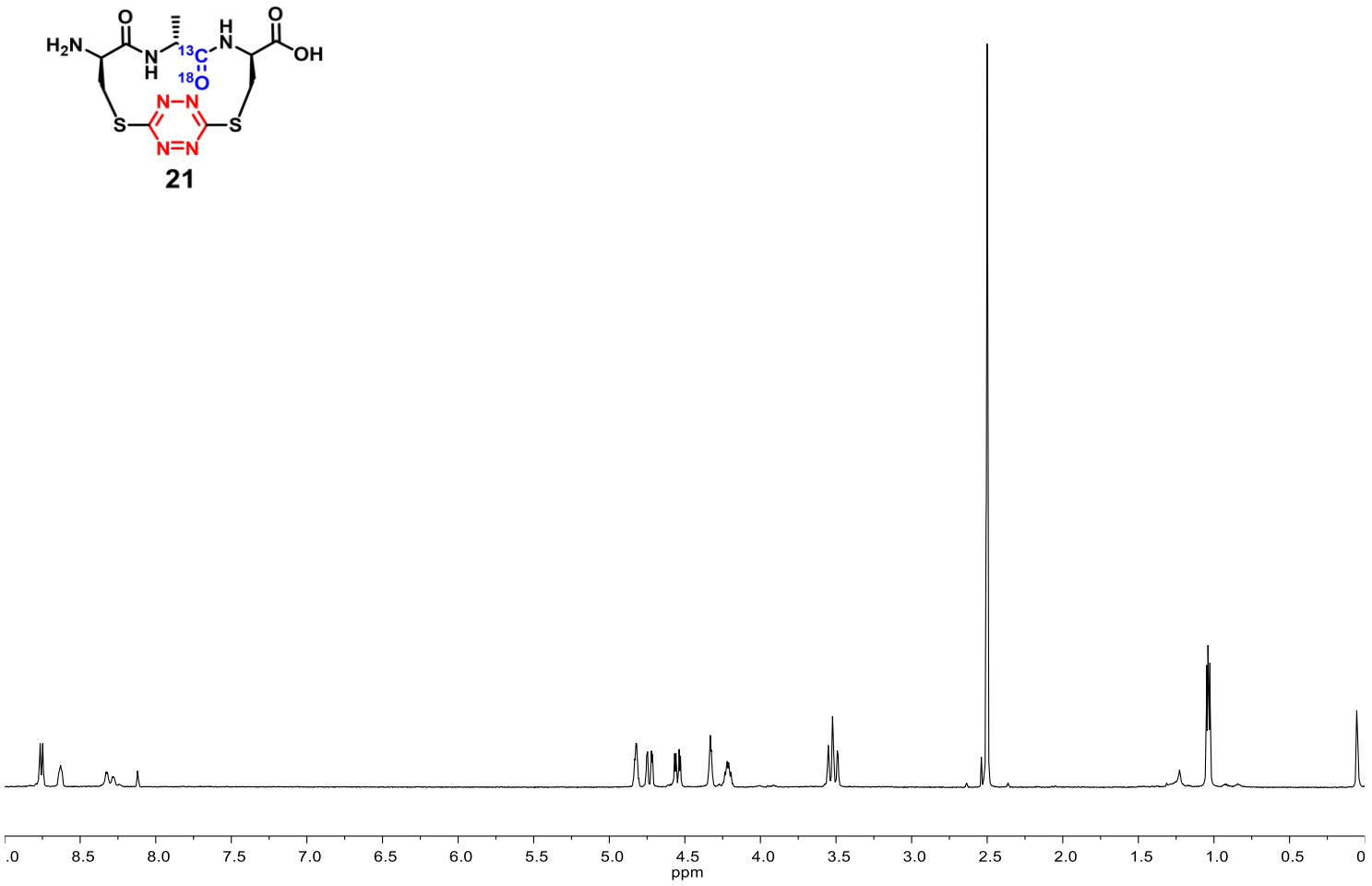

Figure A.40. 500 MHz ^{1}H-NMR Spectrum of Compound 21 in d_6-DMSO

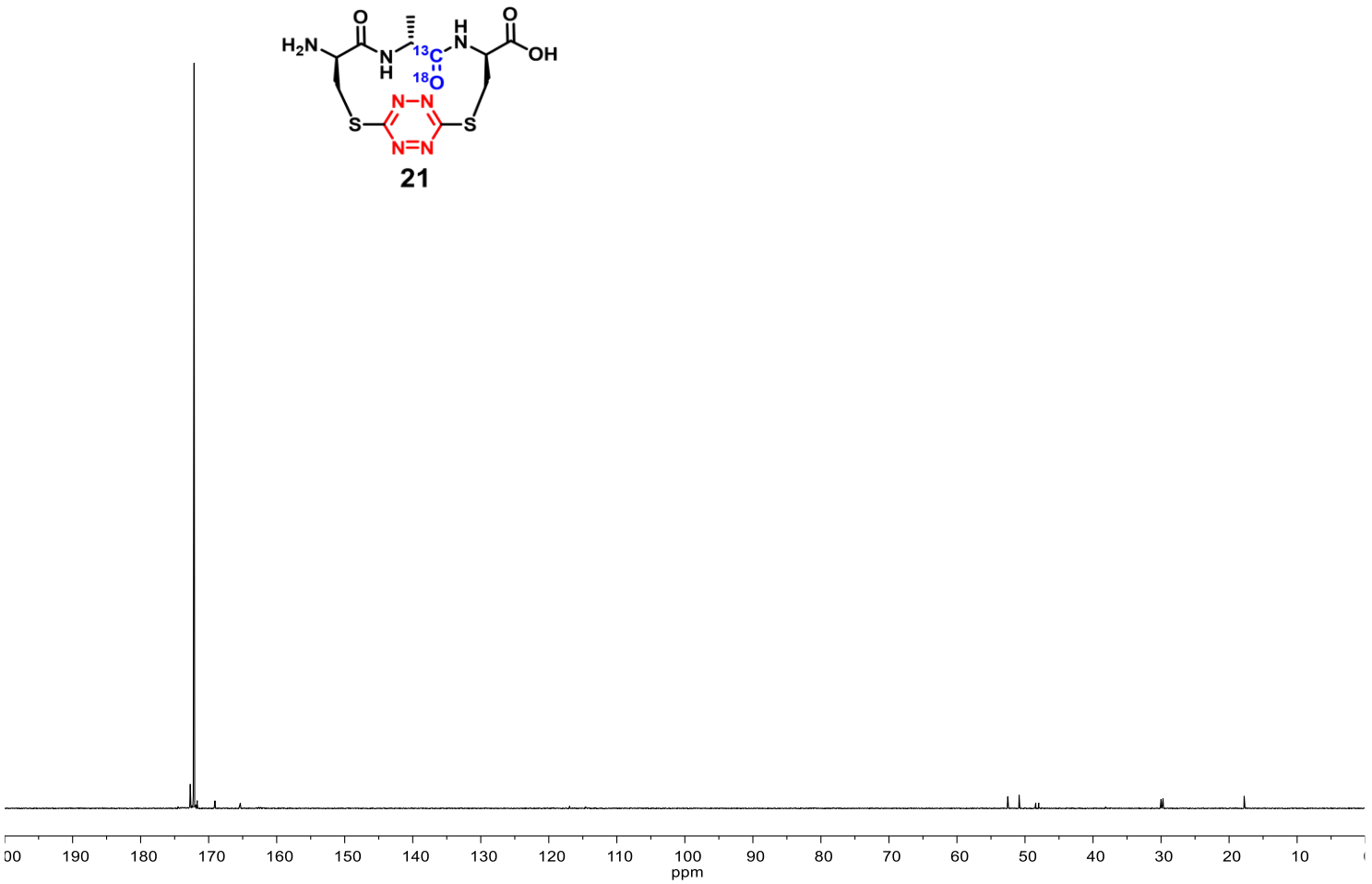

Figure A.41. 125 MHz ^{13}C-NMR Spectrum of Compound 21 in D_2O

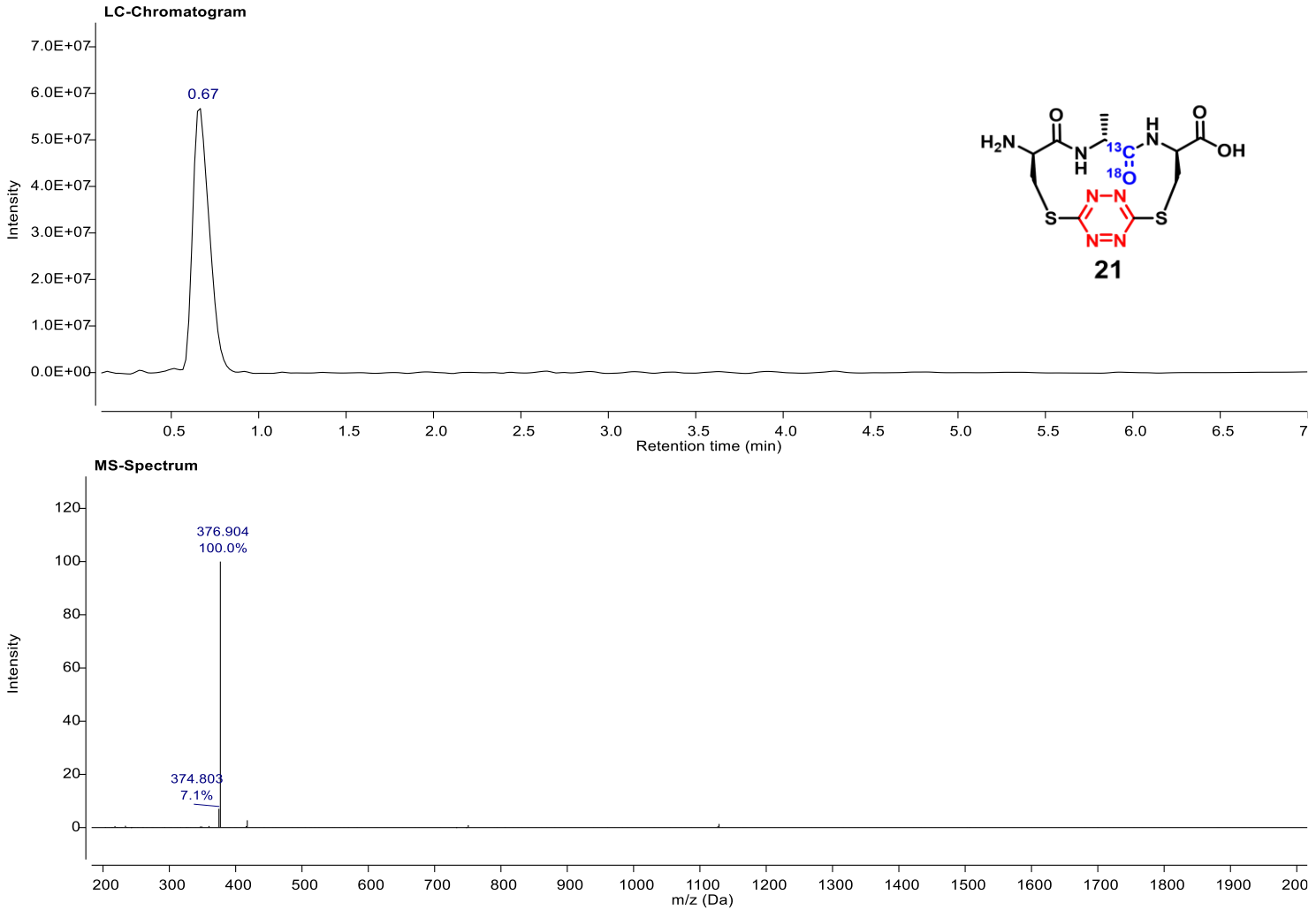

Figure A.42. LC-MS Spectrum of Compound 21 Gradient 5-60 for 7 Minutes

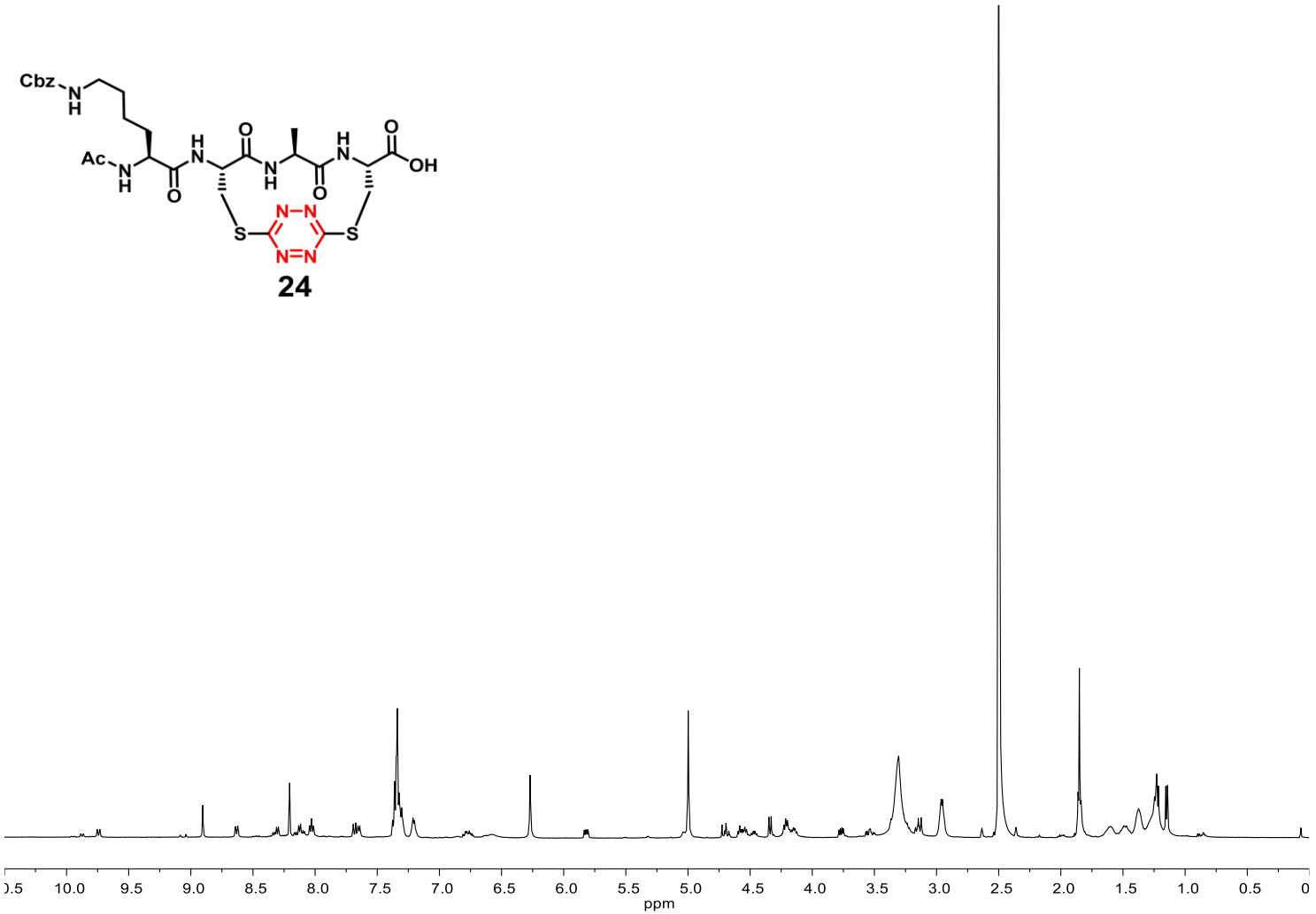

Figure A.43. 500 MHz ^{1}H-NMR Spectrum of Compound 24 in d_6-DMSO

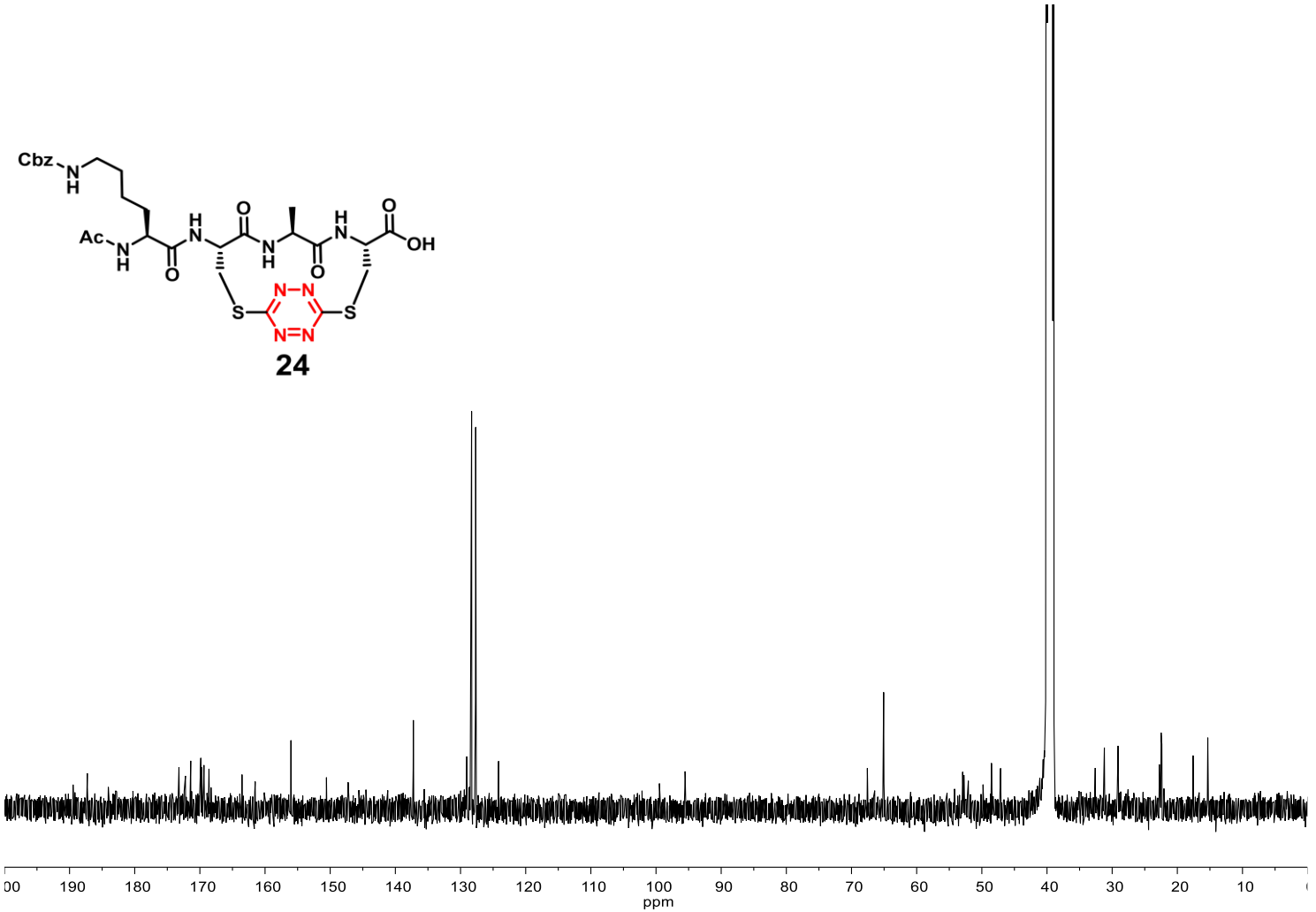

Figure A.44. 125 MHz ^{13}C-NMR Spectrum of Compound 24 in d_6-DMSO

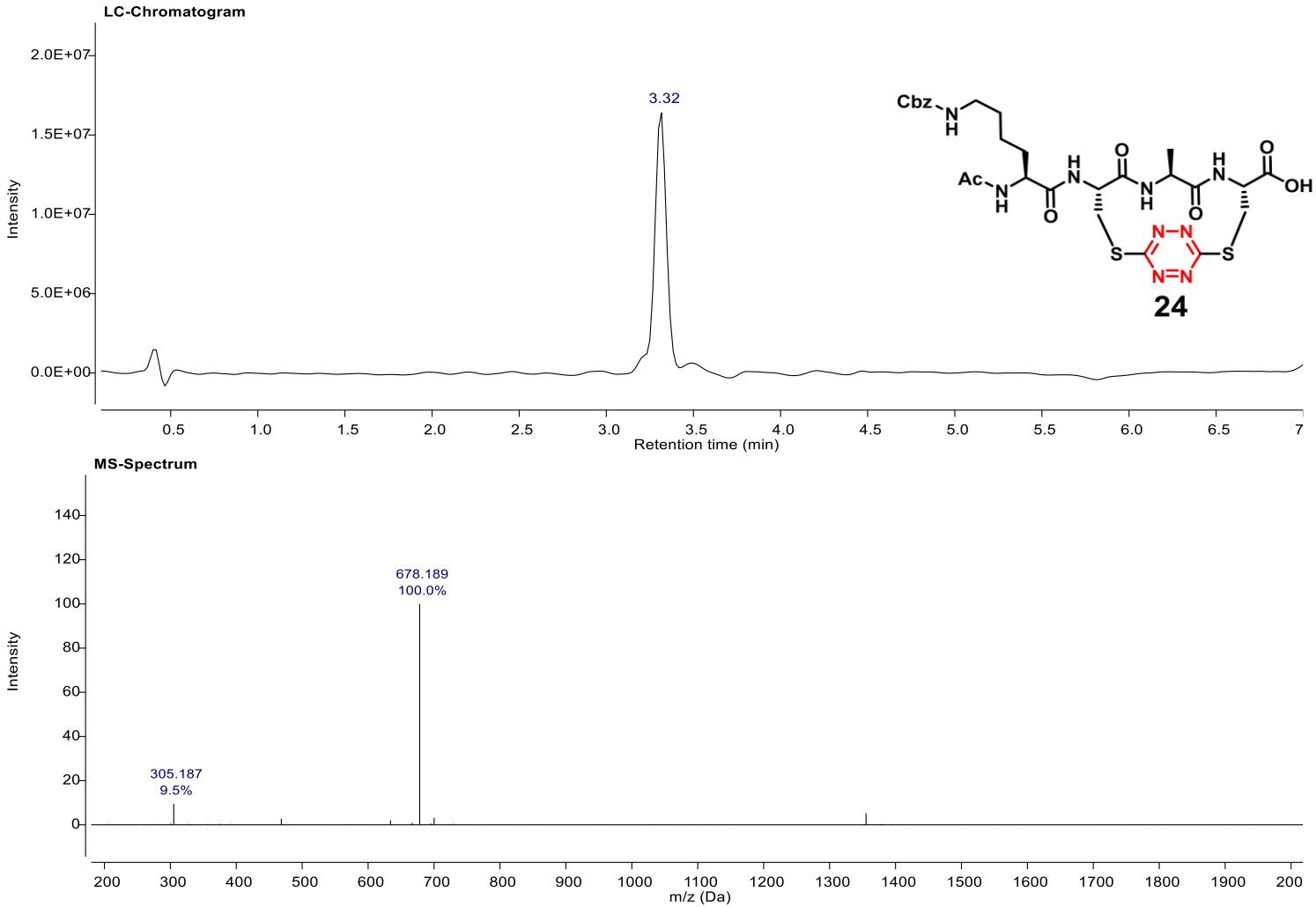

Figure A.45. LC-MS Spectrum of Compound 24 Gradient 5-60 for 7 Minutes

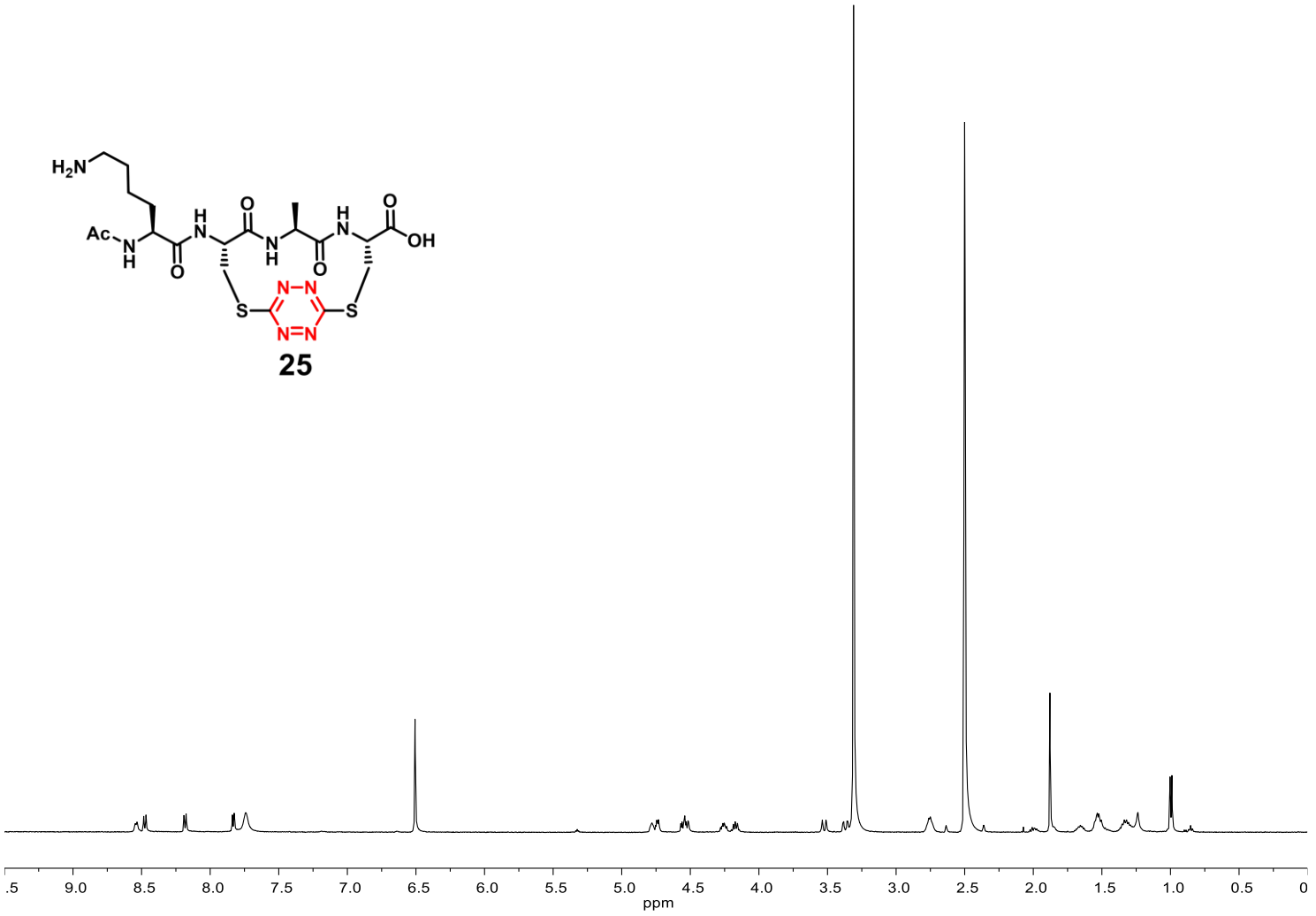

Figure A.46. 500 MHz ^{1}H-NMR Spectrum of Compound 25 in d_6-DMSO

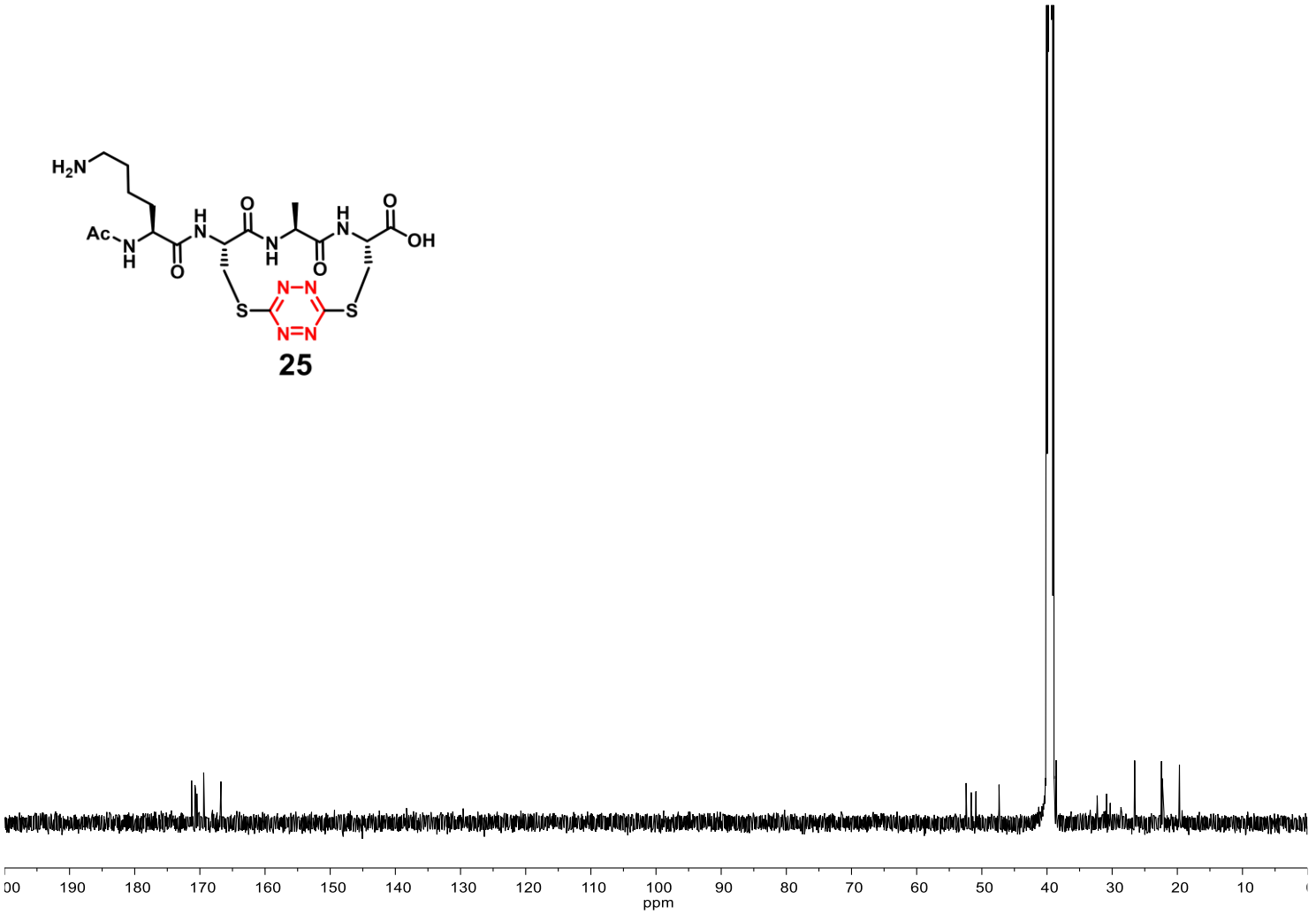

Figure A.47. 125 MHz ^{13}C-NMR Spectrum of Compound 25 in d_6-DMSO

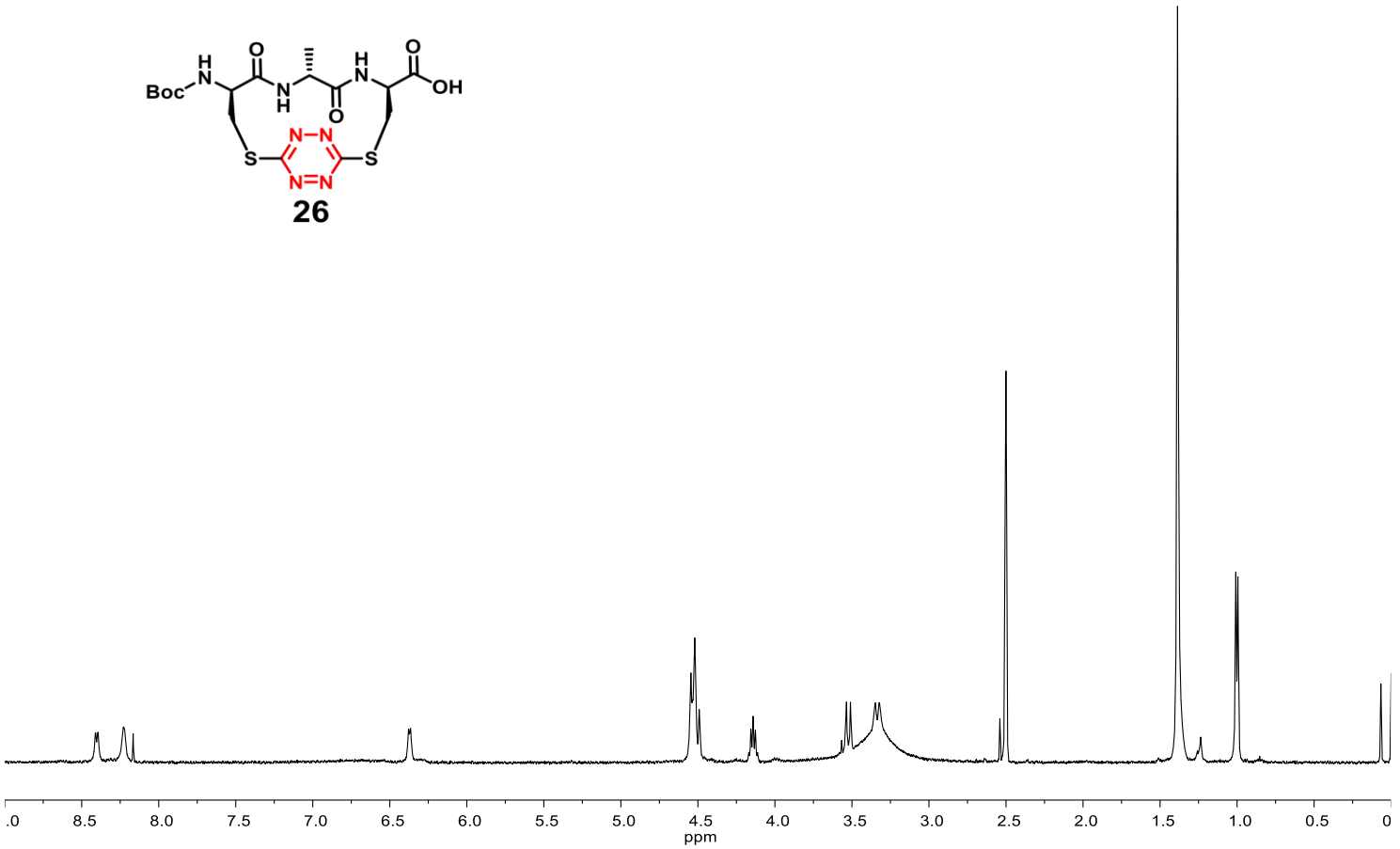

Figure A.48. 500 MHz ^{1}H-NMR Spectrum of Compound 26 in d_6-DMSO

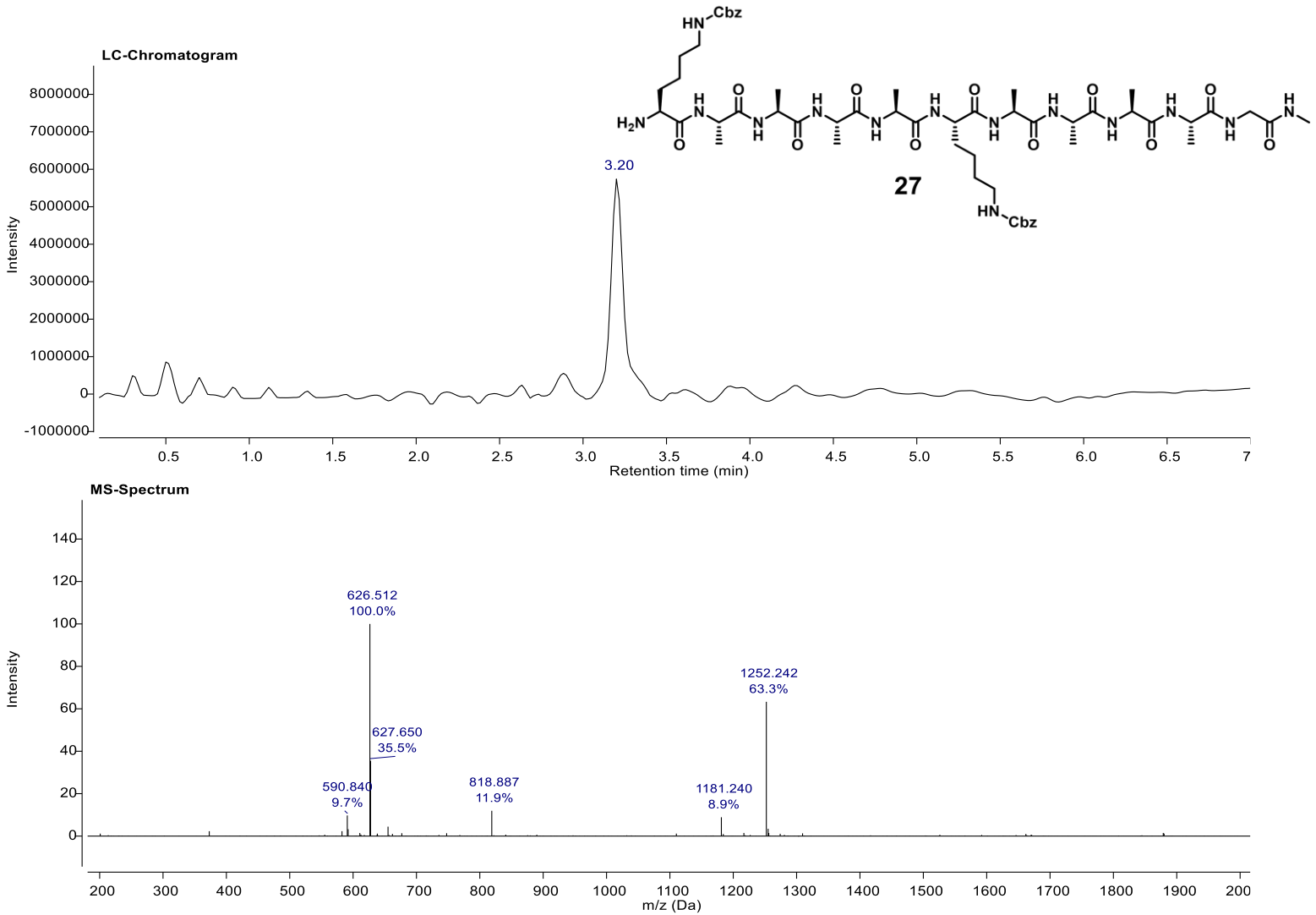

Figure A.49. LC-MS Spectrum of Compound 27 Gradient 5-60 for 7 Minutes

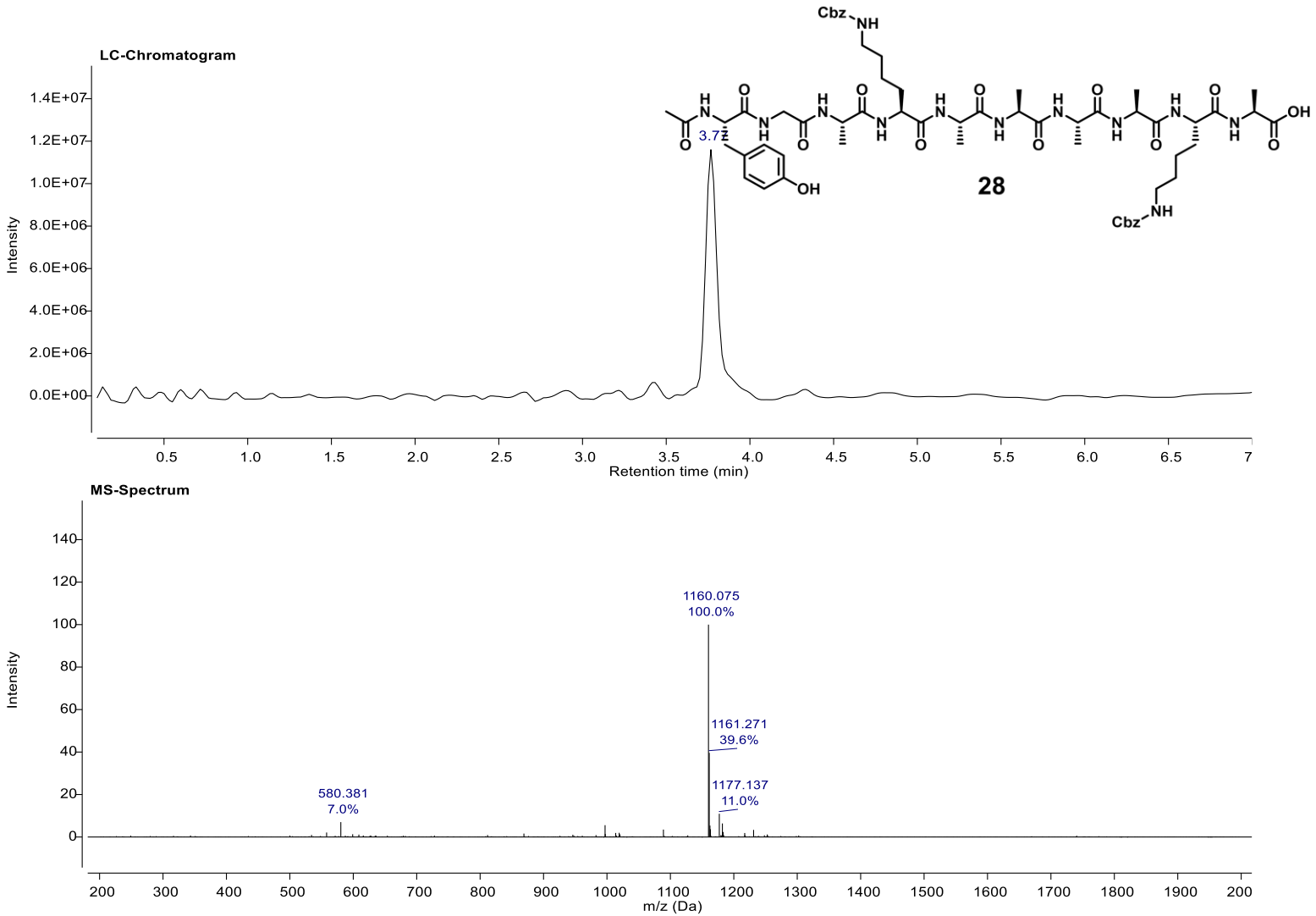

Figure A.50. LC-MS Chromatogram of Compound 28 Gradient 5-60 for 7 Minutes

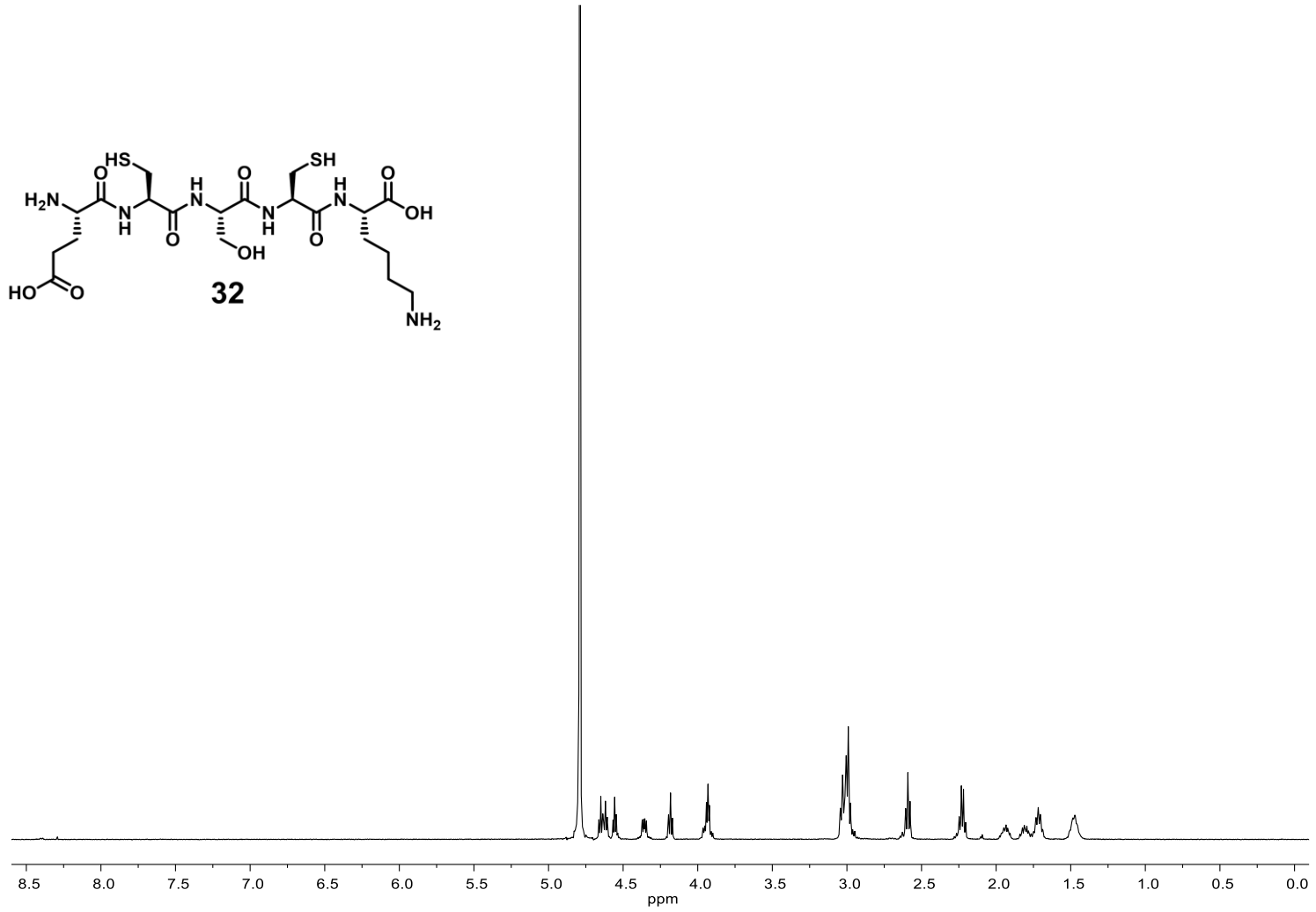

Figure A.51. 500 MHz ^{1}H-NMR Spectrum of Compound 32 in D_2O

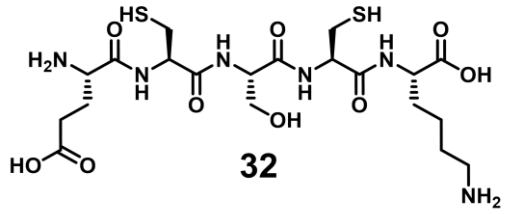

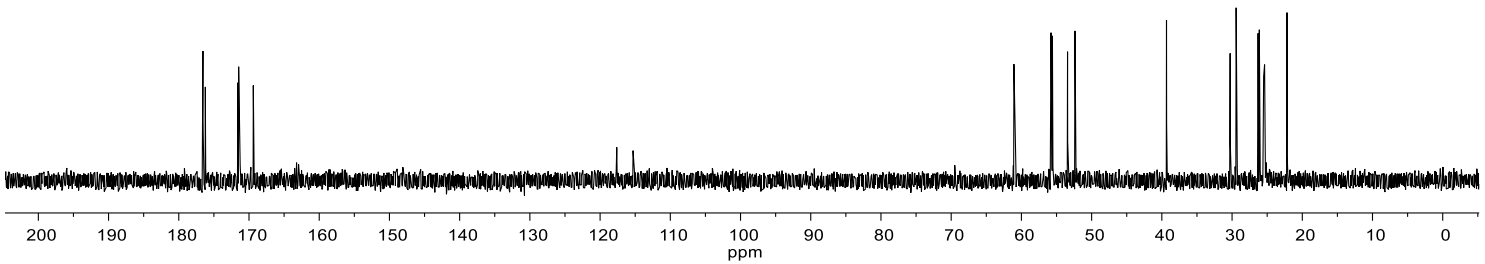

Figure A.52. 125 MHz ^{13}C-NMR Spectrum of Compound 32 in D_2O

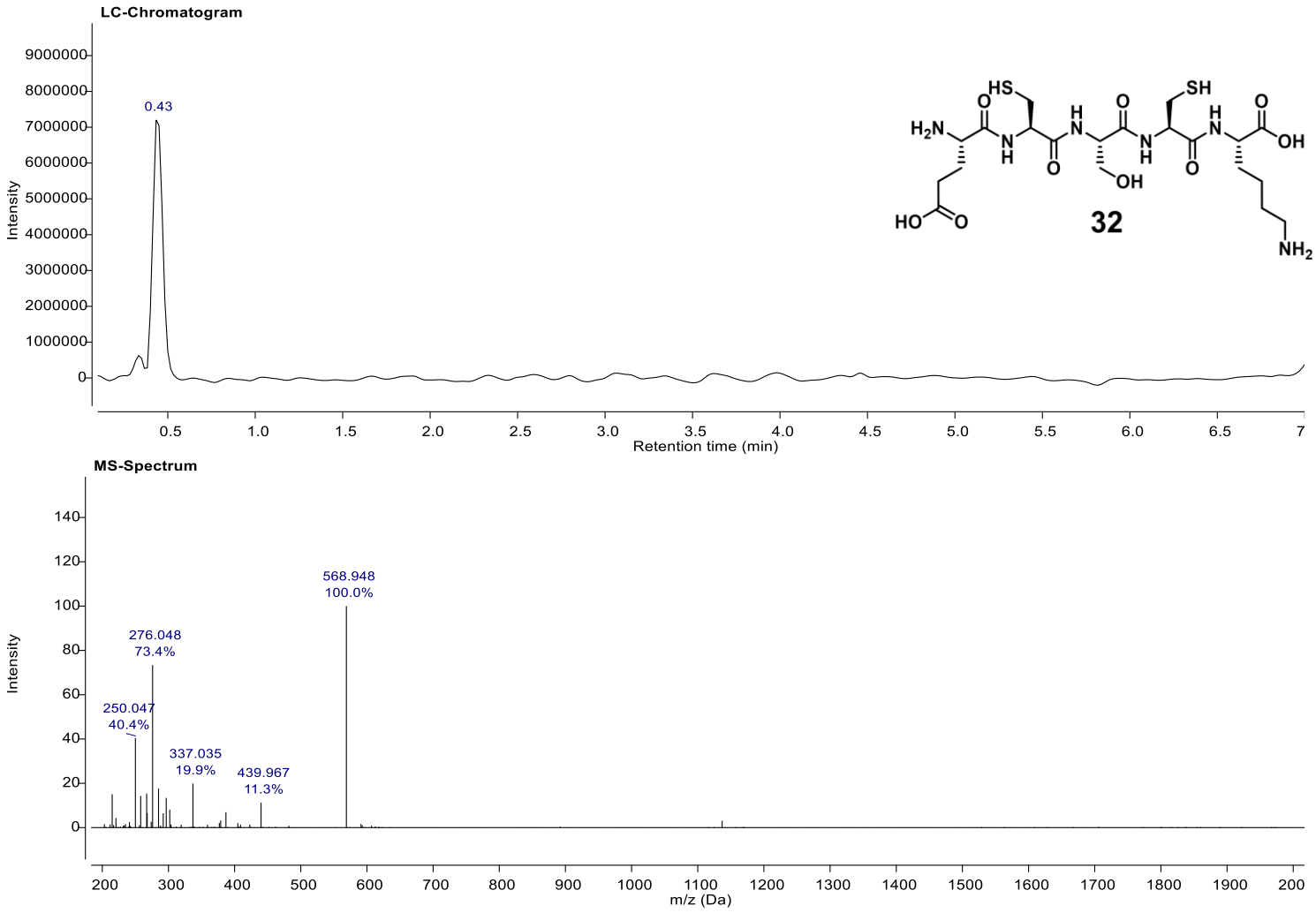

Figure A.53. LC-MS Spectrum of Compound 32 Gradient 5-60 for 7 Minutes

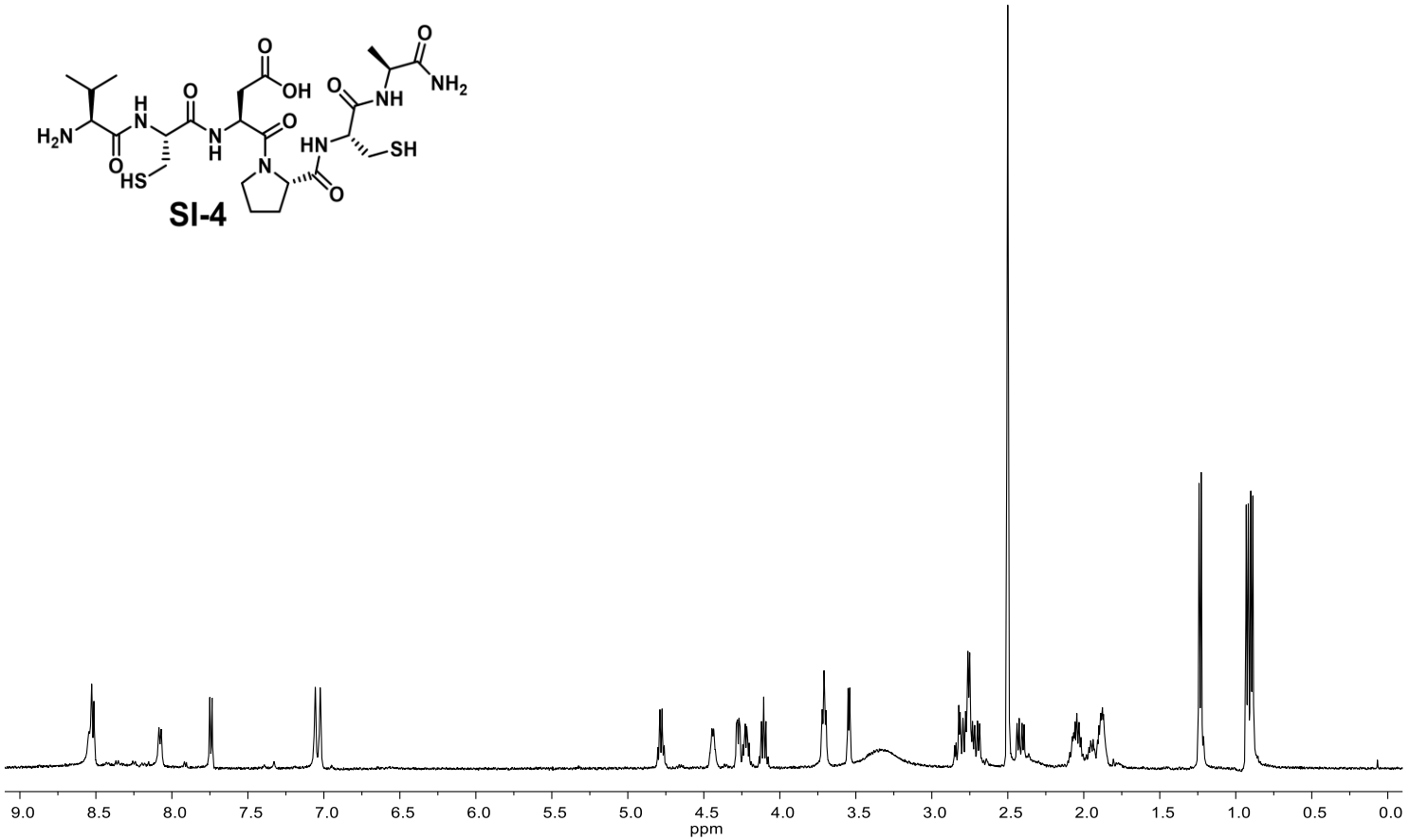

Figure A.54. 500 MHz ^{1}H-NMR Spectrum of Compound SI-4 in d_6-DMSO

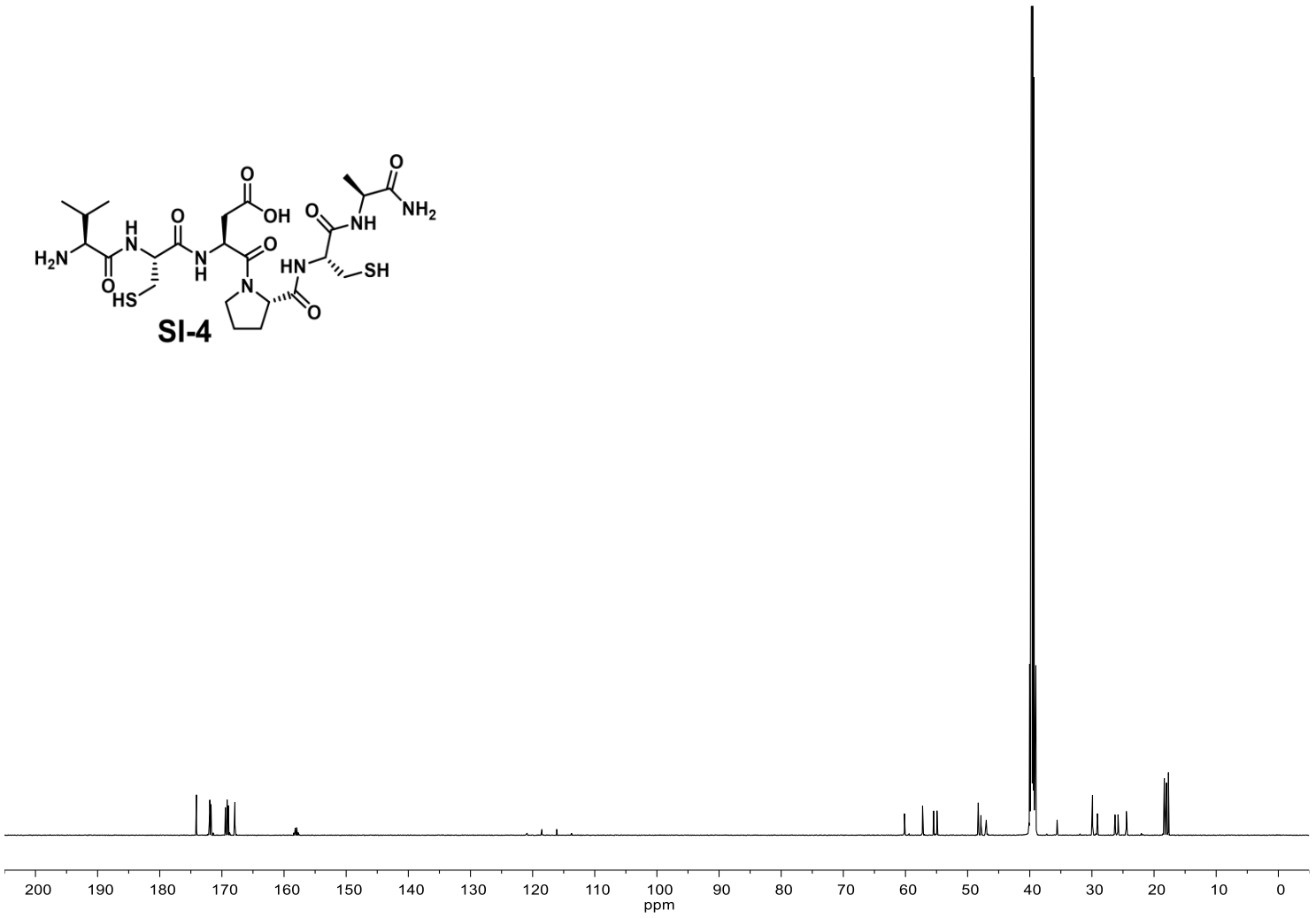

Figure A.55. 125 MHz ^{13}C-NMR Spectrum of Compound SI-4 in d_6-DMSO

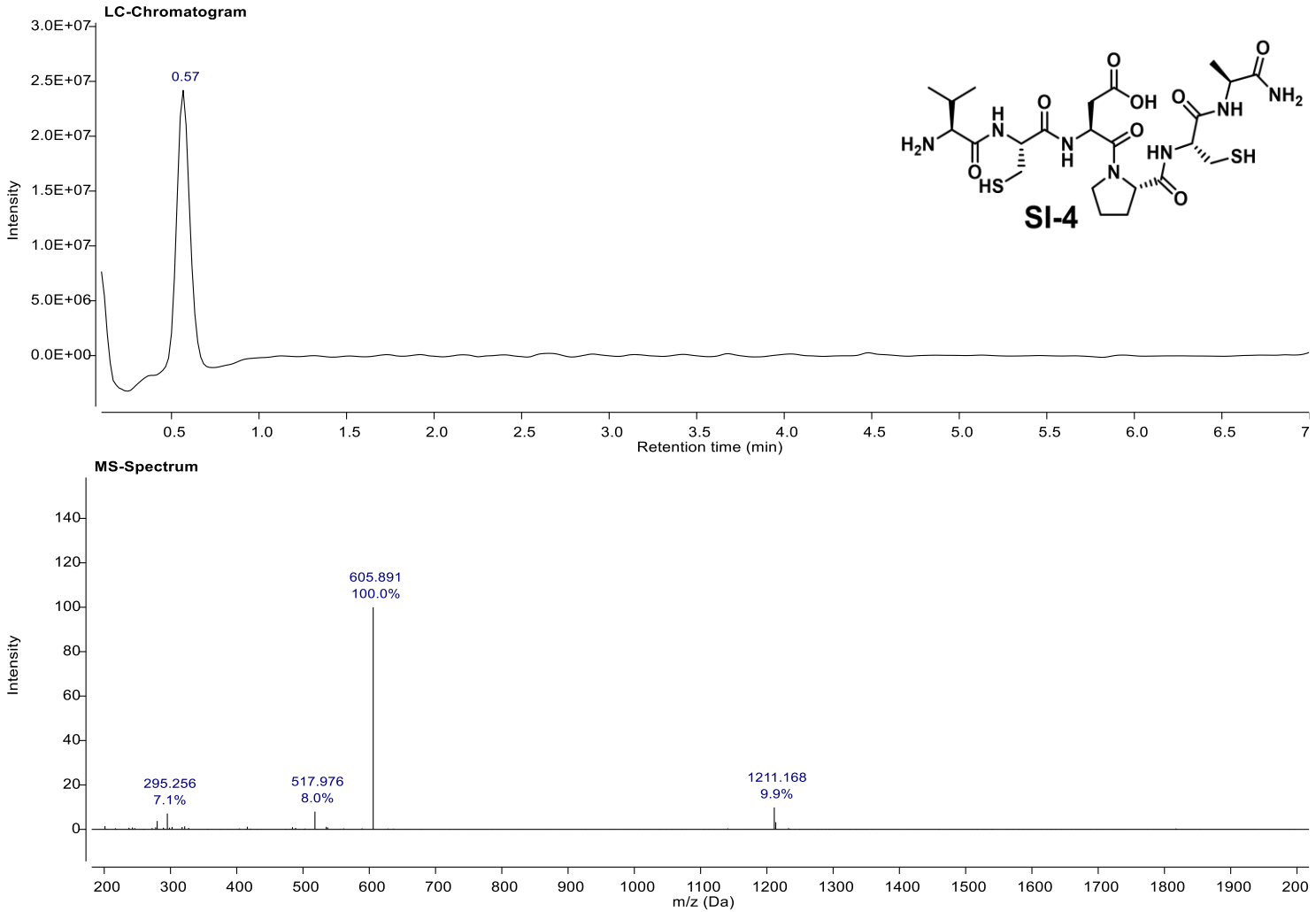

Figure A.56. LC-MS Spectrum of Compound SI-4 Gradient 5-60 for 7 Minutes

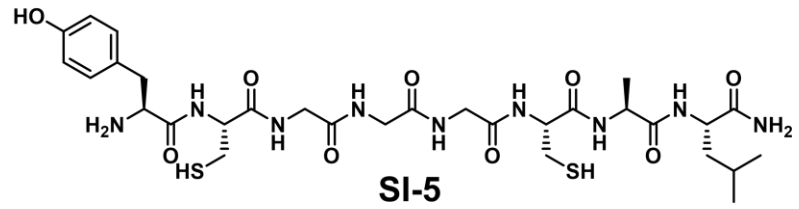

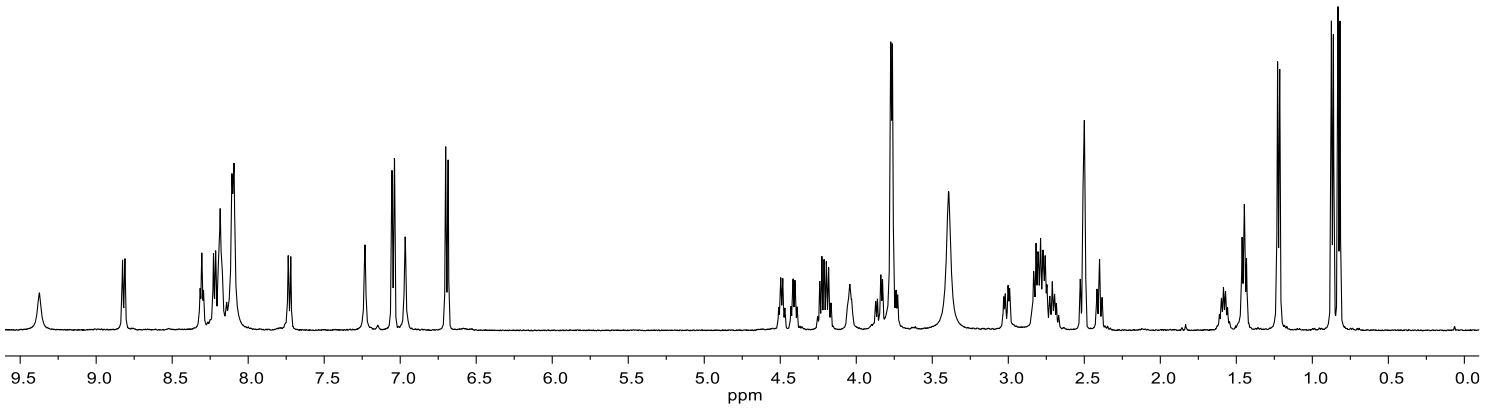

Figure A.57. 500 MHz ^{1}H-NMR Spectrum of Compound SI-5 in d_6-DMSO

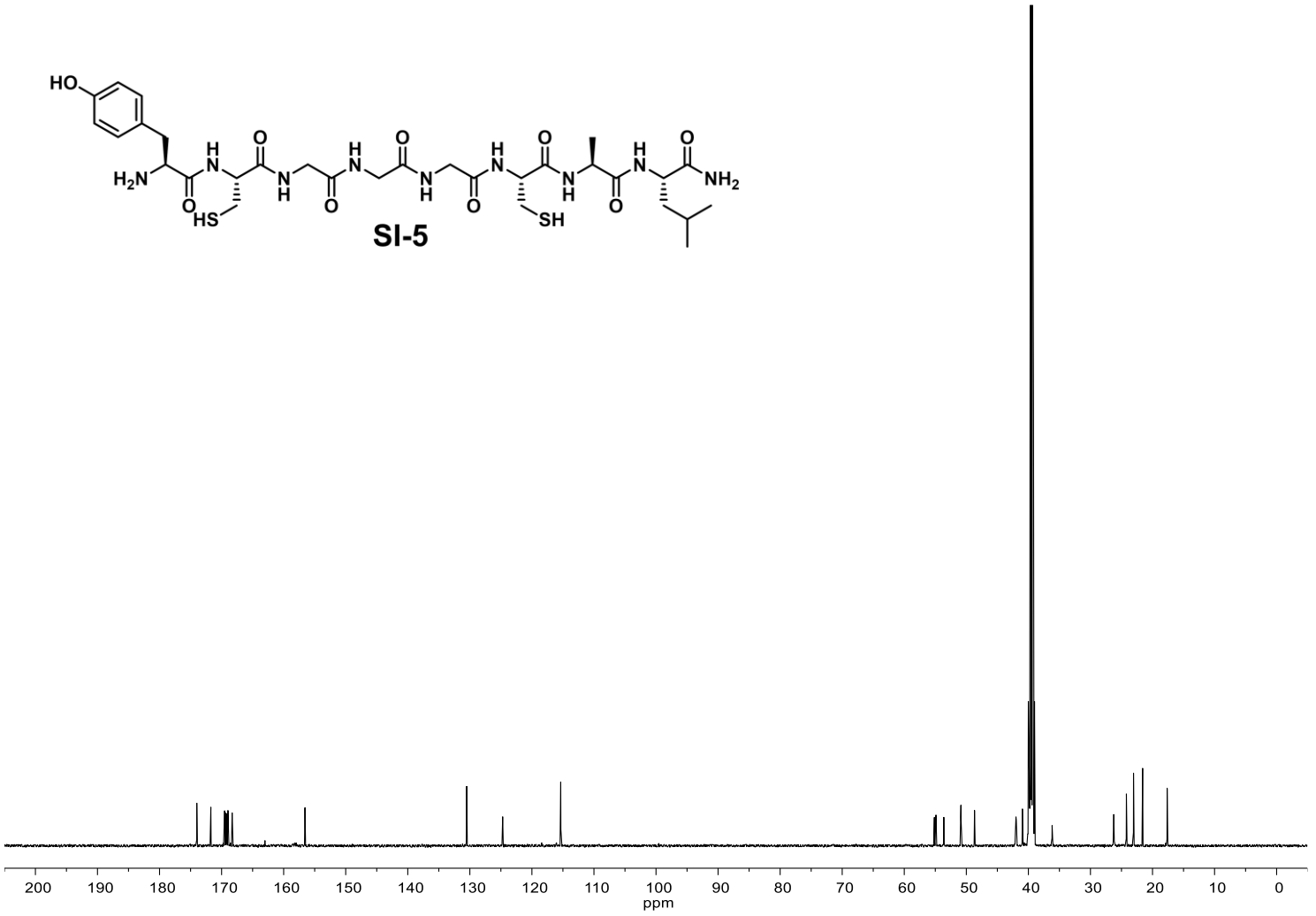

Figure A.58. 125 MHz ^{13}C-NMR Spectrum of Compound SI-5 in d_6-DMSO

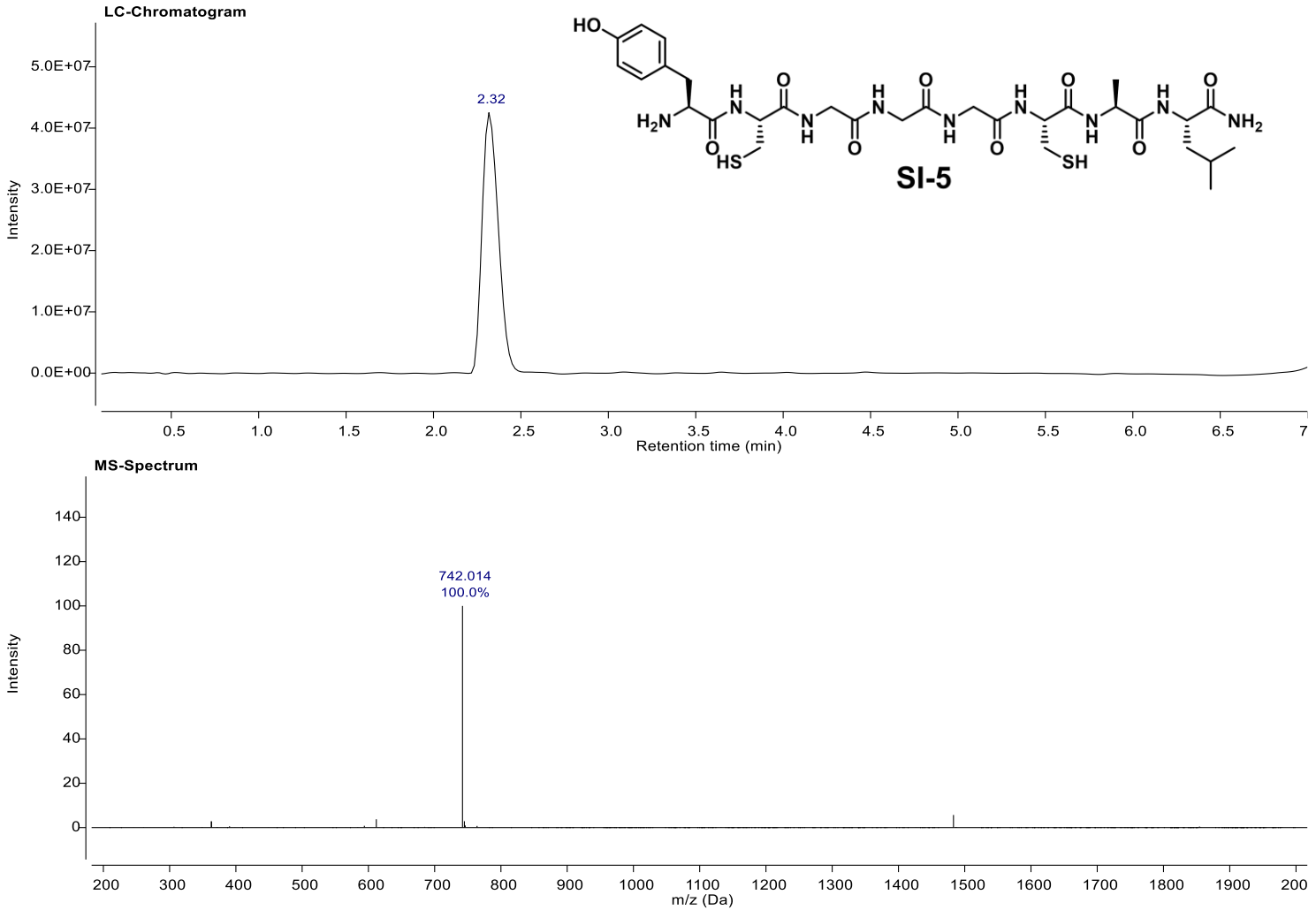

Figure A.59. LC-MS Spectrum of Compound SI-5 Gradient 5-60 for 7 Minutes

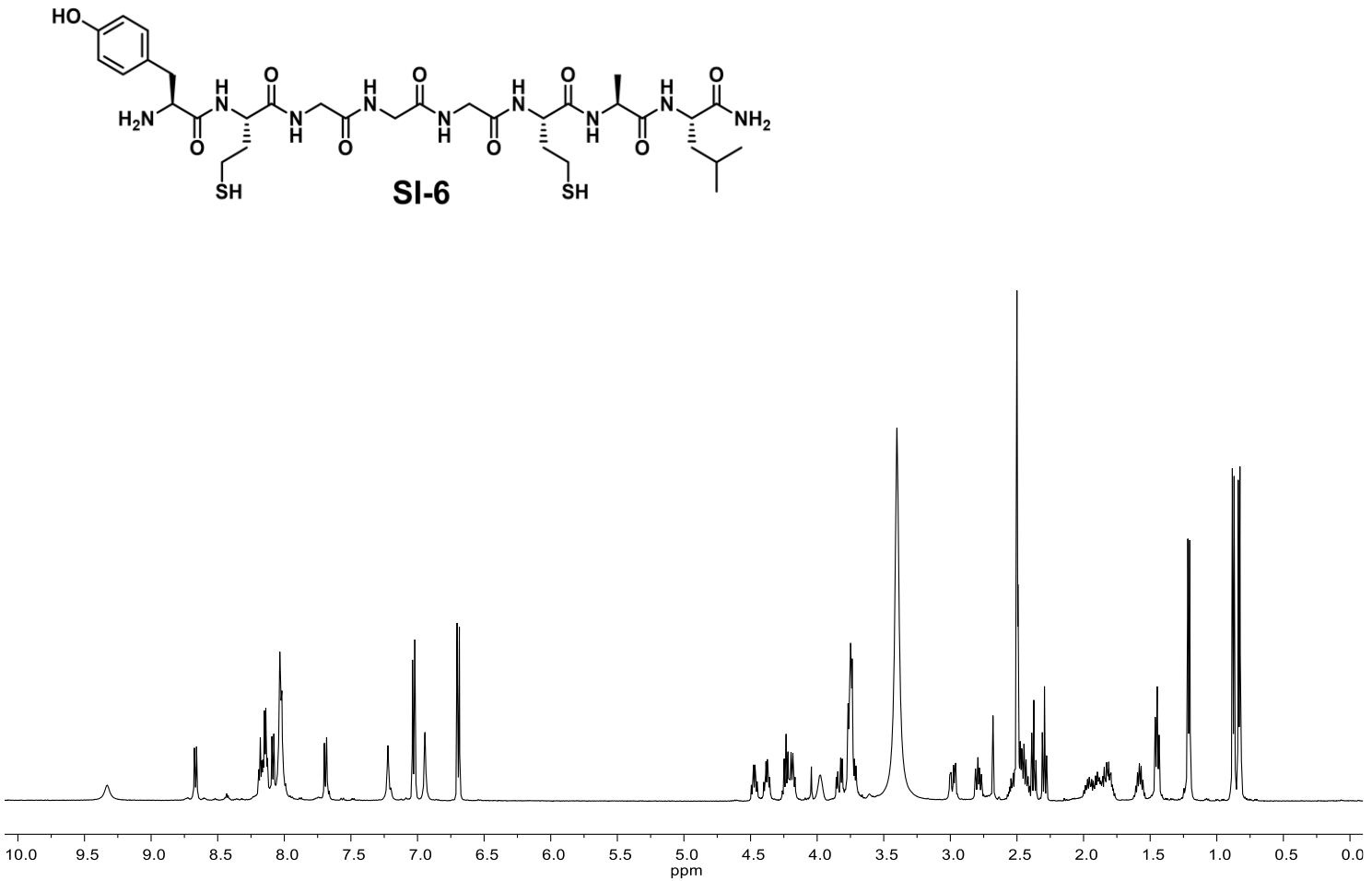

Figure A.60. 500 MHz ^{1}H-NMR Spectrum of Compound SI-6 in d_6-DMSO

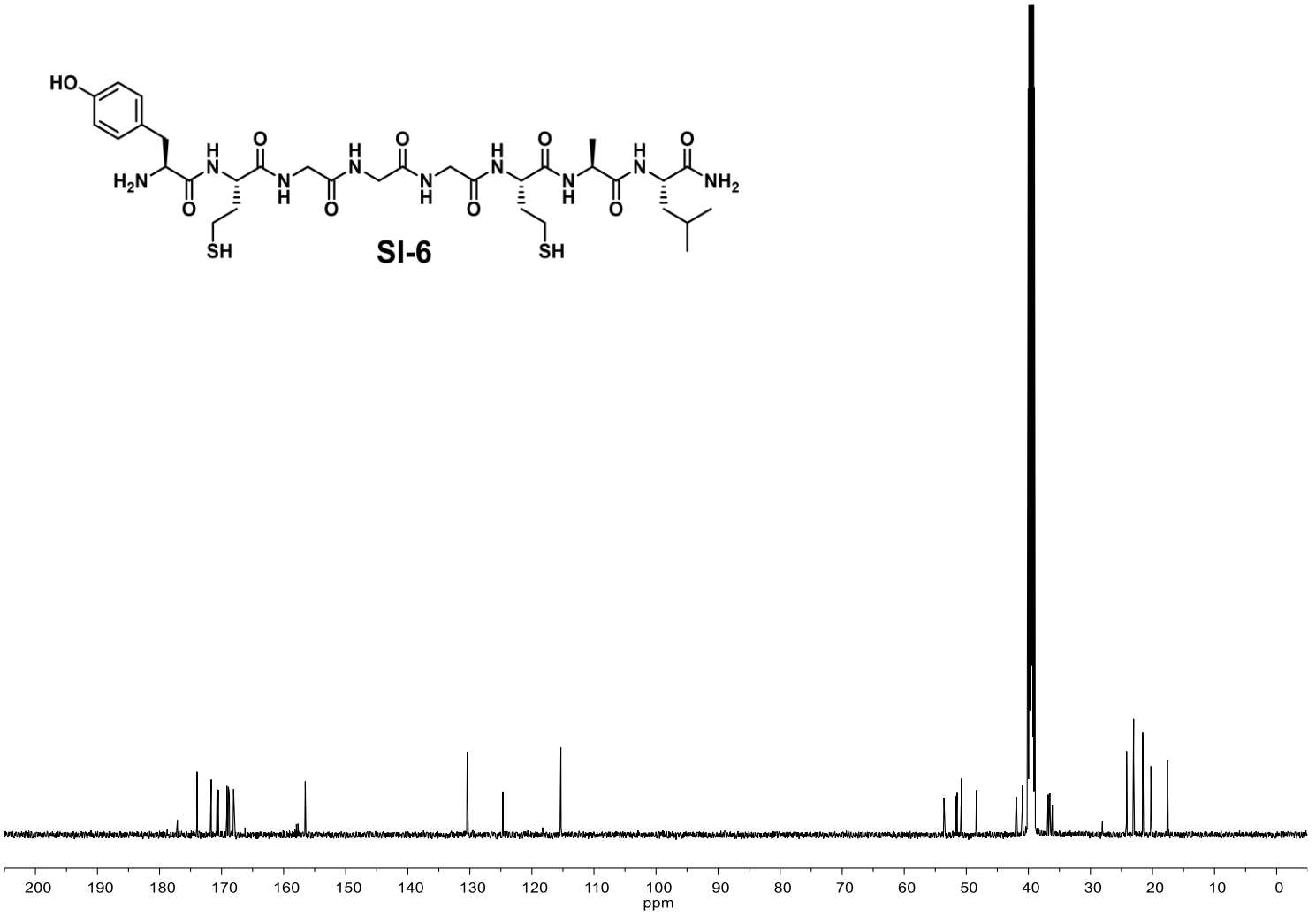

Figure A.61. 125 MHz ^{13}C-NMR Spectrum of Compound SI-6 in d_6-DMSO

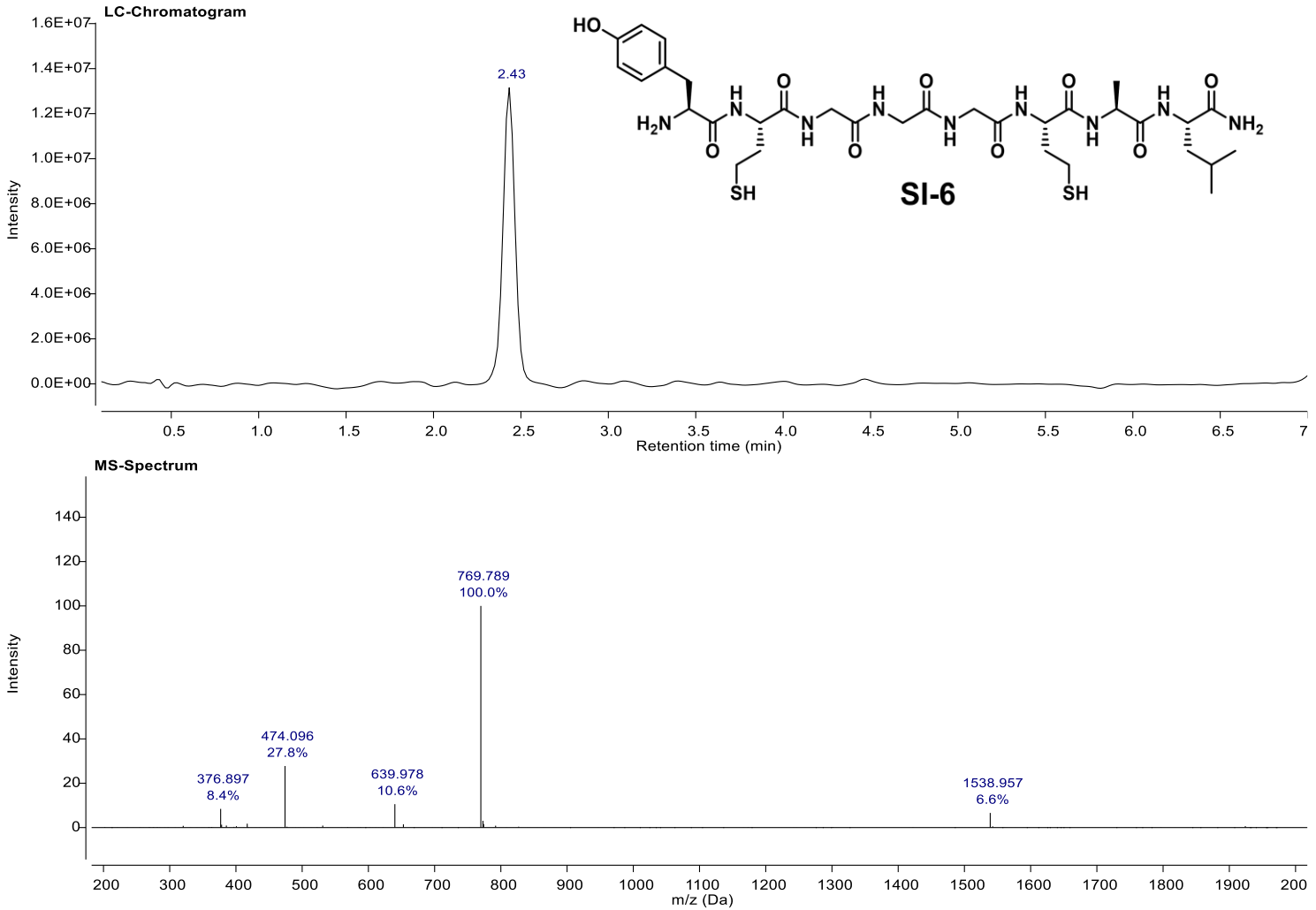

Figure A.62. LC-MS Spectrum of Compound SI-6 Gradient 5-60 for 7 Minutes

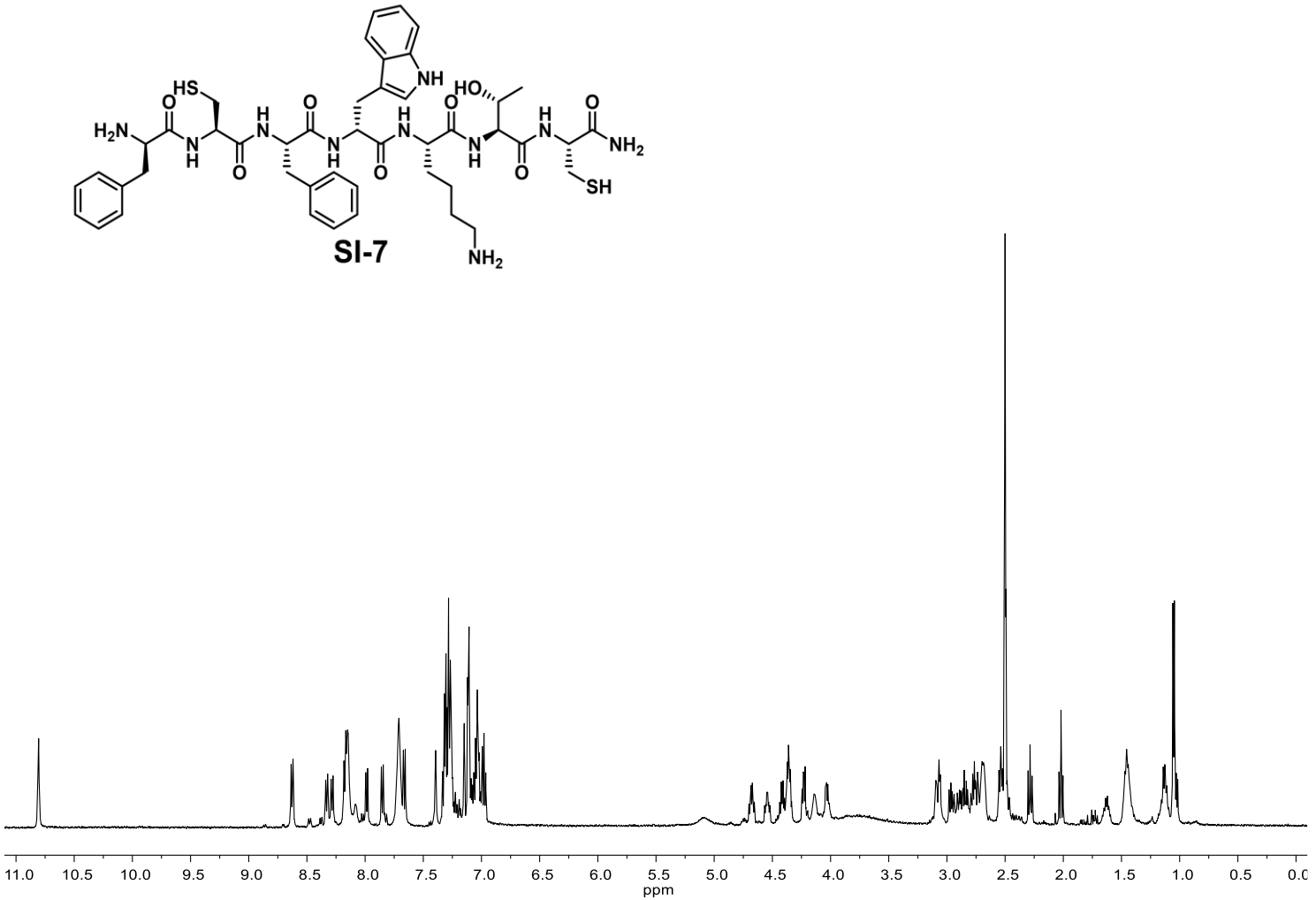

Figure A.63. 500 MHz ^{1}H-NMR Spectrum of Compound SI-7 in d_6-DMSO

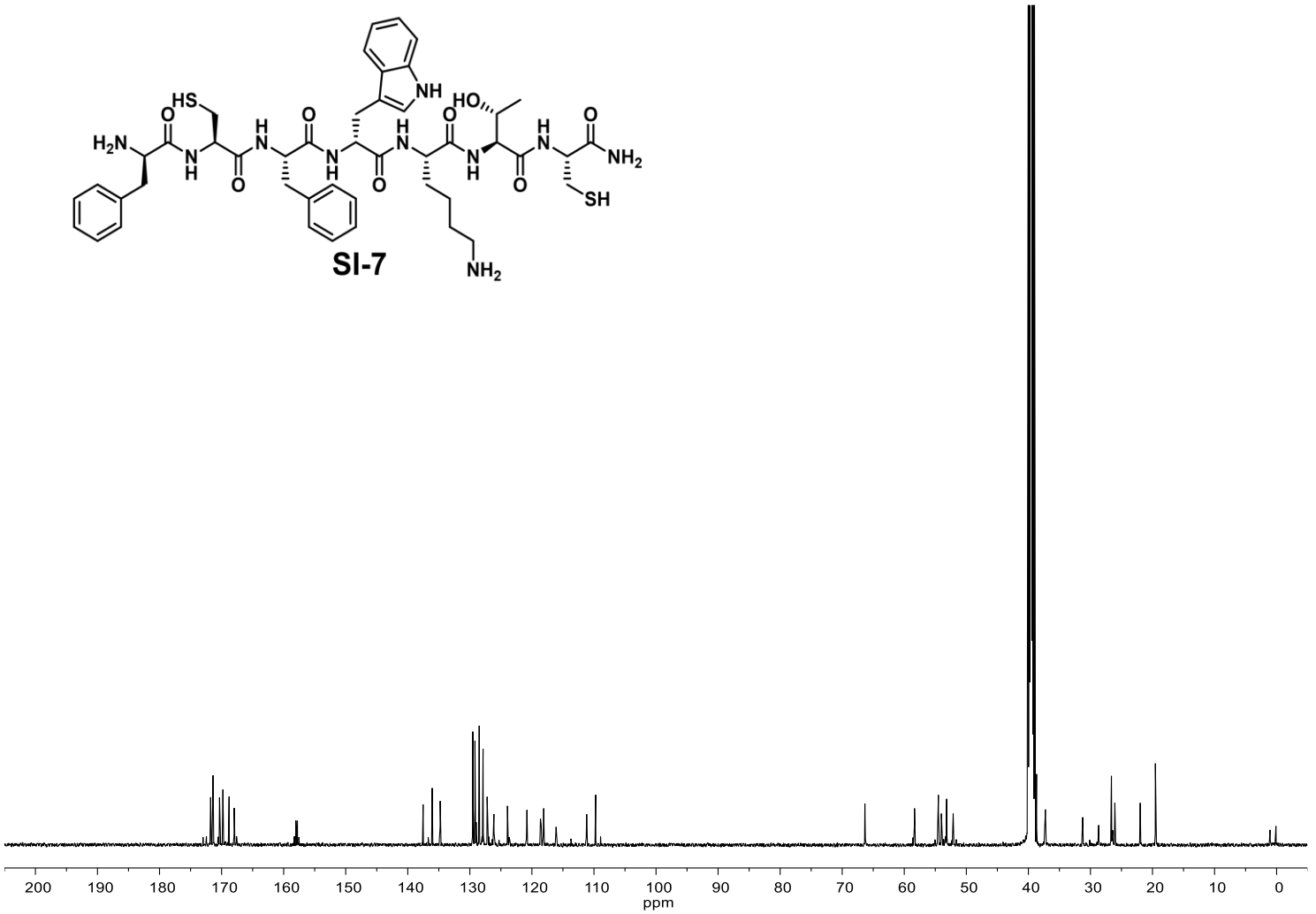

Figure A.64. 125 MHz ^{13}C-NMR Spectrum of Compound SI-7 in d_6-DMSO

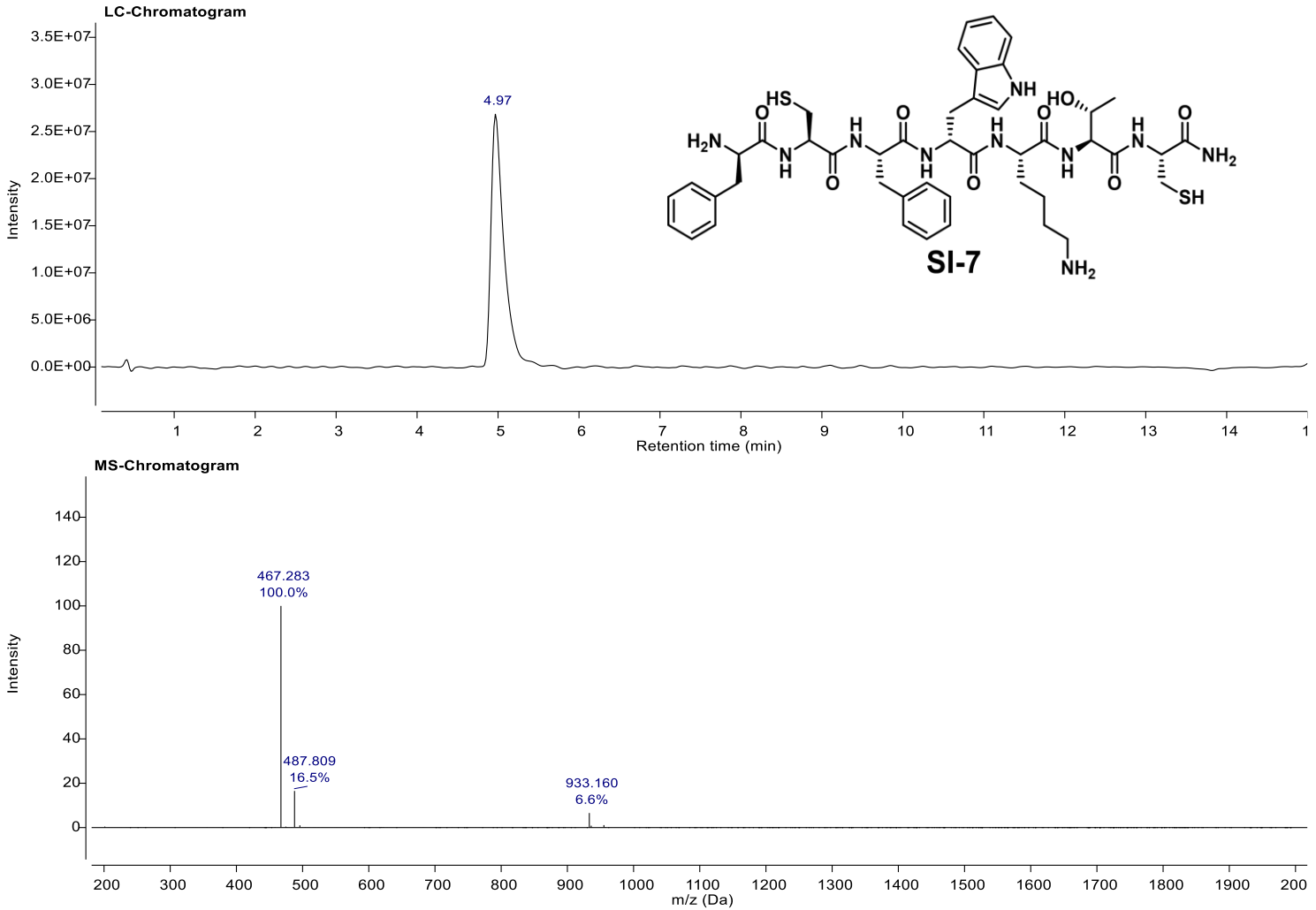

Figure A.65. LC-MS Spectrum of Compound SI-7 Gradient 5-60 for 15 Minutes

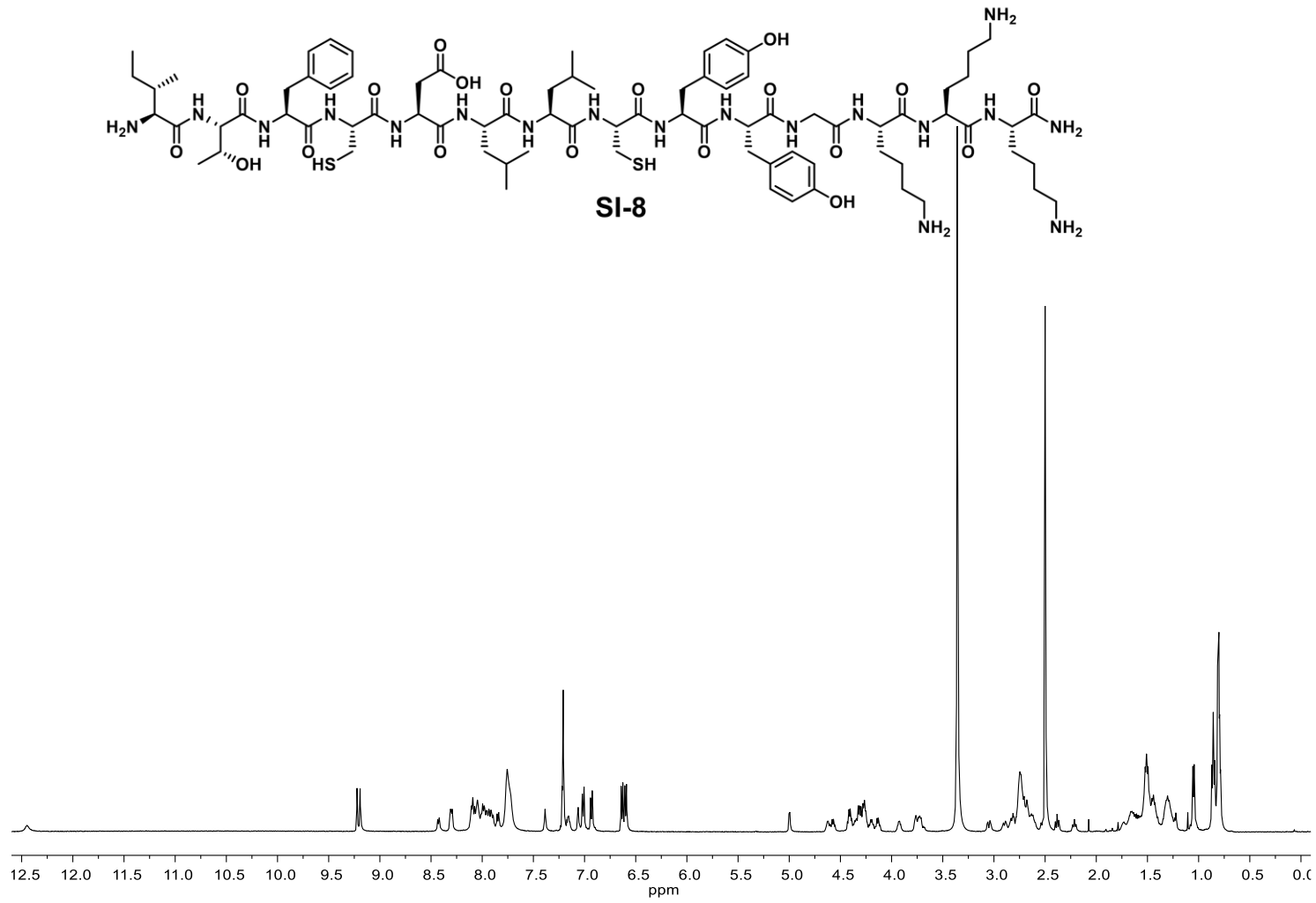

Figure A.66. 500 MHz ^{1}H-NMR Spectrum of Compound SI-8 in d_6-DMSO

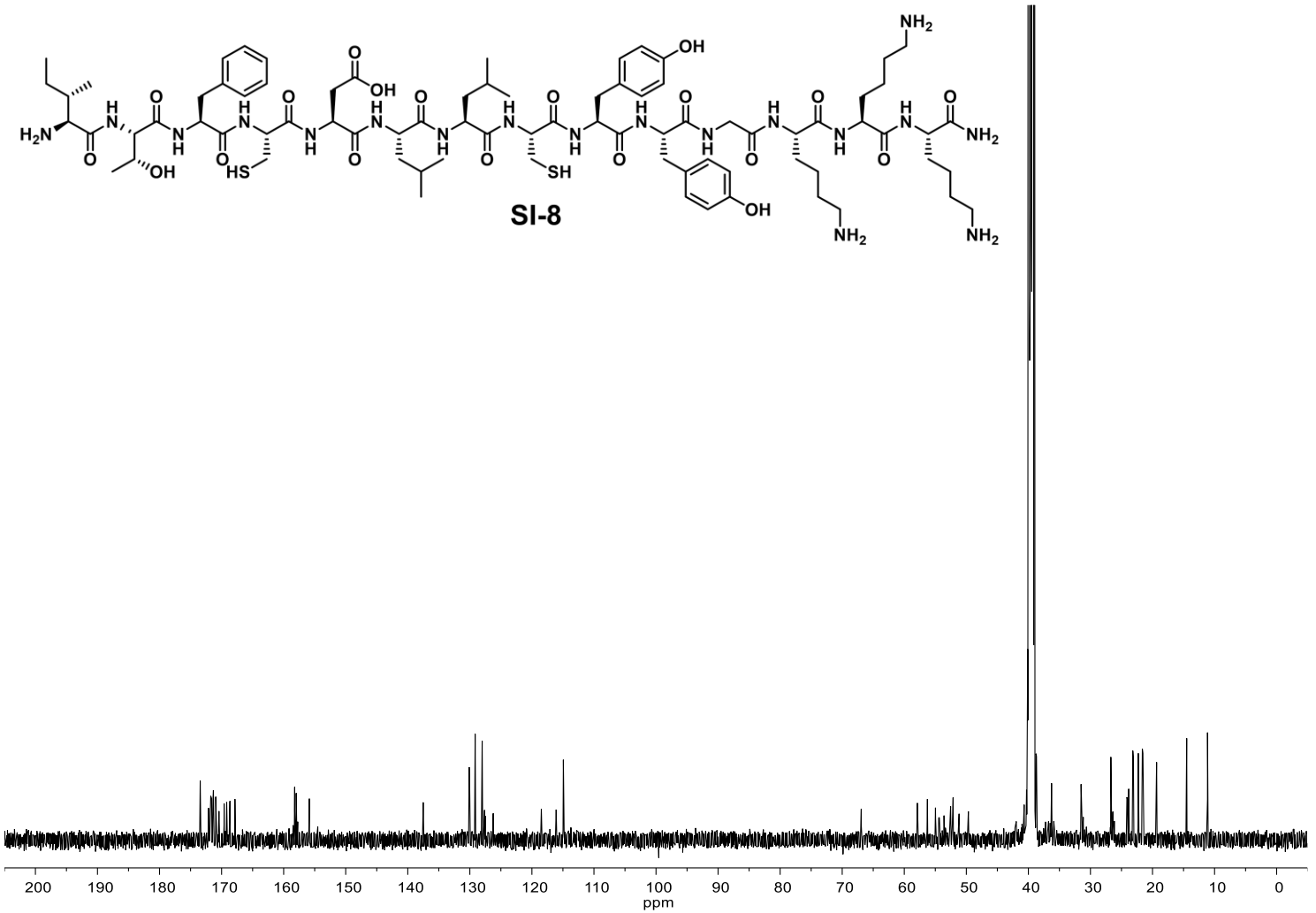

Figure A.67. 125 MHz ^{13}C-NMR Spectrum of Compound SI-8 in d_6-DMSO

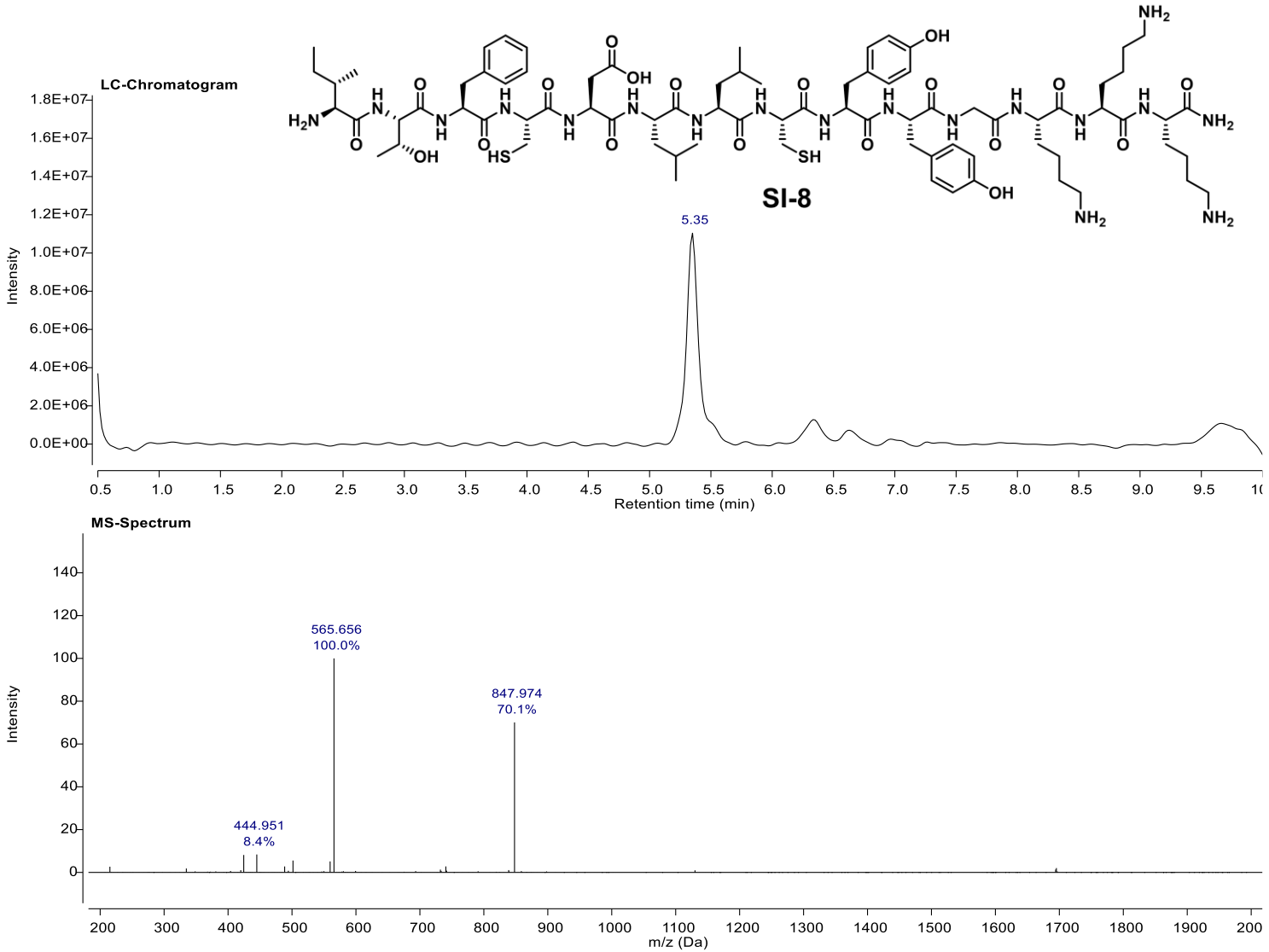

Figure A.68. LC-MS Spectrum of Compound SI-8 Gradient 5-60 for 10 Minutes

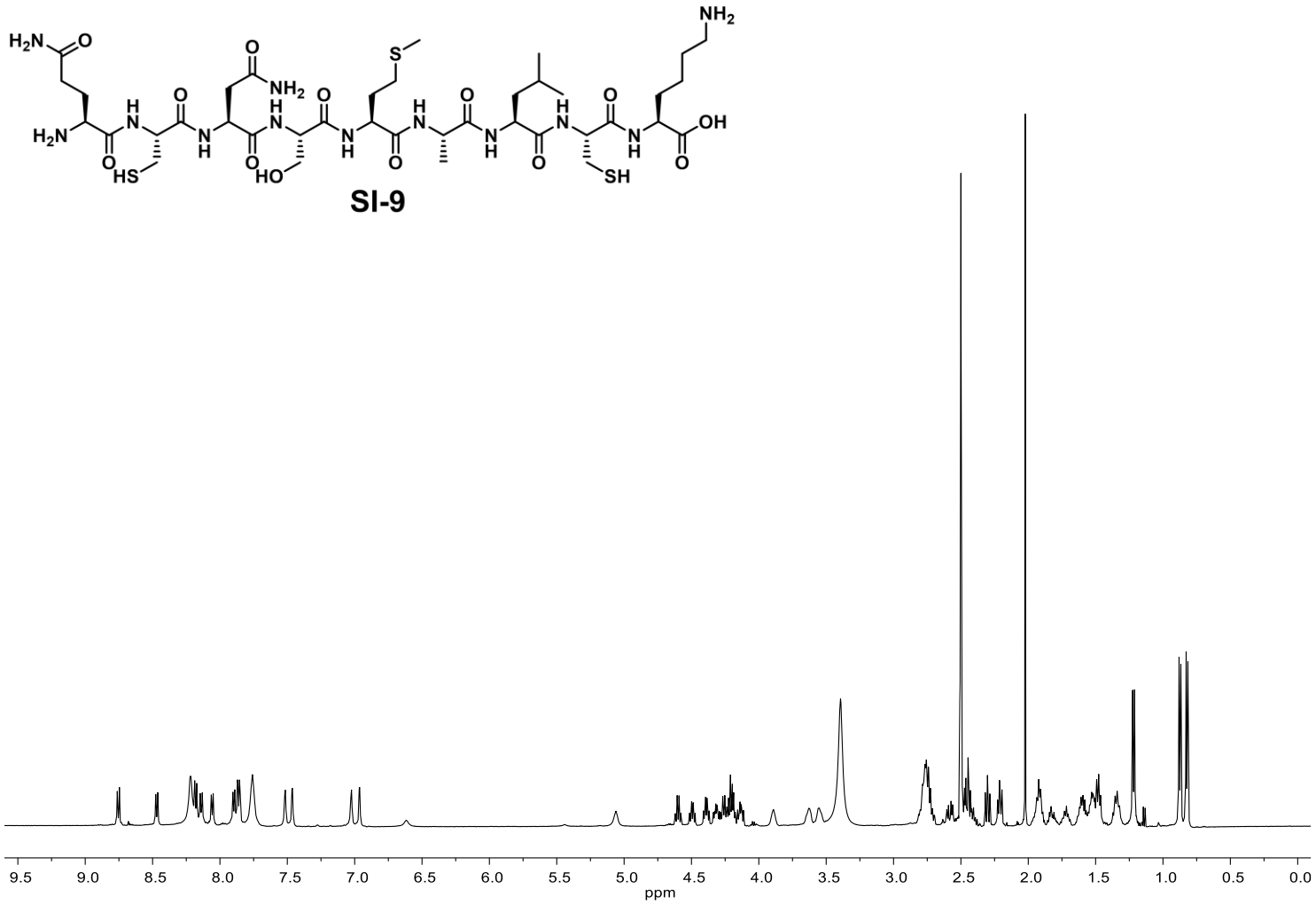

Figure A.69. 500 MHz ^{1}H-NMR Spectrum of Compound SI-9 in d_6-DMSO

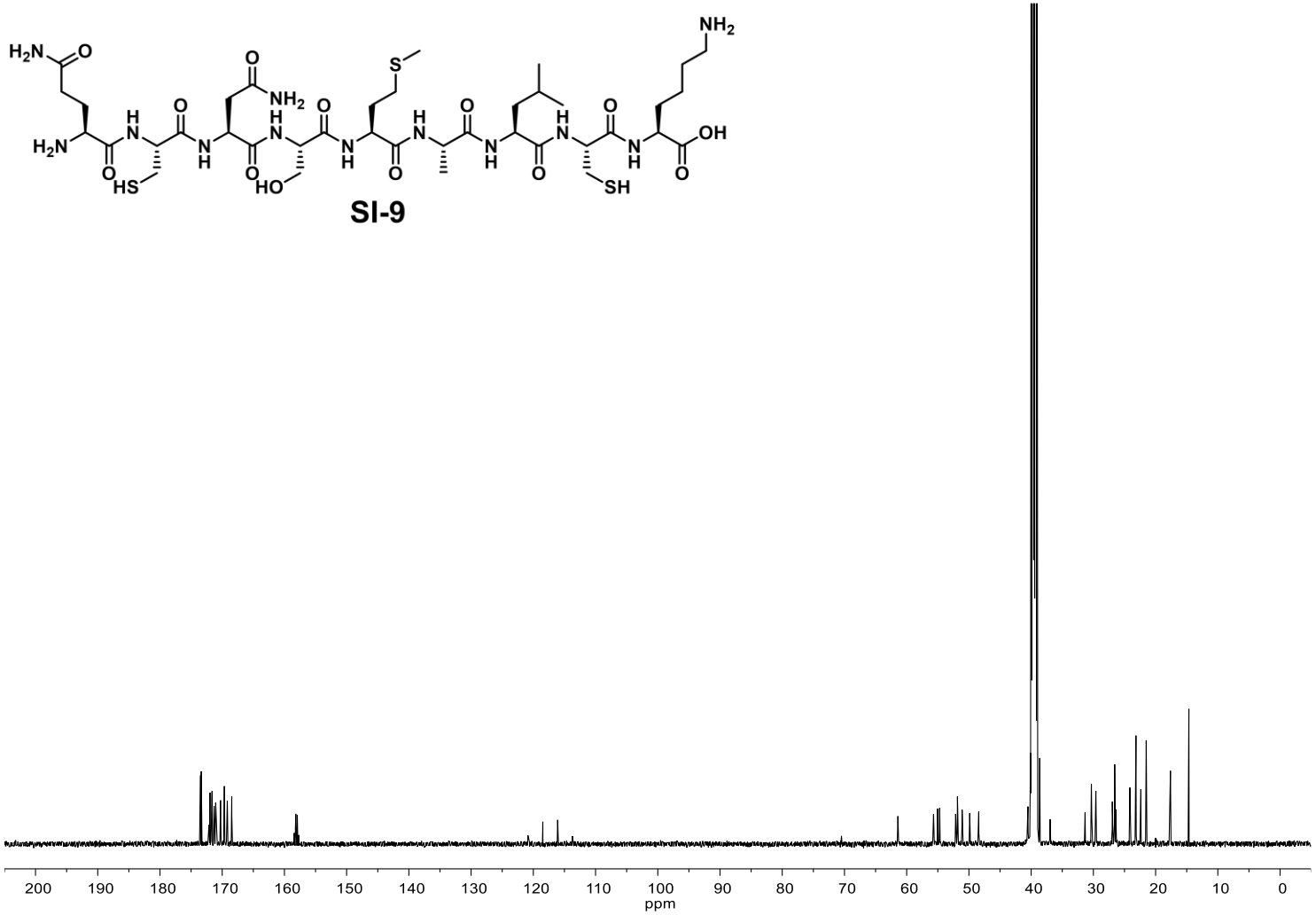

Figure A.70. 125 MHz ^{13}C-NMR Spectrum of Compound SI-9 in d_6-DMSO

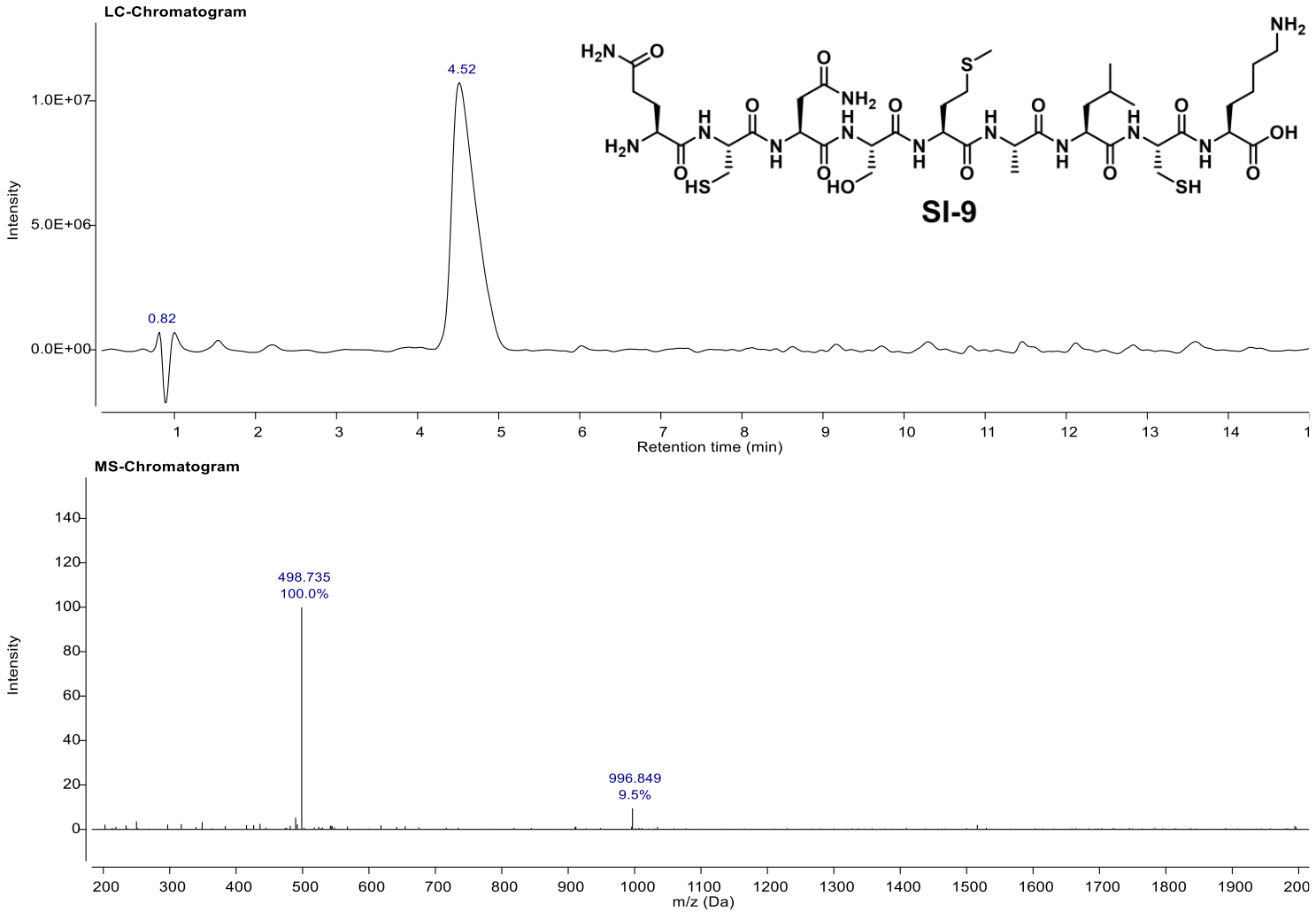

Figure A.71. LC-MS Spectrum of Compound SI-9 Gradient 5-60 for 15 Minutes

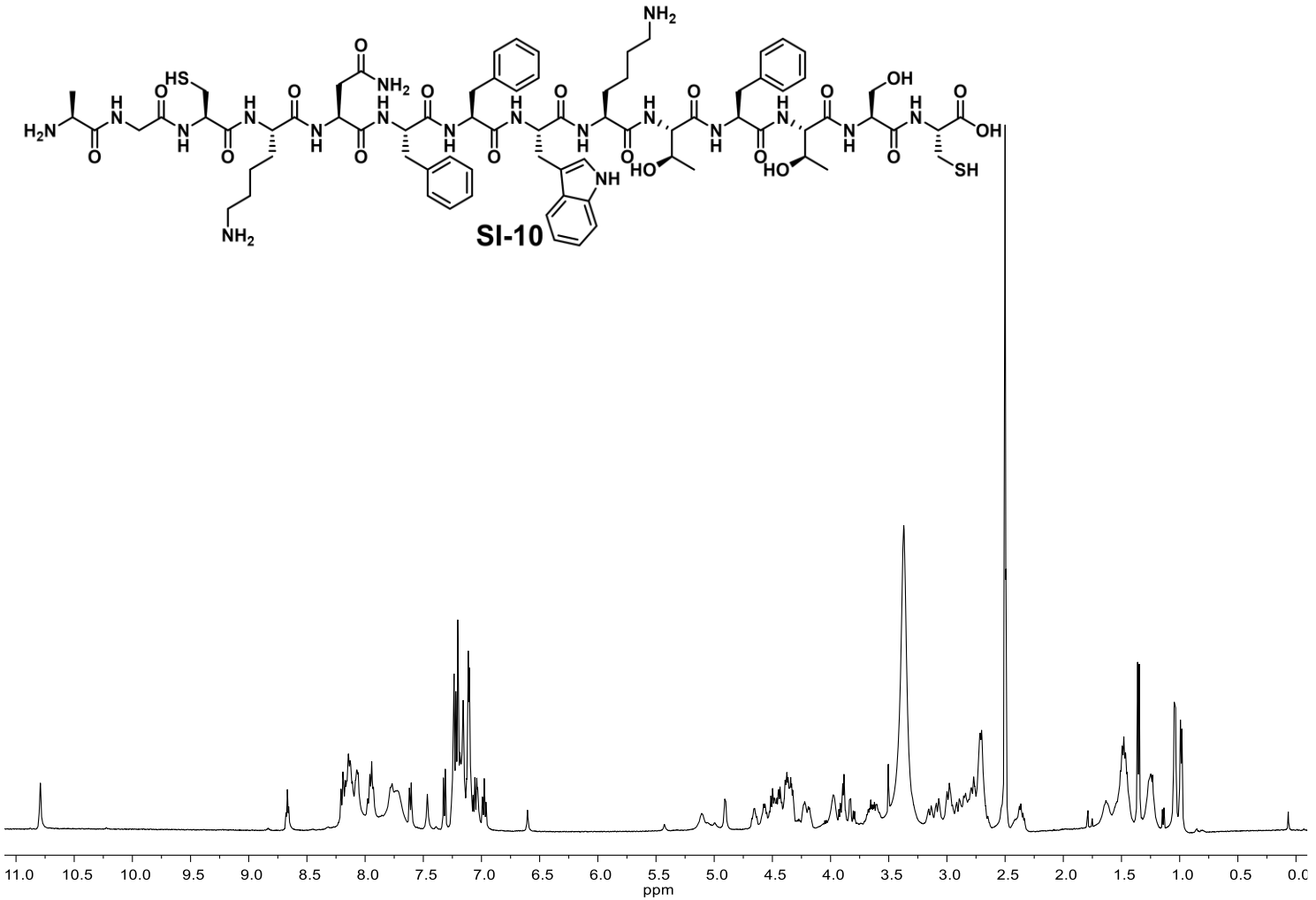

Figure A.72. 500 MHz ^{1}H-NMR Spectrum of Compound SI-10 in d_6-DMSO

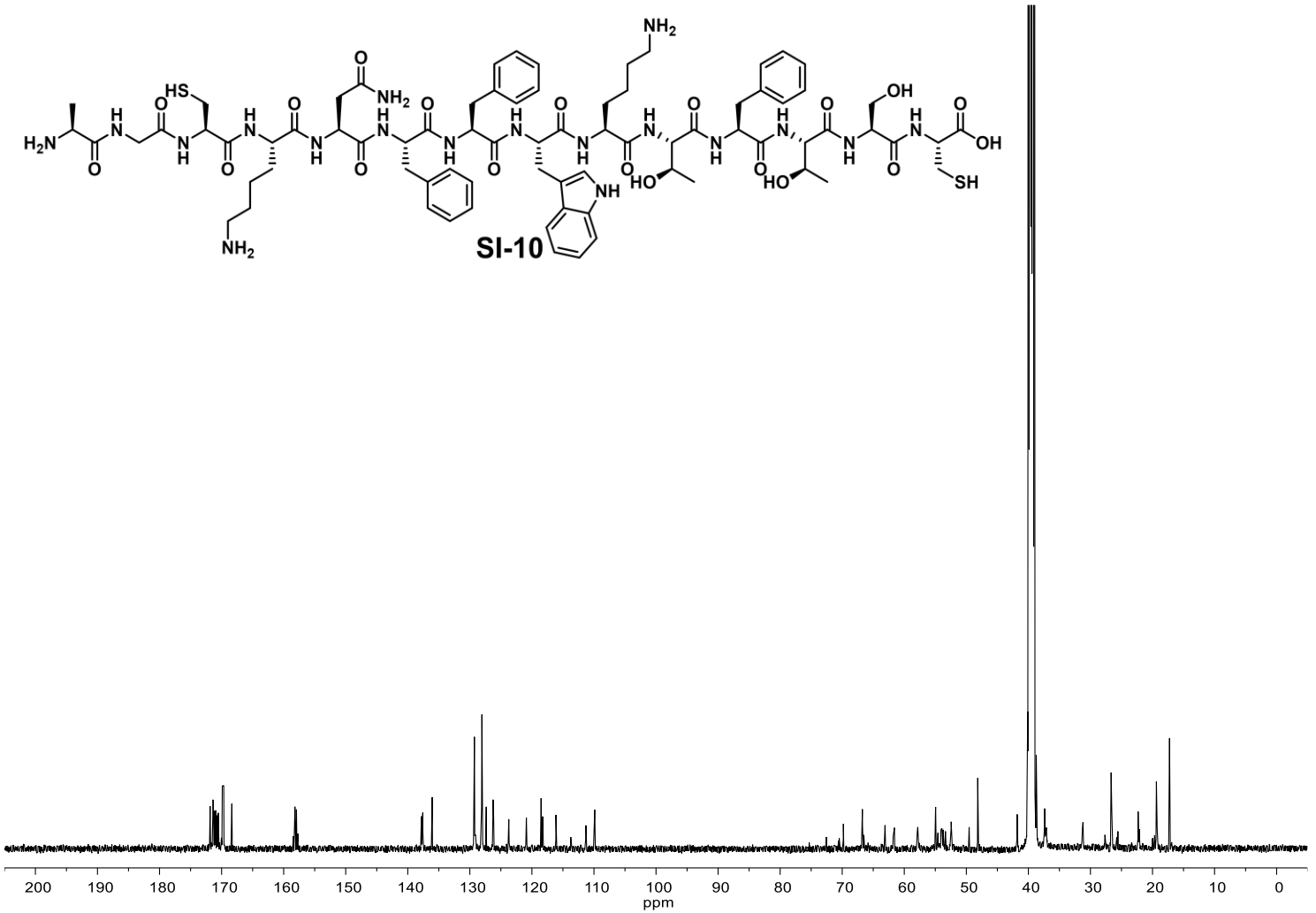

Figure A.73. 125 MHz ^{13}C-NMR Spectrum of Compound SI-10 in d_6-DMSO

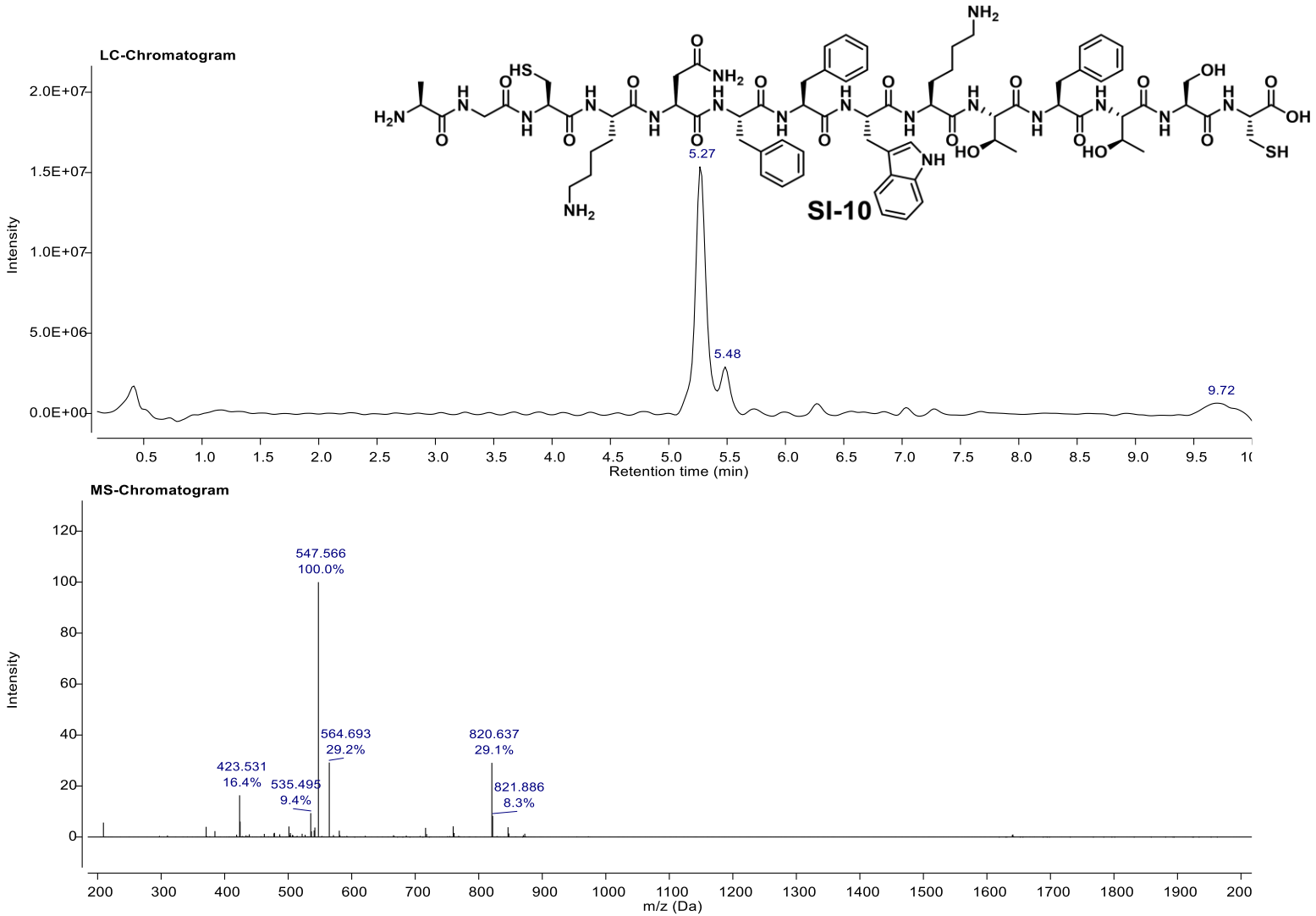

Figure A.74. LC-MS Spectrum of Compound SI-10 Gradient 5-60 for 10 Minutes

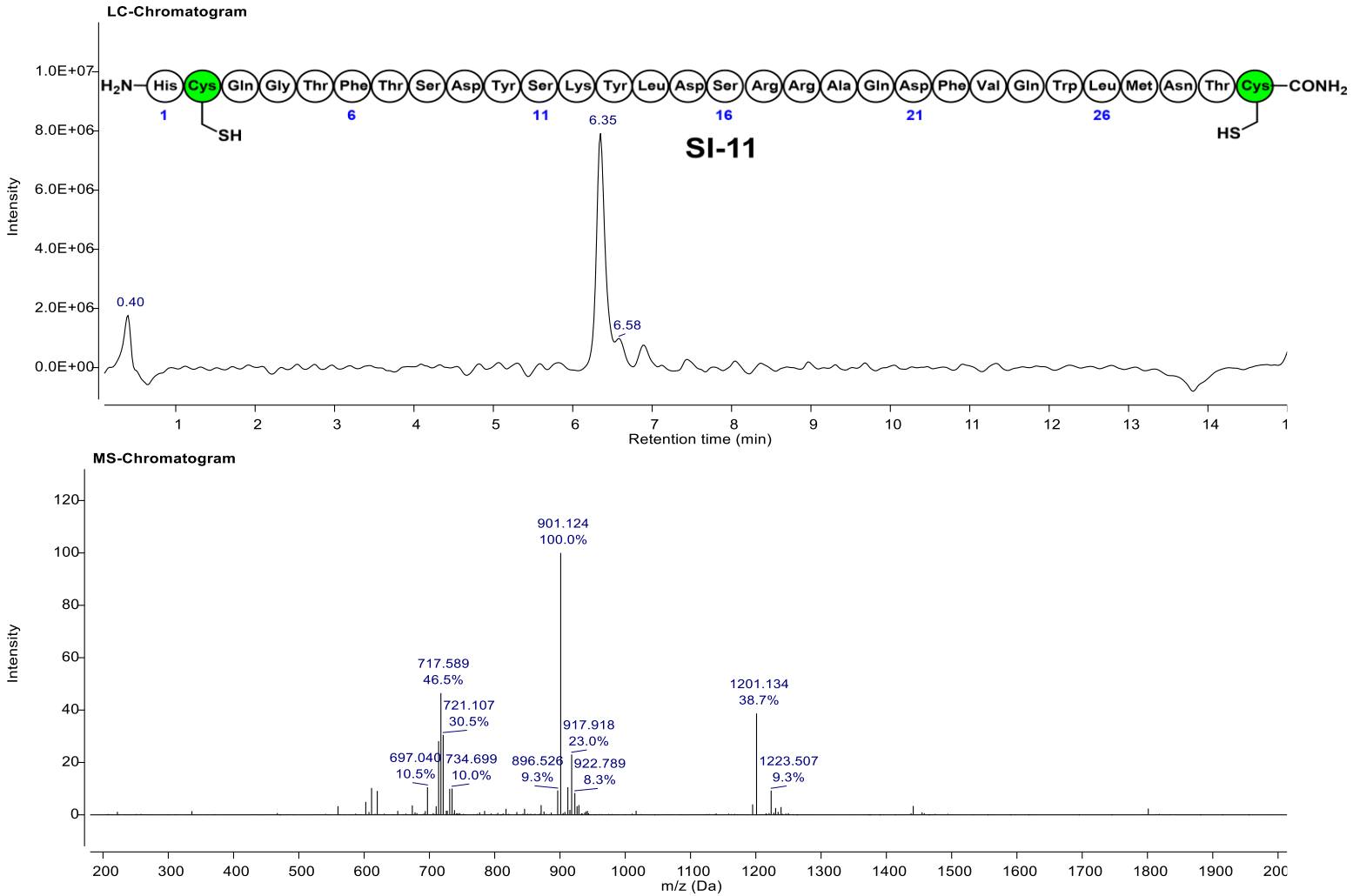

Figure A.75. LC-MS Spectrum of Compound SI-11 Gradient 5-60 for 15 Minutes

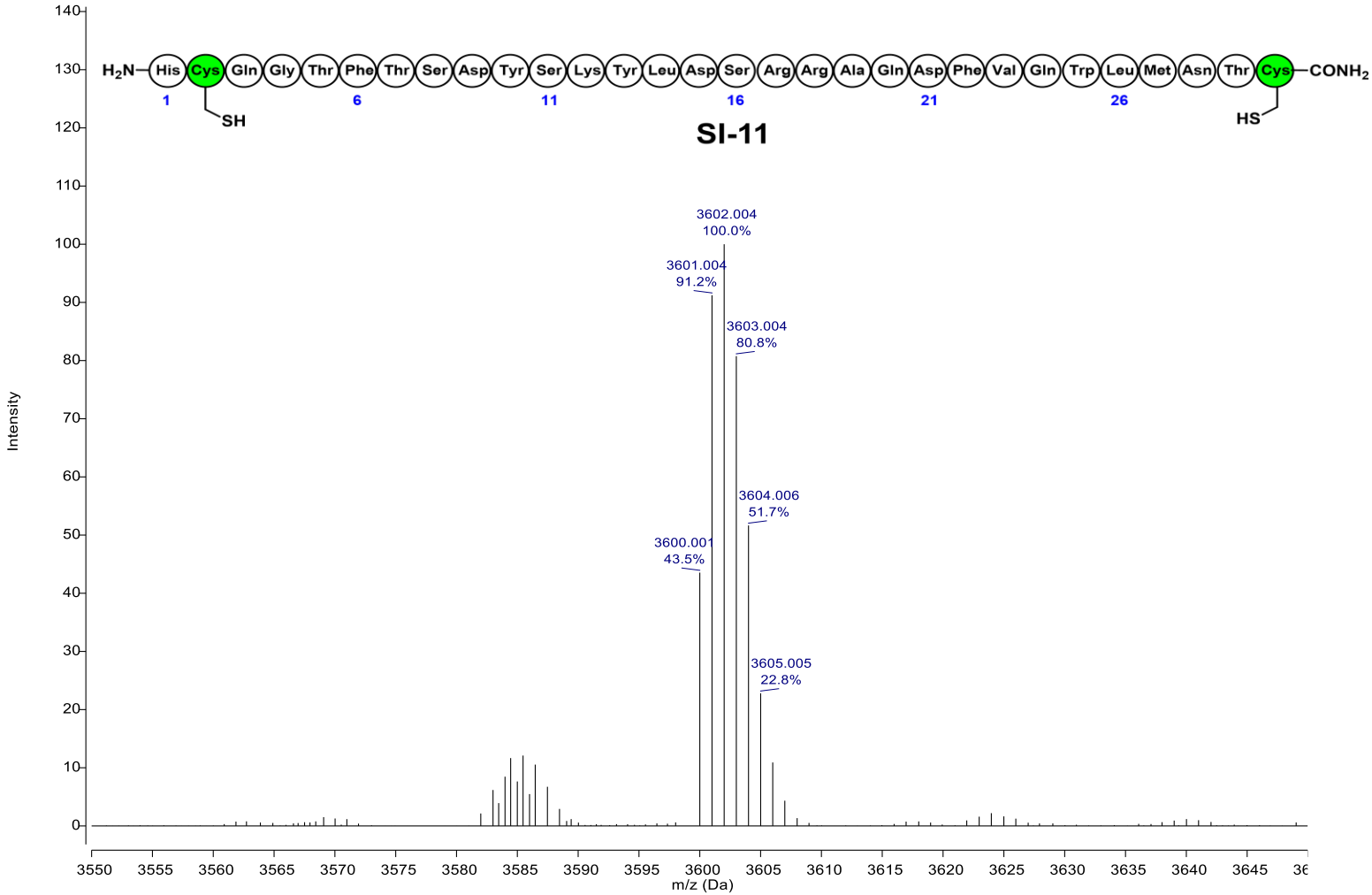

Figure A.76. MALDI-TOF-MS Spectrum of Compound SI-11

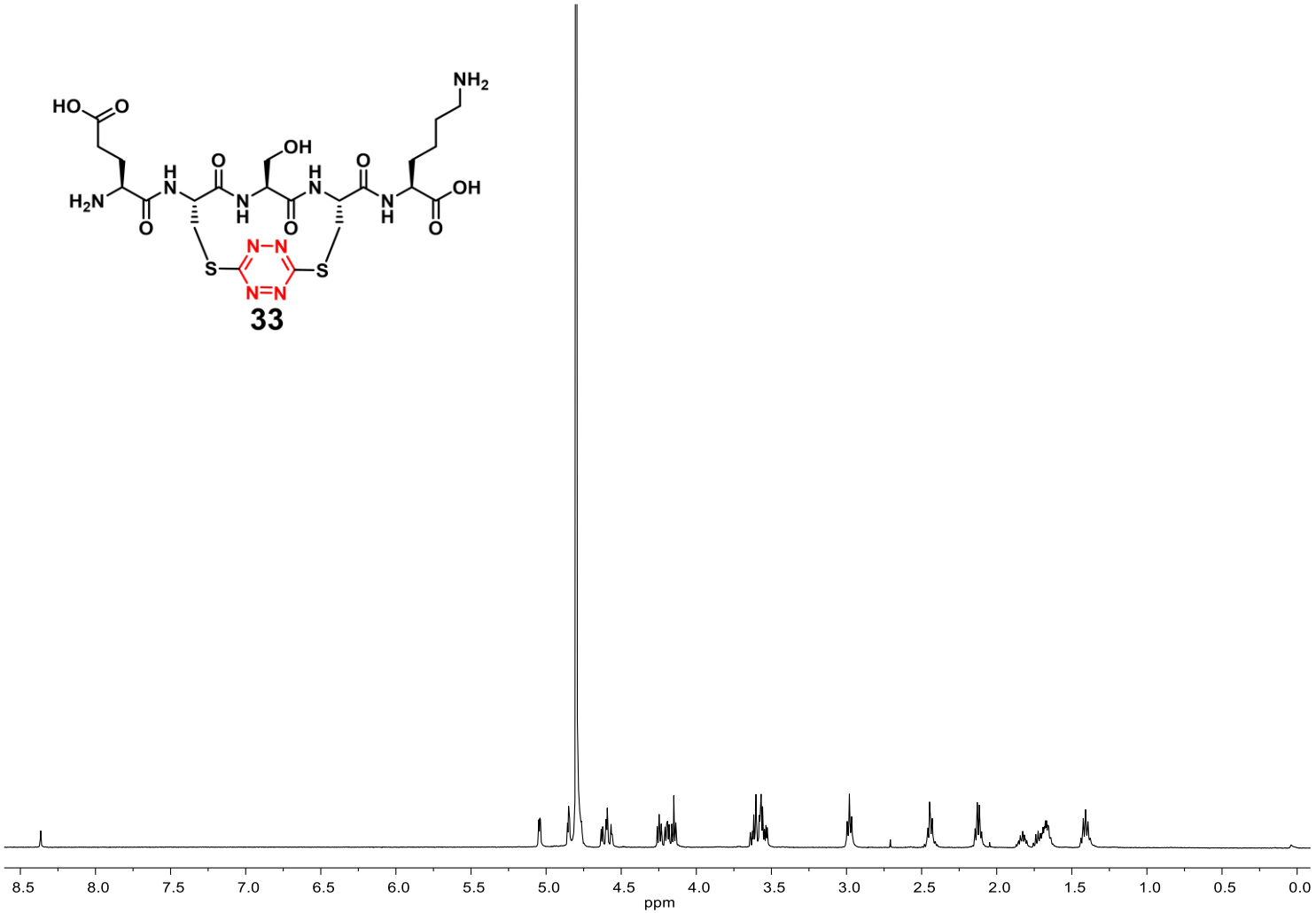

Figure A.77. 500 MHz ^{1}H-NMR Spectrum of Compound 33 in D_2O

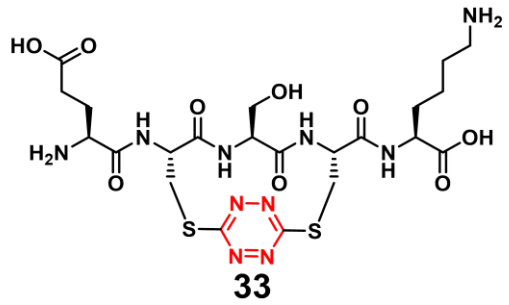

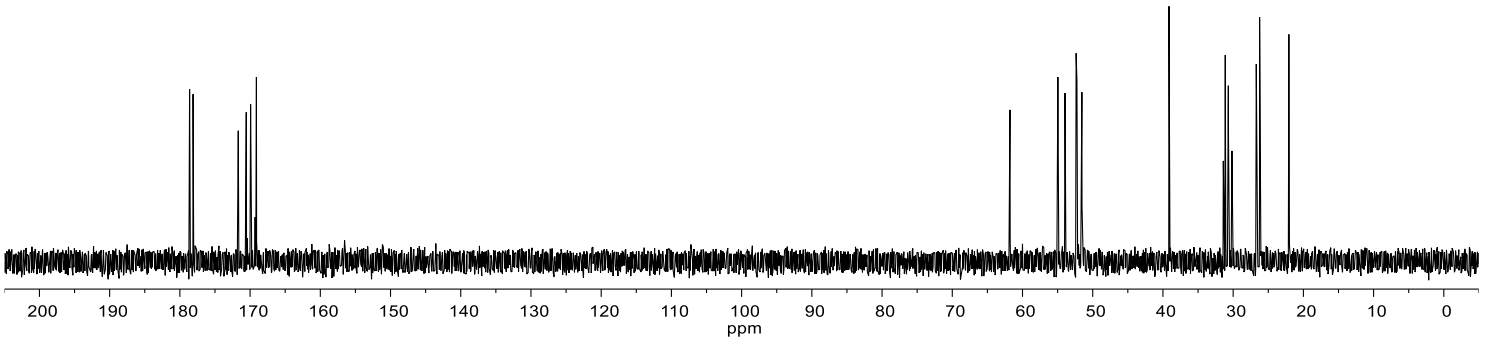

Figure A.78. 125 MHz ^{13}C-NMR Spectrum of Compound 33 in D_2O

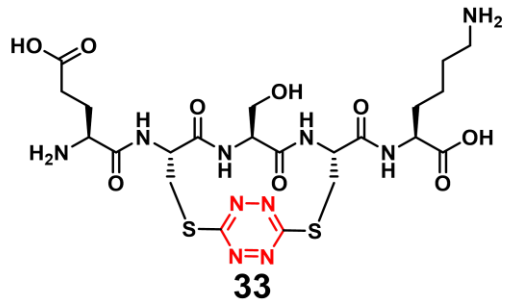

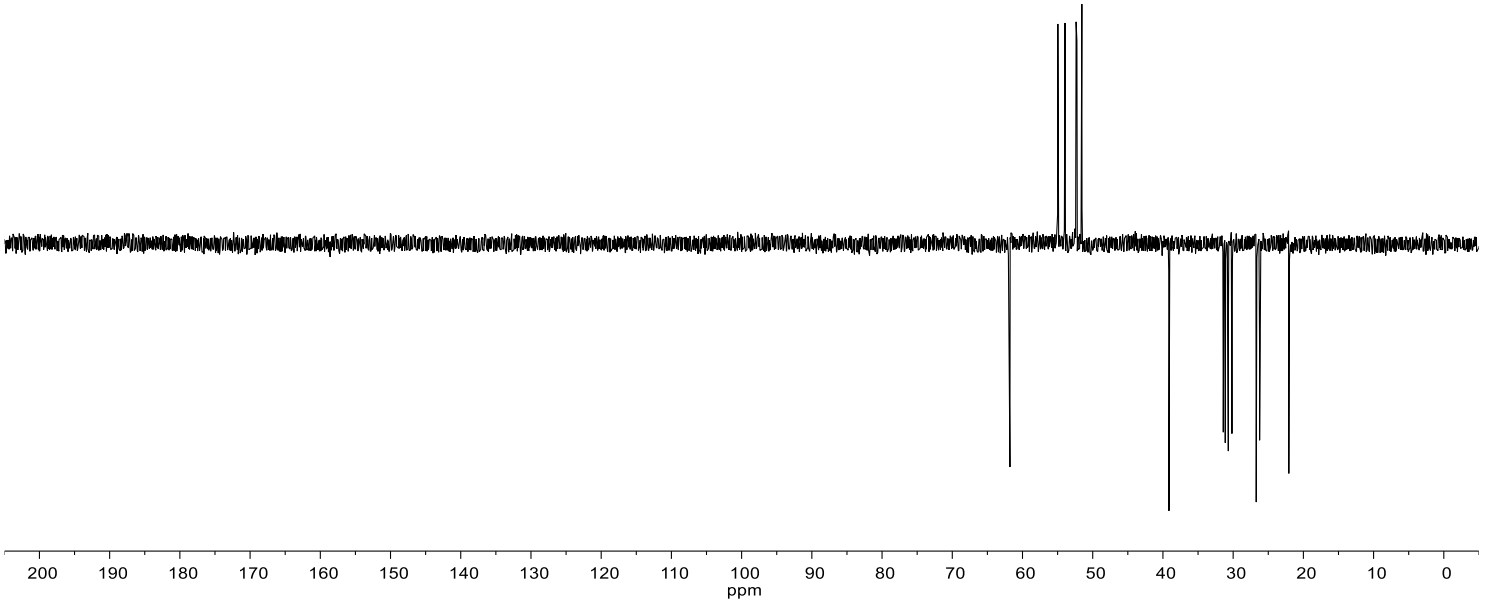

Figure A.79. 125 MHz ^{13}C-NMR DEPT 135 Spectrum of Compound 33 in D_2O

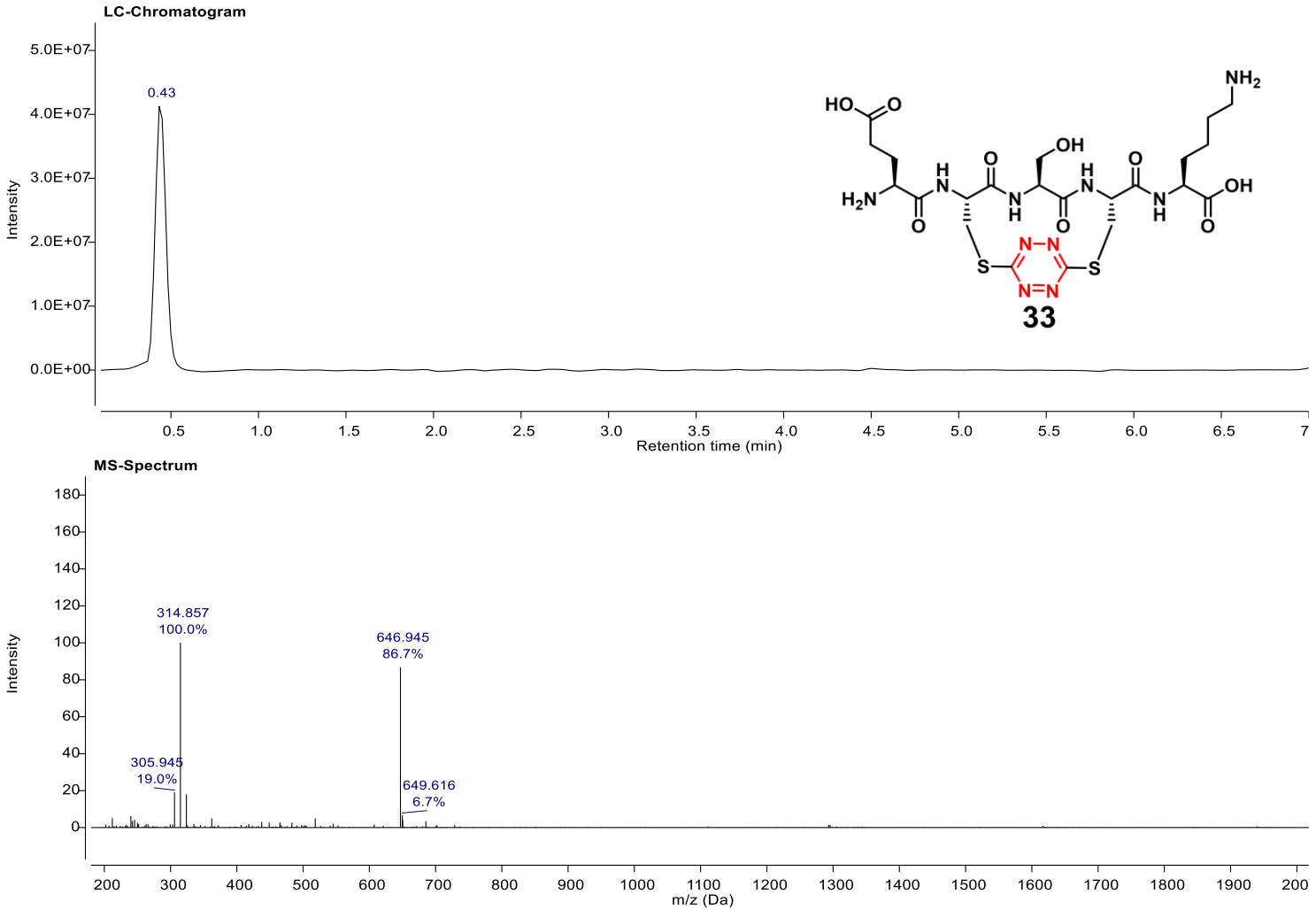

Figure A.80. LC-MS Spectrum of Compound 33 Gradient 5-60 for 7 Minutes

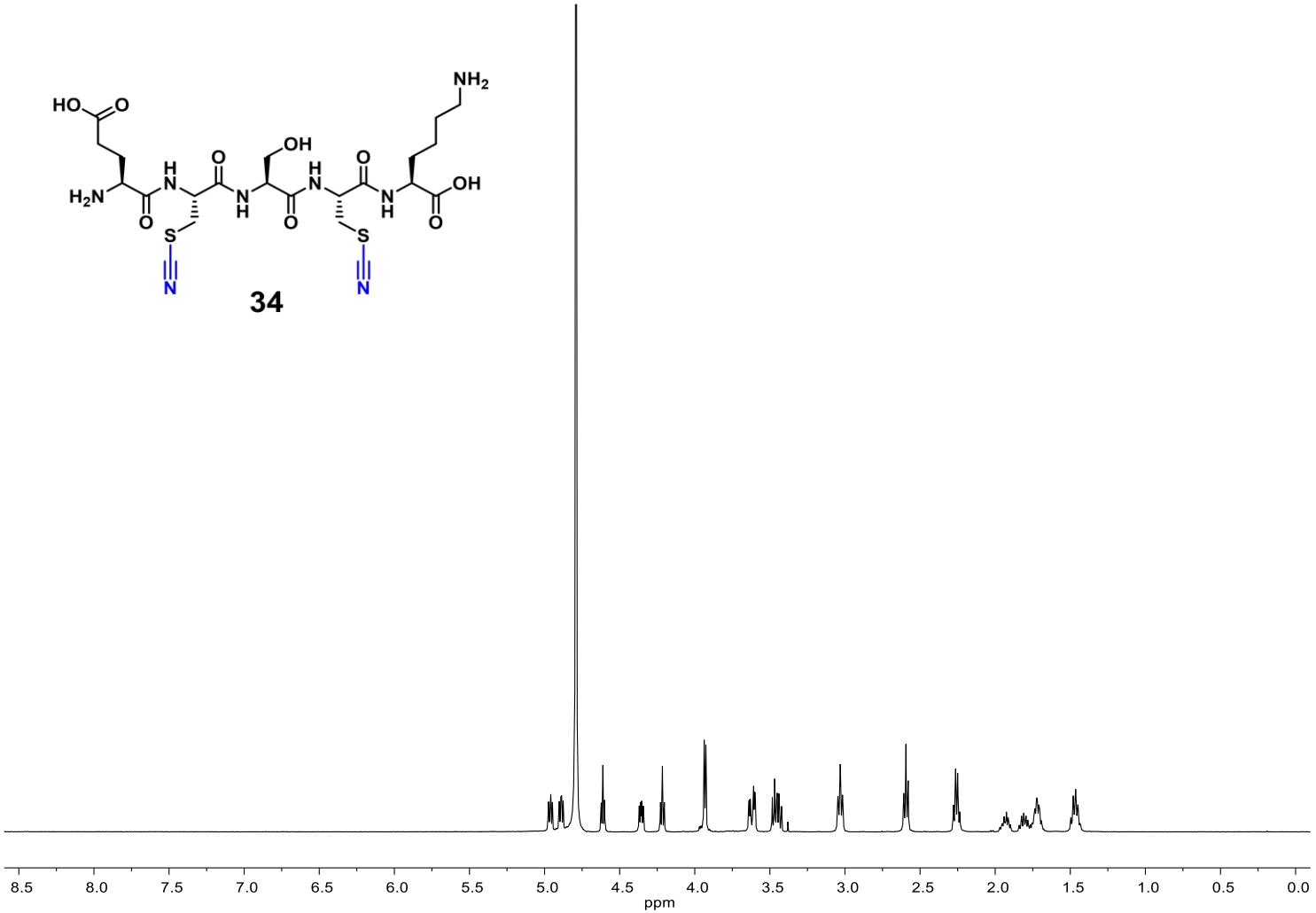

Figure A.81. 500 MHz ^{1}H-NMR Spectrum of Compound 34 in D_2O

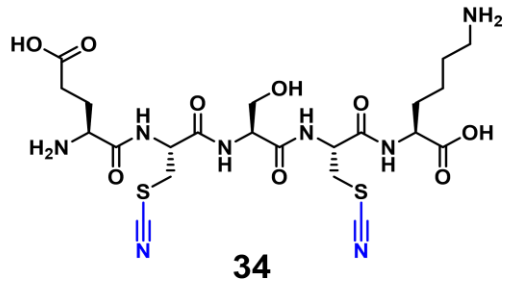

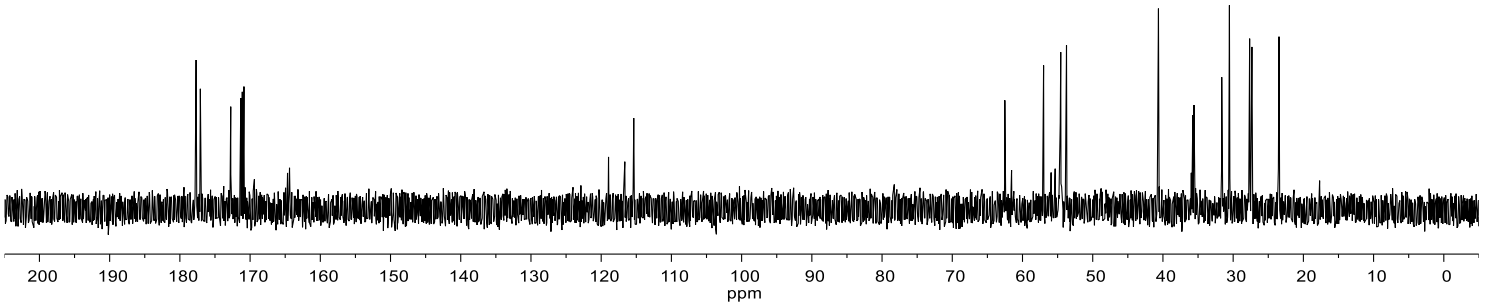

Figure A.82. 125 MHz ^{13}C-NMR Spectrum of Compound 34 in D_2O

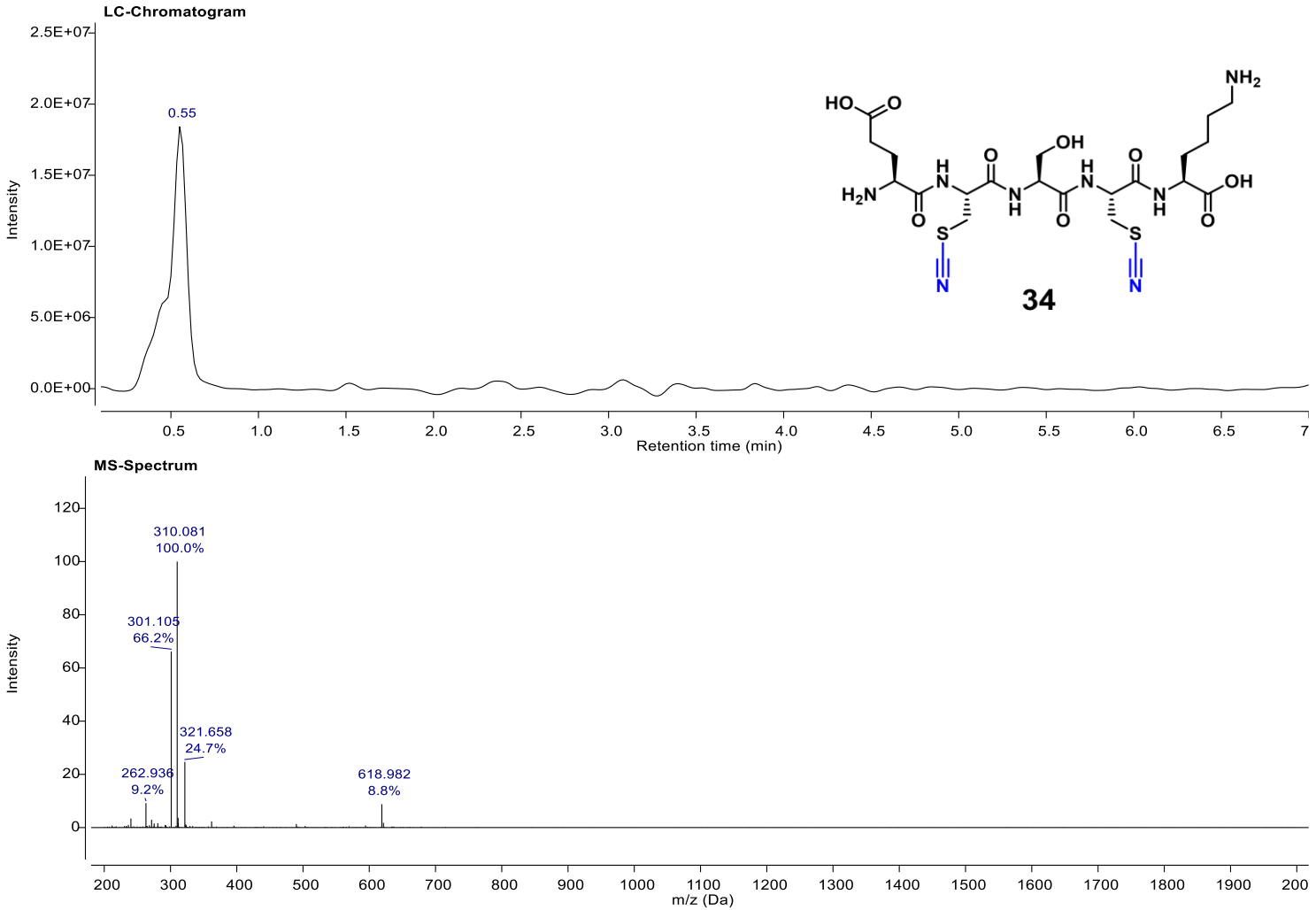

Figure A.83. LC-MS Spectrum of Compound 34 Gradient 5-60 for 7 Minutes

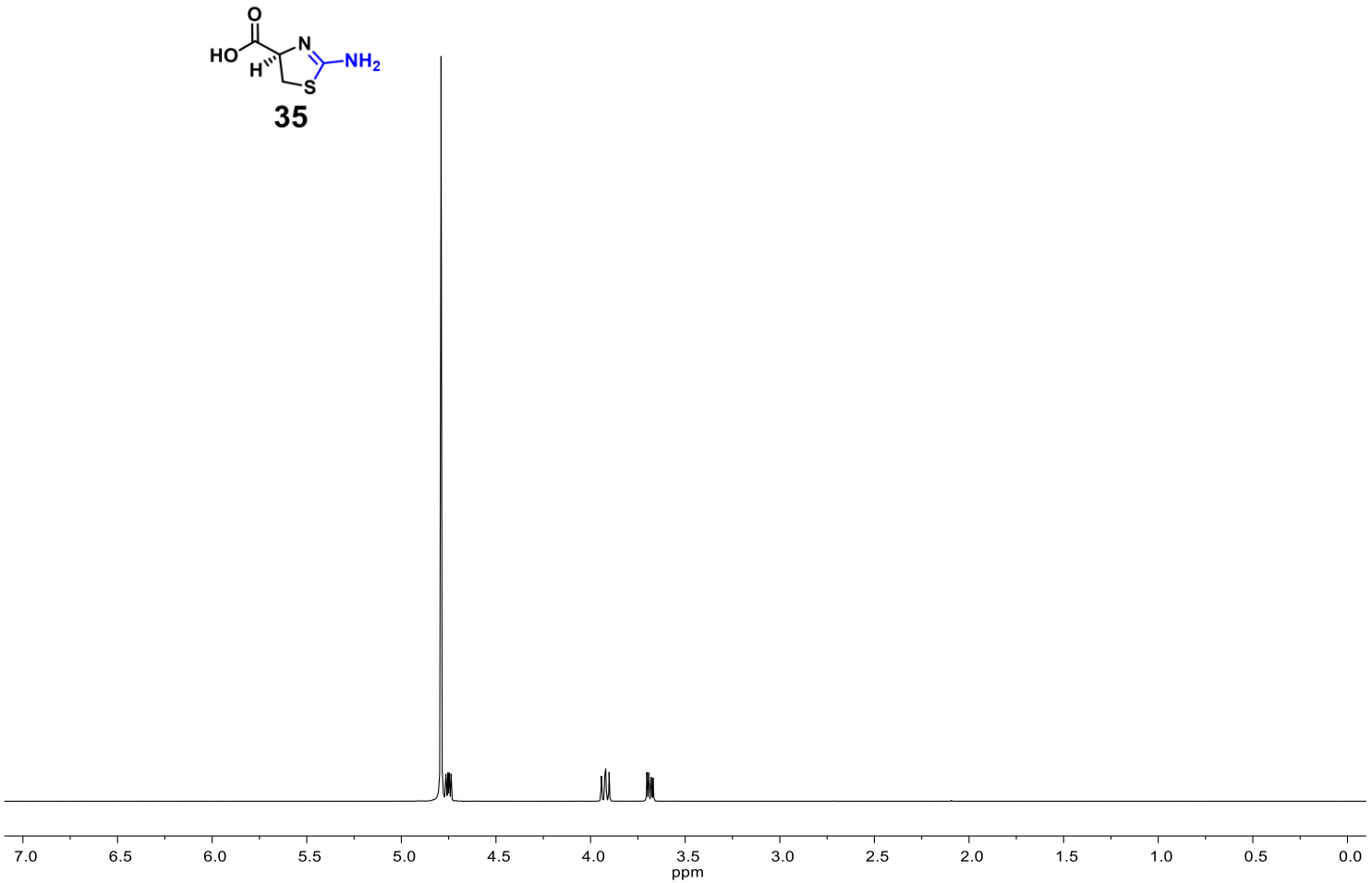

Figure A.84. 500 MHz ^{1}H-NMR Spectrum of Compound 35 in D_2O

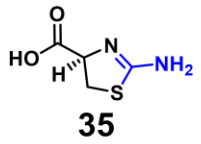

35

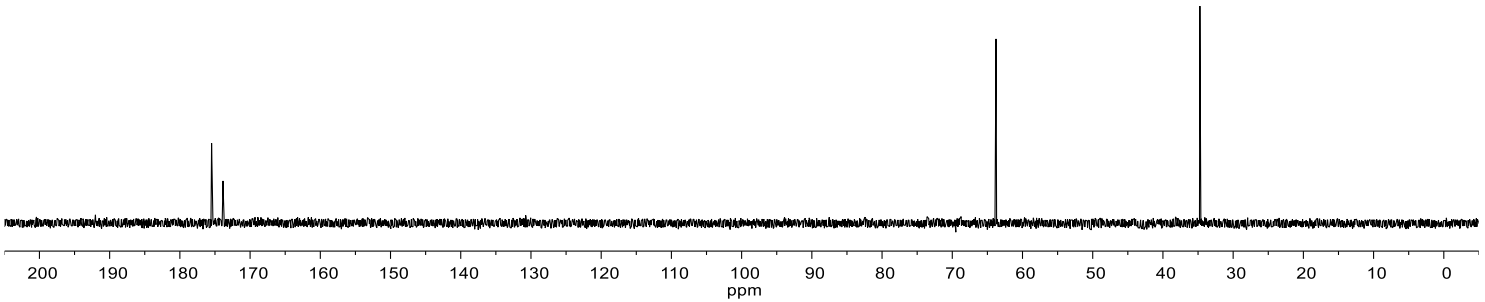

Figure A.85. 125 MHz ^{13}C-NMR Spectrum of Compound 35 in D_2O

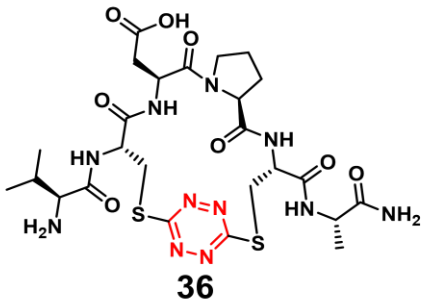

36

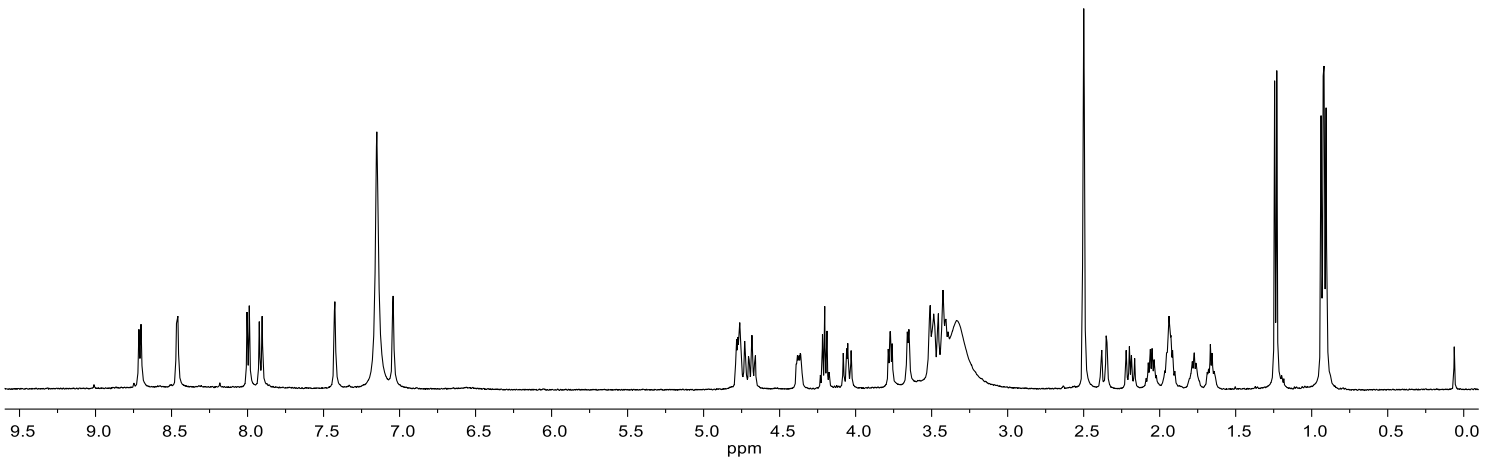

Figure A.86. 500 MHz ^{1}H-NMR Spectrum of Compound 36 in d_6-DMSO

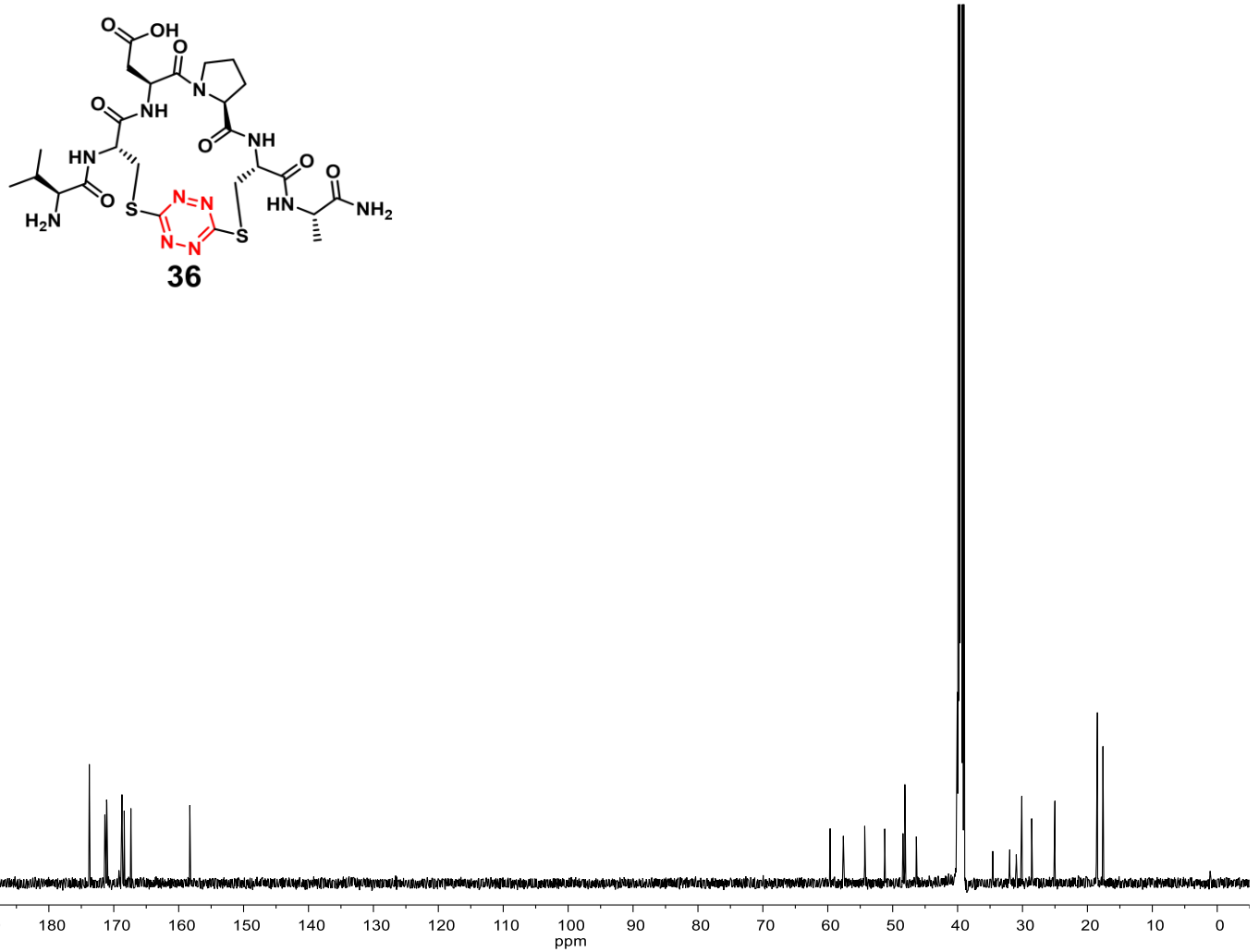

Figure A.87. 125 MHz ^{13}C-NMR Spectrum of Compound 36 in d_6-DMSO

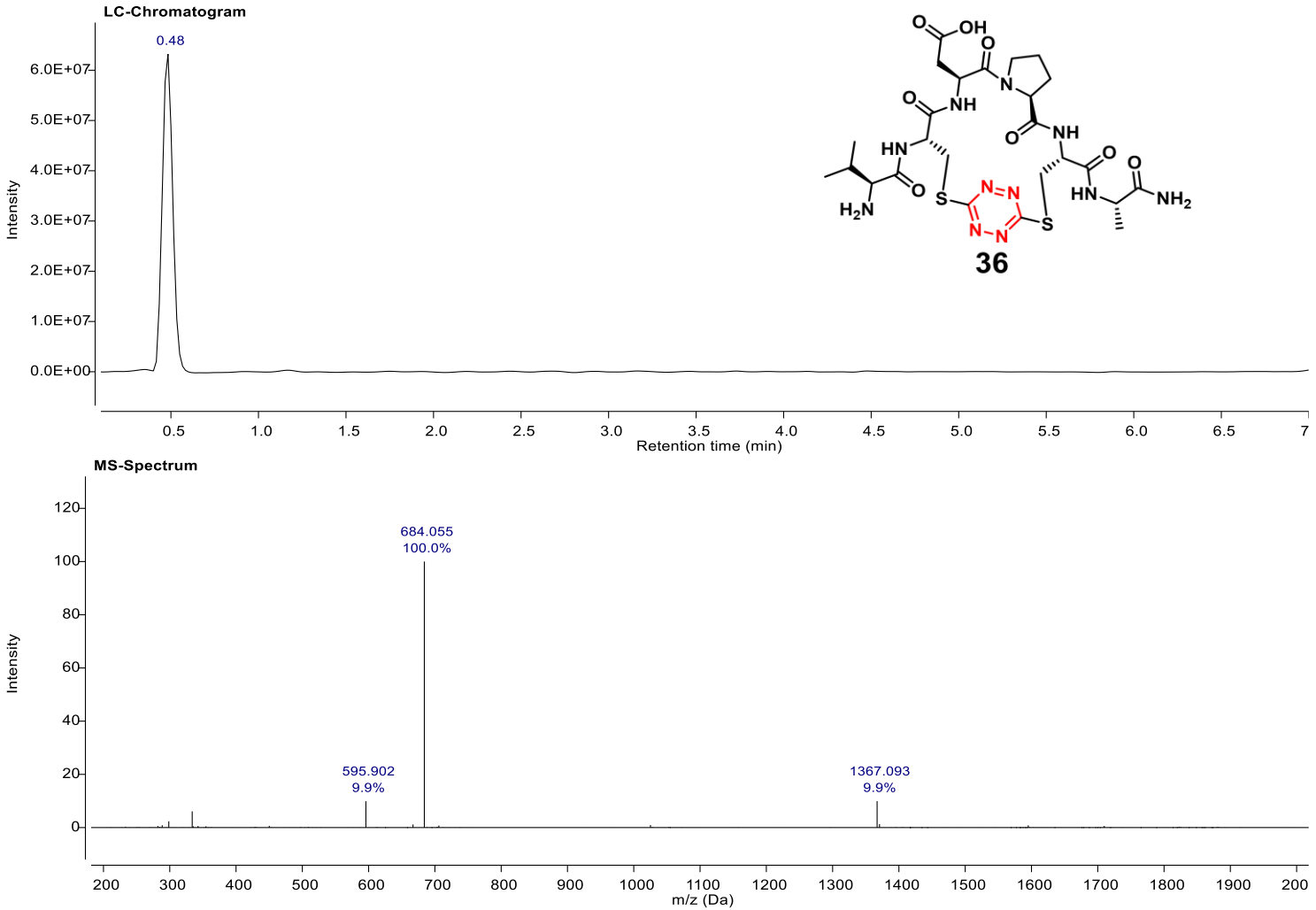

Figure A.88. LC-MS Spectrum of Compound 36 Gradient 5-60 for 7 Minutes

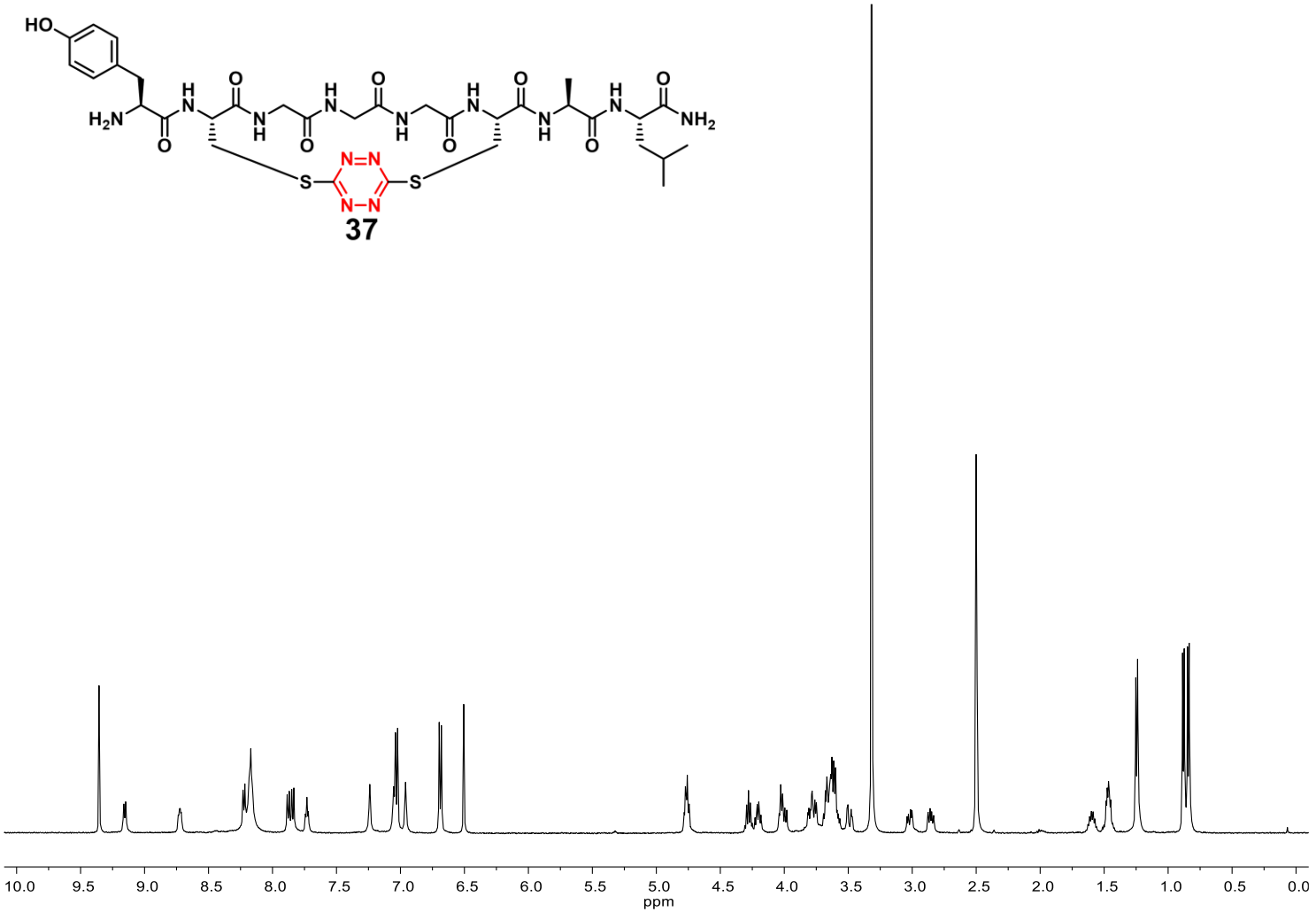

Figure A.89. 500 MHz ^{1}H-NMR Spectrum of Compound 37 in d_6-DMSO

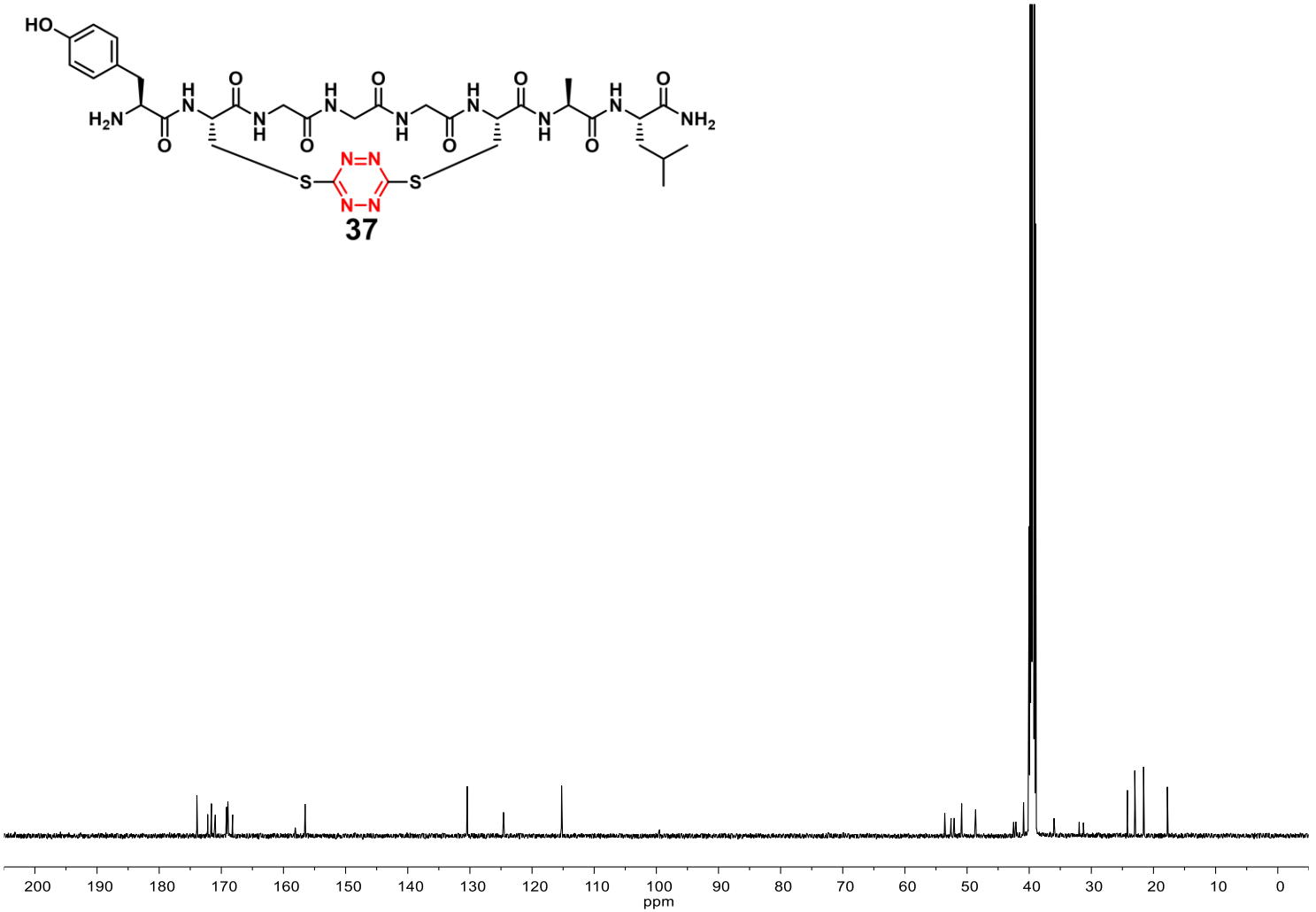

Figure A.90. 125 MHz ^{13}C-NMR Spectrum of Compound 37 in d_6-DMSO

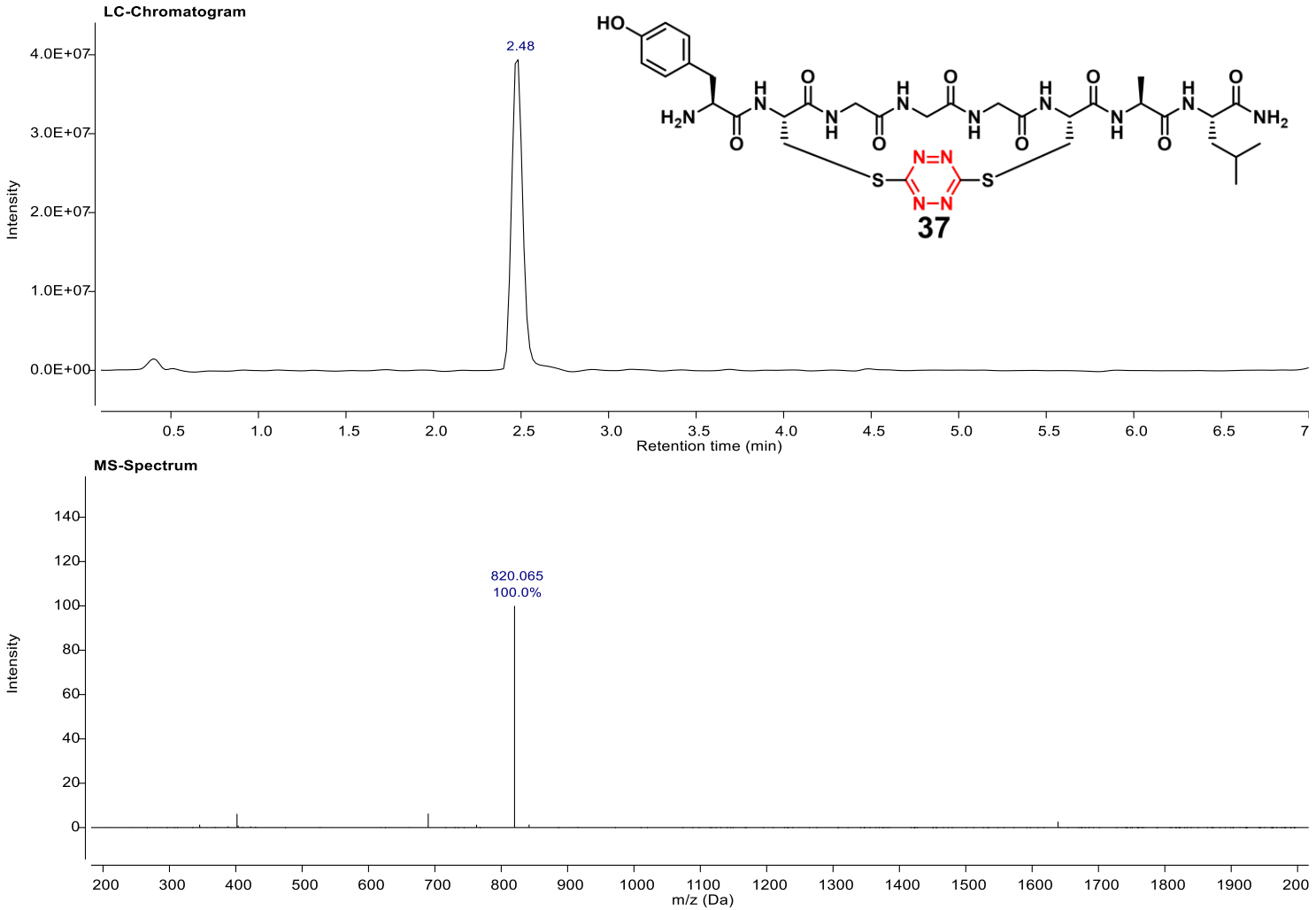

Figure A.91. LC-MS Spectrum of Compound 37 Gradient 5-60 for 7 Minutes

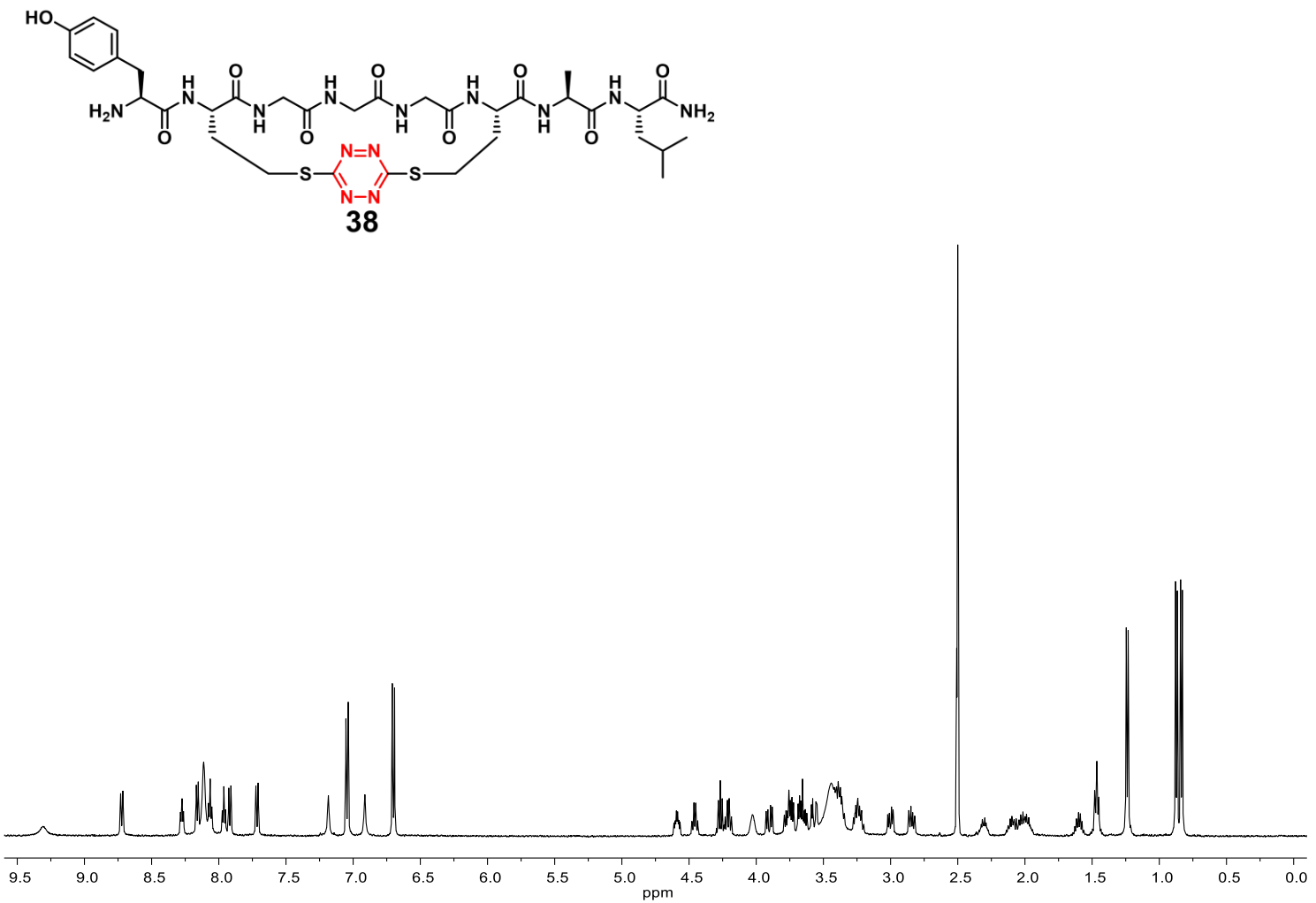

Figure A.92. 500 MHz ^{1}H-NMR Spectrum of Compound 38 in d_6-DMSO

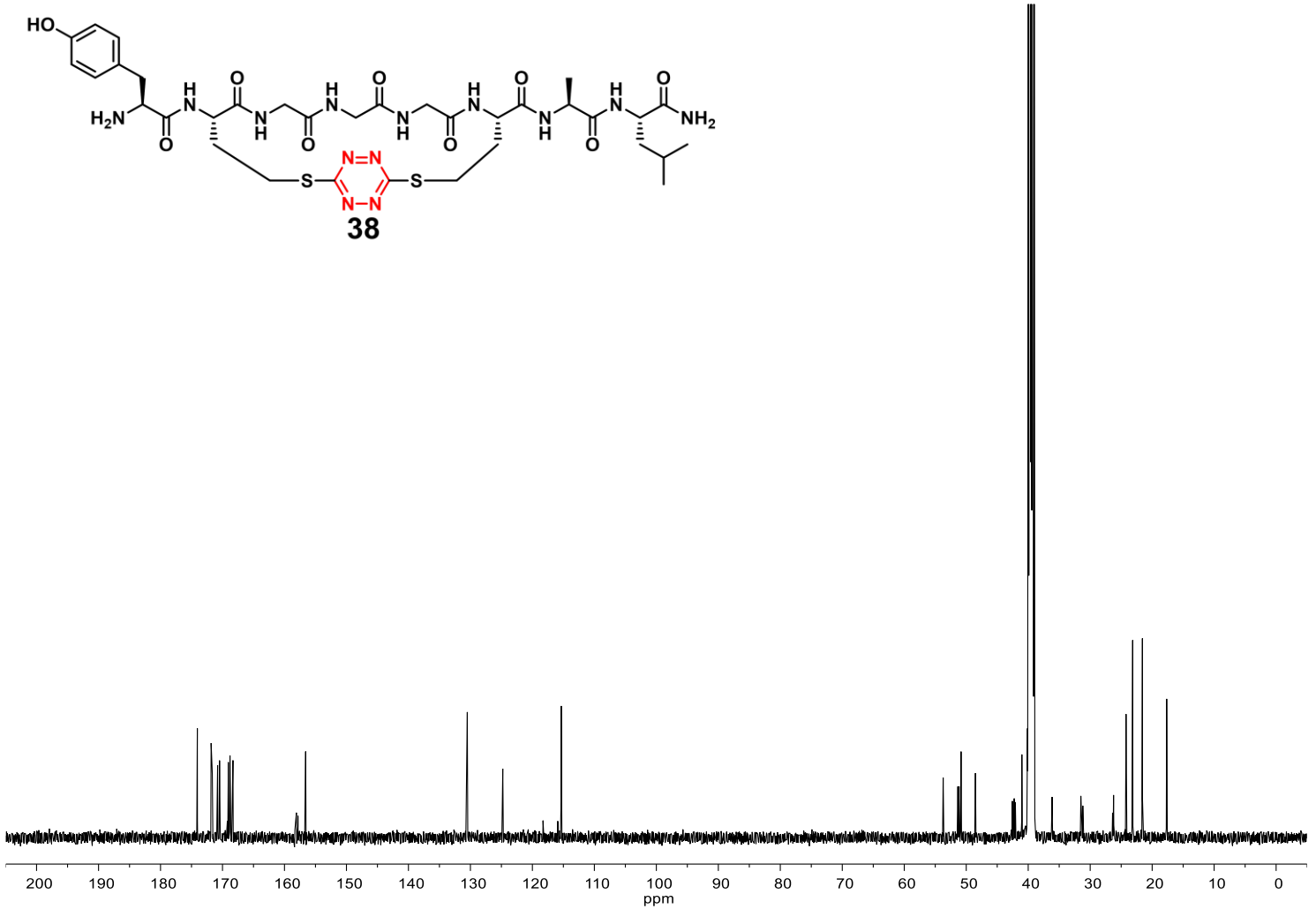

Figure A.93. 125 MHz ^{13}C-NMR Spectrum of Compound 38 in d_6-DMSO

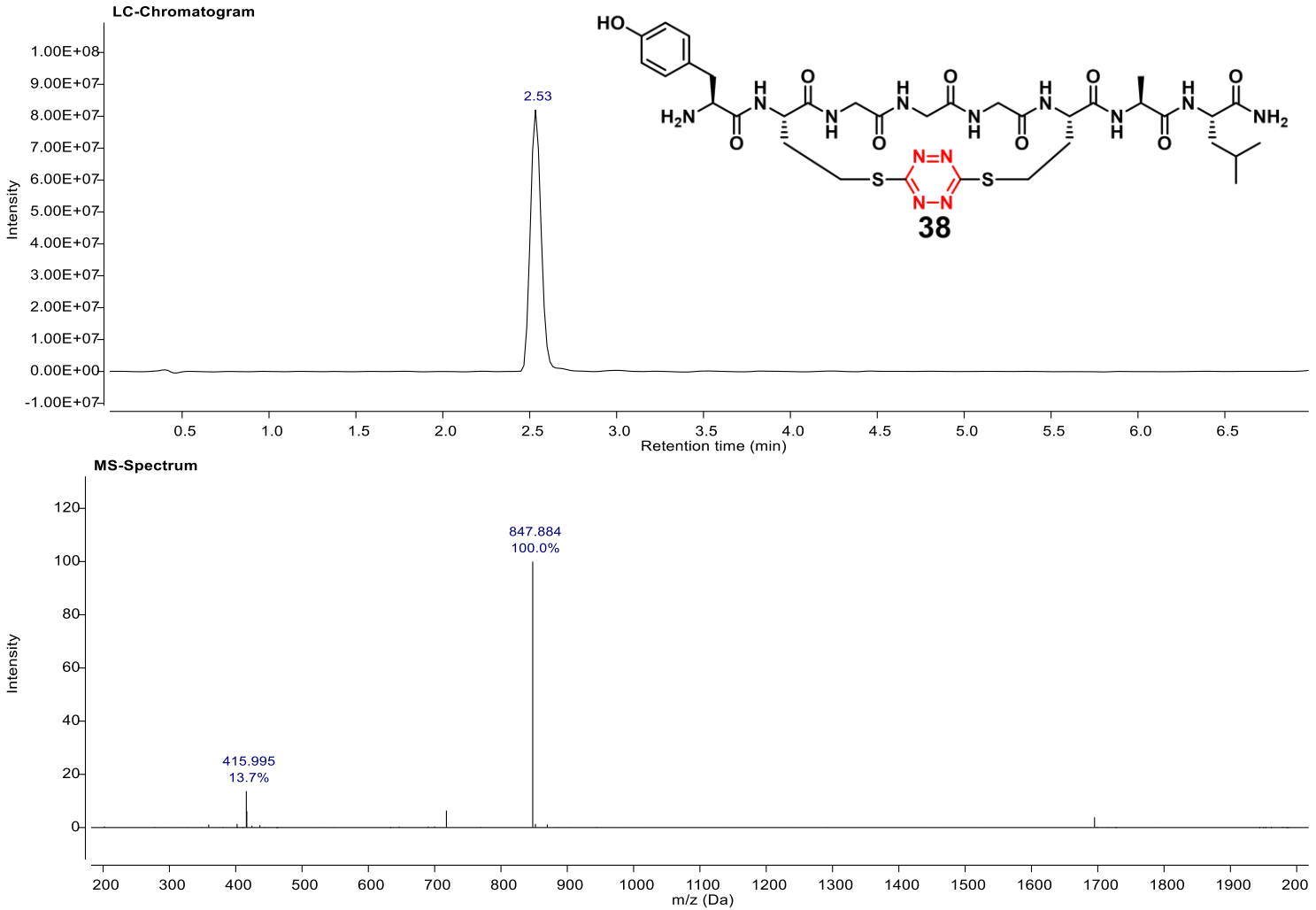

Figure A.94. LC-MS Spectrum of Compound 38 Gradient 5-60 for 7 Minutes

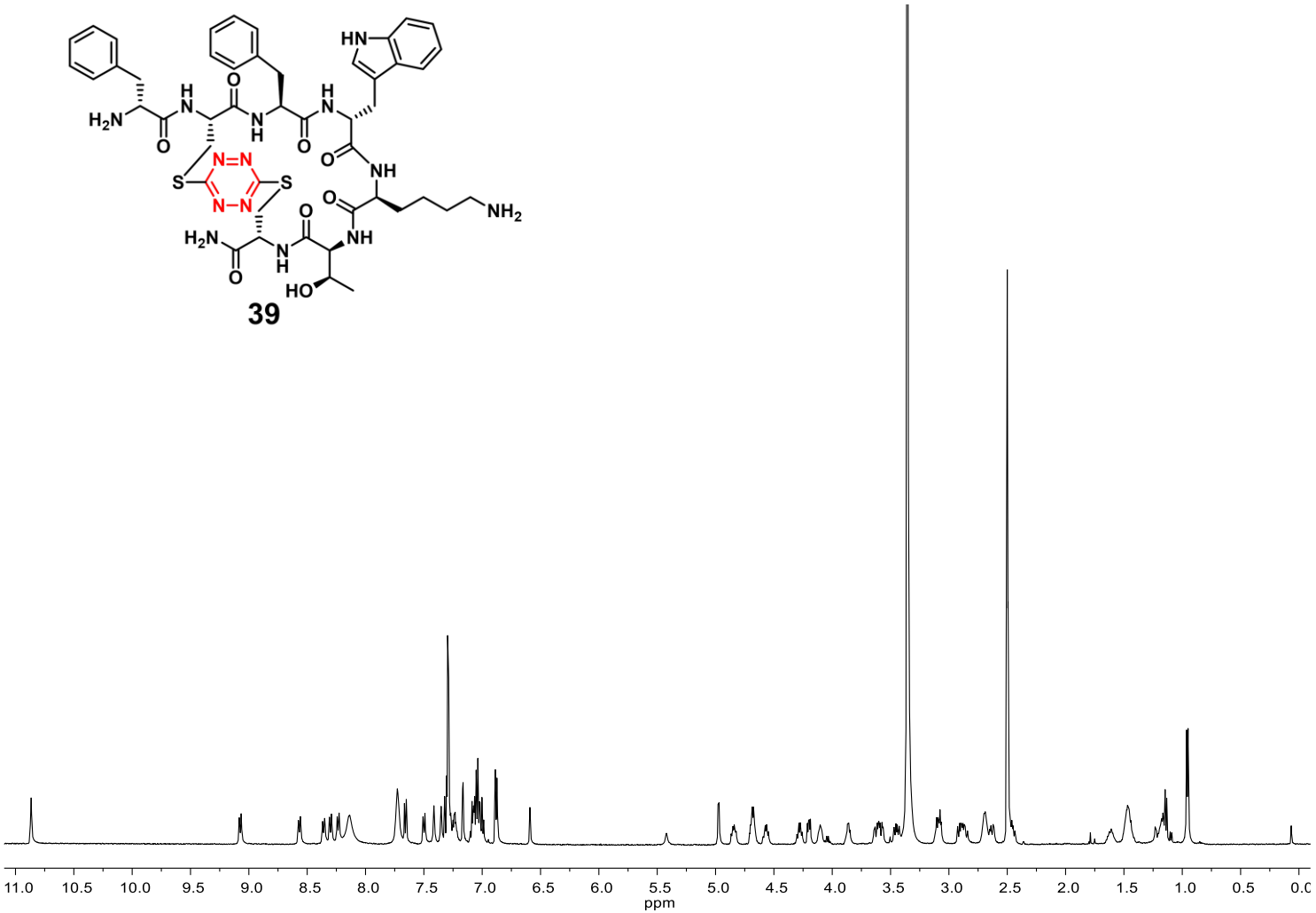

Figure A.95. 500 MHz ^{1}H-NMR Spectrum of Compound 39 in d_6-DMSO

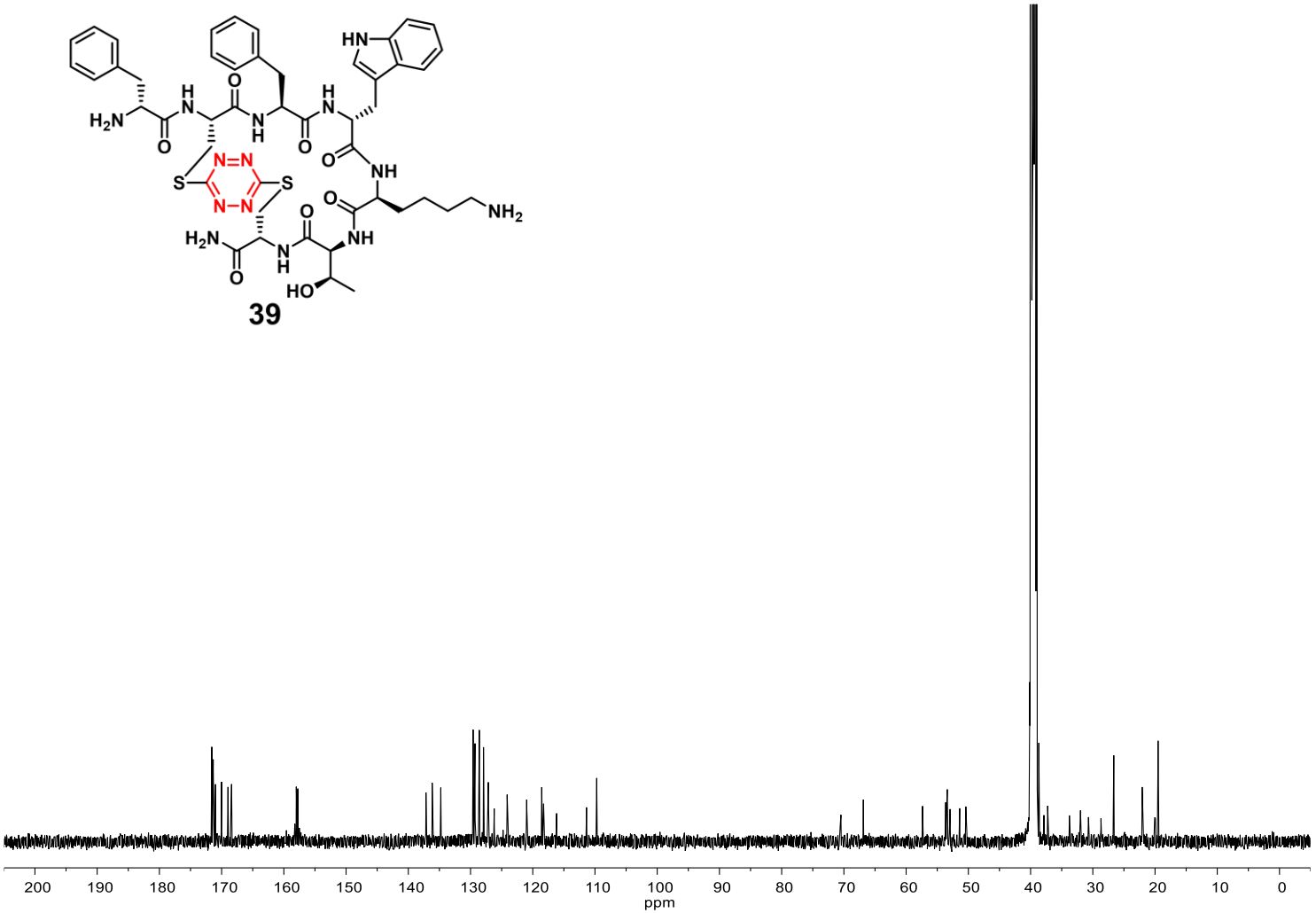

Figure A.96. 125 MHz ^{13}C-NMR Spectrum of Compound 39 in d_6-DMSO

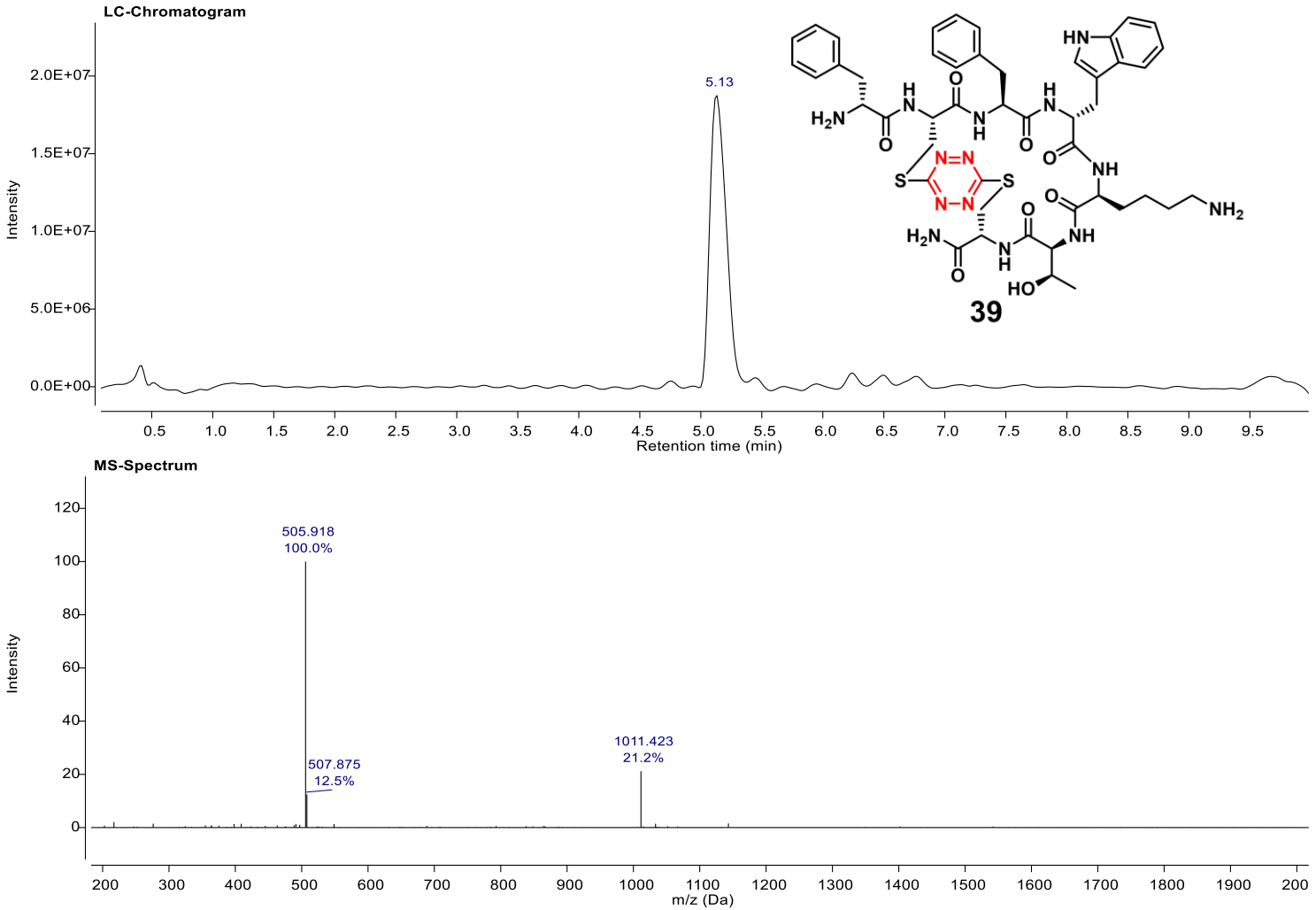

Figure A.97. LC-MS Spectrum of Compound 39 Gradient 5-60 for 10 Minutes

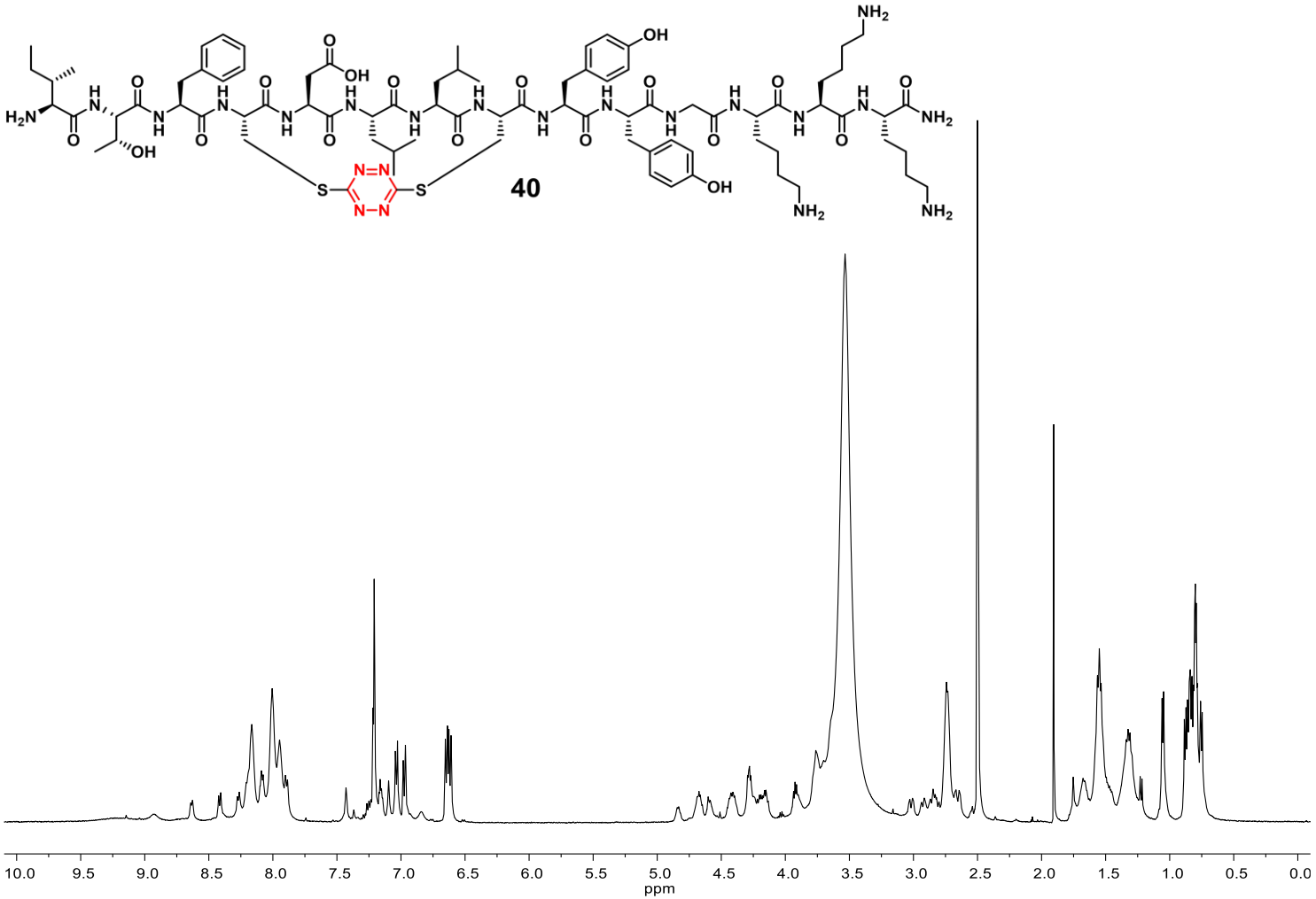

Figure A.98. 500 MHz ^{1}H-NMR Spectrum of Compound 40 in d_6-DMSO

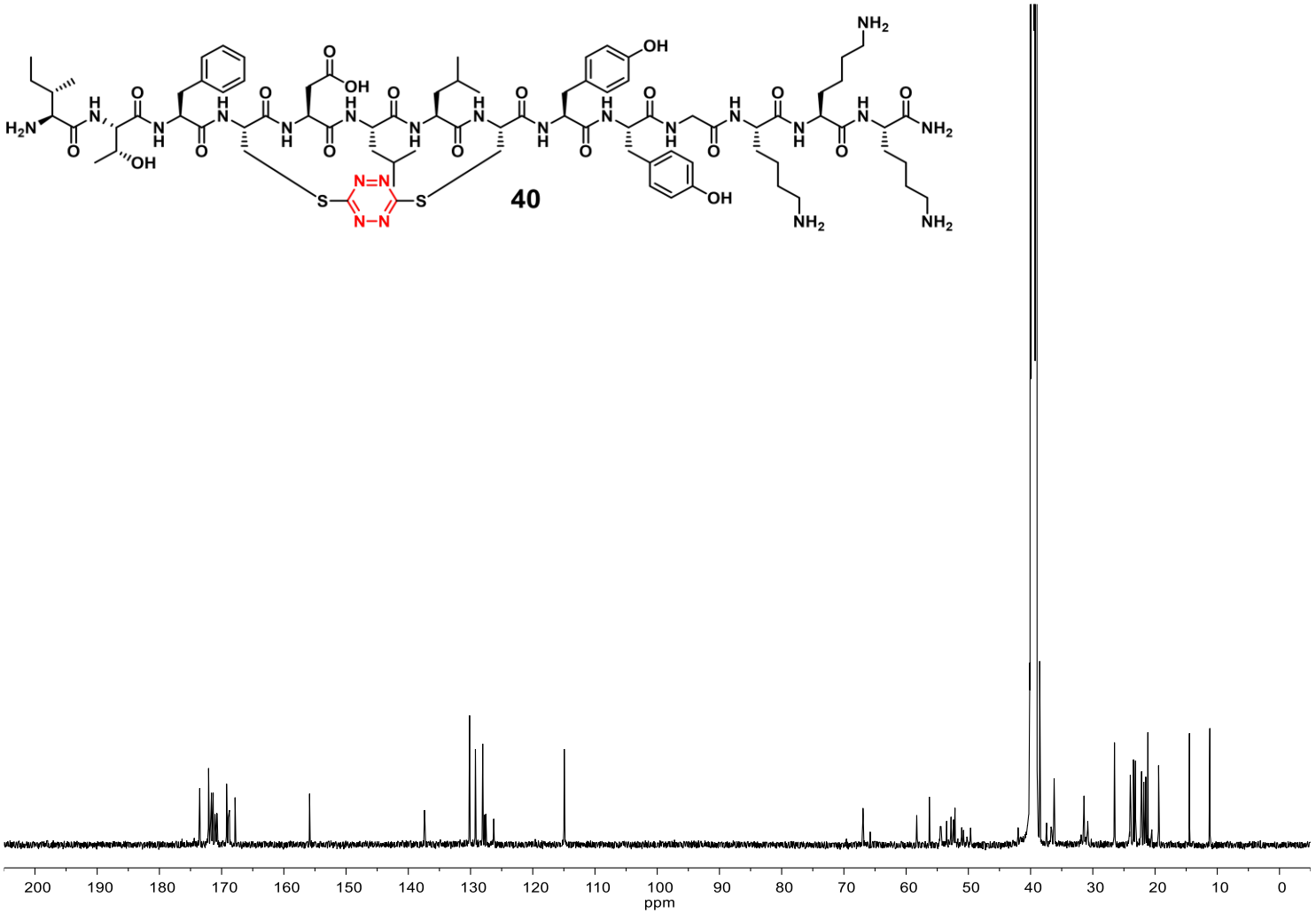

Figure A.99. 125 MHz ^{13}C-NMR Spectrum of Compound 40 in d_6-DMSO

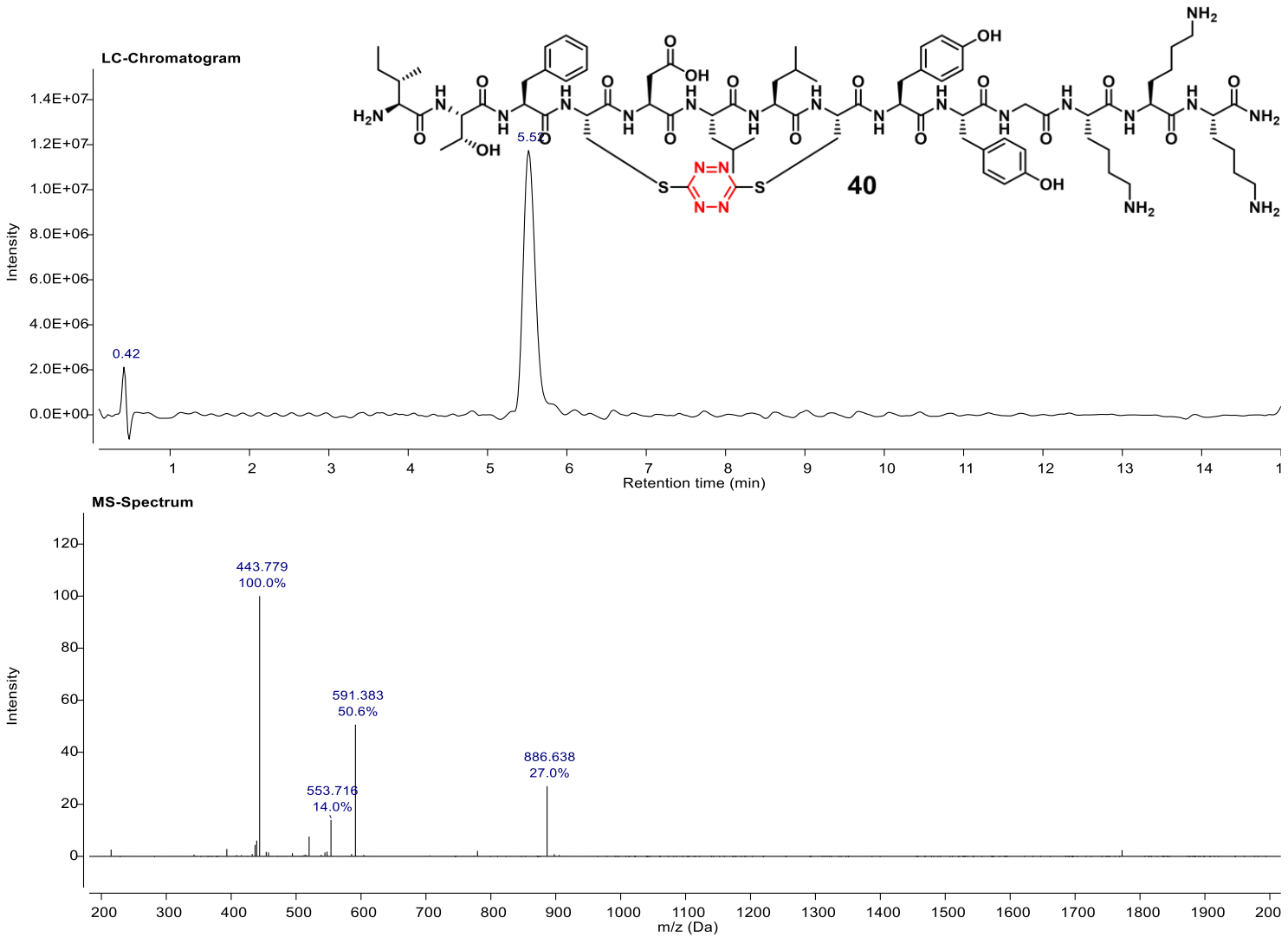

Figure A.100. LC-MS Spectrum of Compound 40 Gradient 5-60 for 15 Minutes

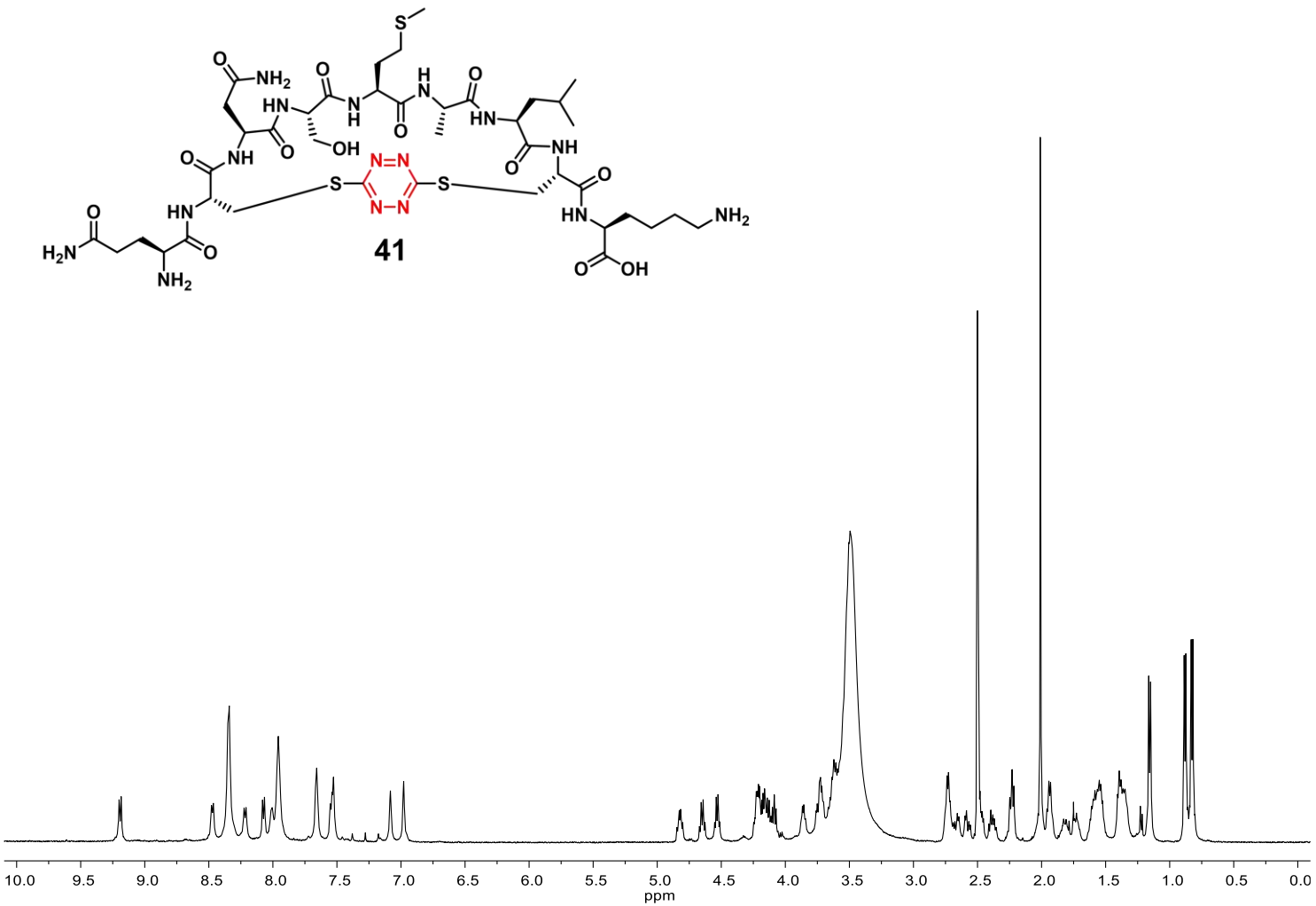

Figure A.101. 500 MHz ^{1}H-NMR Spectrum of Compound 41 in d_6-DMSO

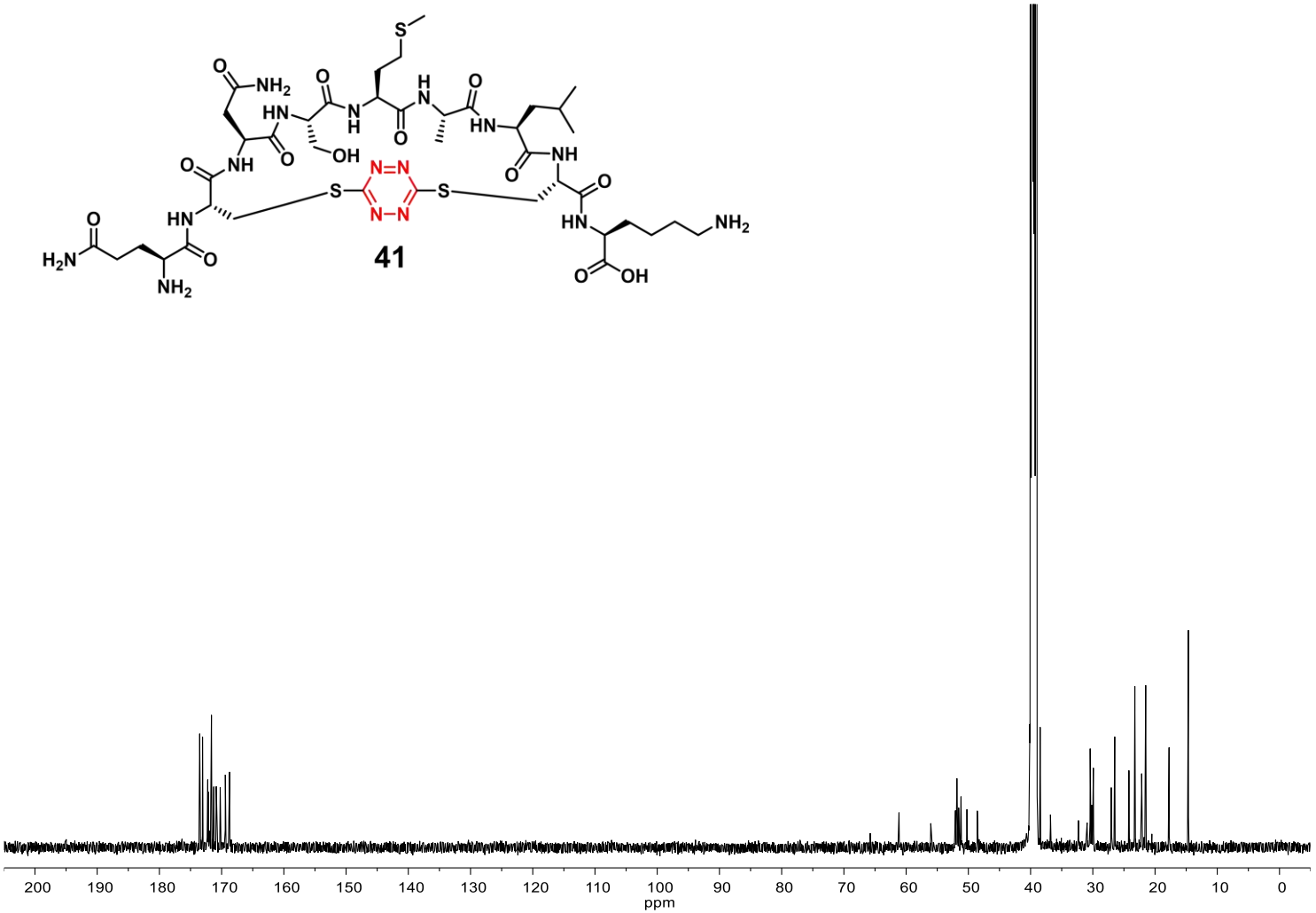

Figure A.102. 125 MHz ^{13}C-NMR Spectrum of Compound 41 in d_6-DMSO

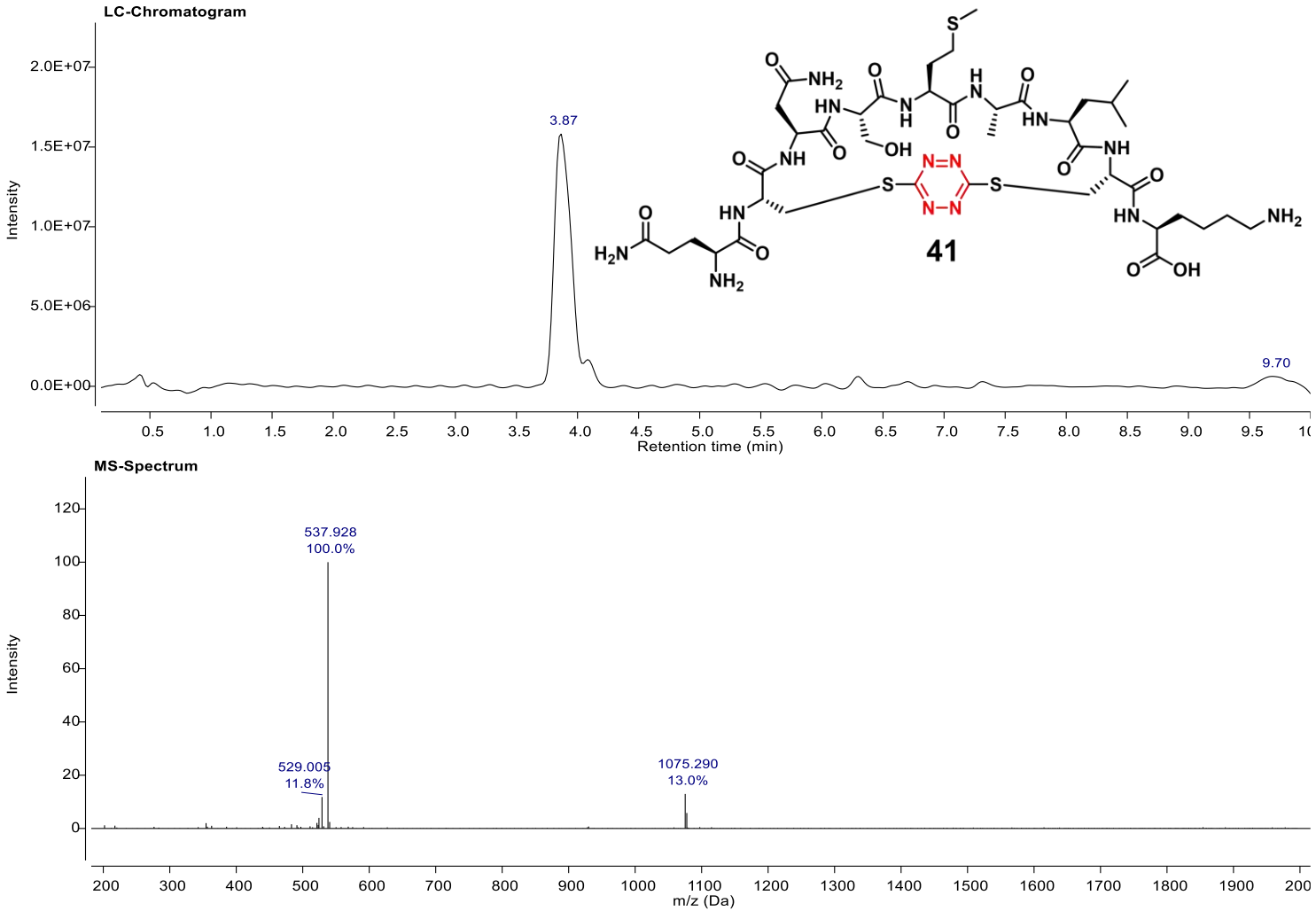

Figure A.103. LC-MS Spectrum of Compound 41 Gradient 5-60 for 10 Minutes

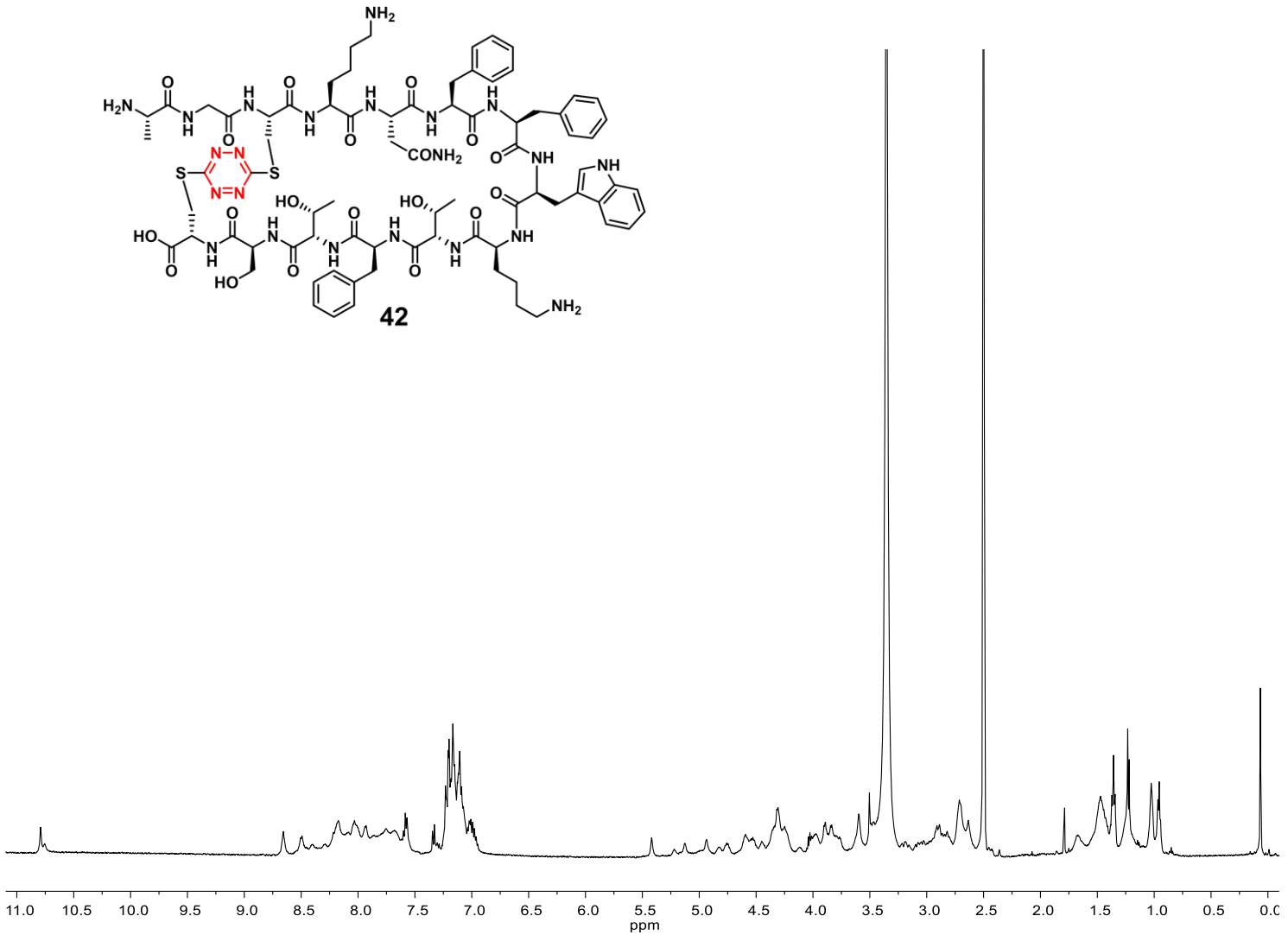

Figure A.104. 500 MHz ^{1}H-NMR Spectrum of Compound 42 in d_6-DMSO

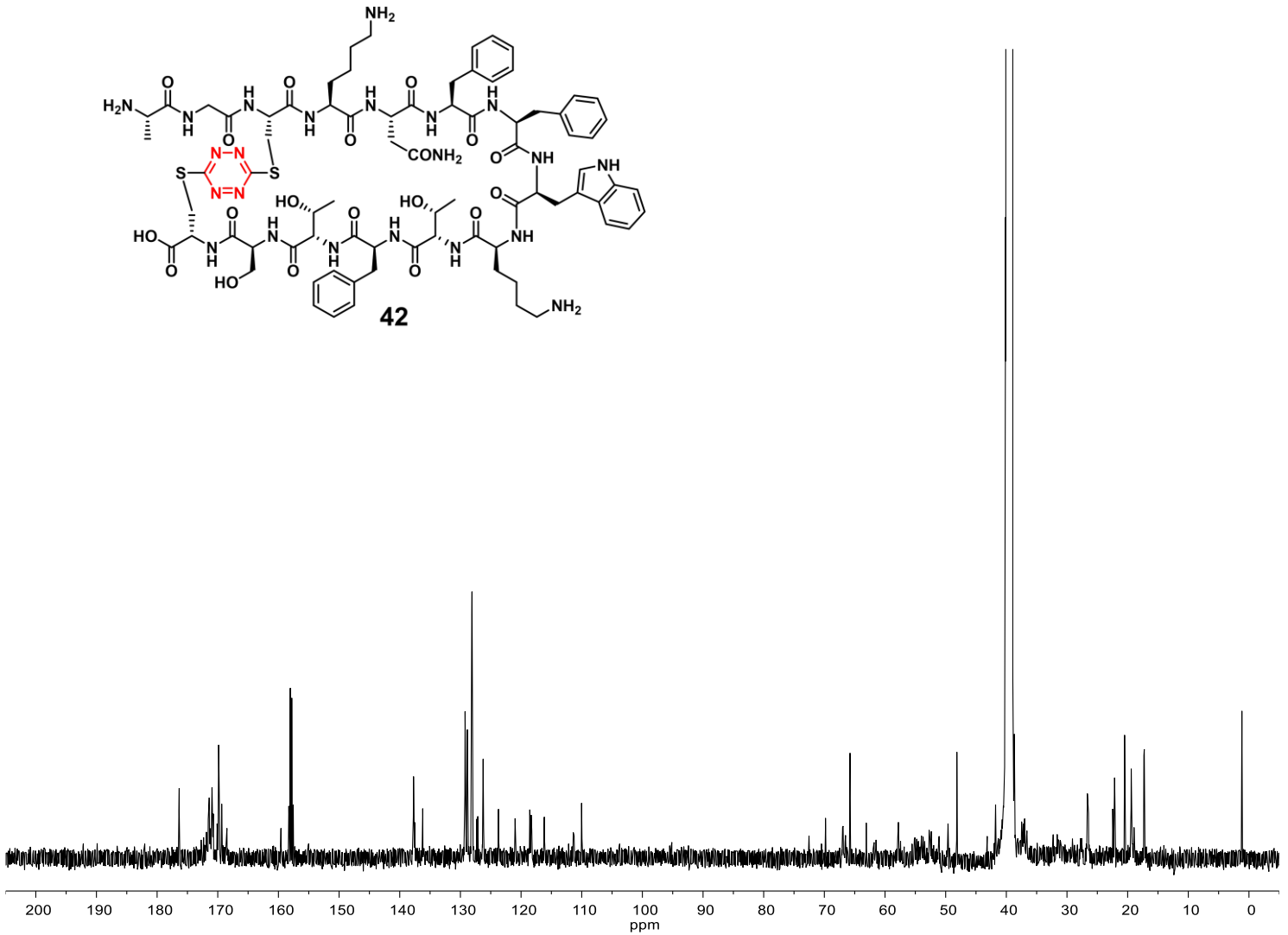

Figure A.105. 125 MHz ^{13}C-NMR Spectrum of Compound 42 in d_6-DMSO

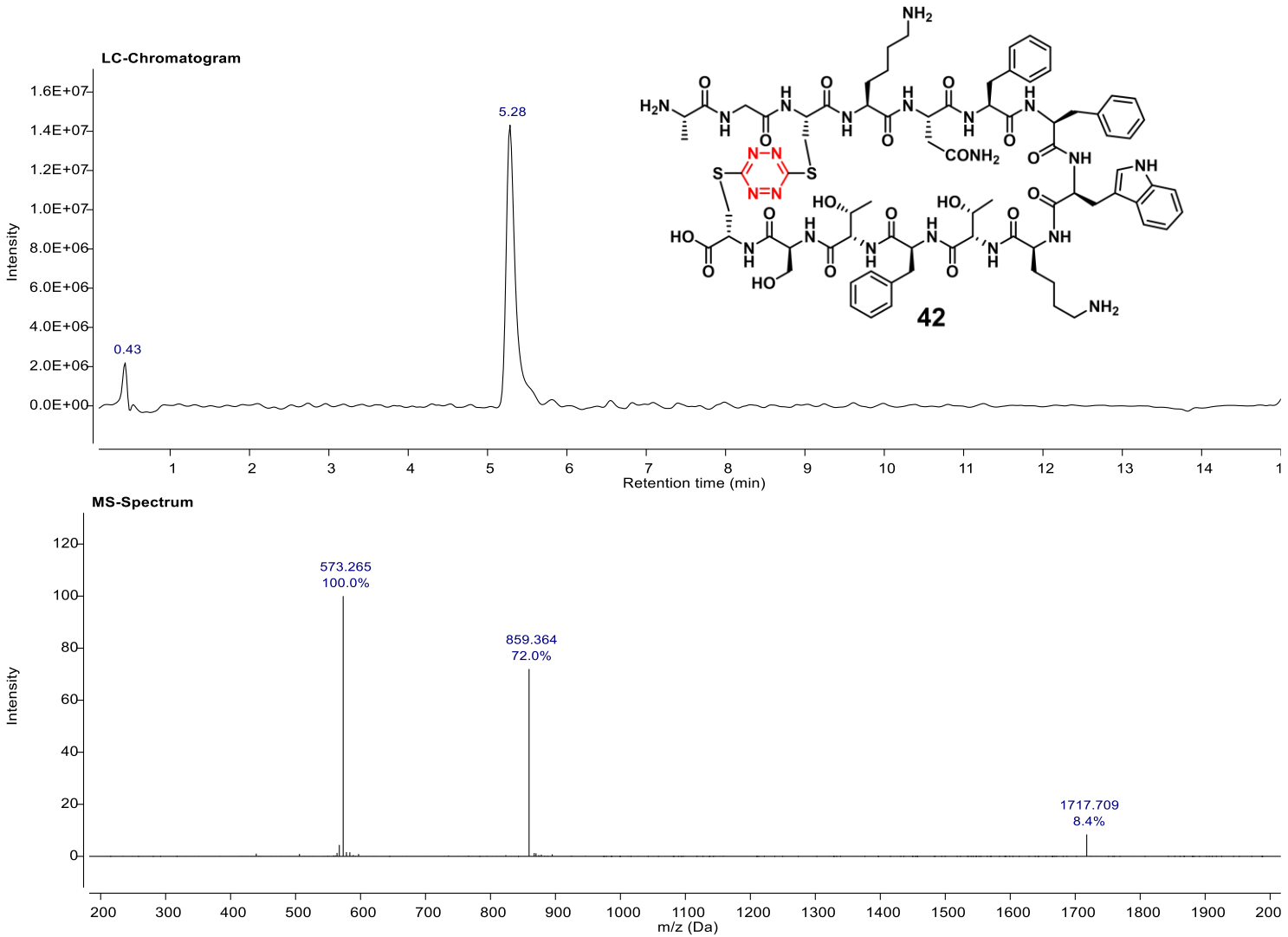

Figure A.106. LC-MS Spectrum of Compound 42 Gradient 5-60 for 15 Minutes

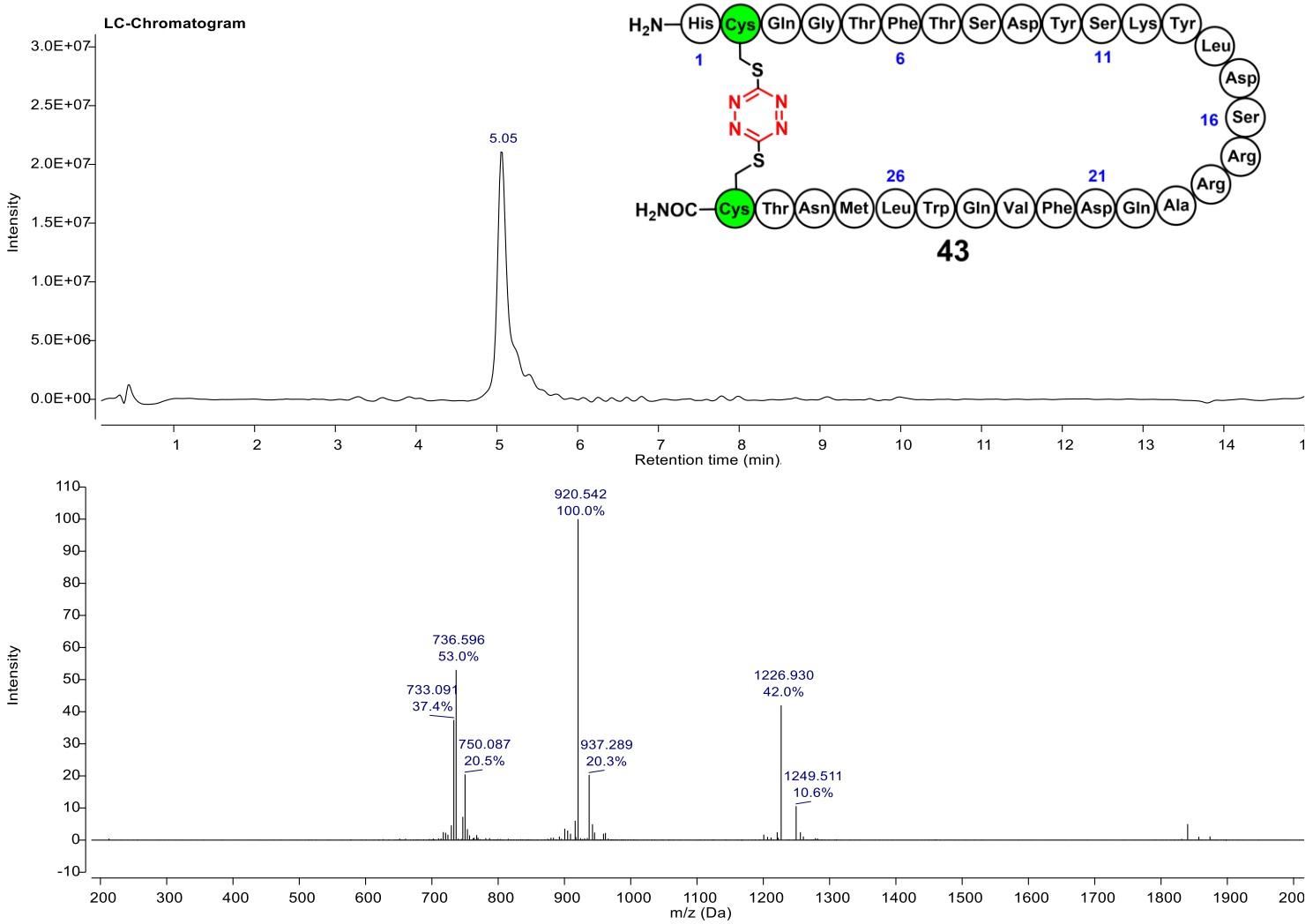

Figure A.107. LC-MS Spectrum of Compound 43 Gradient 5-60 for 15 Minutes

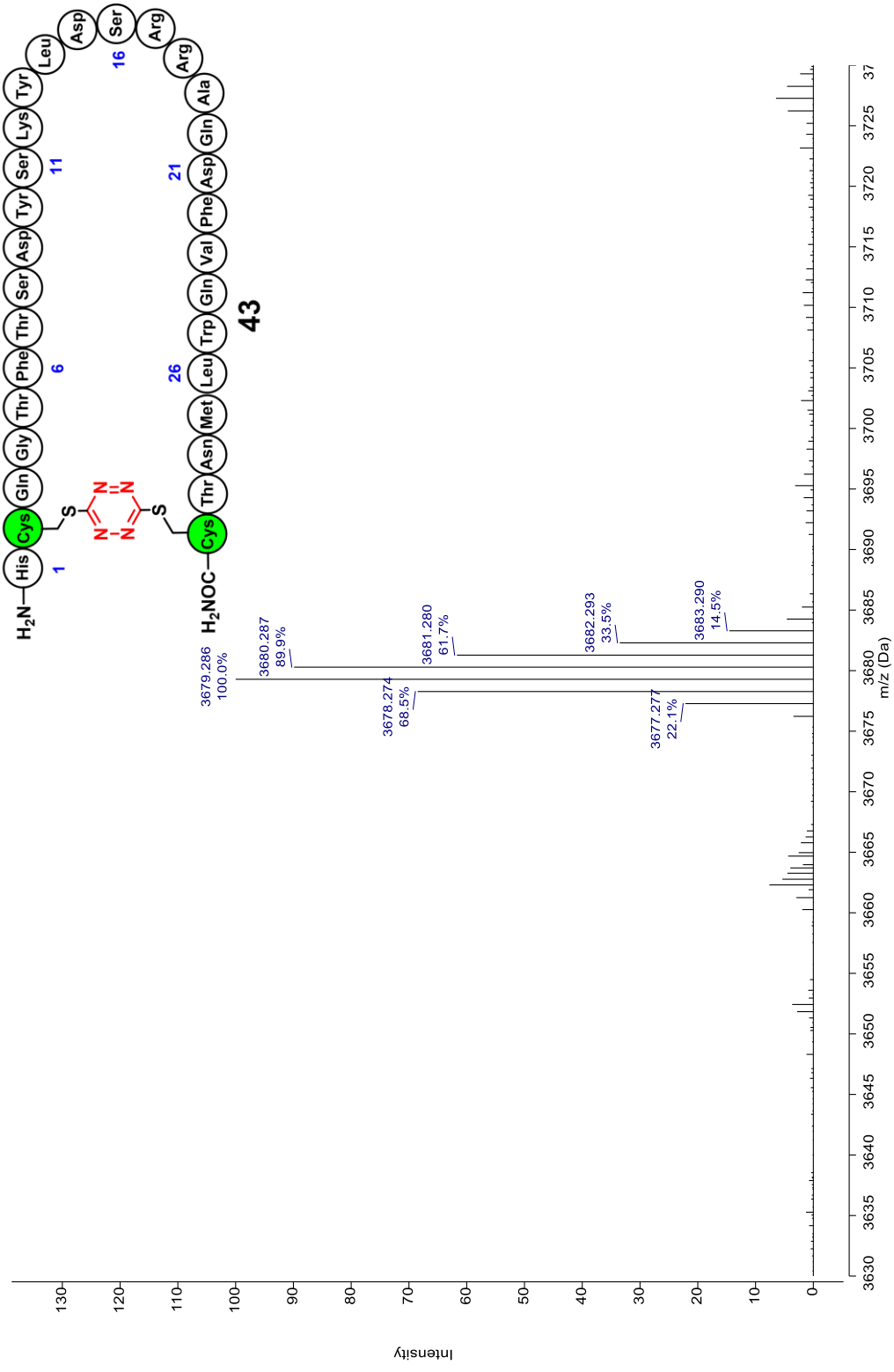

Figure A.108. MALDI-TOF-MS Spectrum of Compound 43

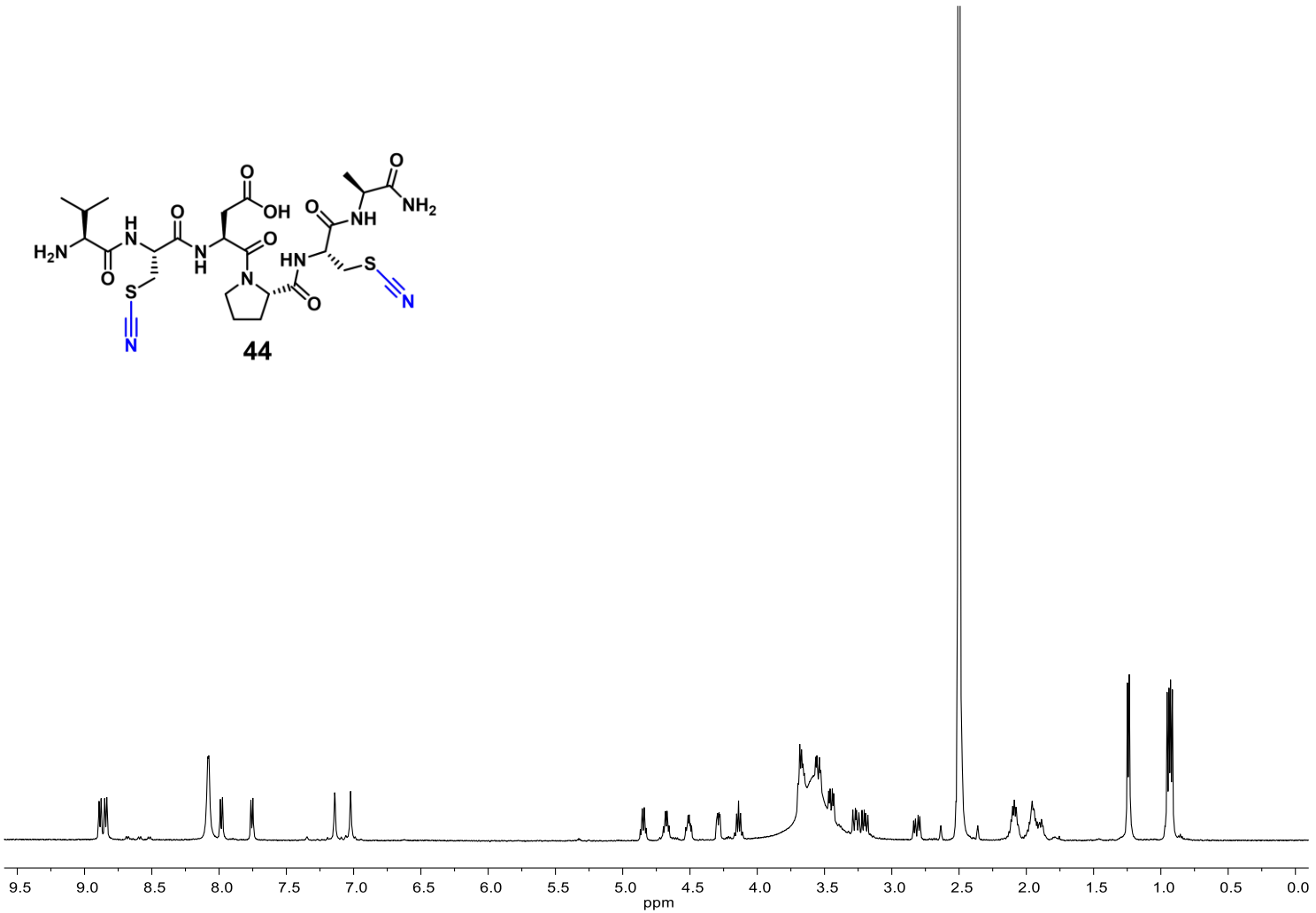

Figure A.109. 500 MHz ^{1}H-NMR Spectrum of Compound 44 in d_6-DMSO

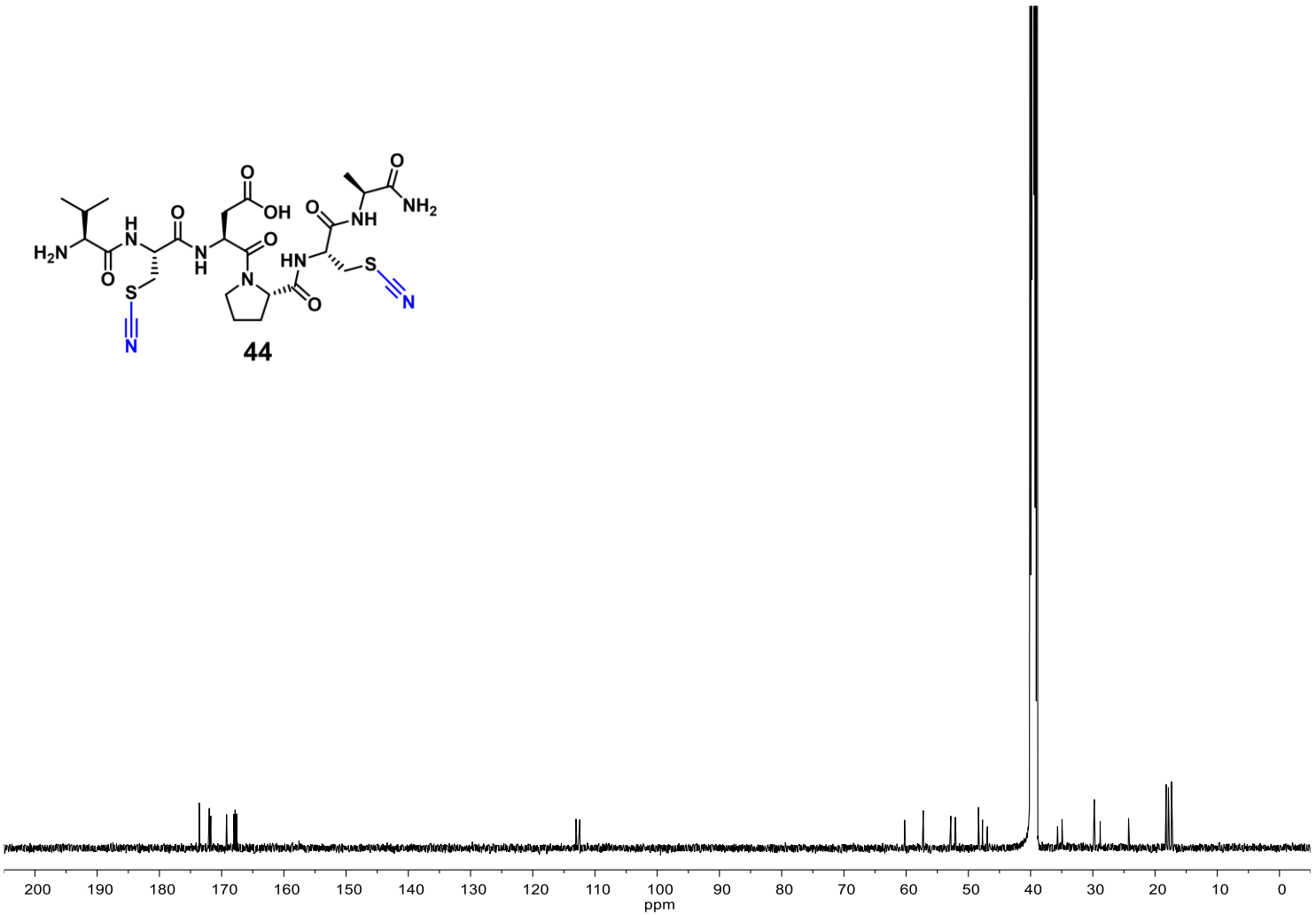

Figure A.110. 125 MHz ^{13}C-NMR Spectrum of Compound 44 in d_6-DMSO

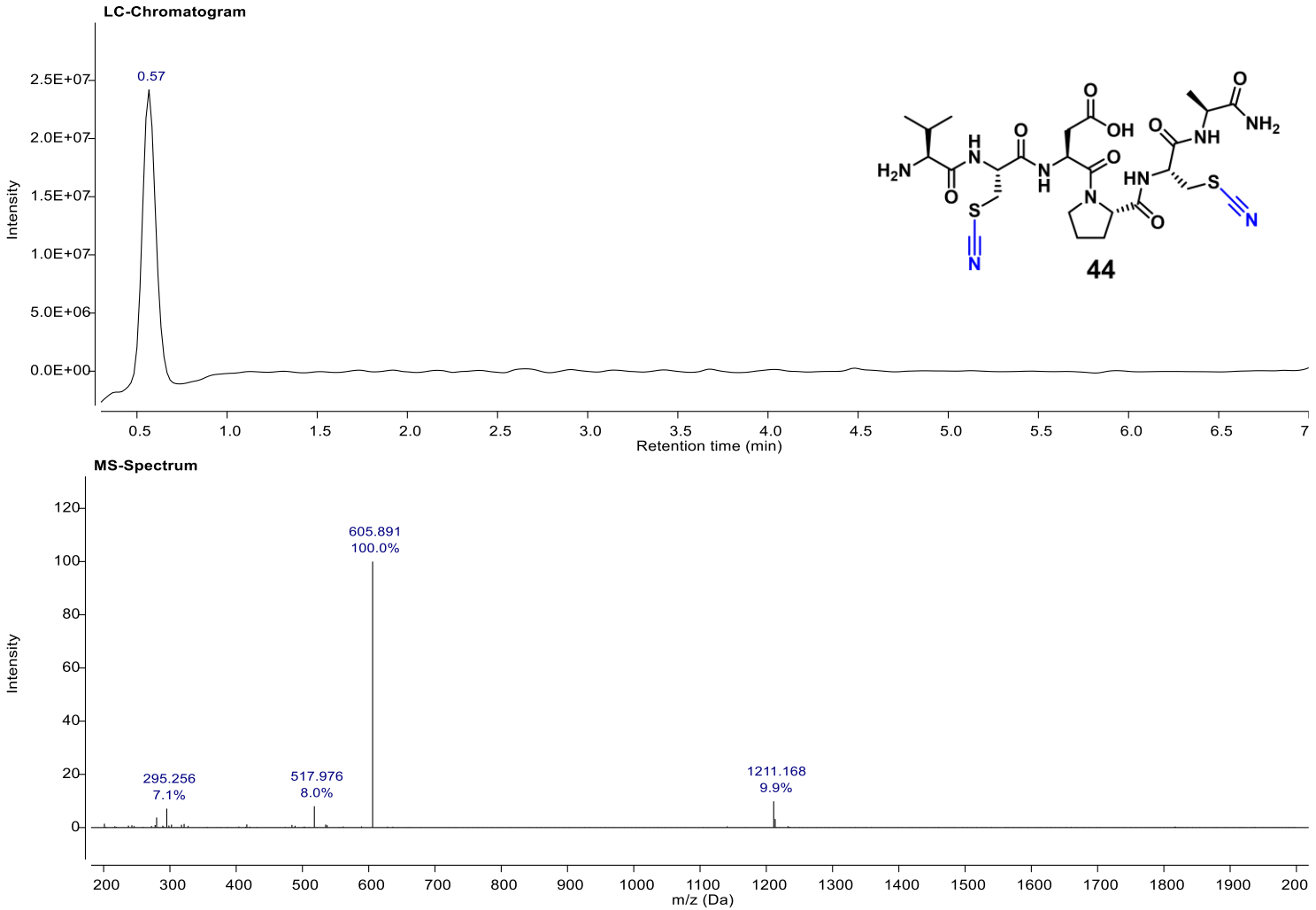

Figure A.111. LC-MS Spectrum of Compound 44 Gradient 5-60 for 7 Minutes

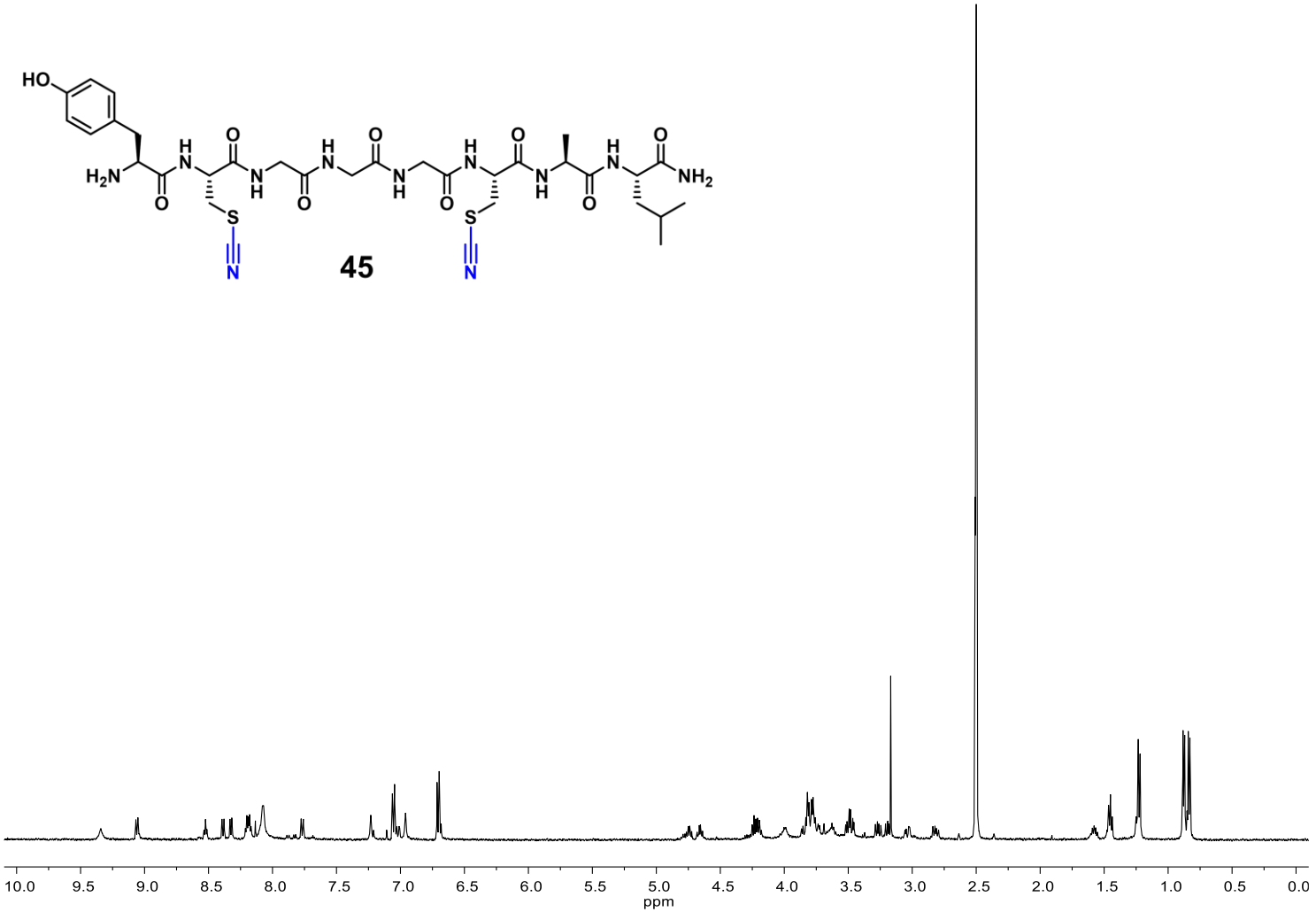

Figure A.112. 500 MHz ^{1}H-NMR Spectrum of Compound 45 in d_6-DMSO

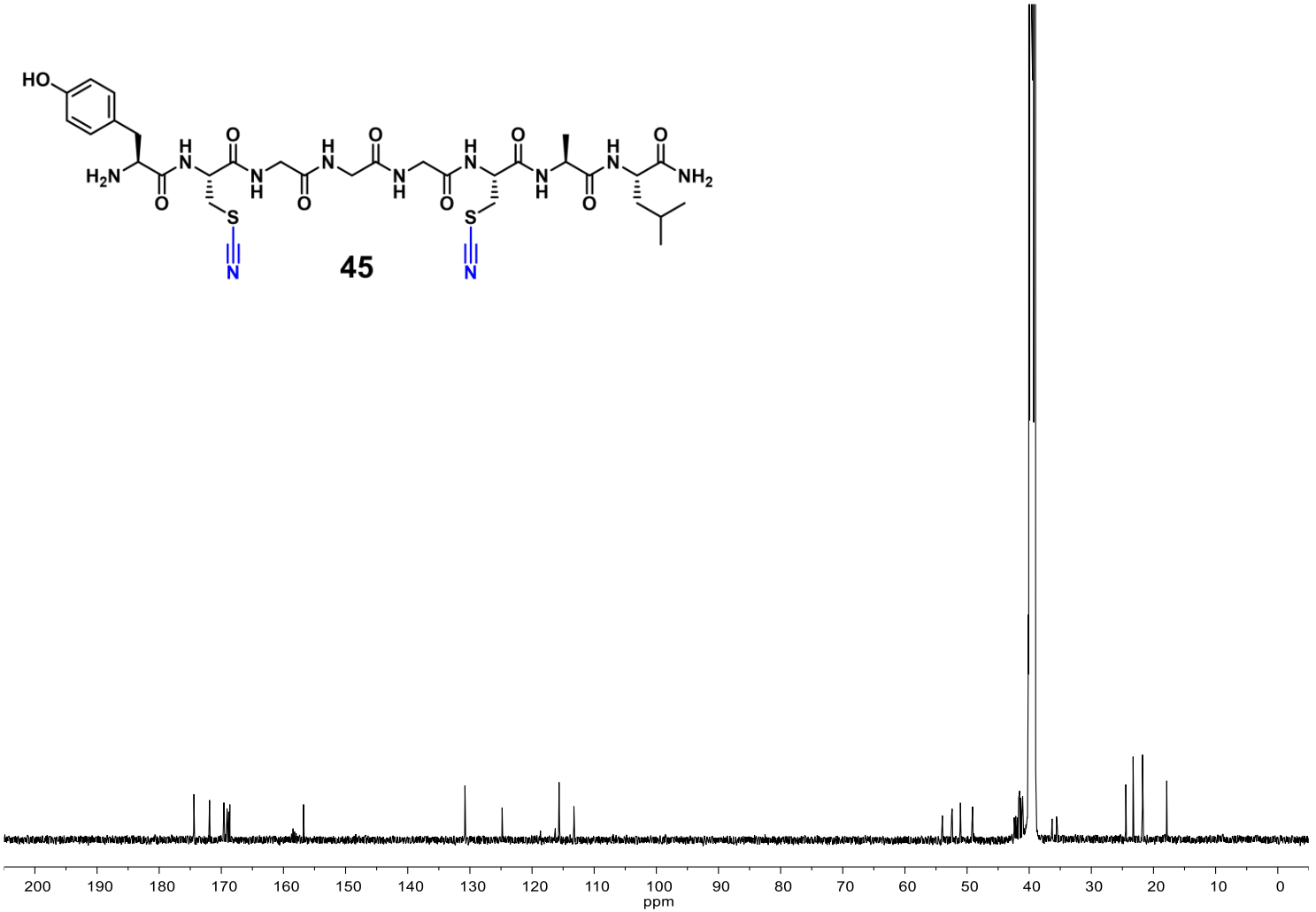

Figure A.113. 125 MHz ^{13}C-NMR Spectrum of Compound 45 in d_6-DMSO

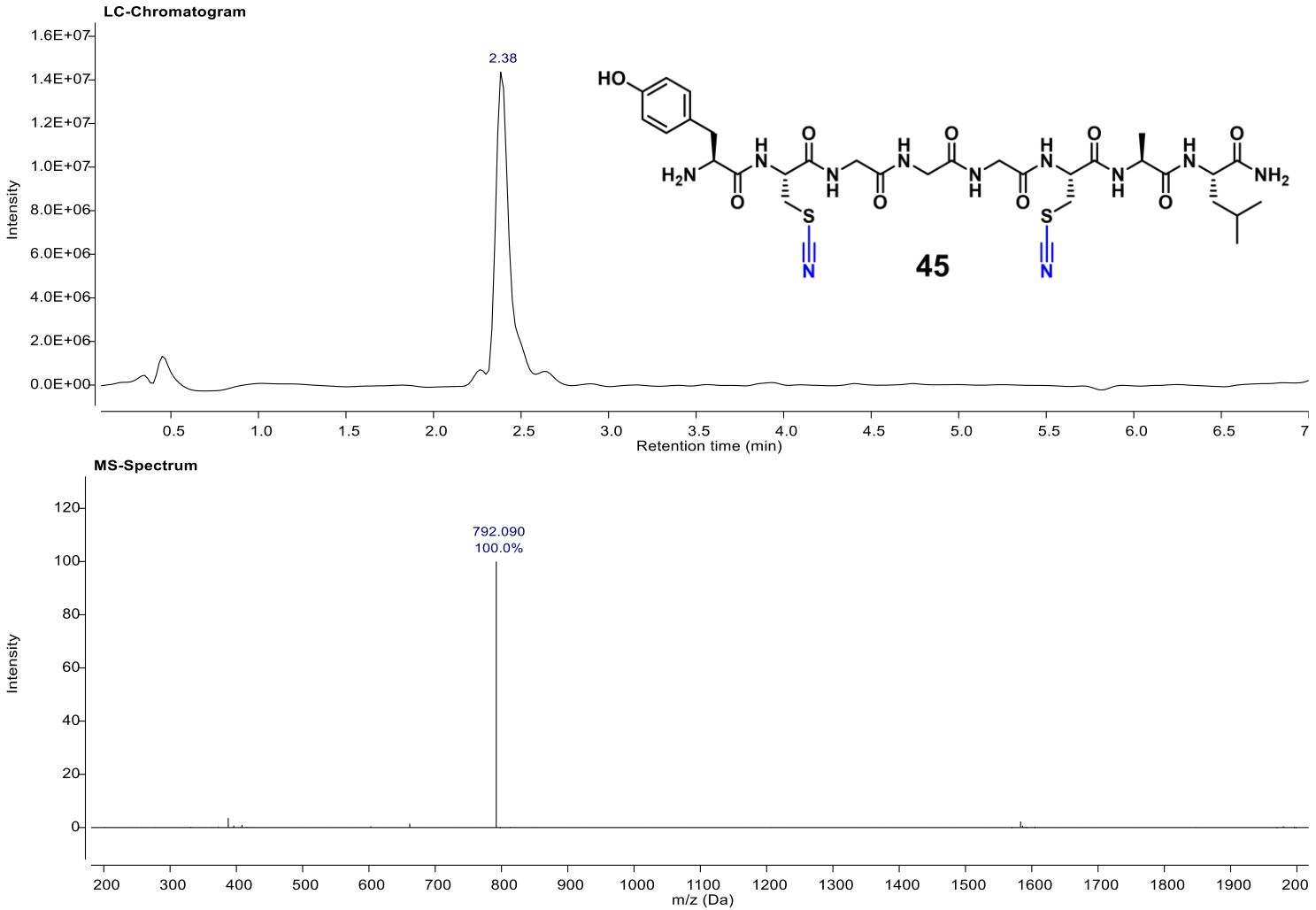

Figure A.114. LC-MS Spectrum of Compound 45 Gradient 5-60 for 7 Minutes

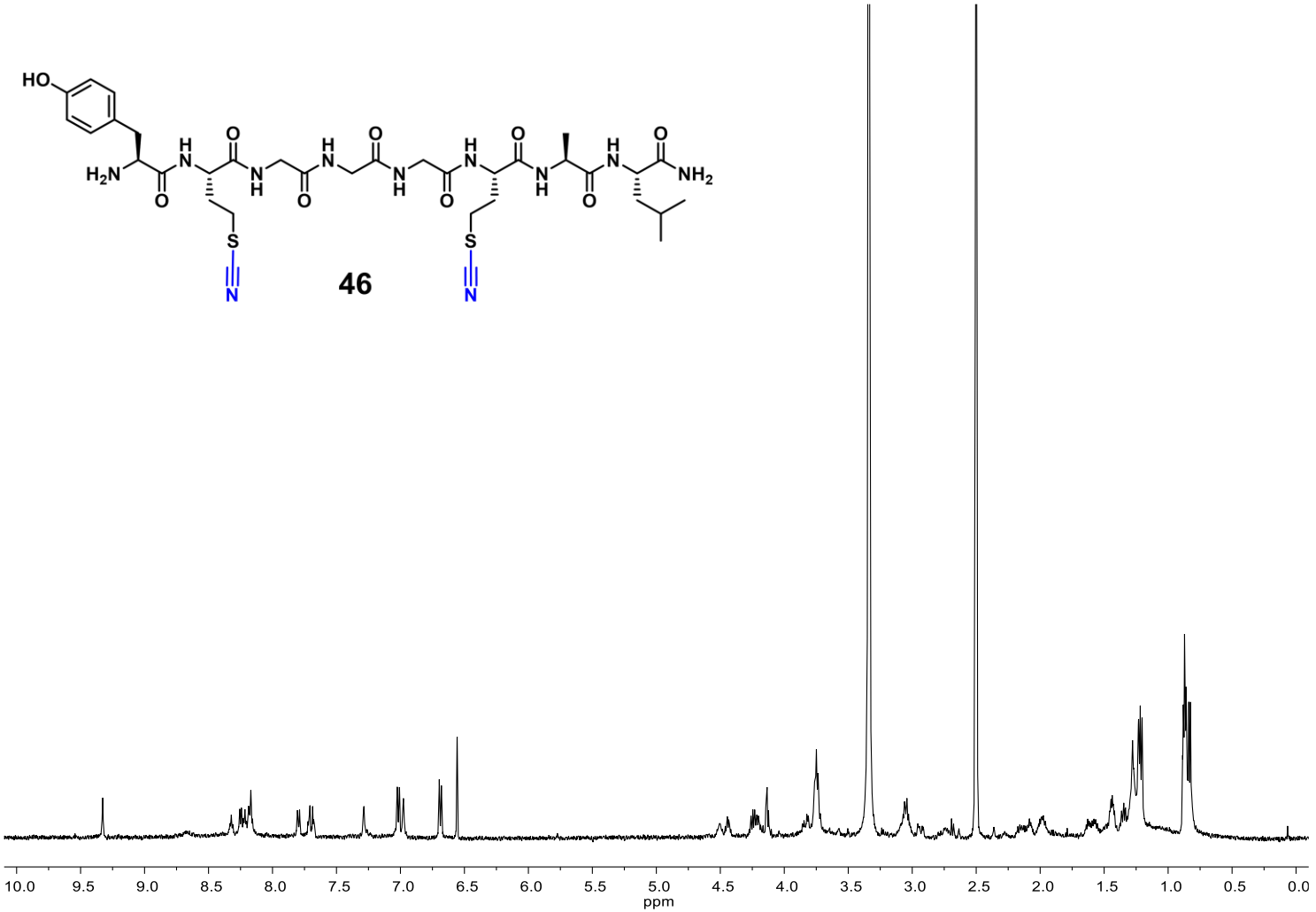

Figure A.115. 500 MHz ^{1}H-NMR Spectrum of Compound 46 in d_6-DMSO

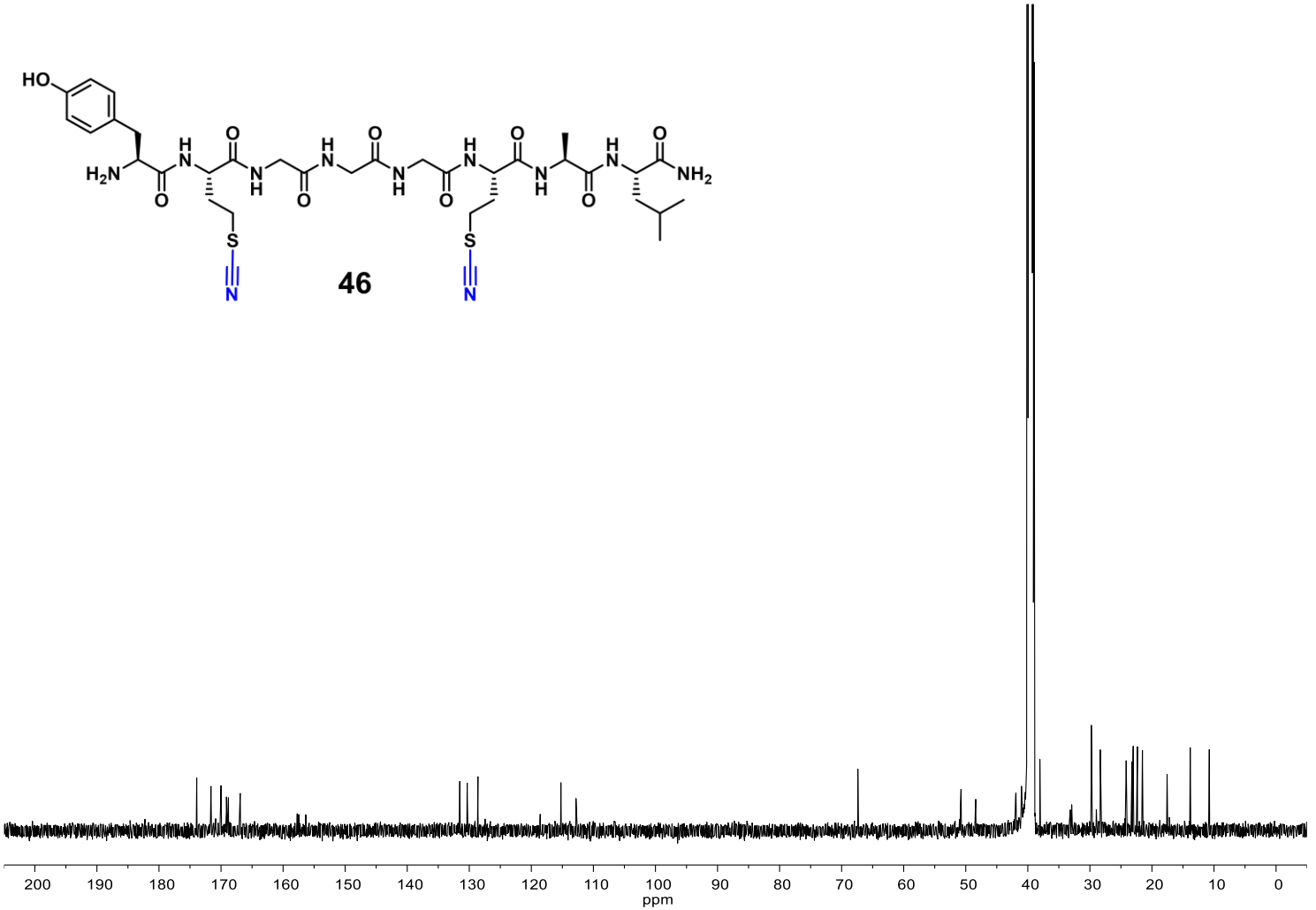

Figure A.116. 125 MHz ^{13}C-NMR Spectrum of Compound 46 in d_6-DMSO

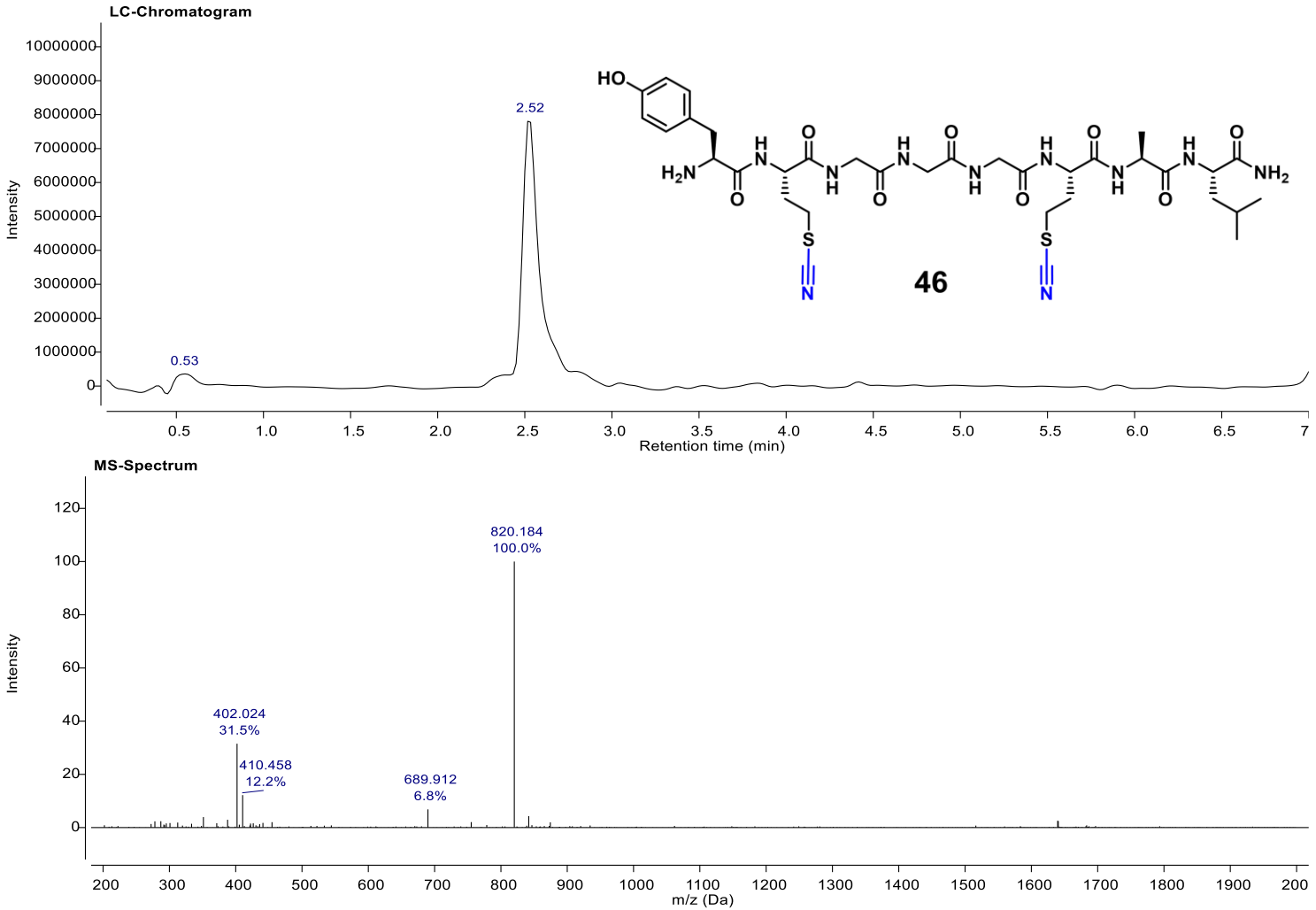

Figure A.117. LC-MS Spectrum of Compound 46 Gradient 5-60 for 7 Minutes

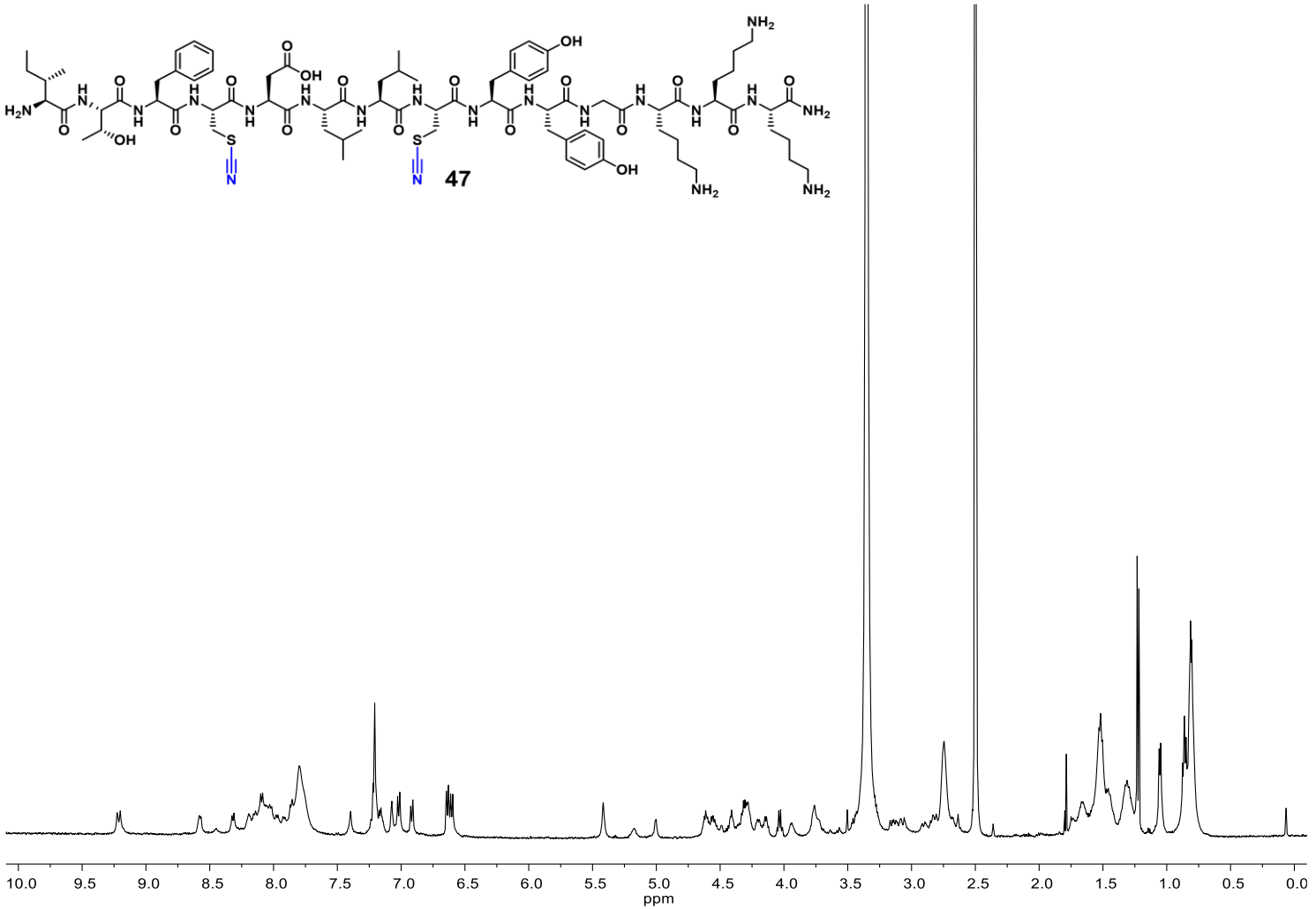

Figure A.118. 500 MHz ^{1}H-NMR Spectrum of Compound 47 in d_6-DMSO

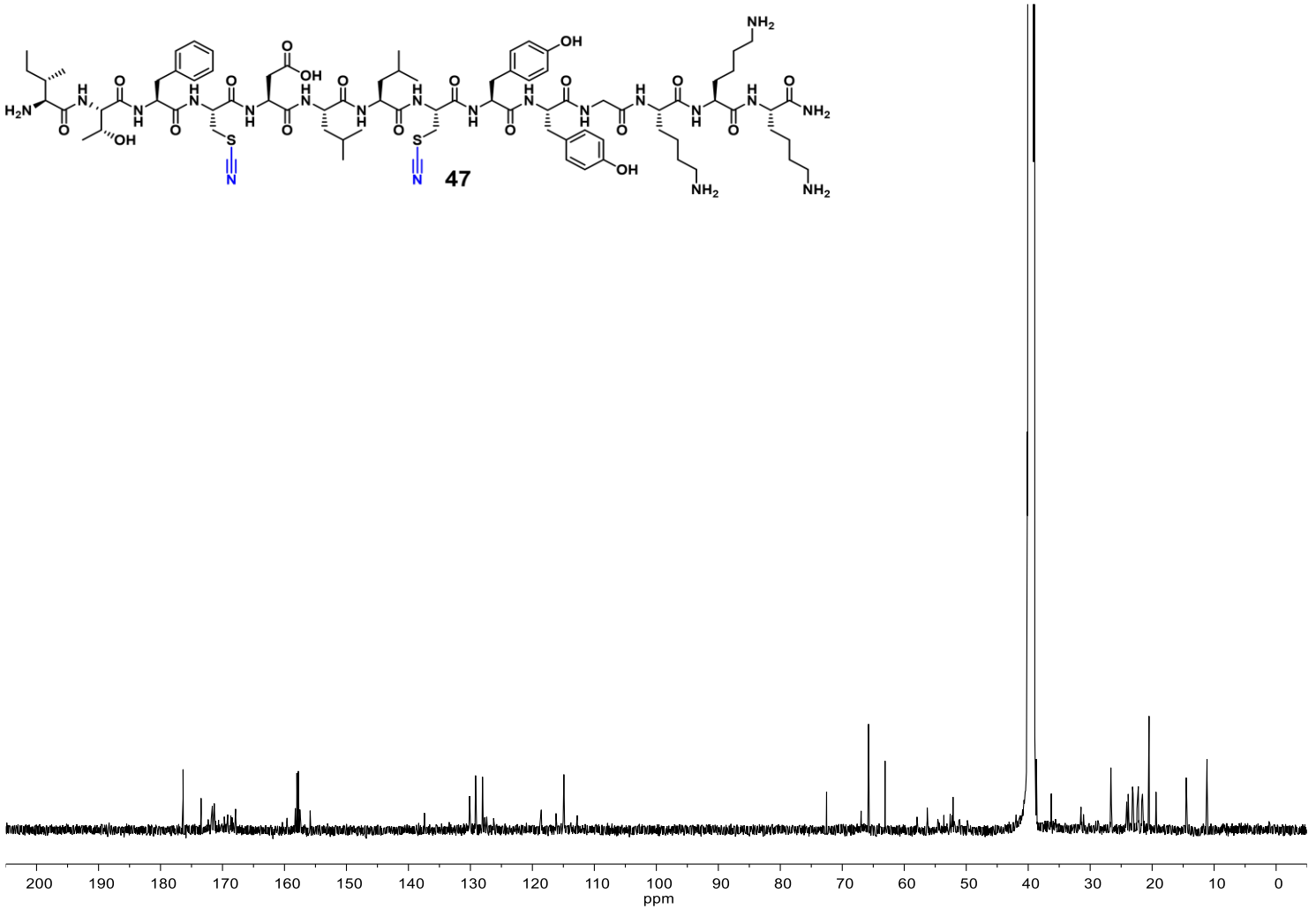

Figure A.119. 125 MHz ^{13}C-NMR Spectrum of Compound 47 in d_6-DMSO

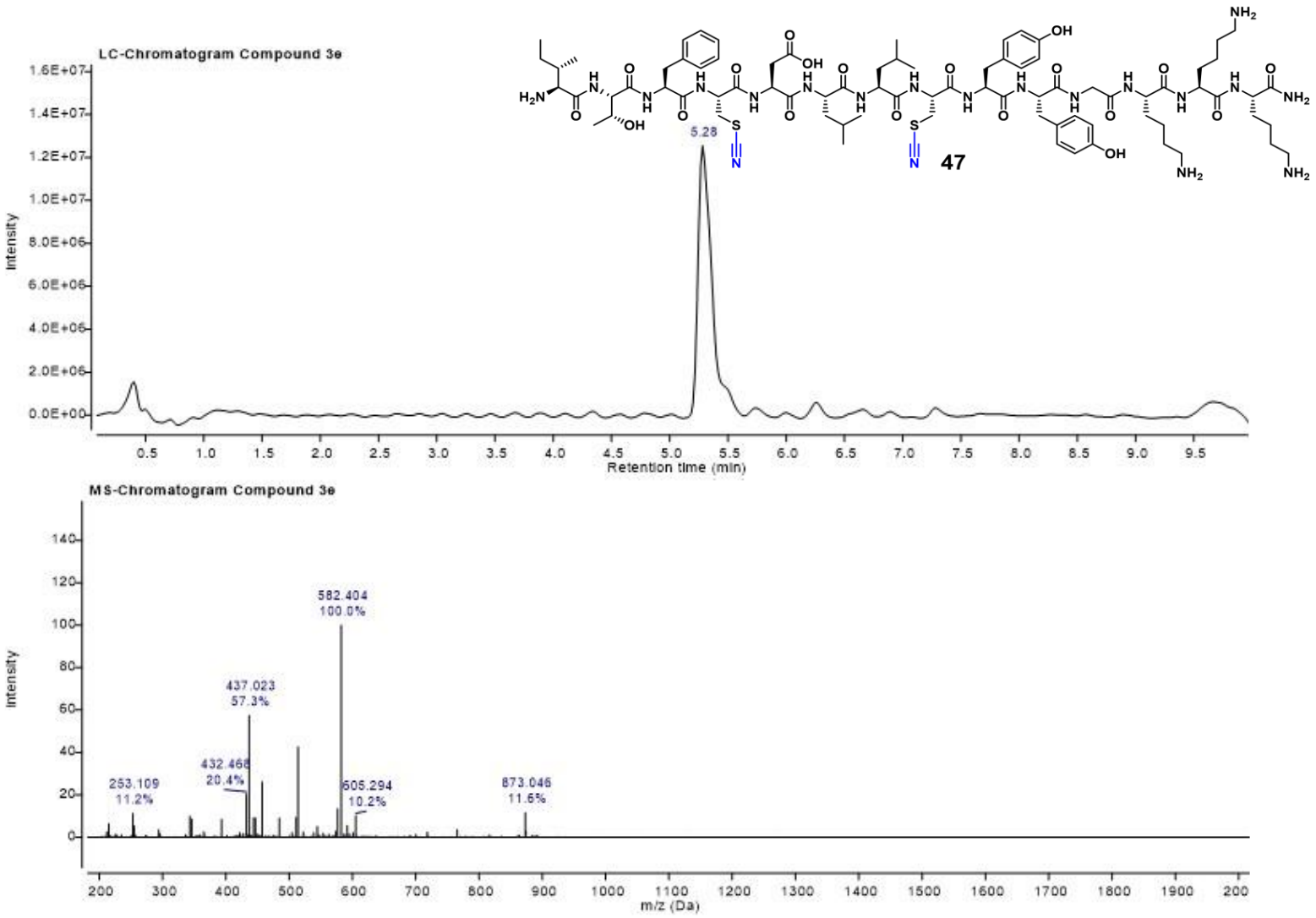

Figure A.120. LC-MS Spectrum of Compound 47 Gradient 5-60 for 10 Minutes

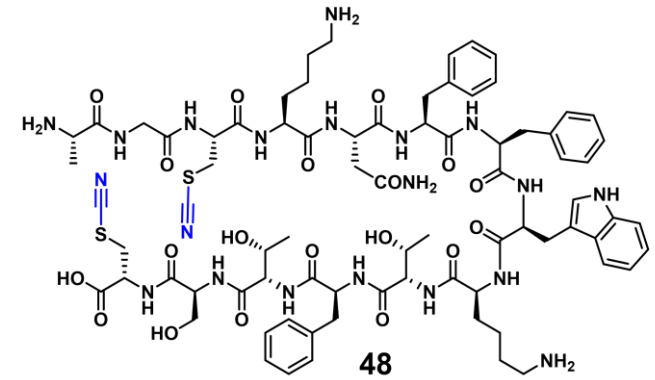

Figure A.121. 500 MHz ^{1}H-NMR Spectrum of Compound 48 in d_6-DMSO

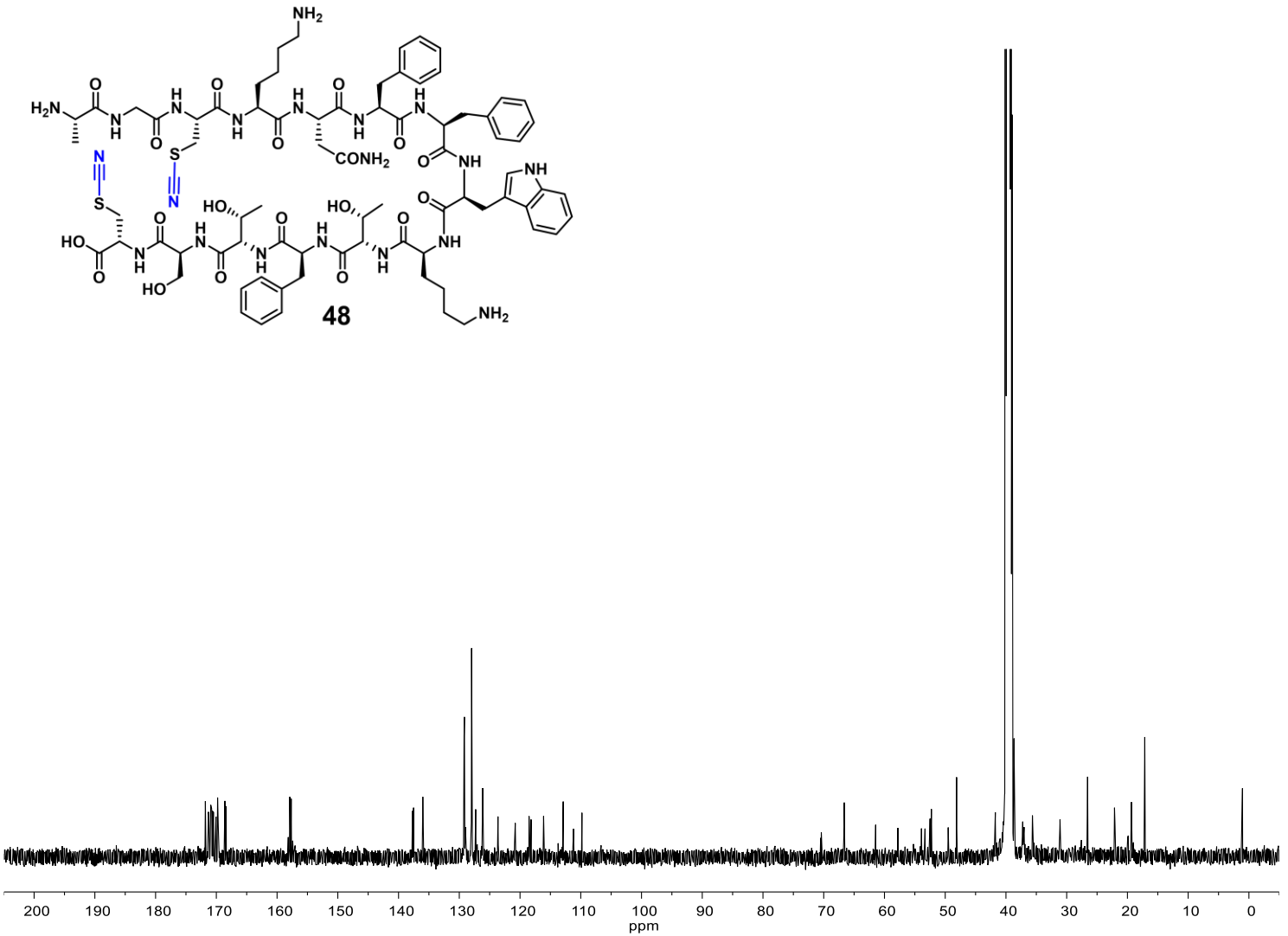

Figure A.122. 125 MHz ^{13}C-NMR Spectrum of Compound 48 in d_6-DMSO

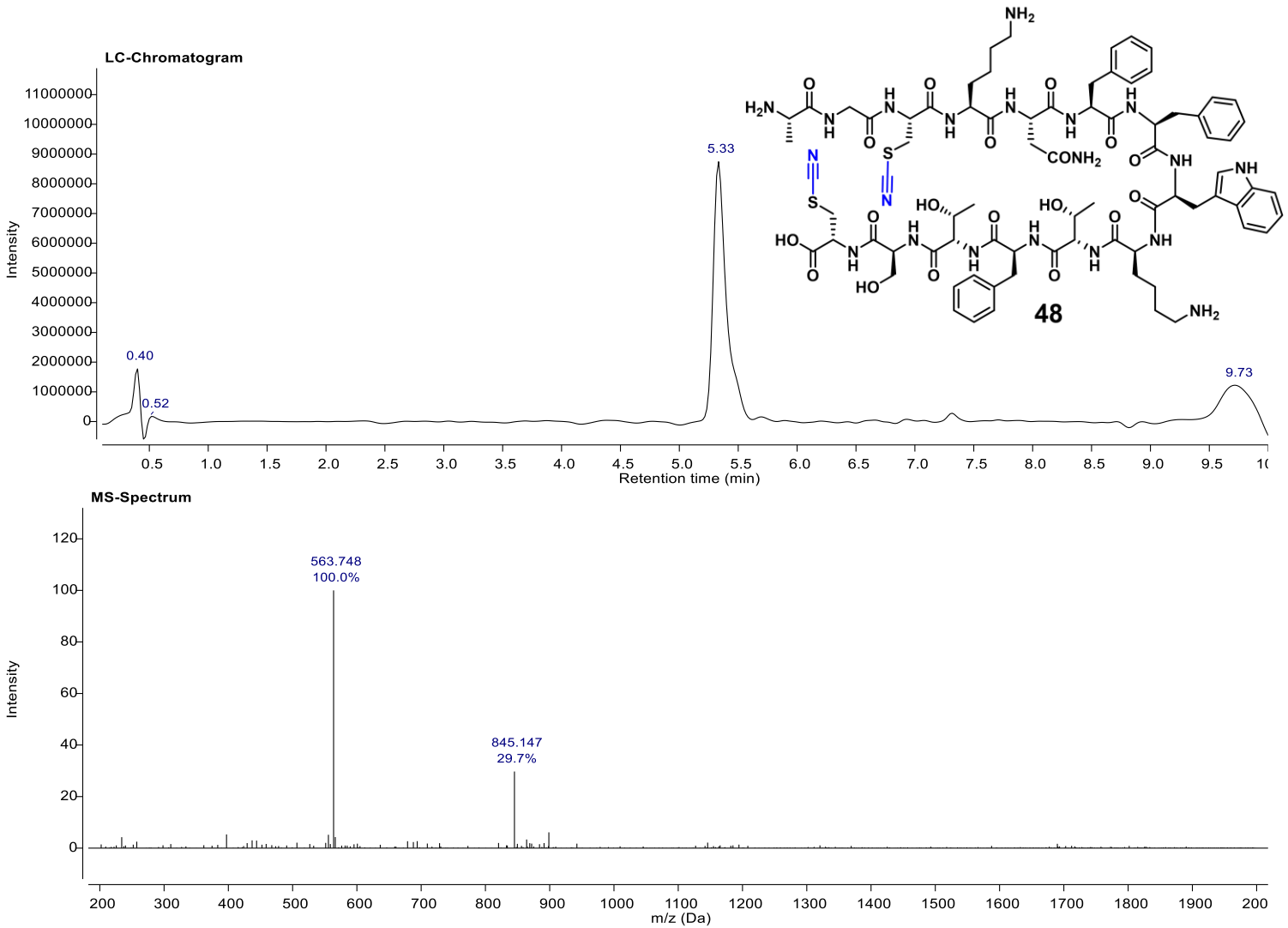

Figure A.123. LC-MS Spectrum of Compound 48 Gradient 5-60 for 10 Minutes

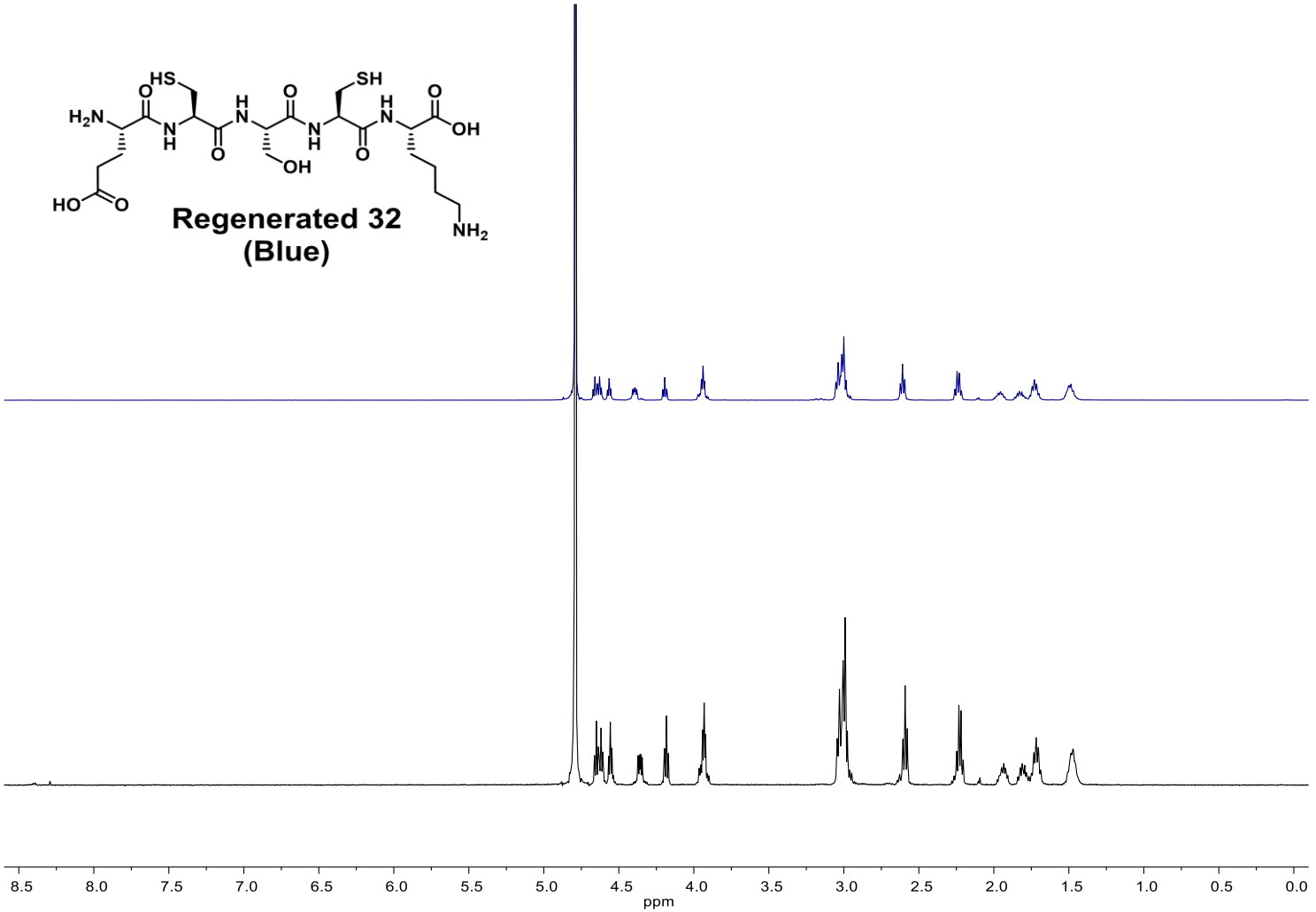

Figure A.124. 500 MHz ^{1}H-NMR Spectrum of Regenerated 32 in D_2O

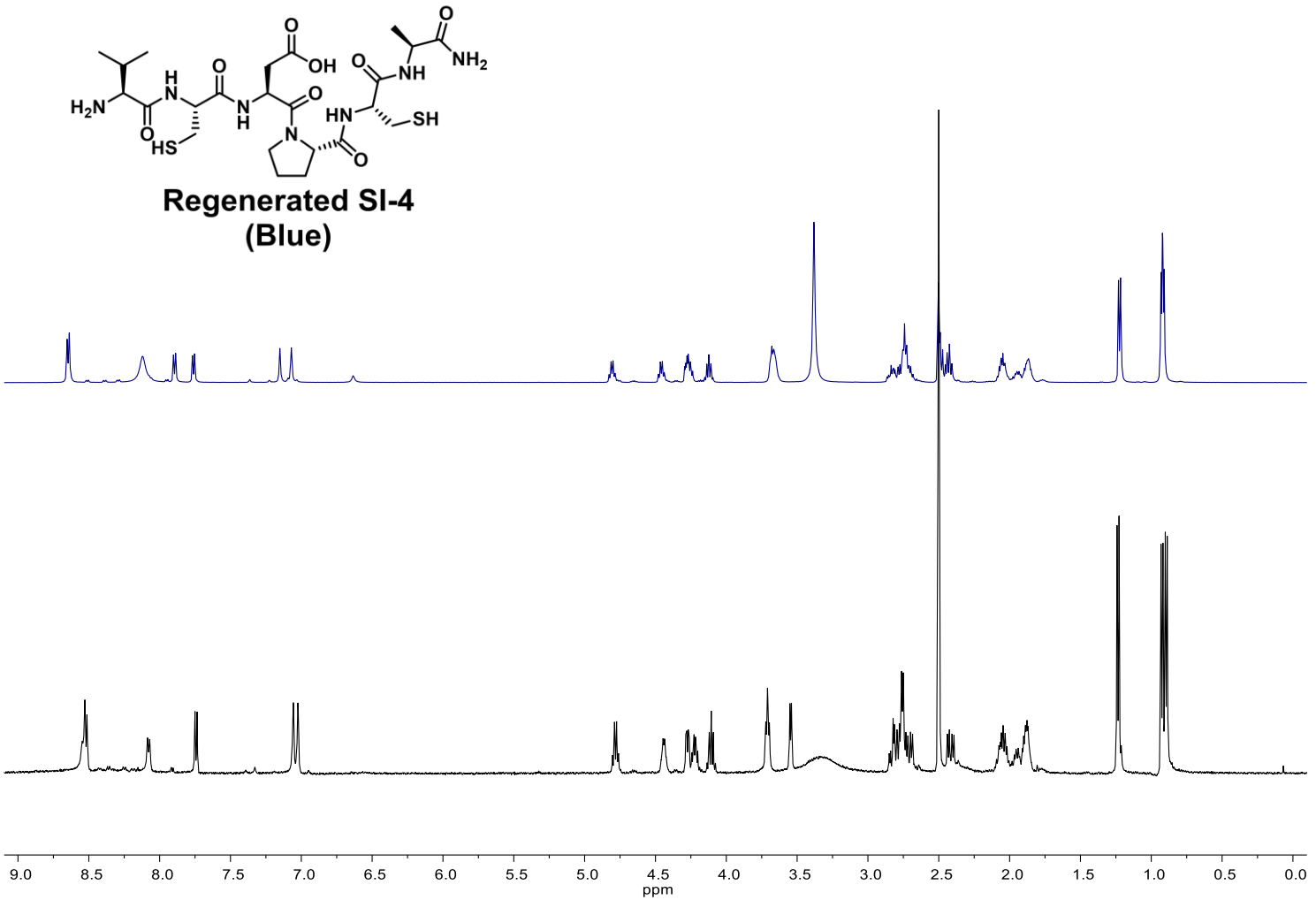

Figure A.125. 500 MHz ^{1}H-NMR Spectrum of Regenerated SI-4 in d_6-DMSO

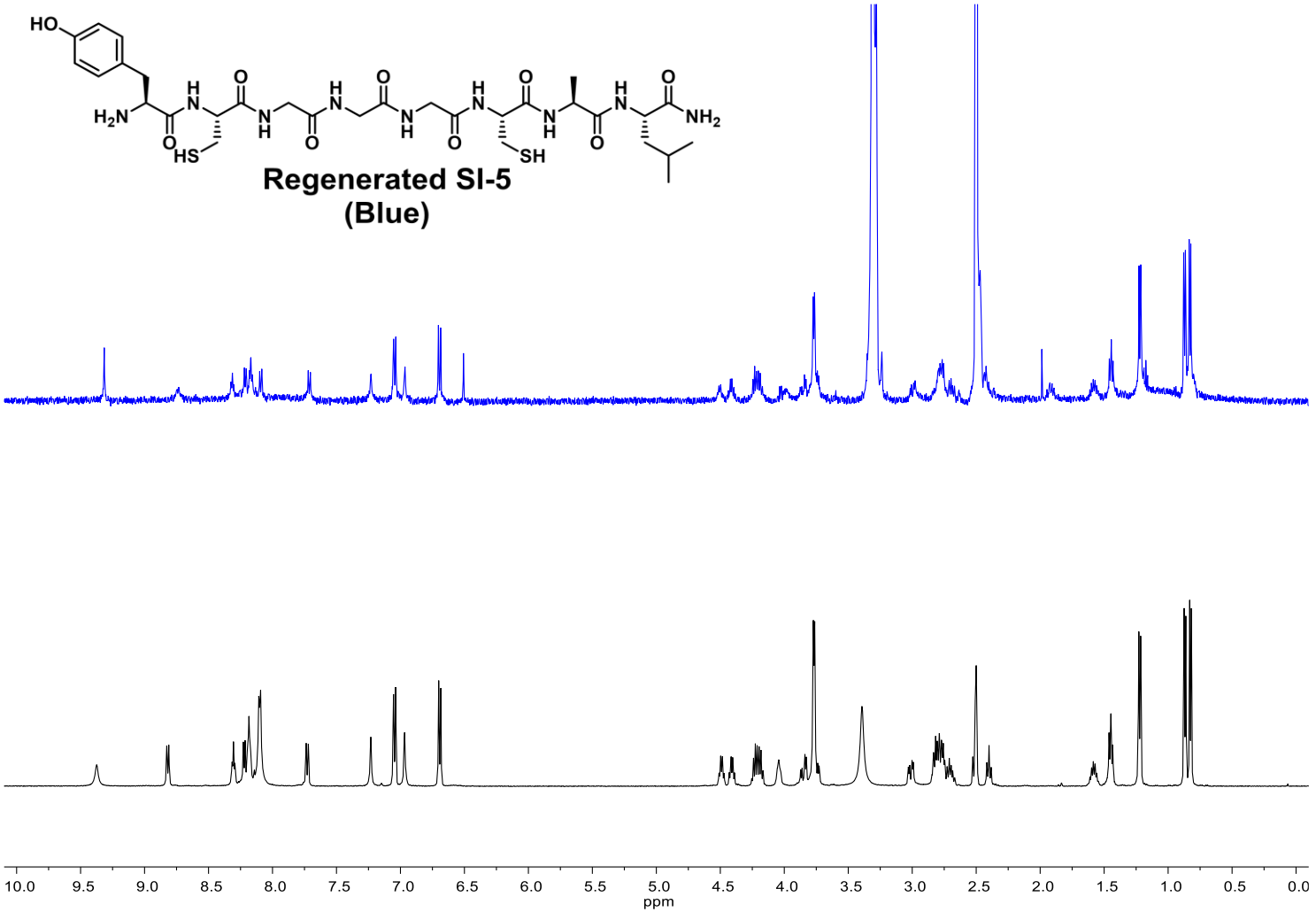

Figure A.126. 500 MHz ^{1}H-NMR Spectrum of Regenerated SI-5 in d_6-DMSO

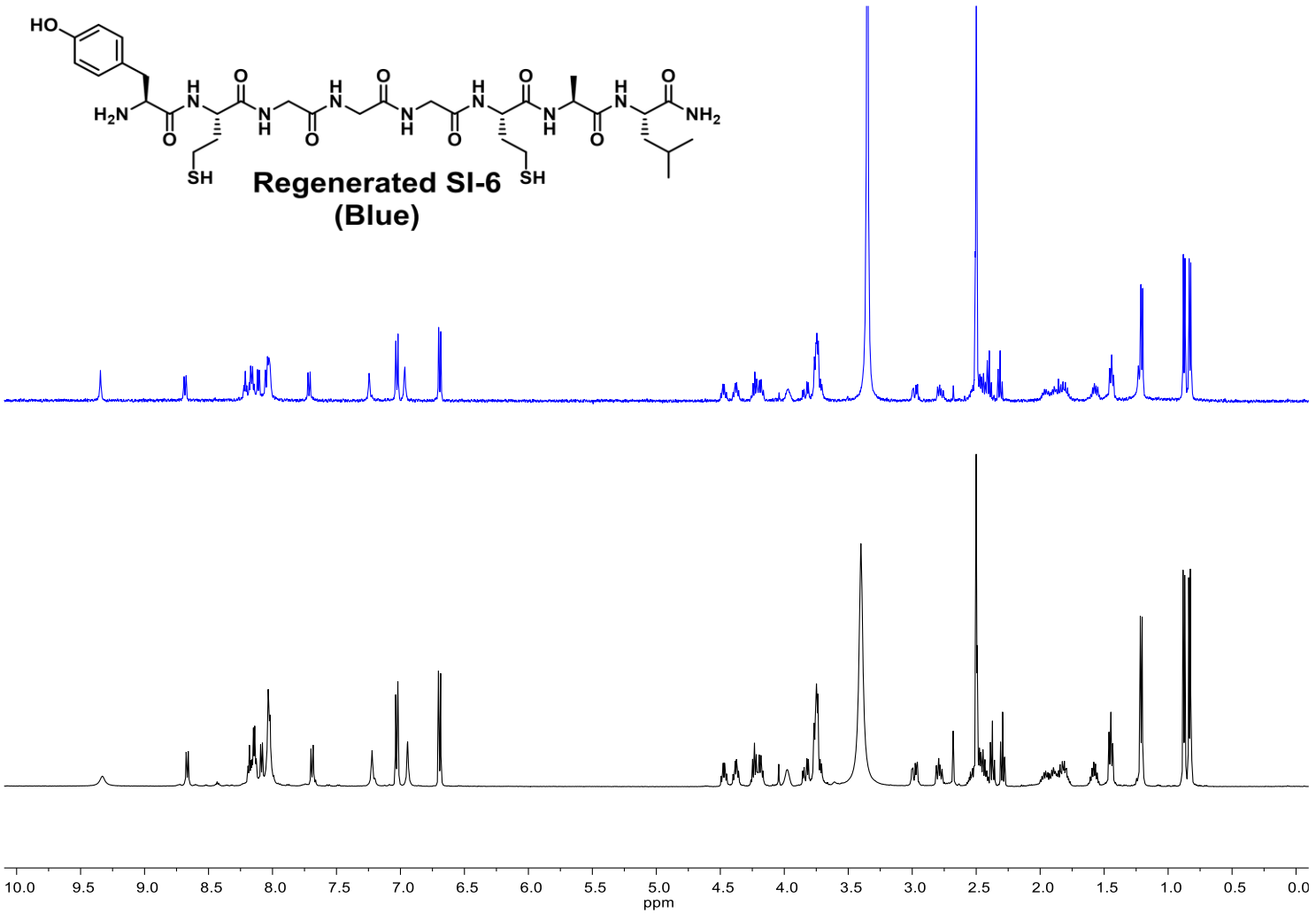

Figure A.127. 500 MHz ^{1}H-NMR Spectrum of Regenerated SI-6 in d_6-DMSO

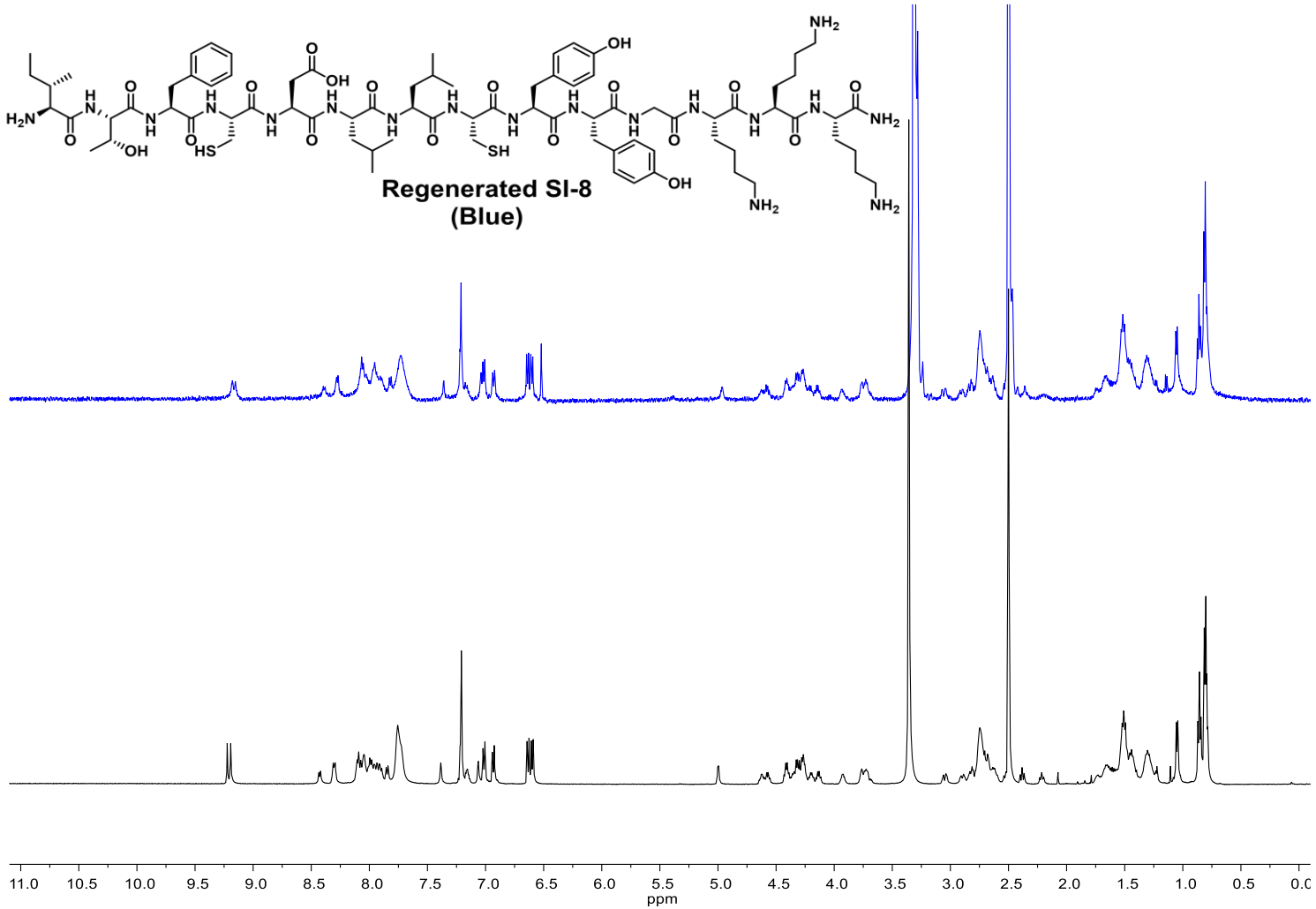

Figure A.128. 500 MHz ^{1}H-NMR Spectrum of Regenerated SI-8 in d_6-DMSO

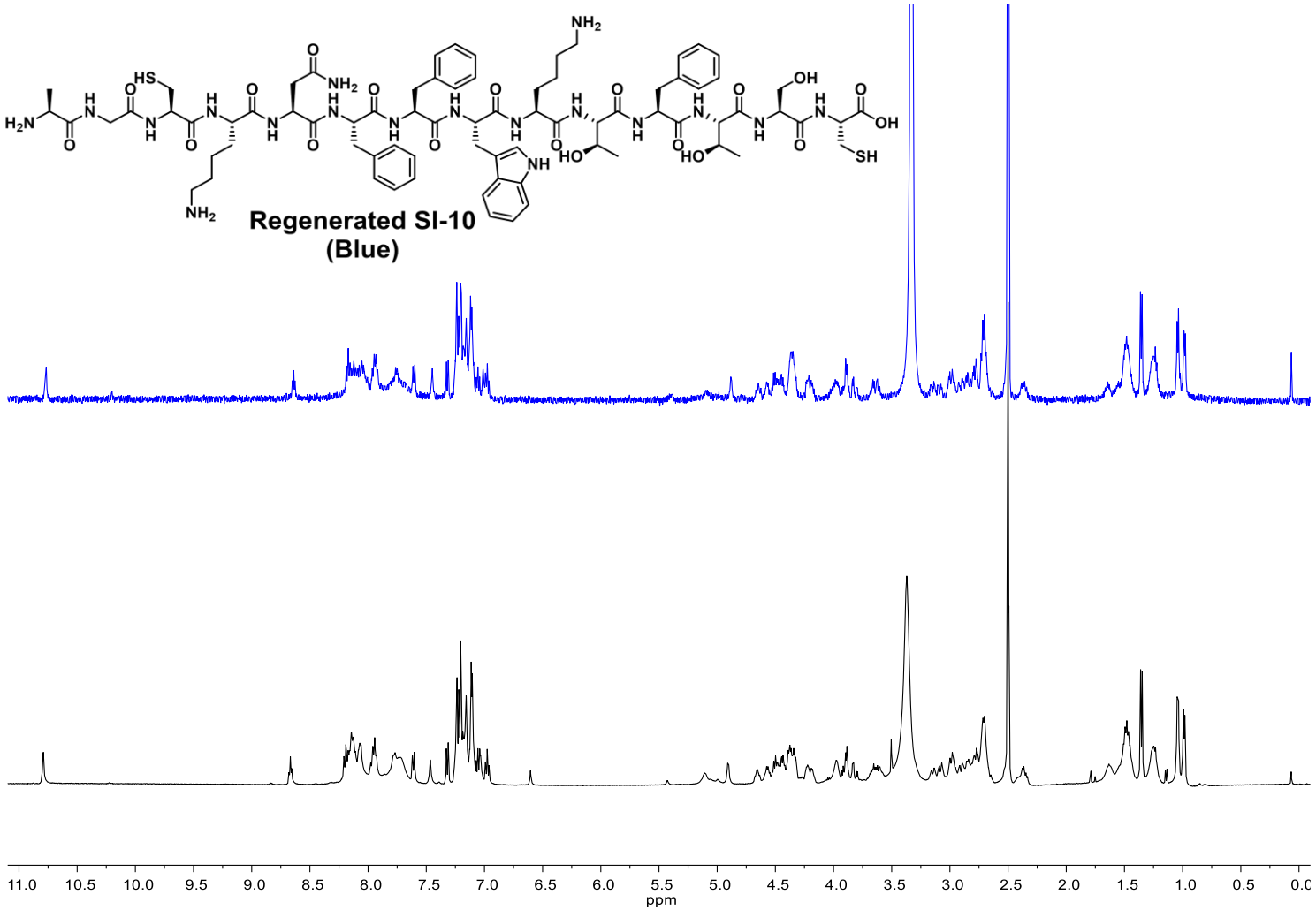

Figure A.129. 500 MHz ^{1}H-NMR Spectrum of Regenerated SI-10 in d_6-DMSO

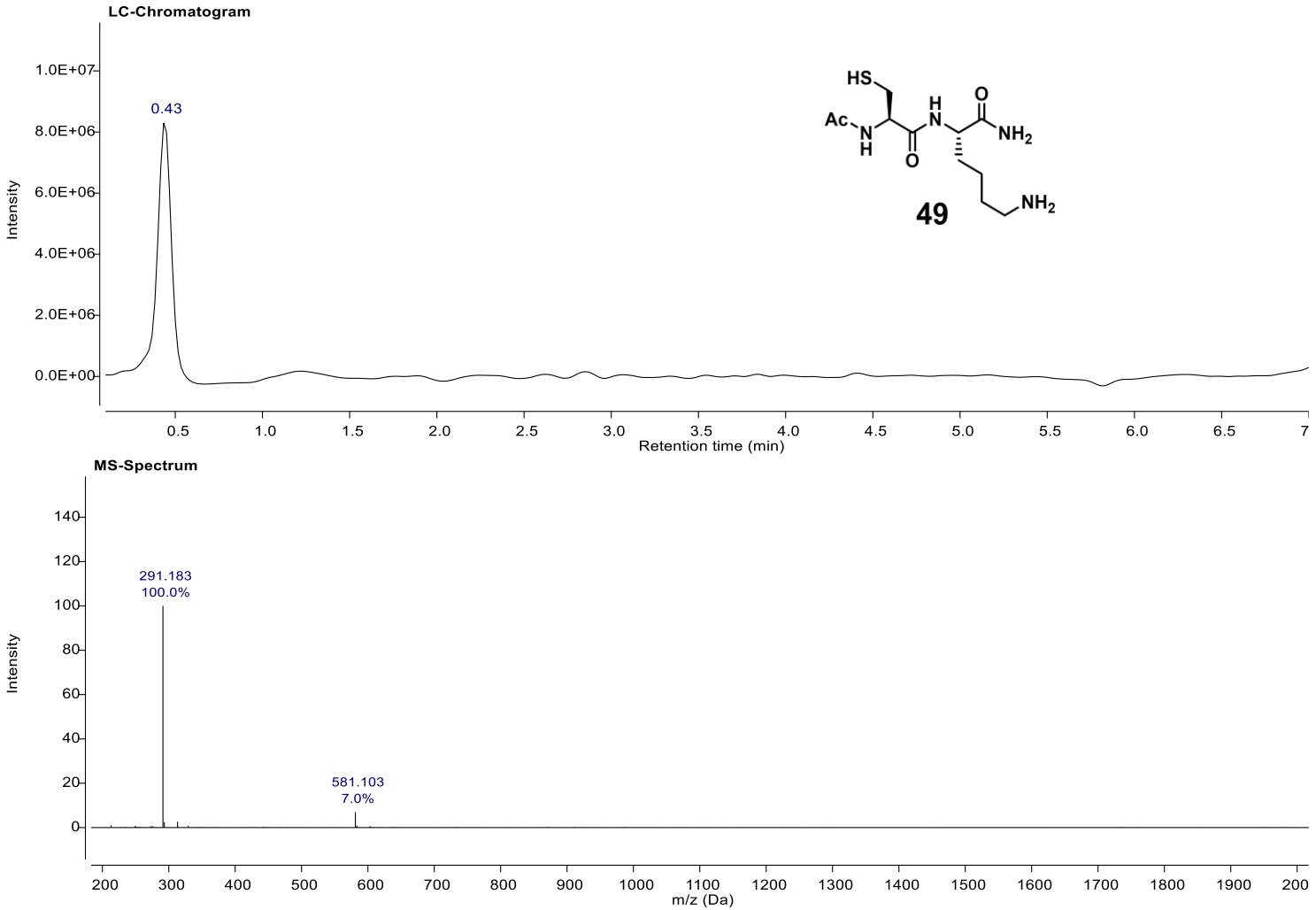

Figure A.130. LC-MS Spectrum of Compound 49 Gradient 5-60 for 7 Minutes

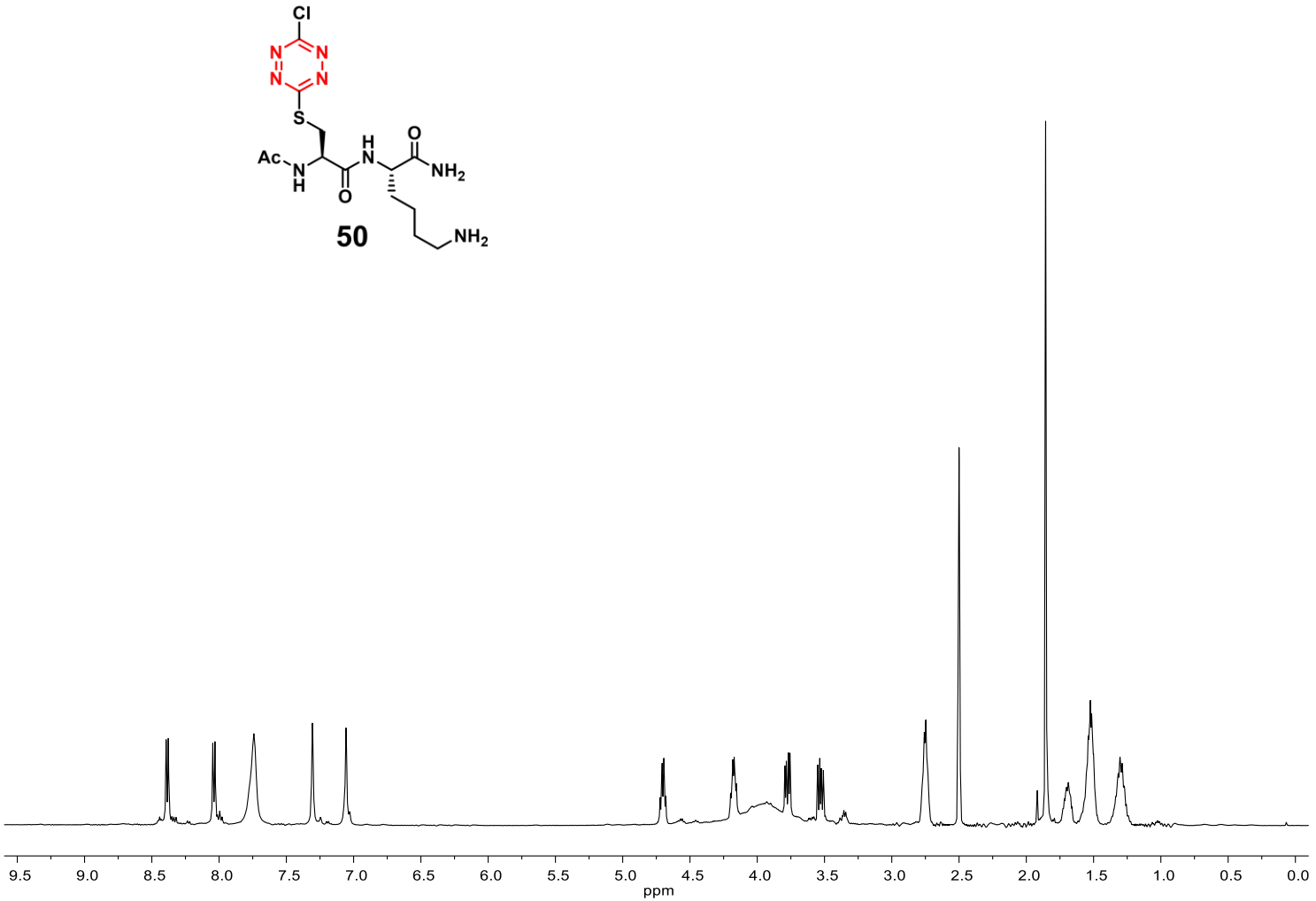

Figure A.131. 500 MHz ^{1}H-NMR Spectrum of Compound 36 in d_6-DMSO

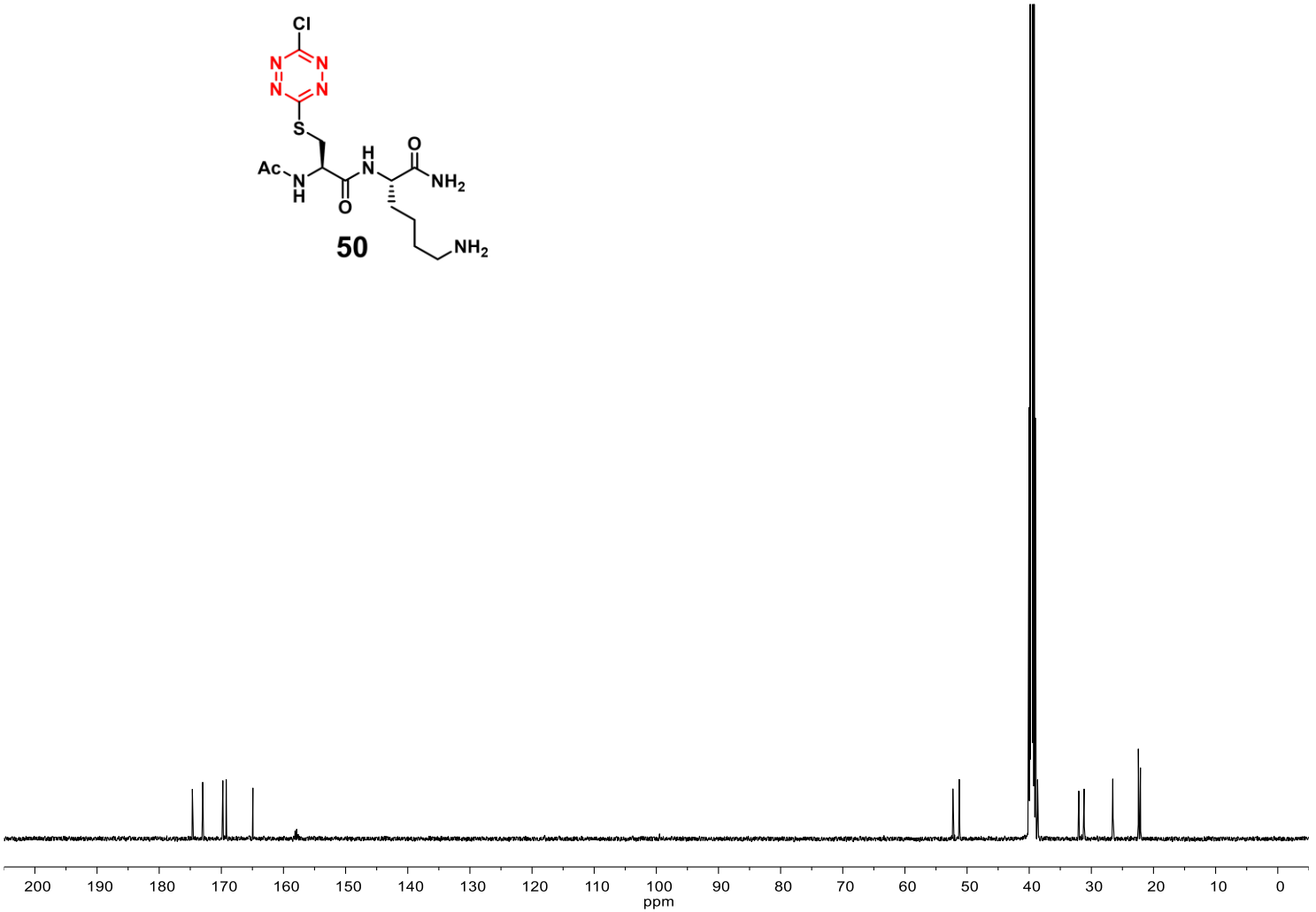

Figure A.132. 125 MHz ^{13}C-NMR Spectrum of Compound 50 in d_6-DMSO

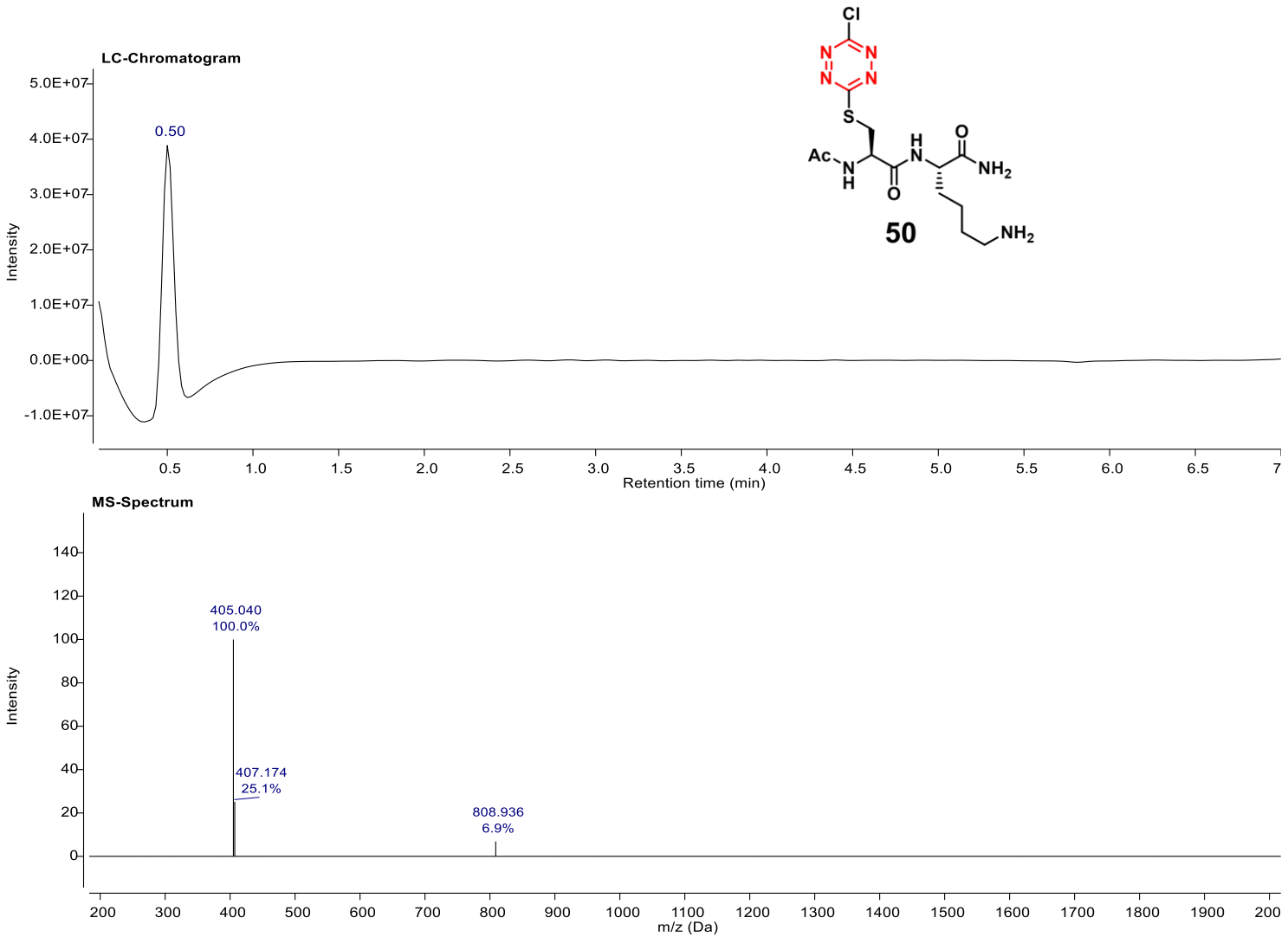

Figure A.133. LC-MS Spectrum of Compound 50 Gradient 5-60 for 7 Minutes

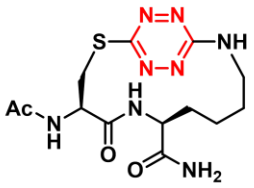

51

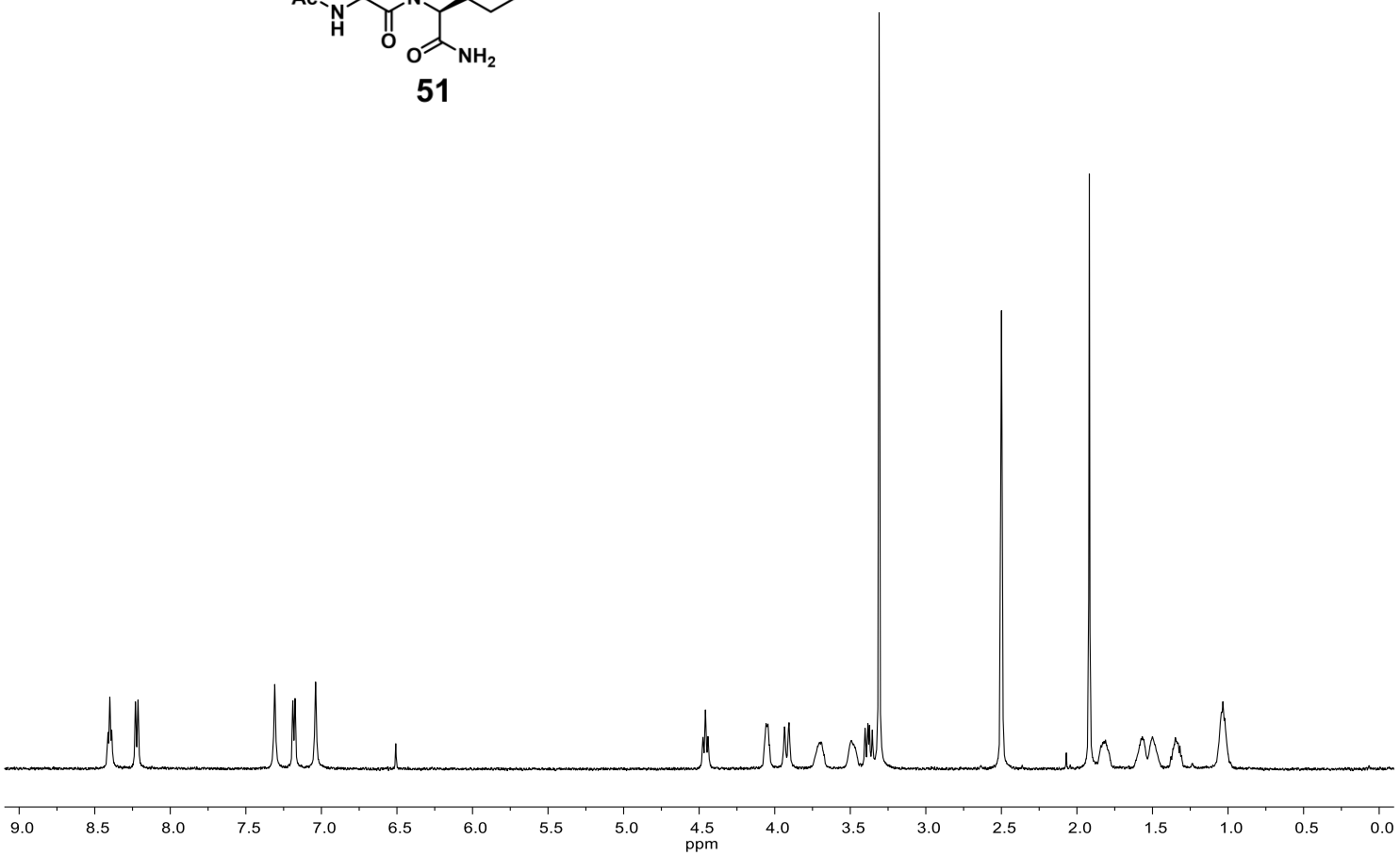

Figure A.134. 500 MHz ^{1}H-NMR Spectrum of Compound 51 in d_6-DMSO

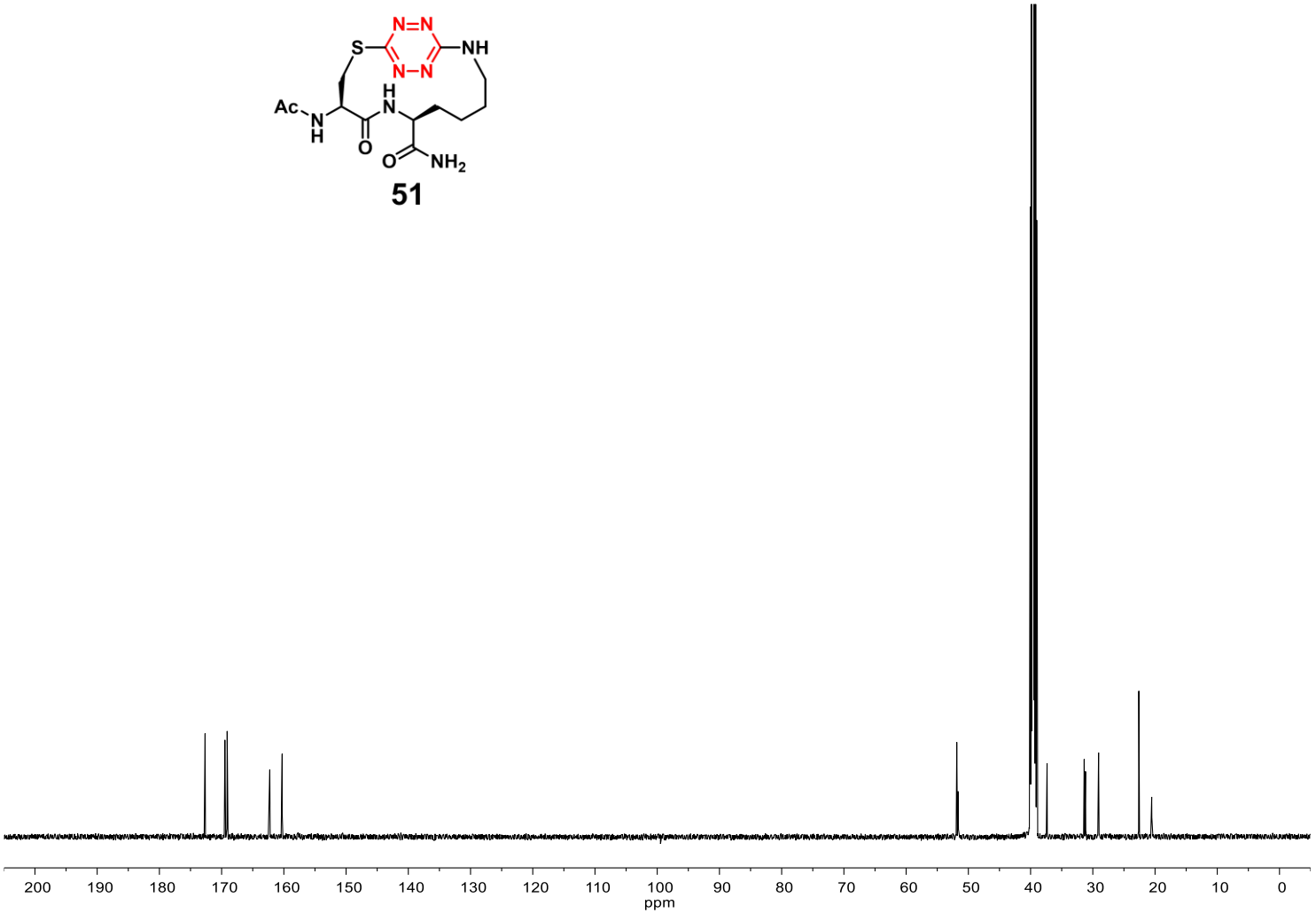

Figure A.135. 125 MHz ^{13}C-NMR Spectrum of Compound 51 in d_6-DMSO

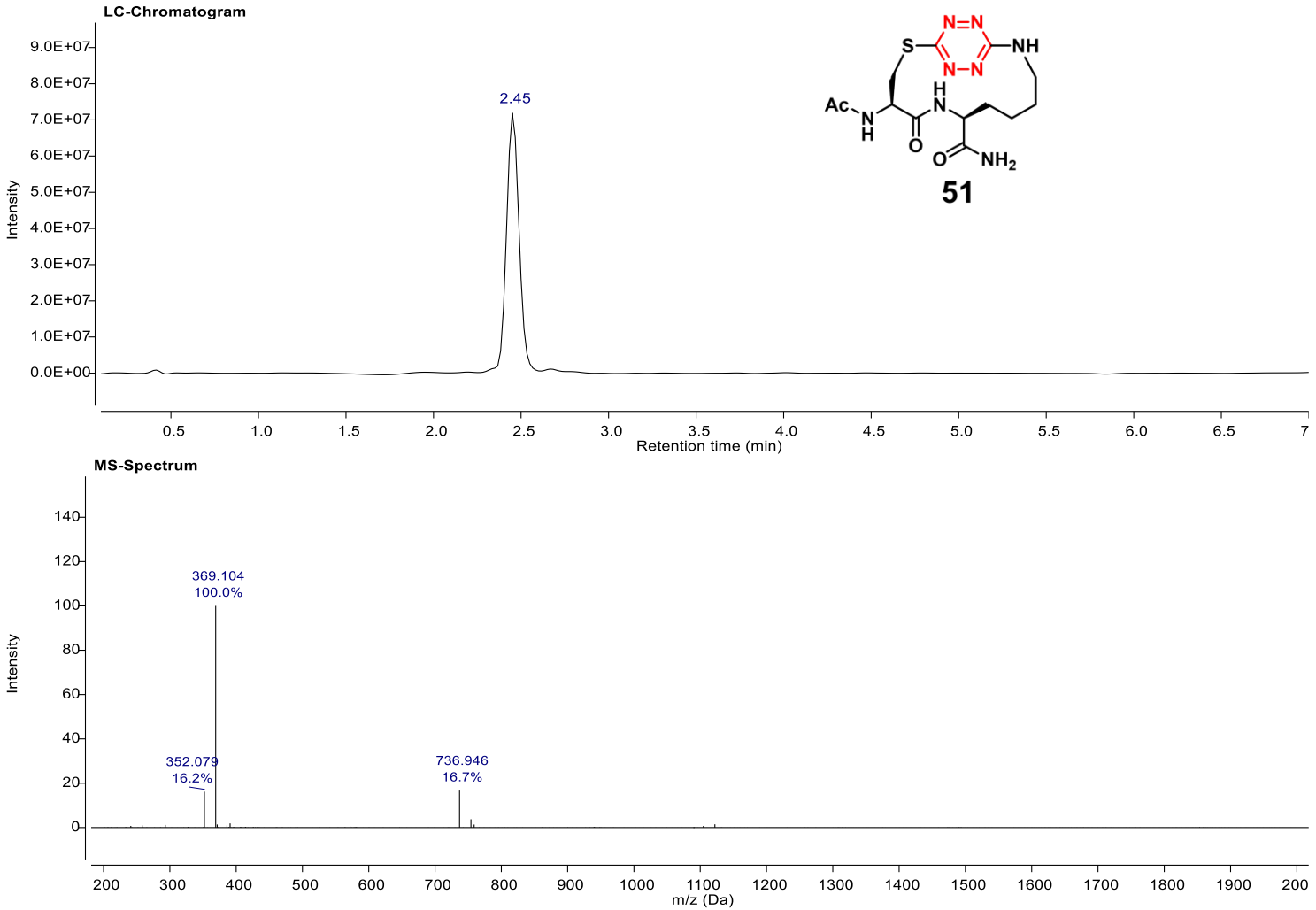

Figure A.136. LC-MS Spectrum of Compound 51 Gradient 5-60 for 7 Minutes

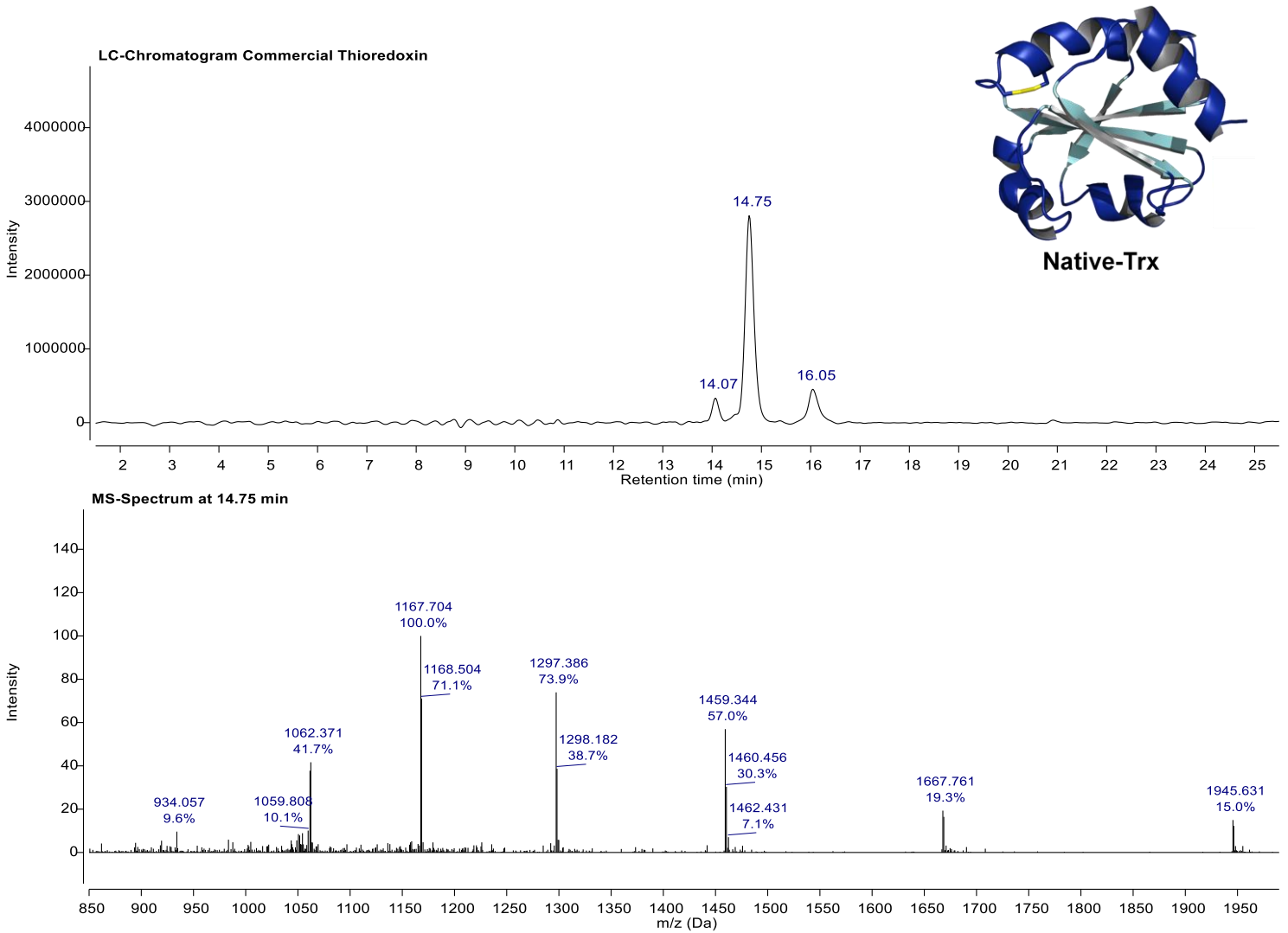

Figure A.137. LC-MS Spectrum of Native Thioredoxin C4-Column Gradient 20-70 for 27 Minutes

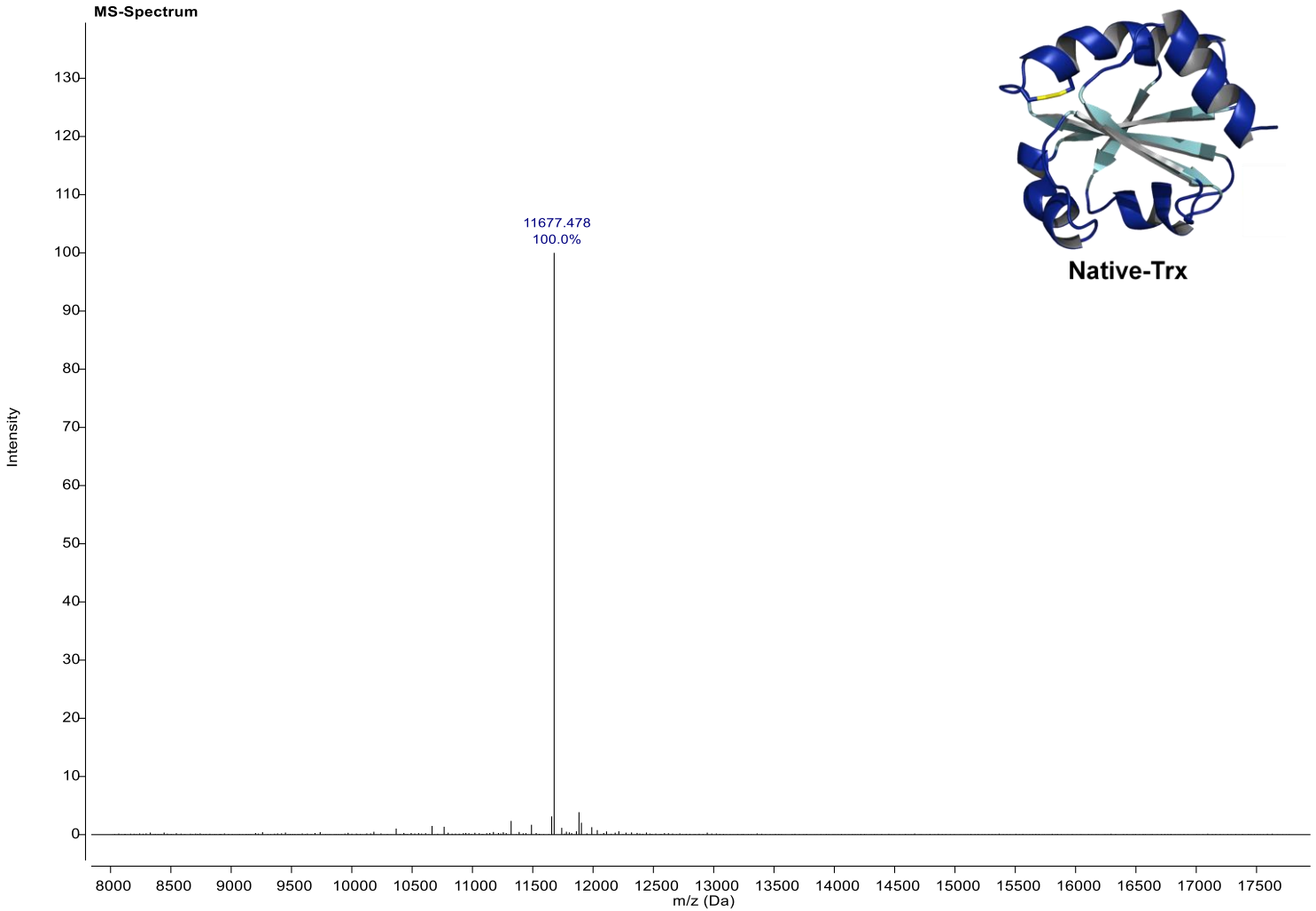

Figure A.138. MALDI-TOF-MS Spectrum of Native Thioredoxin

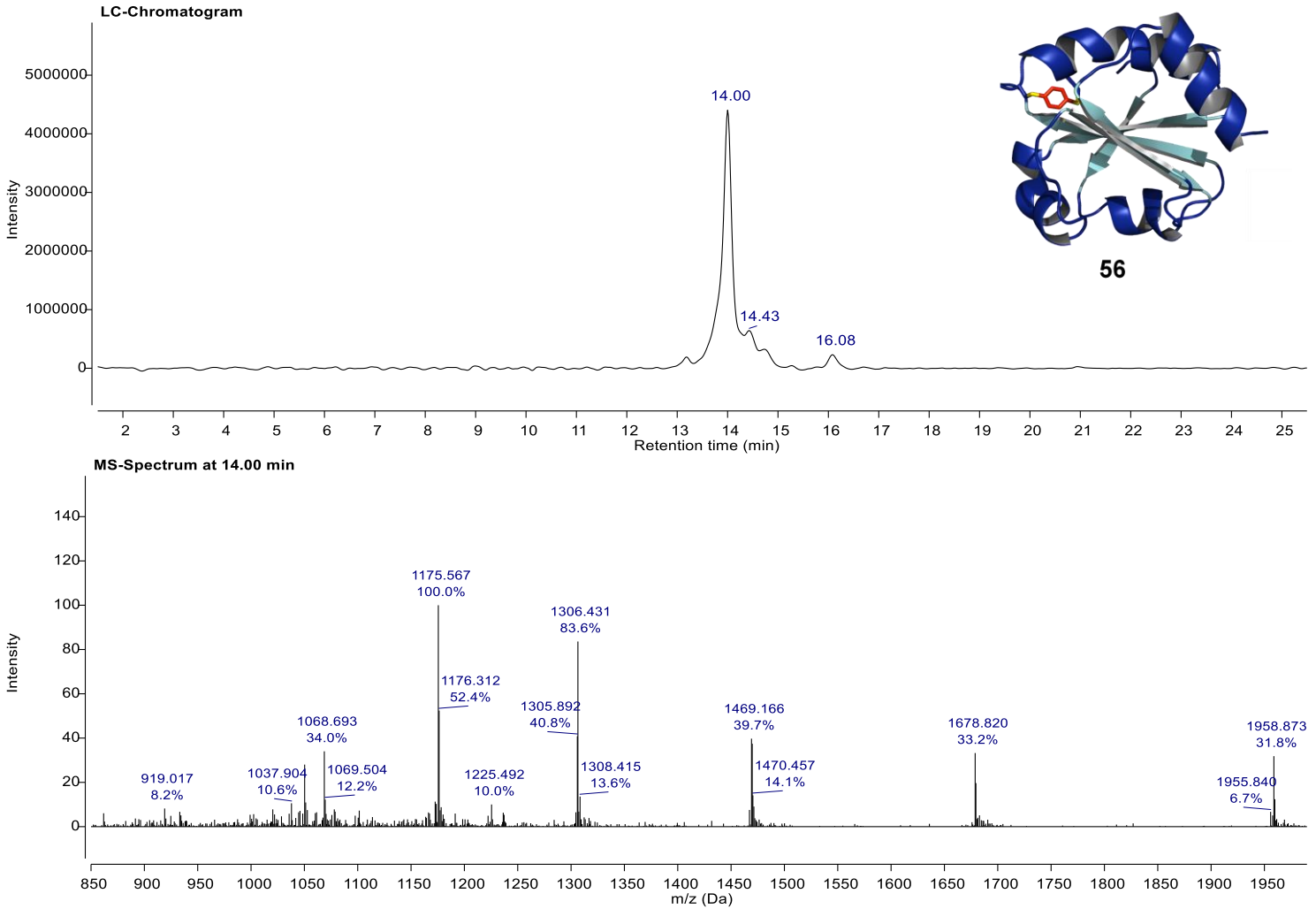

Figure A. 139. LC-MS Spectrum of Protein 56 C4-Column Gradient 20-70 for 27 Minutes

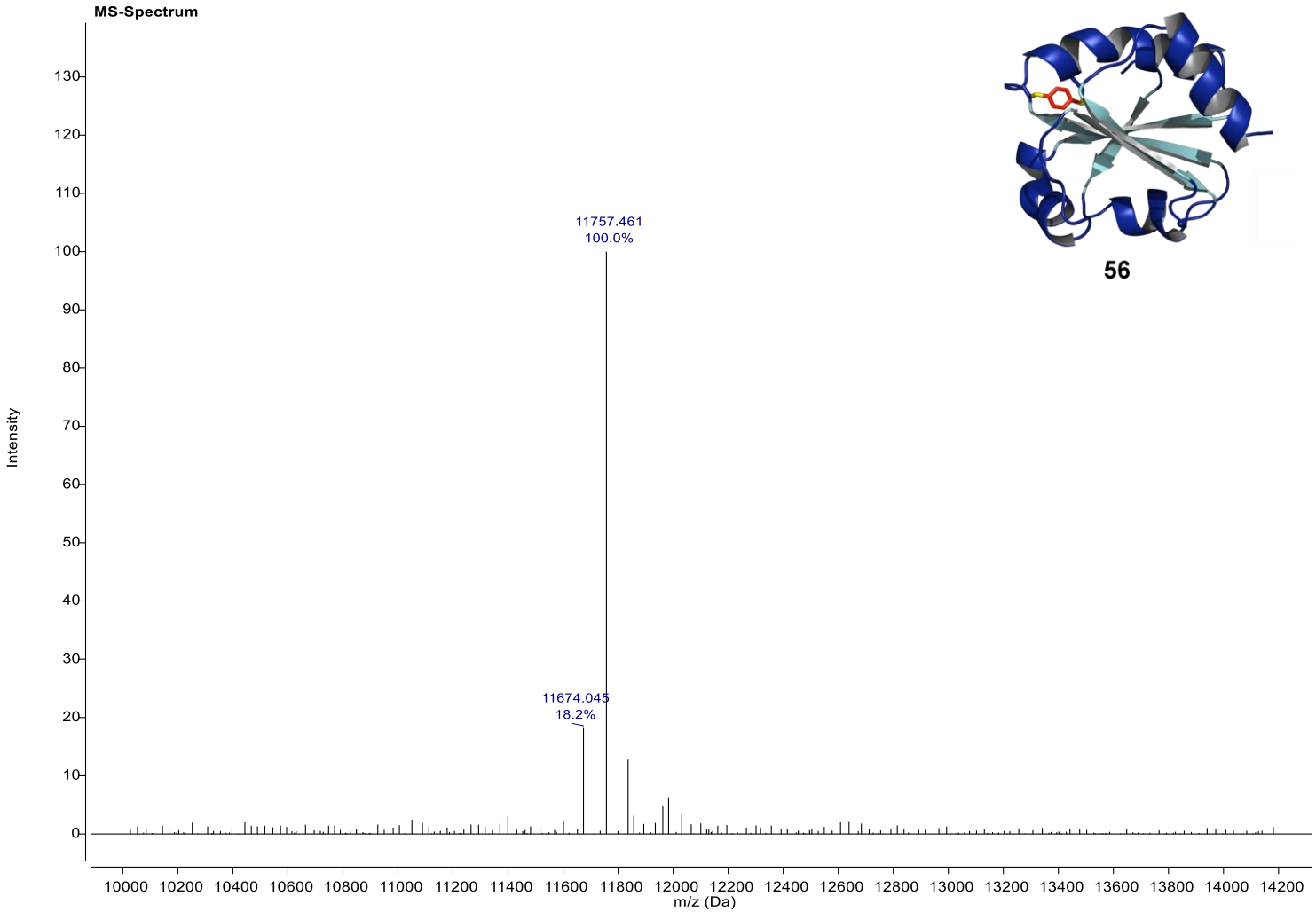

Figure A.140. MALDI-TOF-MS Spectrum of Protein 56

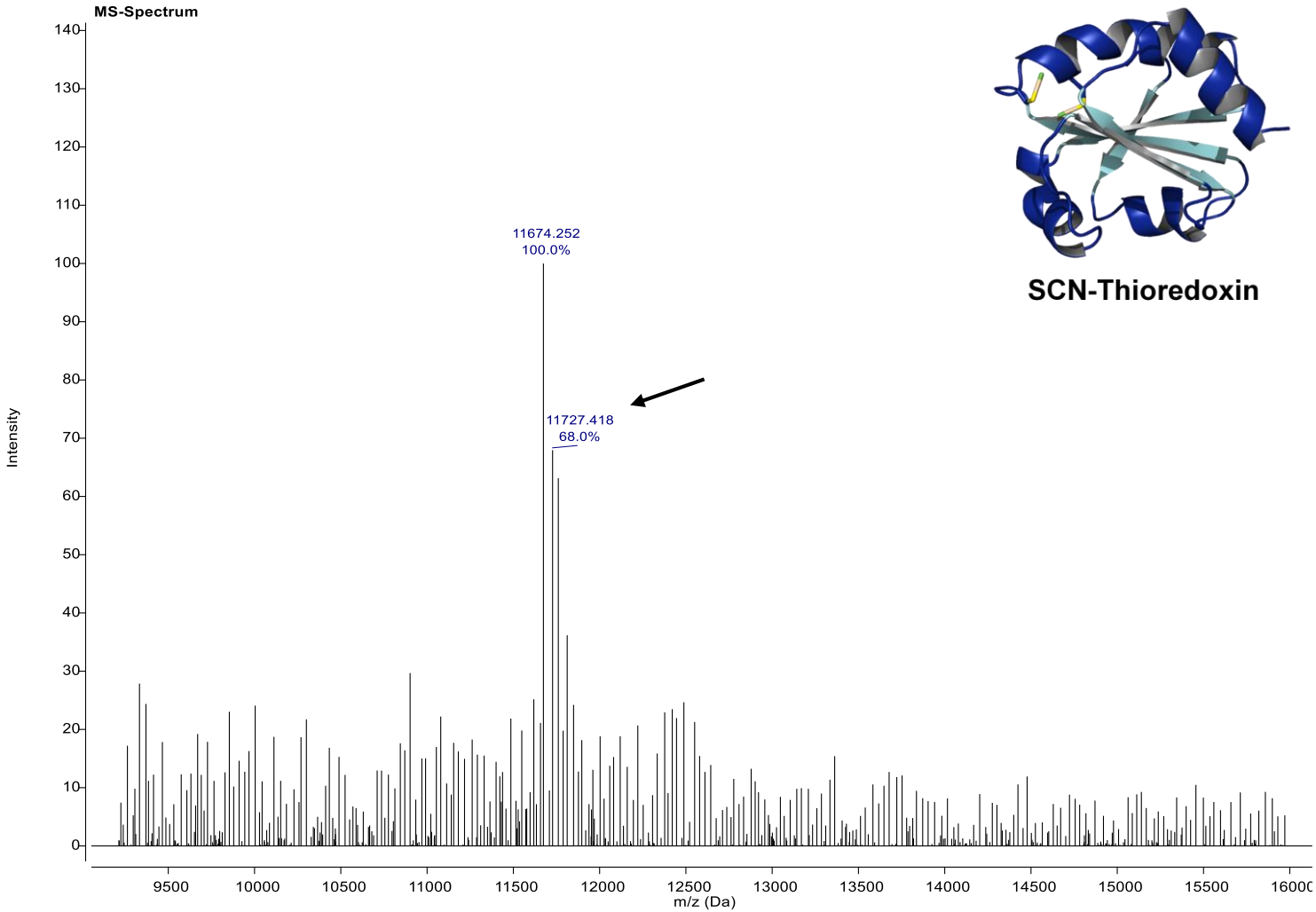

Figure A.141. MALDI-TOF-MS Spectrum of Dithiocyanate Thioredoxin-Flashlamp Conditions

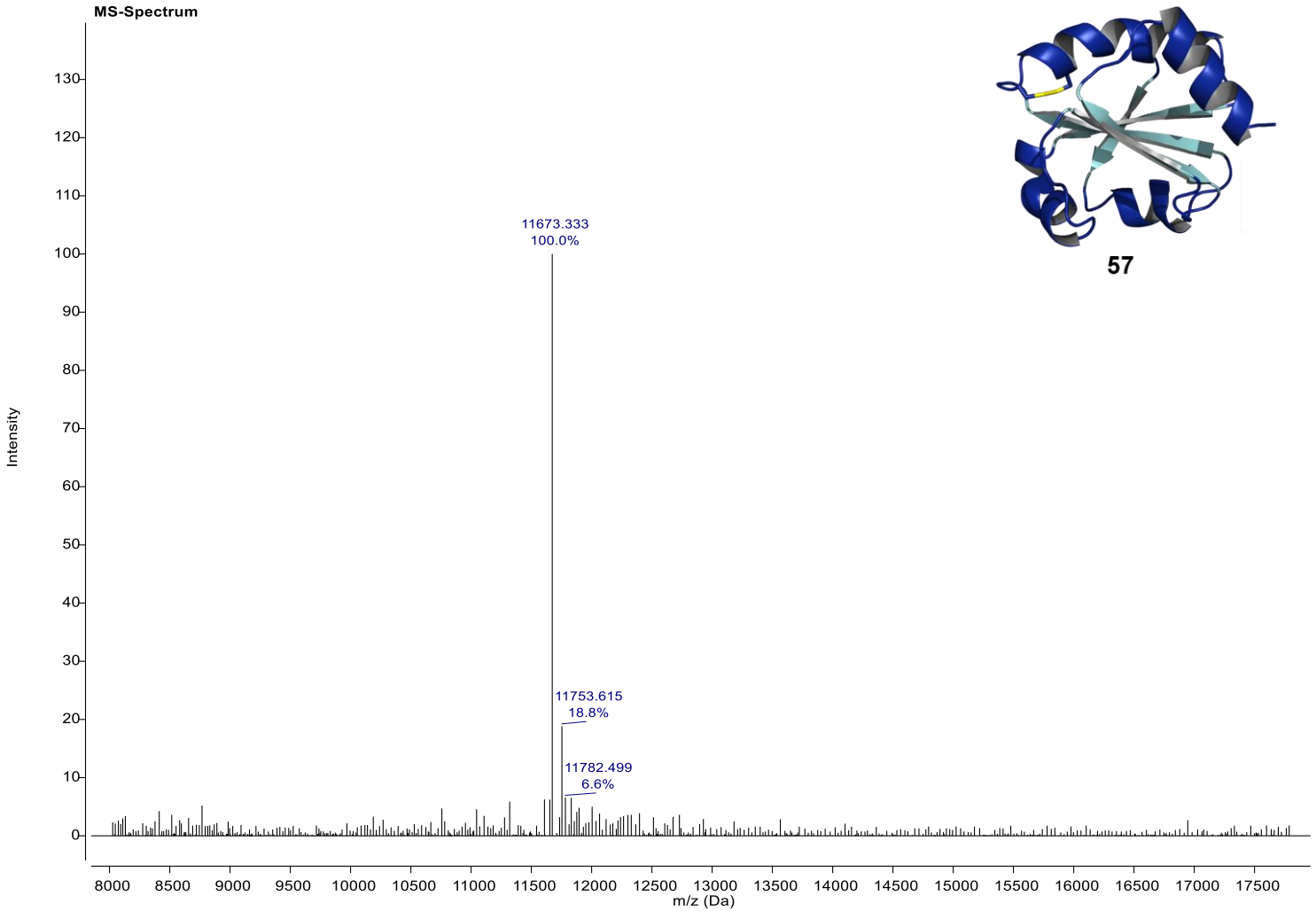

Figure A.142. MALDI-TOF-MS Spectrum of Regenerated Protein 57-Flashlamp Conditions

About the Author

Steve was born in rural Rochester, Indiana in 1981and grew up in this farming community. His father worked at Pike Lumber Company, a sawmill in the neighboring town of Akron. After graduating from Rochester High School in 1999, Steve went to work for Pike Lumber for several years to receive training as a sawmill hand, dry kiln operator, carpenter as well as many other areas towards training for a management pathway. To measure his management ability Pike had sent Steve to guidance counselor for testing and after receiving the results the counselor told Steve "you have management ability, but have you ever considered chemistry, because your score is off the chart in that field". Steve just scoffed at the thought of attending college and continued to work at Pike. However, in 2005 while watching the evening news saw Roy Vagelos addressing Congress on behalf of the National Academy of Science, equating science funding and more importantly science research to the overall future health of the country as well as the need to transition more people from factory wok into higher skilled positions. This was Steve's calling to chemistry and began to attend community college at Indiana University-Purdue University Fort Wayne (IPFW) on Saturdays to earn basic college credits.

Steve then transferred to Indiana University-Purdue University Indianapolis (IUPUI) as a full-time student where, after four years, received a Bachelor of Science degree in chemistry from Purdue University. While at IUPUI, Steve was a Workshop Leader in PLTL (Peer-Led Team Learning) Mentoring Program, worked as an organic laboratory teaching assistant (TA) and conducted three years of undergraduate research in the laboratory of Professor Martin O'Donnell contributing to several research projects in solid-phase synthesis of unnatural peptides and peptidomimetics.

Steve then moved to Philadelphia to pursue a graduate career at the University of Pennsylvania working under the guidance of Professor Amos B. Smith, III. Steve focused on the development of methods for stapling and unstapling peptides and proteins with *s*-tetrazine.

Following the defense of his doctoral work, Steve will move to Groton, CT to begin work at Pfizer as a senior scientist working in the anti-body drug conjugate (ADC) division.